AUXIN-INDUCED ACTIN CYTOSKELETON REARRANGEMENTS REQUIRE AUXIN RESISTANT 1
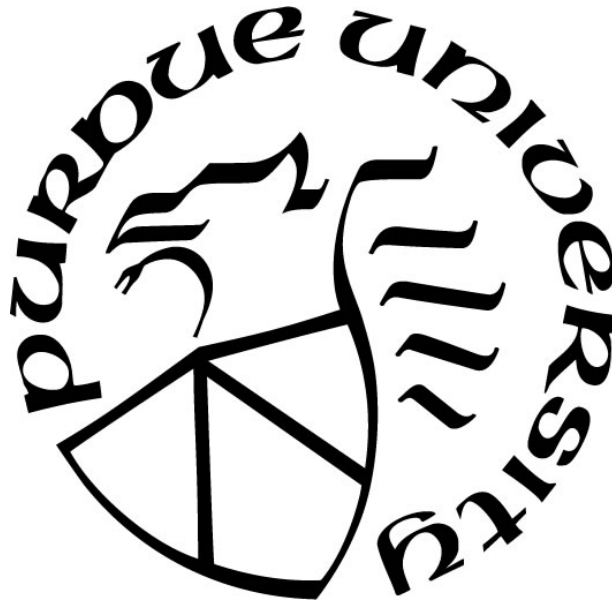
by

Ruthie S. Arieti

A Dissertation

Submitted to the Faculty of Purdue University

In Partial Fulfillment of the Requirements for the degree of

Doctor of Philosophy

Department of Biological Sciences, College of Science

West Lafayette, Indiana

August 2019

THE PURDUE UNIVERSITY GRADUATE SCHOOL
STATEMENT OF COMMITTEE APPROVAL

Dr. Christopher J. Staiger, Chair
    Department of Biological Sciences

Dr. Anjali S. Iyer-Pascuzzi
    Department of Botany and Plant Pathology

Dr. Tesfaye Mengiste
    Department of Botany and Plant Pathology

Dr. Chunhua Zhang
    Department of Botany and Plant Pathology

Dr. Jian-Kang Zhu (*through December 2018*)
    Department of Horticulture and Landscape Architecture

Approved by:
    Dr. Jason R. Cannon
        Head of the Graduate Program

    Dr. Janice P. Evans
        Head of Biological Sciences

In memory of
Karen L. Imhof
1957–2015

&

Alice E. Mapes
1962–2018

ACKNOWLEDGMENTS

Nobody accomplishes anything alone. I am grateful to all who contributed.

My advisor Chris J. Staiger is an amazing, thorough teacher and mentor and I deeply appreciate his patience, largely reasonable expectations, and generosity. BossChris granted me unusual freedom, and guided my every step. I respect him as a scientist and an honorable man. My committee members provided excellent suggestions and insights. Dr. Iyer-Pascuzzi taught me about root cell types, which started this project; Dr. Mengiste was always positive, encouraging, and kind; Dr. Zhang attended every lab meeting, offering recommendations and support; Dr. Zhu made time to listen to my status updates. Sincere thanks for sharing your knowledge and time.

I also owe a great deal to my lab members. Hongbing Luo was patient no matter how often I asked her the same question. When I had to Teaching Assist, Chao Cai showed me how. Lingyan Cao taught me how to image roots and believed in me from the very beginning. Weiwei Zhang reminded me that we are only ever getting closer to the truth, that no science will ever be perfect. Knowing I could count on Shelli Taylor for support—administrative and personal—contributed to my sanity. Being able to work in such a collaborative environment is a privilege and I am lucky to have worked with each of you.

The friends I met here will surely be lifetime friends. Jacob W. Jeffries, Rachel M. McCoy, and Dr. Jessica C. Page were my family here. Jacob and Rachel helped me with molecular work and took doting care of Violet and Mr. Snaggles whenever needed. Jessica helped me practice Every. Single. Presentation. Samy A. Belteton and I shared many discussions about cytoskeletal research and I will be forever thankful that he fixed my angle/parallelness macro.

My friends from back home are my logical family and I couldn'ta done it without your good times and emotional support. S. Kristin Farthing edited every major document I submitted here. Jessica M. Harris always brings the fun, even as the first to visit me in Indiana. Shane A. King's worldly wisdom always provided perspective. My Aunt, Peg Jones, understands how science works—and more frequently does not "work [out as expected]"—and genuinely cared about my progress.

To the other Chris, the #1 Chris, who sure ain't my boss and does not try to be, Chris Voeglein, I cherish you the ut-utmost. Giving up your cushy job and bright city life was a real sacrifice and I hope to eventually make it all worth your while. More words would feel cheap. 💗

TABLE OF CONTENTS

LIST OF TABLES

LIST OF FIGURES

LIST OF ABBREVIATIONS

2,4-D	2,4-Dichlorophenoxyacetic acid (synthetic auxin)
35S	Promoter derived from the cauliflower mosaic virus
AAAP	Amino acid/auxin permease
ABCB	ATP-BINDING CASSETTE/B
ABP(s)	Actin-binding protein(s)
ABP1	AUXIN BINDING PROTEIN 1 (putative auxin receptor)
abp1-c1	ABP1 CRISPR knockout
Abp 140p	A yeast actin-binding protein
ACT	ACTIN
ADF	ACTIN DEPOLYMERIZING FACTOR
AFB	Auxin responsive F-box proteins
ANOVA	Analysis of variance
ARF	AUXIN RESPONSE FACTOR
Arp	Actin-related protein
Aux/IAA	AUXIN/INDOLE-3-ACETIC ACID (transcriptional repressor)
AUX1	AUXIN RESISTANT 1 (auxin importer)
BDM	2,3-Butanedione monoxime (myosin inhibitor)
BFA	Brefeldin A
BRK	BRICK
BRI1	BRASSINOSTEROID INSENSITIVE 1 (brassinosteroid receptor)
BSM	BELAYA SMERT
BUI	BENT UPPERMOST INTERNODE 1 (*see* RMD, FH)
CA	Constitutively active
CDPK	CALCIUM-DEPENDENT PROTEIN KINASE
CesA	Cellulose synthase
CNGC	CYCLIC NUCLEOTIDE-GATED CHANNEL
Col-0	Columbia-0 (Arabidopsis ecotype)
CP	CAPPING PROTEIN
CPD	CYTOCHROME P450 MONOOXYGENASE CYP90A1 (brassinosteroid biosynthesis gene)
Cyt D	Cytochalasin D (pharmacological inhibitor of actin turnover)
d	Day(s)
DGH	Dark-grown hypocotyl
DGR	Dark-grown root
DN	Dominant negative
DR5-GUS	Synthetic auxin-responsive promoter (transcriptional reporter)
EMS	Ethyl methanesulphonate
EPC	Epidermal pavement cell
ER	Endoplasmic reticulum
EZ	Root elongation zone
F-actin	Filamentous actin
fABD2	Second ACTIN-BINDING DOMAIN OF ARABIDOPSIS FIMBRIN1
FFT	Fast Fourier Transform
FH	FORMIN, formin homology
FIJI	Fiji is just ImageJ (Image analysis software)
fiz	FRIZZY mutant (*DN-act*)
G-actin	Monomeric (globular) actin
GAP	ARF-GTPASE-ACTIVATING PROTEIN
GFP	GREEN FLUORESCENT PROTEIN
GH3	GRETCHEN HAGEN 3 (auxin conjugating enzyme)
h, hr	Hour(s)
HSD	Honestly significant difference (statistical test)
IAA	Indole-3-acetic acid
IAA$^-$	Deprotonated IAAH
IAAH	Protonated IAA (lipophilic form)
JASP	Jasplakinolide (pharmacological actin stabilizer)
JMP	Data analysis software
k_m	Michaelis-Menton constant (substrate concentration for ½ max enzymatic reaction rate)
KO	Knockout
Lat B	Latrunculin B (pharmacological inhibitor of actin polymerization)
LAX	LIKE AUX1
LGR	Light-grown root
LIM	LIM-domain containing proteins

MAMP	Microbe-associated molecular pattern	s	Second(s)
MDR	MULTIDRUG RESISTANCE (*see* ABCB)	SAUR	SMALL AUXIN UP-RNA
		SCAR	SUPPRESSOR OF CAMP RECEPTOR DEFECTS (part of the Arp2/3 regulatory complex)
min	Minute(s)		
MS	Murashige and Skoog (plant growth medium)		
NAA	1-Naphthylacetic acid	SKP1	S PHASE KINASE-ASSOCIATED PROTEIN (F-box protein, *see* SCF$^{TIR1/AFB}$)
ND	No difference		
NE	Not evaluated		
NPA	1-N-naphthylphthalamic acid (auxin transport inhibitor)	SCF$^{TIR1/AFB}$	SKP1–CULLIN1–F-BOX–TRANSPORT INHIBITOR RESPONSE 1 (auxin receptor complex)
NR	No predictive relationship		
Os	*Oryza sativa*	SMIFH2	Small molecule inhibitor of Formin Homology 2 domains
OX	Overexpression/overexpressing		
P83	*See* AUX1	SPK1	SPIKE 1
PA	Phosphatidic acid	T-DNA	Transfer DNA
PAT	Polar auxin transport	TIBA	Tri-iodobenzoic acid
PBP	Pentabromopseudilin (myosin inhibitor)	TIR	TRANSPORT INHIBITOR RESPONSE 1 (auxin receptor; F-box protein, *see* SCF$^{TIR1/AFB}$)
PGM1	PHOSPHOGLUCOMUTASE 1 (glucose-to-starch–converting enzyme)		
		TIRF	Total internal reflection fluorescence microscopy
PGP	P-GLYCOPROTEINS (*see* ABCB)	TMK	TRANSMEMBRANE KINASE
		TWD1	TWISTED DWARF 1
PIN	PIN-FORMED (auxin exporter)	VAEM	Variable angle epifluorescence microscopy
PID	PINOID KINASE	VLN	VILLIN
PLD	PHOSPHOLIPASE D	WAV	WAVY ROOT 5 (*see* AUX 1)
PLIM	Pollen LIM		
PM	Plasma membrane	WAVE	WASP FAMILY VERPROLIN HOMOLOGOUS PROTEIN (part of the Arp2/3 regulatory complex)
PRF	PROFILIN		
RIC	ROP INTERACTIVE CRIB MOTIF-CONTAINING		
		WLIM	LIM-DOMAIN CONTAINING PROTEIN
RMD	RICE MORPHOLOGY DETERMINANT (*see* BUI, FH)	WS	Wassilewskija (Arabidopsis ecotype)
		xi3KO	Myosin xi triple knockout mutant
ROI	Region of interest	*xi4KO*	Myosin xi quadruple knockout mutant
ROP	Rho-like GTPases of plants	YFP	Yellow fluorescent protein

ABSTRACT

Author: Arieti, Ruthie (Ruth) Sophia, Ph.D.
Institution: Purdue University
Degree Received: August 2019
Title: Auxin-Induced Actin Cytoskeleton Rearrangements Require AUXIN RESISTANT 1.
Committee Chair: Christopher J. Staiger

The actin cytoskeleton is required for cell expansion and is implicated in cellular responses to the plant growth hormone auxin. However, the molecular and cellular mechanisms that coordinate auxin signaling, cytoskeletal remodeling, and cell expansion are poorly understood. Previous studies have examined actin cytoskeleton responses to long-term auxin treatment, but plants respond to auxin over short timeframes, and growth changes within minutes of exposure to the hormone. To correlate actin arrays with degree of cell expansion, we used quantitative imaging tools to establish a baseline of actin organization, as well as of individual filament behaviors in root epidermal cells under control conditions and after treatment with a known inhibitor of root growth, the auxin indole-3-acetic acid (IAA). We found that cell length was highly predictive of actin array in control roots, and that short-term IAA treatment stimulated denser, more longitudinal, and more parallel arrays by inducing filament unbundling within minutes. By demonstrating that actin filaments were more "organized" after a treatment that stopped elongation, we show there is no direct relationship between actin organization and cell expansion and refute the hypothesis that "more organized" actin universally correlates with more rapidly growing root cells. The plasma membrane-bound auxin transporter AUXIN RESISTANT 1 (AUX1) has previously been shown necessary for archetypal short-term root growth inhibition in the presence of IAA. Although AUX1 was not previously suspected of being upstream of cytoskeletal responses to IAA, we used *aux1* mutants to demonstrate that AUX1 is necessary for the full complement of actin rearrangements in response to auxin, and that cytoplasmic auxin in the form of the membrane permeable auxin 1-naphthylacetic acid (NAA) is sufficient to stimulate a partial actin response. Together, these results are the first to quantitate actin cytoskeleton response to short-term auxin treatments and demonstrate that AUX1 is necessary for short-term actin remodeling.

CHAPTER 1.   INTRODUCTION

It is surprising that despite human reliance on plants, we do not understand the molecular mechanisms of plant growth—neither "why" nor "how". This chapter focuses on current understanding of actin's role in plant cell growth. Actin is an asymmetric protein monomer that polymerizes to form dynamic structures within a cell; these dynamic structures support a multitude of intracellular activities. Plant cells may appear relatively static, but they constantly respond to signals within the cell, within the organism, and from the external environment. Actin plays a role in almost all plant cell processes: innate immunity against microbial pathogens, cytoplasmic streaming, vesicle trafficking, chromatin remodeling, gravitropism, organelle positioning and vacuole morphology, and cell expansion. Actin assembly and disassembly is constant, and cytoplasmic streaming constantly moves vesicles over actin tracks. Short timelapse movies of actin activity provide a good visual of how dynamic plant cells truly are.

1.1   Actin as a Polymerizing Protein

Actin protein structure is highly conserved across kingdoms, indicating that the structure originated at least a billion years ago, before these kingdoms diverged (Gunning et al., 2015). Actin is abundant in eukaryotic cells and can interact with more proteins than any other protein (Dominguez and Holmes, 2011). Although for decades the presence of an actin cytoskeleton was considered a defining criterion of Eukaryotes, cytoskeletal proteins have been discovered in bacteria.

An actin-like protein found in some Prokaryotes, MreB, is similarly shaped to eukaryotic actin monomers, forms helical filaments of approximately the same size as actin (51 Å for MreB vs. 55 Å for actin), and is involved in cell shape determination and establishing polarity (Cabeen and Jacobs-Wagner, 2010), two functions that actin supports in plant cells. The prokaryotic MreB is present in rod-shaped bacteria species (Cabeen and Jacobs-Wagner, 2010), substantiating the importance of polymerizing proteins in cell polarity and function.

Globular actin monomers (G-actin) exhibit asymmetry: the "pointed" or "minus" end has two different sized subdomains, and a cleft that binds ATP and a divalent cation; the "barbed" or "plus" end has two similarly sized subdomains but lacks the ATP binding cleft (Shetterline and

Sparrow, 1994). Filaments always form in a predictable way. Because the monomer ends are different, each face has distinct properties that affect how a monomer interacts with other monomers and with other proteins.

In the rate-limiting step for polymerization, three ATP-loaded actin subunits come together in the pointed-end-to-barbed-end orientation (**Figure 1.1**), forming an "actin seed", and the start of a two-stranded helix, that then adds more G-actin subunits, polymerizing to form filamentous actin (F-actin). Filaments are highly symmetric with 13 subunits forming half of each right-handed twist (**Figure 1.1**; Sheterline and Sparrow, 1994). Shortly after monomer addition, ATP is hydrolyzed to ADP-P_i and then P_i is released to create ADP-G-actin subunits. Monomers can still remain incorporated within a filament even after ATP hydrolysis, although only free monomers may exchange ADP for ATP. The state of bound ATP, ADP-P_i, or ADP affects actin protein conformation, which in turn influences a filament's ability to be bound by accessory proteins (Sheterline and Sparrow, 1994).

Recombinant actin cannot be expressed and purified from bacteria because the protein requires accessory proteins to fold properly (Frydman and Hartlt, 1996; Hansen et al., 1999). Native actin can be extracted from organisms, and actin derived from rabbit skeletal muscle or from corn pollen is frequently used for in vitro experiments (Gibbon et al., 1999; Blanchoin et al., 2000; Doolittle et al., 2013; Li et al., 2015b). Recent work shows plant actin can be expressed and purified from *Dictyostelium discoideum* (Kijima et al., 2016). Polymerization in vitro requires ATP, a physiological salt concentration, and a divalent cation like Mg^{2+} (Sheterline and Sparrow, 1994; Li et al., 2015a). In vitro, ATP-loaded monomers are more likely to add to the barbed end and ADP-bearing subunits are more likely lost from the pointed end; this balance of growth and loss is called "treadmilling". Actin polymerization within plant cells does not exhibit treadmilling; rather, actin polymerization in vivo appears difficult to parse, the result of probabilistic events that feed back on one another, and is best described by the term "stochastic dynamics" (Staiger et al., 2009). Polymerization within cells is constant and uses more than 600 ATP-loaded subunits per filament per second (Staiger et al., 2009), creating a highly energy-intensive process. Accessory proteins break down filamentous structures, ATP is exchanged for ADP on monomers, and ATP-loaded monomers are recycled to the monomer pool. The most parsimonious interpretation of this vast energy expenditure is that the polymerization into filaments and construction of structures serves a purpose worthy of such an investment.

1.2   Actin in Cell Biological Processes

While purified actin protein will treadmill in in vitro experiments, its behavior in building filaments and higher order structures is different within a cell because actin monomers and polymerized filaments are controlled by a variety of regulatory proteins or "actin-binding proteins" (ABPs). In yeast, ABPs compete for actin, which shapes the cell's actin array (Rotty et al., 2013; Burke et al., 2014; Rotty and Bear, 2014; Suarez and Kovar, 2016). Cells have many different ABPs, and the activity of each ABP is regulated by upstream signaling molecules. Discrete combinations of activated and inactivated ABPs enable a plethora of pathways to regulate actin behavior and, therefore, the actin network in a cell. Plants specifically are notorious for having evolved multiple isoforms within protein families (see below). For example, birds and mammals have no more than 6 actin isoforms but the Arabidopsis genome codes for 8 known isoforms and maize codes for as many as 21 (Perrin and Ervasti, 2010; Šlajcherová et al., 2012). The high number of isoforms of plant proteins is thought to be a strategy to counter the fact that most plant cells are stationary (Šlajcherová et al., 2012; Kijima et al., 2016).

1.2.1   Actin-Binding Proteins Control the Actin Network

ABPs control actin structures in many ways (see **Figure 1.1**), including:

- Filament nucleation;
- Enhancing filament polymerization;
- Inducing a filament break;
- Capping filament length;
- Bundling or crosslinking filaments together;
- Annealing two filament segments; and
- Severing filament bundles.

Each of these activities builds, sculpts, or demolishes specific structures within the cell. ABPs themselves are regulated by upstream signaling, either by phosphorylation of the protein (ex., actin depolymerizing factor, ADF; Carlier et al., 1997; Smertenko et al., 1998; Allwood et al., 2001; Henty et al., 2011; Suarez et al., 2011; Henty-Ridilla et al., 2014; Huang et al., 2014) or by binding signaling molecules like calcium (ex., villin, VLN; Huang et al., 2005; Khurana et al., 2010; Bao et al., 2012; van der Honing et al., 2012) or phosphatidic acid (PA; ex., capping protein, CP; Li et al., 2012a, 2012b; Pleskot et al., 2013; Li et al., 2014b, 2015c, 2016). Stimuli further

upstream are perceived by receptors. These stimuli can be initiated by the cell towards itself, by other cells within the organism (ex. hormones are secreted, which can affect the cell producing the signal as well as distal cells), or by environmental stimuli (ex., pathogen- or damage-associated molecular patterns).

1.3   Visualizing the Actin Cytoskeleton

Actin can be visualized by fixing cells and staining actin arrays with the fungal toxin phalloidin (which binds only F-actin) conjugated to fluorescent molecules, though cell fixation is time-intensive, can produce artifacts, and harms living cells (Cooper, 1987; Melak et al., 2017). Live cell fluorescent imaging of plants with genetically encoded actin reporters is more commonly used, because these techniques do not require laborious cell fixation and allow dynamic processes to be visualized as they occur (Dyachok et al., 2014). The plant actin field generally uses secondary reporters: for example, green fluorescent protein (GFP) fused to the second actin-binding domain of the Arabidopsis actin crosslinking protein, fimbrin (GFP-fABD2; Sheahan et al., 2004; Dyachok et al., 2014). Another fluorescent reporter widely used to study actin in plants is the yellow fluorescent protein (YFP) derivative Venus, fused to a portion of the yeast ABP Abp140p (Lifeact-Venus; Era et al., 2009). Though Lifeact-Venus can produce growth defects in some cell types (Dyachok et al., 2014), it allows visualization of some structures that GFP-fABD2 does not (van der Honing et al., 2011). The GFP-fABD2 construct, behind either a *35S* or *Ubiquitin 10* promoter, allows for the best visualization of actin filaments in all plant cell types, with minimal negative effects on whole plant growth (Dyachok et al., 2014); however, this construct can be silenced in some actin-binding protein mutants (Li et al., 2015a). Overall, both Lifeact-Venus and GFP-fABD2 report individual actin filament behaviors quite well. Recent work used a long linker sequence between actin and the fluorescence protein to express directly-labeled actin in Arabidopsis protoplasts and tobacco (Kijima et al., 2018). The long linker appeared to interfere with normal actin polymerization less than previous attempts to label actin alone (Sheahan et al., 2004; Melak et al., 2017; Kijima et al., 2018). These constructs have not yet been evaluated for potential effects on actin dynamics or the ability to complement *ACTIN* mutants (Kijima et al., 2018).
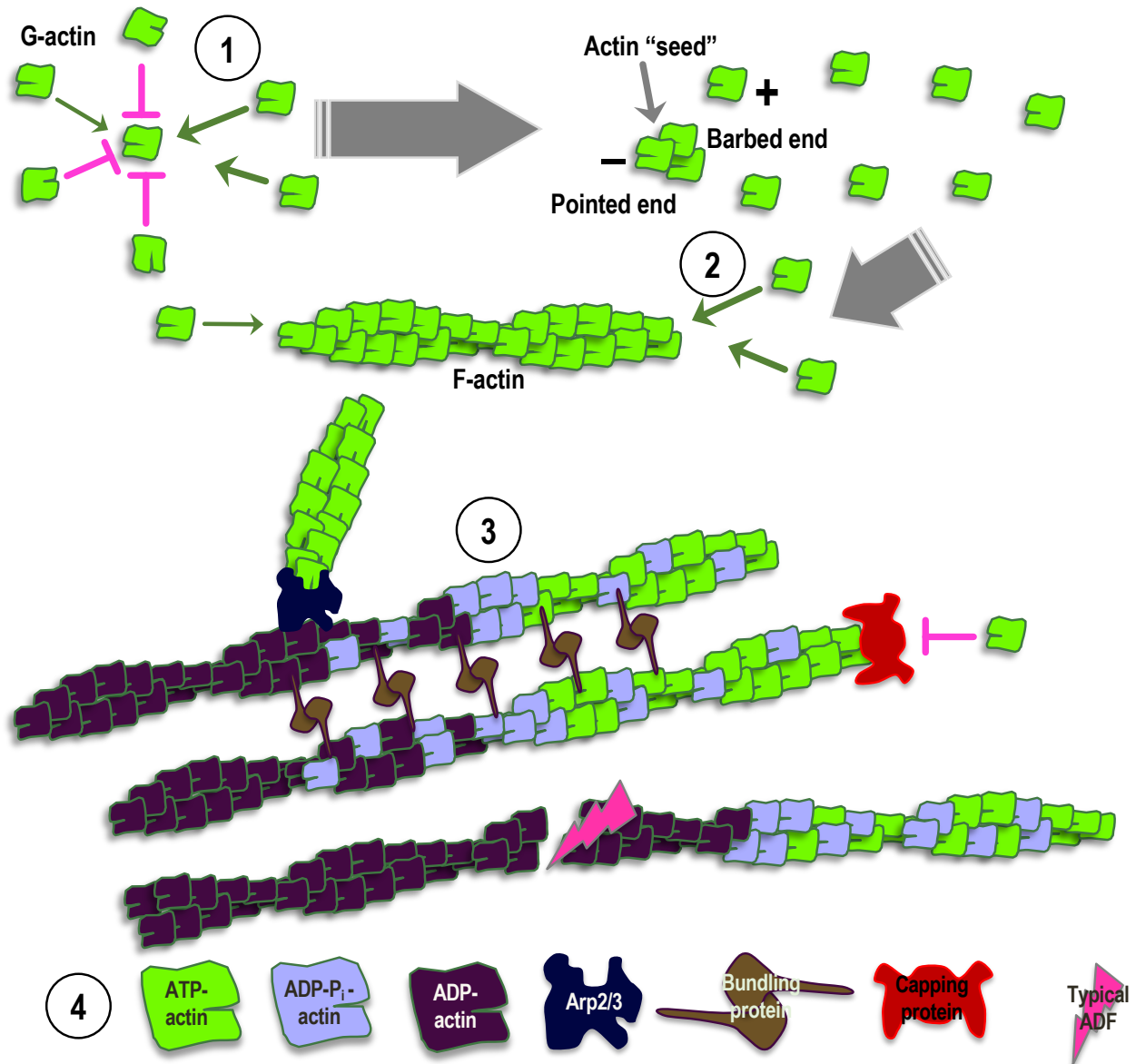
Figure 1.1 Actin Nucleation and Filament Regulation by Actin-Binding Proteins.

① **Nucleation:** Three actin monomers must come together in a specific orientation for polymerization to occur.

② **Elongation:** Monomers are more likely to add to the barbed end and less likely to add to the pointed end.

③ As filaments age, ATP is hydrolyzed to ADP-P_i and then to ADP, changing the probabilities that actin-binding proteins (ABP) will bind each region of the filament.

④ ABPs control filament behavior and the entire actin array. Selected ABPs represented here include: The **Arp2/3 multiprotein complex** produces a branched nucleation from the side of a mother filament. **Capping protein** binds to filament barbed ends, preventing barbed end elongation. **Bundling proteins** crosslink filaments. **Typical ADF** binds to ADP-actin to induce a filament break.

1.3.1 Actin Organization and Stochastic Dynamics and How to Measure Them

Because ABP are differentially activated and inactivated by upstream signals, different stimuli work through ABPs to affect actin behavior and overall organization. Presumably, a single stimulus in isolation would always affect levels of second messengers to the same extent, and, therefore, affect ABP regulation and actin organization in a predictable way. However, the precise nature of how actin responds to stimuli is not always visually apparent.

Precise measurements can suggest or implicate cellular mechanisms involved in stimulus response (Blancaflor and Gilroy, 2000). It is possible to evaluate multiple parameters from still images of an actin array: the quantity of pixels in an image occupied by fluorescence; skewness of pixel intensity distribution; average filament angle in relation to the cell's longitudinal axis; degree of filament parallelness to one another; number of fluorescent peaks and range of intensities in an image; and extent of filament alignment ("entropy" of pixels in a Fast Fourier Transform [FFT] of an image) or the extent to which an FFT deviates from a circular shape, "eccentricity" (Staiger et al., 2009; Ueda et al., 2010; Vidali et al., 2010; Dyachok et al., 2011; van der Honing et al., 2012).

Timelapse movies can be analyzed to discern differences in overall array dynamicity between cell types, or differences between a treatment or mutant vs. control. The correlation coefficient algorithm calculates the pairwise correlation coefficient (i.e., similarity) between all pixels in an image (pixel intensity and pixel location) at all possible time intervals, and plots correlation coefficient curves as a function of time intervals in the movie, with all curves starting at 1 (Vidali et al., 2010). Flatter or shallower curves indicate more cytoskeletal stability over time; steeper curves indicate higher levels of actin dynamicity (i.e., more differences between frames of the timelapse movie, and a faster loss of frame-to-frame "similarity"). Because this algorithm examines the entire actin array in a cell or portion of a cell, it is best for providing a quick assessment of variation between treatment groups and for quantifying vastly different arrays, but is not sufficiently sensitive to account for the variety of dynamic filament behavior (such as annealing behaviors, where filaments change in short order but do not relocate).

The most precise way to evaluate difference in actin behavior in mutants or in response to treatments is to measure individual filament behaviors (Michelot et al., 2006; Staiger et al., 2009; Henty et al., 2011; Li et al., 2012a; Cai et al., 2014; Cao et al., 2016), preferably in vivo. Some filament behaviors (filament elongation rate, maximum filament length, maximum filament

lifetime, severing frequency, filament regrowth after severing, convolutedness, and rate of change of convolutedness) can be measured from entire timelapse movies. Others (frequencies of annealing, bundling and unbundling, and nucleation events and origins) are best quantified from regions of interest cropped from movies because these events can occur more frequently, and differ from the process of filament growth to disappearance. Choosing regions of interest and hand-selecting individual filaments certainly has the potential to introduce bias, but this can be mitigated by working on blinded images and taking regions from multiple cells.

These sorts of quantitative live cell imaging techniques have been used to dissect signaling pathways and demonstrate that ABPs are differentially regulated during plant innate immunity (Li et al., 2015b; Li and Staiger, 2018). Microbial pathogens and symbionts stimulate increased actin filament abundance (Cardenas et al., 1998; Takemoto and Hardham, 2004; Henty-Ridilla et al., 2013b). An immunogenic peptide sequence (or "pattern") associated with bacteria stimulates the increase in density by regulating the ABPs ACTIN DEPOLYMERIZING FACTOR 4 (ADF4) and CAPPING PROTEIN (CP), whereas chitin, a microbe-associated molecular pattern (MAMP) associated with fungi, stimulates an increase in actin filament density by regulating only CP. Mutants for each of these proteins were used to demonstrate that ADF4 and CP are necessary for each sort of MAMP signaling: actin array organization in *adf4* and *cp* mutant plants did not respond to respective stimuli (Henty-Ridilla et al., 2013b, 2014; Li et al., 2015c, 2016). Though both MAMPs cause actin reorganization by increasing actin density, the *cp* and *adf4* results show that different MAMPs can trigger unique responses, reinforcing the idea that specific structures play certain roles and inspiring questions about a purpose behind these different structures.

After sufficient measurements of actin behavior during a cell process or reaction to a stimulus are counted, and differences in mutant responses enumerated (to evaluate variations in response when a protein is absent), actin's behavior and function in that process or in response to that stimulus become clearer. When this strategy (generalized in **Figure 1.2**) is repeated for many, many processes and stimuli over time, we will move closer to understanding actin's functions in plant cells. For this strategy to be productive, measurements of actin behavior and organization must be as consistent and free from bias as possible. Live cell fluorescent imaging in conjunction with quantitative image analysis software are the best tools to reveal how actin operates in plant cells, and to gain insight into what purposes energy intensive actin organization and reorganization serve.

Figure 1.2 The Basics of Signaling to Actin.

① Ligand stimulates the cell by binding to a specialized receptor, or enters through a transporter, or by passing directly through the plasma membrane.

② Ligand binding to its receptor stimulates second messengers (sometimes requiring a coreceptor, not shown).

❷ Alternatively, stimulus entry to the cell in and of itself induces second messengers, binds an intracellular receptor, or the stimulus directly targets actin-binding proteins (ABPs).

③ ABPs are activated or inactivated.

④ Differentially regulated ABPs (or actin monomers) alter individual filament behaviors, which en masse cause overall array reorganization.
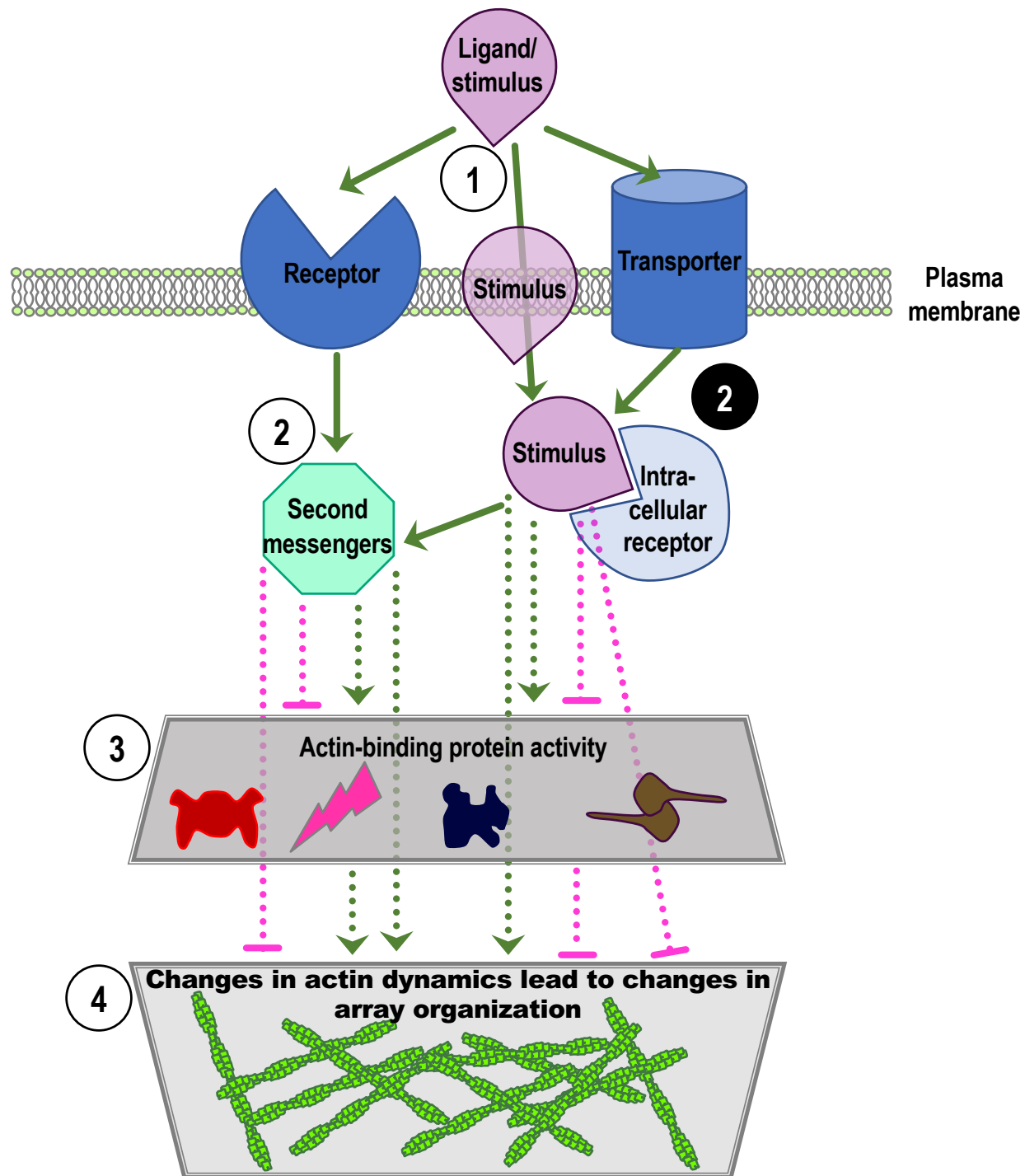
Figure 1.2 The Basics of Signaling to Actin.

1.4   Actin, Plant Growth, and Cell Expansion and Shape

New plant cells emerge from meristems in the tips of roots and shoots. In general, plant cell expansion is driven by the vacuole taking up fluid and exerting turgor pressure on a loosened cell wall. Plant cells are under immense turgor pressure because they expand within the confines of a rigid cell wall (Szymanski and Cosgrove, 2009). Actin filaments provide tracks for vesicle transport from the Golgi to the plasma membrane (PM), and myosins transport vesicles that contain cell wall building materials along these tracks. Upon reaching their destination at the PM, vesicle contents are exocytosed for incorporation to the wall (Geitmann and Nebenführ, 2015; Nebenführ and Dixit, 2018; Zhang et al., 2019).

The necessity of actin for plant cell growth leads to the hypothesis that filaments would behave differently in growing and nongrowing cells (Staiger et al., 2009; Smertenko et al., 2010). The field's general hypothesis states that the appearance of actin filament "organization" causes, coincides with, or is a byproduct of cell expansion, and apparent filament "disorganization" causes, coincides with, or is a byproduct of nongrowth (**Figure 1.3**). However, actin array organization is not predictably different in growing and nongrowing cells from study to study (Gilliland et al., 2003; Holweg et al., 2004; Rahman et al., 2007; Kandasamy et al., 2009; Nick et al., 2009; Yang et al., 2011; Li et al., 2014a; summarized in **Tables 1.1** and **1.2**). In addition, individual actin filaments do not exhibit obviously different behaviors in growing and nongrowing cells in dark-grown hypocotyls (Staiger et al., 2009). Furthermore, what specific activities actin is undertaking, and even how it functions during cell growth, are unknown.

1.4.1   Plant Cells Exhibit Two Kinds of Growth

Two types of growth occur in plant cells. Most cells grow by diffuse growth, where expansion presumably occurs over an entire cell and regional wall properties determine the cell's final shape (Baluska et al., 2003; Hussey et al., 2006). Hypocotyl, leaf, and root epidermal cells undergo diffuse growth and are used as models for its study. Although diffuse expansion is hypothesized to occur over the entire cell, there has been little work definitively showing that this is the case, and it is quite possible that cells grow by depositing new material, for example, mainly towards specific regions of a cell, such as axial end walls. One study that closely examined trichome branch expansion found that this tissue grows diffusely but anisotropically, with new cell wall materials forming a gradient (in which older tissue contains more new cell wall materials) along the sides of

trichome branches (Yanagisawa et al., 2015). Cell wall deposition patterning has not yet been evaluated in other diffusely-growing cell types. The second kind of growth is tip growth, which is elongation at only a specific end of a cell, and cell types include pollen tubes, moss protonema, and root hairs (Mathur, 2004; Hussey et al., 2006).

Actin is required for both diffuse and tip growth, and actin organization within tissues forms observable patterns that are quantifiably consistent (Li et al., 2015a; Szymanski and Staiger, 2018). These characteristics of actin organization have been correlated with cell growth to devise a model for actin and growth that in theory applies universally to plant tissues. Growing pollen tubes and moss protonema have well-characterized and similar actin organizations: dense longitudinal bundles extend the length of the tube and an especially bright actin "fringe" or "collar" stops about 5 μm short of the apex, with only a few bundles extending beyond the collar (Gibbon et al., 1999; Lovy-Wheeler et al., 2005; Vidali et al., 2007). This actin network supports vesicle delivery that is necessary for rapid growth (Peremyslov et al., 2010; Bibeau et al., 2017). Actin accumulations indicate where root hairs start to grow, and the growing tip is continuously enriched in "fine" actin filaments (Baluška et al., 2000; Ketelaar, 2013). "Fine" actin accumulations are also associated with expanding regions in trichomes and epidermal pavement cell (EPC) lobes (Szymanski et al., 1999; Fu, 2002; Fu et al., 2005; Armour et al., 2015), where the denser actin presumably prevents endocytosis of growth hormone transporters so that the transporters create local auxin maxima (Nagawa et al., 2012). Maize root cells exhibit arrays that vary from transverse in the postmitotic region (i.e., the transition zone) to wrinkly and longitudinal in the latter elongation zone (Baluska et al., 1997).
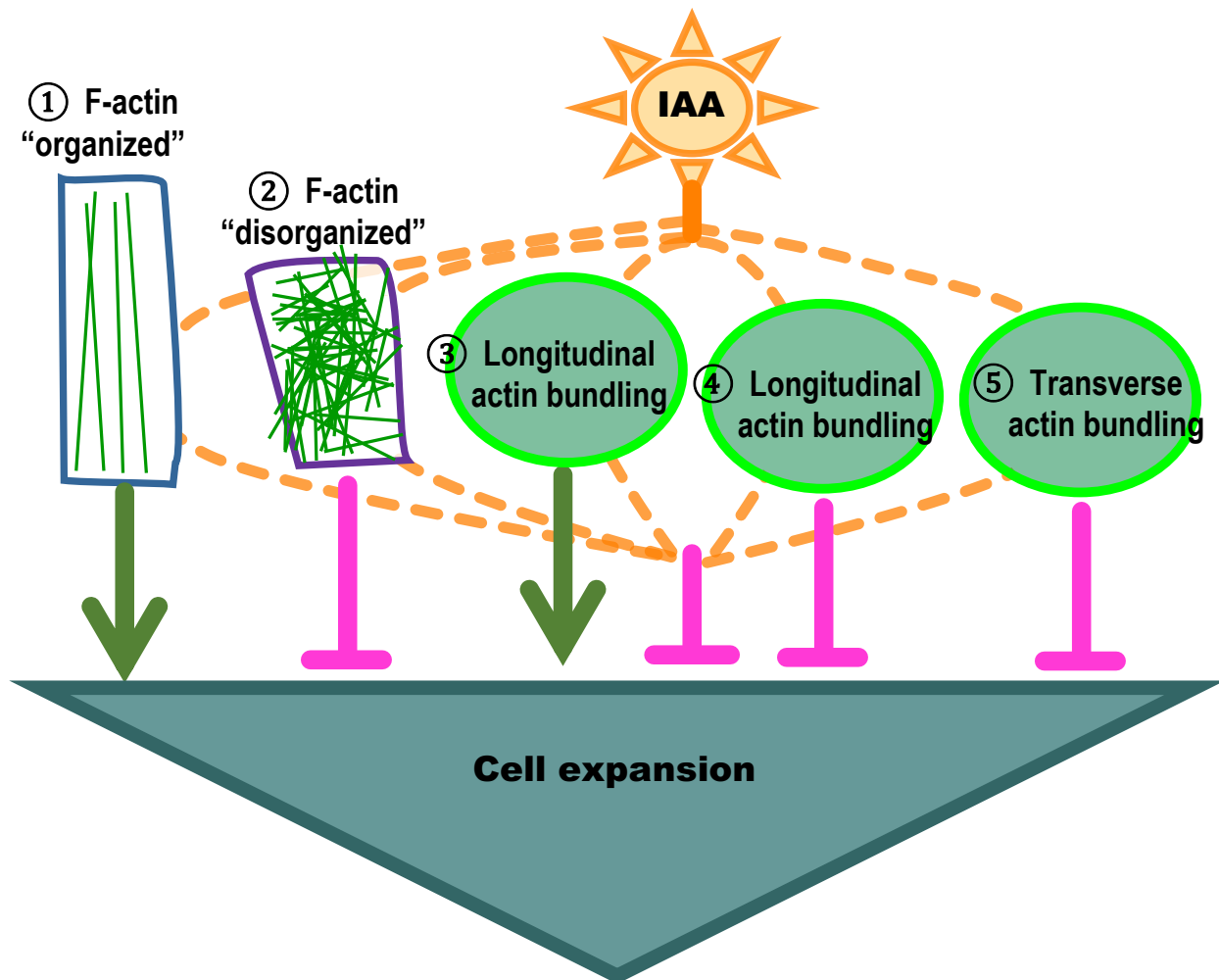
Figure 1.3 Summary of Hypotheses That Tie Actin Organization and Growth.

①   Longitudinally "organized" F-actin precedes, is necessary for, and/or correlates with cell expansion;

②   "Disorganized" F-actin inhibits or disrupts cell expansion;

③   Longitudinal actin bundles are necessary for, or positively correlate with, cell expansion;

④   Longitudinal actin bundles restrict cell expansion;

⑤   Transverse actin bundles inhibit, disrupt, or coincide with cessation of cell expansion.

See **Tables 1.1** and **1.2** for more details.

1.4.2   The Role of the Cell Wall

Plant cell shape is governed by cell wall extensibility (which is determined by material composition) and turgor pressure (Baskin, 2005; Smith and Oppenheimer, 2005; Szymanski and Cosgrove, 2009). All plant cells exhibit an isotropic shape when they divide from the meristem. During expansion, the vacuole's pressure on a loosened cell wall should produce a larger cell with the same isotropic shape, but expanding plant cells exhibit a variety of shapes. The anisotropic growth implies that the vacuole's pressure is exerted equally but affects specific areas of loosened cell wall (Mathur, 2004; Hussey et al., 2006; Szymanski and Cosgrove, 2009; Pei et al., 2012; Yanagisawa et al., 2015). Local cell wall loosening is caused by acidification (i.e., by ATPases) and by wall-loosening enzymes called expansins which can bind to various cell wall components, potentially altering interactions among cellulose and other polysaccharides (Cosgrove, 1998; Cosgrove, 2018).

The rate of plant cell expansion is a function of cell wall deposition (Kotzer and Wasteneys 2006). Actin controls cell wall composition by anisotropic delivery of noncellulosic polysaccharides to the wall (Szymanski and Cosgrove, 2009). Actin filaments provide the means by which materials reach the PM, and microtubules and their accessory proteins coordinate the sites where cellulose microfibrils are polymerized and deposited, enabling the formation of specific cell shapes. In growing pollen tubes and root hairs, materials are delivered down the longitudinal axis to the tip apex; in puzzle-shaped leaf EPC, delivery occurs differentially around the perimeter of the cell. As the major component of cell walls that provides tensile strength, cellulose microfibrils constrain turgor pressure, so it is clear why cellulose placement is a key determinant of cell shape (Baskin, 2005; Smith and Oppenheimer, 2005; Fayant et al., 2010; Wightman and Turner, 2010; Armour et al., 2015). Cellulose synthase (CesA) complexes travel to the PM in Golgi-derived vesicles or small CesA-containing compartments, where they synthesize cellulose microfibrils (Sampathkumar et al., 2013; Zhang et al., 2019).

1.4.3   Pharmacological Treatments that Disrupt Actin Affect Growth

When the actin cytoskeleton is disrupted with pharmacological treatments or mutations, cell expansion is aberrant, and tissues and plants are frequently dwarfed or otherwise display abnormal growth phenotypes. Plant cells treated with actin-destabilizing drugs exhibit altered or halted

vesicle motility distribution (Gu et al., 2005; Voigt et al., 2005; Lee et al., 2008). Growing cells have more diffuse F-actin arrays, whereas cells at late growth stages (mature cells) have less diffuse F-actin and more bundles (Szymanski et al., 1999; Ketelaar et al., 2003). Endosomes (Voigt et al., 2005) and Golgi (Akkerman et al., 2011) are visible near patches of F-actin, and faster moving "actin-associated spherical bodies" (Szymanski et al., 1999), and Golgi (Akkerman et al., 2011) associate along bundles. Furthermore, Golgi stacks exhibit differential motility depending on the type of actin array on which they reside: "wiggling" movements occur in regions of dense F-actin and very fast and directional motility is observed along actin bundles (Akkerman et al., 2011), further indicating that actin organization might regulate vesicle trafficking.

Inhibiting actin polymerization with the drug latrunculin B (Lat B) leads to severe dwarfing in both roots and shoots grown in light and dark conditions (Baluska et al., 2001b). When the same drug is used on pollen tubes, root hairs, and moss protonema, cells stop growing within minutes (Gibbon et al., 1999; Baluška et al., 2000; Vidali et al., 2001; Bibeau et al., 2017).

Destabilizing actin filaments with cytochalasin D (Cyt D) or inhibiting polymerization with Lat B in hypocotyl epidermal cells shows that actin filaments are the tracks on which Golgi are trafficked in cells (Satiat-Jeunemaitre et al., 1996; Hawes and Satiat-Jeunemaitre, 1999; Nebenführ et al., 1999; Crowell et al., 2009; Gutierrez et al., 2009). Research groups have observed unusually distributed clusters of Golgi and increased GFP-CesA signal at the PM in the vicinity of these clusters (Crowell et al., 2009; Gutierrez et al., 2009). Because they observed CesA at the PM, albeit unevenly distributed, Gutierrez et al. (2009) concluded that actin distributes CesA, rather than positions it at specific PM locations. Sampathkumar et al. (2013) report that Golgi-localized CesA in jasplakinolide (JASP, which stabilizes actin)-treated Arabidopsis seedlings follows "disorganized trajectories". By measuring less cellulose per unit dry weight versus controls in an *act2 act7* double mutant and in Lat B-treated wildtype Arabidopsis hypocotyls, they demonstrate a significant change in cell wall assembly following actin disruption (Sampathkumar et al., 2013). This group did not observe significantly slower CesA movement at the PM in the *act2 act7* mutant or in the Lat B-treated hypocotyls, but they report a reduction in both the delivery and recovery of CesA to/from the PM following actin disruption (Sampathkumar et al., 2013). These data imply that actin is involved in CesA trafficking to the PM and endocytosis but does not participate in the act of cellulose deposition, a result supported by recent findings about an actin-associated molecular motor (Sampathkumar et al., 2013; Zhang et al., 2019). This latter work shows that

myosins XI play a substantial role in tethering vesicles that contain cellulose synthase complexes to the PM, potentially by interacting with the exocyst complex (Zhang et al., 2019).

Interestingly, actin-disrupting drugs alter cell shape development only in growing cells, supporting the argument that an intact actin cytoskeleton is necessary for normal cell morphogenesis; perhaps correct vesicle trafficking is most important during the expansion phase (Szymanski et al., 1999; Armour et al., 2015). If cell expansion occurs before drug treatment, the resultant disruptions in actin organization do not alter cell shape (Szymanski et al., 1999).

1.4.4   Mutations that Disrupt Actin Affect Growth

In addition to pharmacological treatments, genetic mutations that affect actin organization and function affect plant growth. There are 8 ACTIN (ACT) isoforms in Arabidopsis: 5 that are expressed in reproductive tissues and 3 vegetative variants. The vegetative variants are divided into two subclasses: ACT2 and ACT8 (subclass 1) and ACT7 (subclass 2), which appear to have diverged more than 200 million years ago (Kandasamy et al., 2001; Gilliland et al., 2002, 2003; Kandasamy et al., 2009). Mutations in the vegetative isoforms cause varying degrees of growth deformations (summarized in **Table 1.1**): stunted roots or root hairs, bulging epidermal cells, and dwarfed cotyledons (though mature plant sizes do not significantly differ, indicating that the isoforms are somewhat functionally redundant).

Growth in double mutants, particularly those lacking ACT7, is severely perturbed: roots are very short compared with wildtype; root hairs are mere bulges or entirely absent; epidermal cells, trichomes, and entire organs are misshapen; and cells and plants are extremely dwarfed at maturity. Actin itself in both single and double mutants exhibits degrees of irregularity, and these differences have been used to support a model that correlates actin organization to extent of cell expansion. Filaments in *act2* root hairs are transverse instead of longitudinal, and the hairs are stunted. *act8* root hairs exhibit "only a mildly altered organization of actin filaments" and are closer in length to wildtype, and *act7* root hairs are nearly wildtype length, corresponding to their lack of any "obvious defect in actin cytoskeletal organization" (Kandasamy et al., 2009). Actin quantity is reduced, and actin organization in double mutants is, like growth phenotypes, severely aberrant, with all double mutant root epidermal cells and hairs exhibiting few, transverse filaments. Expressing *ACT8* under the *ACT7* promoter restores wildtype actin quantity and actin and growth phenotypes, but expressing *ACT7* does not fully restore normal growth in *act2 act8,* indicating that

this isoform has lost some functions since it diverged from the other vegetative actins 200 million years ago (Kandasamy et al., 2009).

Dominant negative mutations to *ACT2* and *ACT8* alter an actin-binding region on the monomer surface, which inhibits or prevents actin polymerization (Nishimura et al., 2003; Kato et al., 2010). Aberrant polymerization in these vegetative actin isoforms causes shorter, thicker, and more stable actin bundles and aggregates, instead of fine F-actin meshworks, resulting in mutants with shorter cells and tissues (Nishimura et al., 2003; Kato et al., 2010). These dominant negative mutations in individual ACT isoforms appear to affect plant growth and ultimate size more than knockout mutations because the dominant negative mutants still express *ACT* and make deformed ACT proteins, which are incorporated into filaments that do not form or function properly (Kandasamy et al., 2001; Gilliland et al., 2002, 2003; Nishimura et al., 2003; Kandasamy et al., 2009; Kato et al., 2010). In the absence of a knocked-out ACT isoform, the knockout mutants upregulate expression of the other vegetative isoforms (Kandasamy et al., 2009). These data demonstrate the necessity of actin polymerization in plant growth.

1.4.5 Mutations in Actin-Binding Proteins Affect Growth

Correlations between actin array and growth in ABP mutants are used to provide much evidence for the conclusion that actin organization relates to or causes cell expansion. However, when the data are examined in bulk, no clear relationships between actin organization and cell size emerge. ABP disruption does affect growth, and this section describes conclusions reached by the field on ABP function in vegetative tissues. However, current data do not clearly support the hypothesis that a specific actin array is related to cell expansion, only that perturbed actin organization affects cell expansion. None of the studies discussed below (and summarized in **Table 1.2**) measures actin organization in conjunction with cell growth rate. Until very recently (see **Chapter 3**), those sorts of experiments were not technically feasible, so here, cell size serves as a passable proxy for the dynamic process of expansion.

Table 1.1 Growth and Actin Phenotypes of Vegetative Actin Mutants.

Actin isoform mutant	Growth phenotype[1]	Actin array phenotype in roots and root hairs
act2[a,b]	**Reduced root hair length** **Narrower cotyledons**	Transverse actin in root hairs
act7[a,b]	**Reduced root length** **Narrower cotyledons** Twisted root epidermal cell files	"no obvious defect"[b]
act8[b]	**Reduced root hair length** **Narrower cotyledons**	"mildly altered"[b]
act2 act7[b]	**Smaller plants** **Smaller EPCs, fewer EPC lobes** Deformed trichomes Oblique anticlinal cell walls	Few, thick, transverse bundles
act2 act8[b]	Absent root hairs	Actin absent from trichoblasts
act7 act8[b]	**Shorter tissues** **Smaller EPCs** Deformed trichomes Swollen root epidermal cells	Few, thick, coiled bundles
act2-2D[2,d] **Dominant negative mutation in** *ACT2*	Shorter tissues, smaller plants Deformed trichomes Fewer, **shorter** root hairs; "caved" trichoblasts[d]	Shorter, thicker filaments
fiz1[2,c] **Dominant negative mutation in** *ACT8*	**Shorter tissues,** smaller plants Kinked or curled stems **Shorter root and shoot epidermal cells**	Absent transvacuolar strands Shorter, thicker, more stable filaments that aggregate at cell end

Bold in columns 2 & 3 indicates parameters that were quantified (rather than subjectively assessed).

[1]Studies examined entire *Arabidopsis thaliana* plants.

[2]Mutant phenotype present in heterozygote and exacerbated in homozygote.

References: [a]Gilliland et al. (2002); [b]Kandasamy et al. (2009); [c]Kato et al. (2010); [d]Nishimura et al. (2003).

Table 1.2 Growth and Actin Phenotypes in Vegetative Tissues of Actin-Binding Protein Mutants.

Actin-binding protein mutant	Tissue	Growth phenotype	Actin array phenotype		Notable differences in filament behavior	
adf4[1,h]	DGH	**Longer hypocotyls, longer cells**	**Density** **Skewness**	⇓ ⇑	**Max filament length** **Filament lifetime** **Severing freq.**	⇑ ⇑ ⇓
[h]	LGR	**Longer roots, longer cells**	NE		NE	
arp2 & *arp3*[1,k]	Guard cells	**Inhibited stomatal opening**	Shorter, thicker actin bundles that accumulate in patches		**Filament elongation rate** ⇑ **Filament shortening rate** ⇑ **Severing freq.** ⇑	
[i]	Leaf EPC	**Shallower lobes**	**Fewer actin patches associated with lobes**		NE	
[i]	Trichomes	Stunted branches Enlarged stalks	Missing diffuse actin signal in branches; increased bundling in stalk		NE	
[f]	DGR	Longer roots	**Actin alignment**	⇓	NE	
[f]	LGR	**Shorter roots, shorter cells in elongation zone**	**Actin alignment**	⇓	NE	
brk1[2,g]	Leaf EPC	Absent lobes	Actin patches absent		NE	
[f]	DGR	Longer roots	**Actin alignment**	⇓	NE	
[e,f]	Various	**Shorter roots, shorter cells in elongation zone** Trichomes lack branches	**Actin alignment** ⇓ Actin appears depleted		NE	
cp[1,j,m]	DGH	**Longer hypocotyls, longer cells**	**Density** **Skewness** **Array dynamicity**	⇑ ⇓ ⇑	**Max filament length** **Filament lifetime** **Annealing freq.**	⇑ ⇑ ⇑
[j,m]	LGR	**Shorter roots, shorter cells**	**Density** **Skewness** **Array dynamicity**	⇑ ⇓ ⇑	NE	

Table 1.2 continued.

CP-OX[1,j,m]	DGH	**Shorter hypocotyls, shorter cells**	**Density** **Skewness** **Array dynamicity**	⇩ ⇧ ⇩	**Max filament length** **Filament lifetime** **Annealing freq.**	⇩ ⇩ ⇩
[1,j,m]	LGR	**Longer roots, longer cells**	**Density** **Skewness** **Array dynamicity**	⇩ ⇧ ⇩	NE	
fh1[1,o]	LGR	**Increased sensitivity to latrunculin B— shorter, wider roots, abnormal root hairs with treatment**	**Density** **Skewness** **Array dynamicity**	⇩ ⇧ ⇩	NE	
fh5/bui/rmd[4,l,t,v]	Various	**Smaller plants** **Shorter shoots, leaves, and roots** **Shorter cells** **More waves in root** **Hypergravitropism**	**Filament intensity peaks** ⇩ **Filament pixel intensity** ⇩ Array appears transverse		NE	
myosin xi-3KO[1,c] ***(myosins xi1, xi2, & xik)***	DGH	**Shorter hypocotyls, shorter cells, narrower cells at hypocotyl base**	**Density** **Skewness** **Av. filament angle** **Parallelness** **Array dynamicity**	⇩ ⇧ ⇧ ⇩ **or ND** ⇩	**Max filament length** **Filament lifetime** **Annealing freq.**	⇧ ⇧ **ND**
[a,c]	LGR	**Shorter roots, shorter, narrower cells** **Increased lateral and adventitious roots** **Increased # stele cells with oblique axial walls**	**Density** **Skewness** **Av. filament angle** **Parallelness** **Array dynamicity**	⇩ ⇧ ⇧ ⇧ ⇩	NE	
[p]	Inflorescence stems	**Reduced tissue elongation rate, reduced tissue diameter, stiffer tissue** **Reduced gravitropism,** impaired amyloplast sedimentation	Density Skewness **Av. filament angle** **Parallelness**	NE NE **ND** **ND**	NE	

Table 1.2 continued.

myosin xi-3KO[1,n] *(various myosins XI KO)*	Various	**Smaller cells, tissues, and plants** **Smaller leaf rosette** **Fewer seeds per silique** **Branched root hairs**	**Longitudinal bundles** ⇓ **Trans-ER strands** ⇓ **Bundles present in root hair apex** ⇑		NE	
myosin xi-4KO[1,n] *(various myosins XI KO)*	Various	**Smaller cells, tissues, and plants** **Smaller leaf rosette** **Fewer seeds per silique** **Branched root hairs**	**Longitudinal bundles** ⇓ **Bundles present in root hair apex** ⇑		NE	
prf1[1,d]	DGH	**Longer hypocotyls, longer cells**	**Density** ⇓ **Skewness** ⇓	**Max filament length** ⇓ **Filament lifetime** ⇑ or ND **Annealing freq.** ND		
[d]	LGR	**Longer roots, longer cells**	**Density** ⇓ **Skewness** ND		NE	
PRF-RNAi[3,r]	Proto-nema	**Isotropic expansion instead of tip growth** **Smaller cells**	**Eccentricity** ⇓		NE	
vln2[4,s]	Various	**Shorter plants** **Shorter internodes, narrower leaf sheaths, narrower roots** **Longer, narrower, thinner, and lighter rice grains** **Wavier roots, shorter cells inside the wave** **Hypergravitropism**	**Av. fluoresc. intensity** ⇓ **Skewness** ⇓	**Max filament length** ⇓ **Filament lifetime** ⇓ **Annealing freq.** ND		
vln2 vln3[1,b,q]	Various	**More breakable stems** **More downward pointing inflorescences** **Reduced stem diameter, fewer cells** Wavier roots	**Filament pixel intensity** ⇓ **Skewness** ⇓ **# fluorescence peaks** ⇑		NE	

Table 1.2 continued.

vln4[1,u]	Root hairs	**Reduced root hair length, growth rate** Aberrant cytoplasmic streaming velocity and direction	**Skewness**	⇩	NE

Bold in columns 3–5 indicates parameters that were quantified (rather than subjectively assessed).

DGH = Dark-grown hypocotyls; DGR = Dark-grown roots; EPC = Epidermal pavement cells; LGR = Light-grown roots; ND = No difference; NE = Not evaluated.

[1]*Arabidopsis thaliana*; [2]Maize (*Zea maize*); [3]Moss (*Physcomitrella patens*); [4]Rice (*Oryza sativa*).

References: [a]Abu-Abied et al. (2018); [b]Bao et al. (2012); [c]Cai et al. (2014); [d]Cao et al. (2016); [e]Dyachok et al. (2008); [f]Dyachok et al. (2011); [g]Frank et al. (2002); [h]Henty et al. (2011); [i]Li et al. (2003); [j]Li et al. (2012a); [k]Li et al. (2013); [l]Li et al. (2014a); [m]Li et al. (2014b); [n]Peremyslov et al. (2010); [o]Rosero et al. (2013); [p]Talts et al. (2016); [q]van der Honing 2012; [r]Vidali et al. (2007); [s]Wu et al. (2015); [t]Yang et al. (2011); [u]Zhang et al. (2011b); [v]Zhang et al. (2011c).

ADF4 is a member of the ADF/cofilin family that is present across Eukaryotes (Ruzicka et al., 2007; Bernstein and Bamburg, 2010). ADF4 severs actin filaments, returning subunits to the monomer pool and increasing filament turnover. Knockout-mutant growth in light-grown roots and dark-grown hypocotyls is affected by loss of the protein—measured tissues are longer and contain longer cells (Henty et al., 2011). Filament density in mutants is reduced and bundling increased; these characteristics are attributed to increased filament lengths and lifetimes and a more than 50% reduction in severing events (Henty et al., 2011). These, plus data from other ABP mutants, originate the hypothesis that increased maximum filament lengths and lifetimes lead to larger cells and tissues (Li et al., 2014b, 2015a). The idea is that longer filaments can extend to cell peripheries and that persistent filaments can last in order to support vesicle traffic traveling to the wall for incorporation. But this correlation does not always hold, especially as additional data from other ABP mutants accumulates, as data presented below and in **Table 1.2** will demonstrate.

Actin-related proteins 2 and 3 (Arp2/3) are two subunits of the 7 subunit Arp2/3 complex. This actin-binding complex is a nucleation factor that, when activated, mimics the shape of two actin monomers coming together to form an actin seed, increasing the probability that a "third" monomer will join and overcome the rate-limiting step to filament polymerization. Arp2/3 binds the side of an existing "mother" filament and always creates a branch at a 70° angle (Machesky et al., 1994; Mullins et al., 1997, 1998; Blanchoin et al., 2000; reviewed in Yanagisawa et al., 2013). Arp2/3 is critical in lamellipodia function in animal cells where Arp2/3-driven actin polymerization produces force that moves a crawling cell forward. In animal cell crawling, actin polymerization generates force. But calculations in Szymanski and Cosgrove (2009) demonstrate that actin polymerization cannot produce enough force to overcome the pressure of the plant cell vacuole, so force itself is unlikely to cause plant cell growth. Arp2/3 is necessary to create actin meshworks associated with endocytosis in yeast (Galletta et al., 2008; Mooren et al., 2012). In plants, disruption to critical members of the complex, or upstream activation factors (e.g., the SCAR/WAVE complex), has substantial effects on cell development (Li et al., 2003; Basu et al., 2004; Frank et al., 2004; Basu et al., 2008; Yanagisawa et al., 2013).

Genetic screens for altered cell shape in maize and Arabidopsis EPC, as well as in Arabidopsis trichomes, uncovered key regulators of Arp2/3-driven actin polymerization: the SCAR/WAVE and ARP2/3 complexes. The *brick1* (*brk1*) mutant affects EPC morphogenesis in maize leaves (Frank and Smith, 2002; Frank et al., 2003, 2004). The phenotype results from a

single base-pair substitution in a gene for the smallest subunit of the WAVE/SCAR complex, necessary for activation of the ARP2/3 complex (Frank et al., 2004). Wildtype maize leaves have lobed rectangular EPC and, while the *brk1* mutant exhibits normal elongation and organ development, EPC lobes fail to develop (Frank and Smith, 2002; Frank et al., 2003).

In wildtype, lobes appear to begin growing from regions where F-actin is enriched; *brk1* lacks these regions of enrichment (Frank and Smith, 2002), suggesting that F-actin might coordinate lobe outgrowth. Another set of mutants that exhibit abnormal EPC lobe morphology are four *arp2/3* mutants of Arabidopsis (Li et al., 2003). In *arp* mutant plants, EPC are less lobed compared to wildtype and, like *brk1*, lack actin-enriched patches at lobe bases. In these cells, F-actin is distributed throughout the cell. The *arp* mutant trichomes have short branches and their swollen bases—phenocopied by cytochalasin treatment of wildtype trichomes—are extensively bundled, and lack diffuse F-actin. Li et al. (2003) conclude that cell shape differentiation requires an Arp2/3 complex to correctly localize F-actin nucleation. Unlike wildtype trichome branches that exhibit a wall thickness gradient, a*rp2* mutant trichome branches have uniform wall thickness that is almost twice as thick as wildtype (Yanagisawa et al., 2015). Fluorescent BRK1 and Arp2/3 normally localize at branch tips where they produce a diffuse actin network within a "microtubule-depleted zone" but in *arp2*, the actin network lacks directionality, as do Golgi trafficking along it (Yanagisawa et al., 2015). Microtubules lay down cellulose, which contributes to the cell wall thickness gradient in wildtype; the authors of this study suggest that Arp2/3 and actin determine the location of the microtubule-depleted zone, and thus the cell wall thickness gradient, as well as direct and deliver organelles in coordination with cell expansion (Yanagisawa et al., 2015). The actin nucleation complex Arp2/3, together with its regulatory proteins, appears critical for the feedback among cellular processes and actin that is necessary for normal cell expansion, potentially implying a more complex role for actin in growth than a simple model where extensive, thick actin bundles inhibit trichome expansion.

The FORMIN (FH) family comprises a second actin nucleation factor in plants, and some isoforms of the highly differentiated protein family—there are roughly 20 isoforms in Arabidopsis—can also elongate, cap, and bundle actin filaments, as well as bind microtubules (Blanchoin and Staiger, 2010; Cvrčková, 2012, 2013; van Gisbergen and Bezanilla, 2013). It is thought that formins nucleate filaments from organelle membranes or the PM (Li et al., 2015b). Unlike Arp2/3, the family is thought not to need to nucleate from the side of an existing filament.

FH in Arabidopsis are divided into two classes: Class I, which contains a transmembrane domain, and Class II, which lacks the transmembrane domain but largely retains their ability to bind the PM (Cvrčková, 2013; van Gisbergen and Bezanilla, 2013). High functional redundancy across isoforms makes it difficult to study effects of a single knockout mutant, but it is possible to use inhibitors or pharmacological treatments that exacerbate a preexisting phenotype to the level that it can be observed and quantified (Cvrčková, 2012; Rosero et al., 2013; Cvrčková, 2013). A T-DNA insertion mutant for the Arabidopsis Class I *FH1* exhibited reduced root growth and fatter roots only in the presence of Lat B compared with wildtype on the same dose, indicating that FH1 plays a role in polarized growth. Even without Lat B, actin in *fh1* was less dense, more bundled, and less dynamic (Rosero et al., 2013). A mutation in just a single Class II *FH*, in rice, *fh5/bui/rmd* (*OsFH5/BENT UPPERMOST INTERNODE 1/RICE MORPHOLOGY DETERMINANT*), causes a more apparent phenotype in both plant growth and actin organization, where cells and tissues are shorter and actin filament intensities are reduced (indicating fewer filaments) and appear transverse compared with wildtype (Yang et al., 2011; Zhang et al., 2011c; Li et al., 2014a). These findings support the classical hypothesis that actin filaments need to be longitudinal for axial cell expansion to occur.

The actin monomer pool in plant cells is thought to be enormous. To tightly control polymerization, most actin monomers are bound by the ABP PROFILIN (PRF; 5 isoforms in Arabidopsis) at monomer pointed ends (Gibbon et al., 1999; Henty-Ridilla et al., 2013a). Profilin inhibits nucleation and addition of monomers to pointed ends, but allows addition on barbed ends. FHs work with PRF to nucleate and elongate filaments with these PRF-bound monomers specifically (Yang et al., 2011; Henty-Ridilla et al., 2013a; Li et al., 2015b; Cao et al., 2016). Moss protonema require PRF for tip growth. When RNAi constructs were used to reduce expression of all three *Physcomitrella patens PRF*, actin filaments in the tissue were less "eccentric." In these cells, only isotropic growth occurred, and typical tip growth no longer took place (Vidali et al., 2007), showing the protein is necessary to maintain polar growth and supporting the model that longitudinal actin is necessary for growth.

Dark-grown hypocotyls and light-grown roots are longer in Arabidopsis *prf1* mutants, as well as epidermal cells in both mutant tissues. Overall actin arrays in *prf1* cells are less dense in both roots and shoots, and less skewed/bundled in shoots, indicating fewer filaments despite similar quantities of actin (Cao et al., 2016). Mutant maximum filament lengths and elongation

rates are reduced—notably the fastest elongating filaments are affected by the mutation—but average filament lifetimes are longer or no different from wildtype. Loss of PRF1 reduces both side and end nucleation events, and increases de novo nucleation events. Wildtype plants treated with the FH inhibitor SMIFH2 phenocopy the reduction in nucleation events, and *prf1* treated with the inhibitor exhibits no further reduction in nucleation events, indicating that PRF1 is active in FH-mediated filament nucleation from filament ends and sides (Cao et al., 2016).

Loss of PRF1 has a clear effect on plant growth, but the data in Cao et al. (2016) further confound the issue of what role actin plays in expansion. Density in *prf1* cells is reduced, as well as bundling, while plants themselves are larger. If actin's role in expansion is to provide tracks for vesicle delivery, it is difficult to understand how loss of tracks, particularly the fastest-elongation population of tracks, could result in plants of increased size. The authors suggest that perhaps trafficking of specific vesicles related to hormone transport is affected (Cao et al., 2016).

Capping protein (CP) is an obligate heterodimer that caps filament barbed ends to control filament elongation (Li et al., 2012a, 2014c). The *cp* knock-down mutants and CP-overexpressing lines (*CP-OX*) have opposite effects on actin organization and filament behaviors and, interestingly, opposite effects on plant and cell size. Even more fascinating, *cp* or *CP-OX* each affects actin array organization (in terms of density and skewness/bundling) and dynamicity identically within each genotype's light-grown roots and dark-grown hypocotyls. But, even though, ex., *cp* mutant shoots and roots exhibit the same actin phenotypes, the mutation inversely affects tissue and cell size (see **Table 1.2**). For example, the loss of CP in *cp* results in increased density and dynamicity and reduced skewness/bundling in both roots and shoots. But dark-grown *cp* hypocotyls are longer with longer cells, and light-grown roots are shorter with shorter cells. *CP-OX* exhibits the exact opposite actin arrays, dynamicity, and tissue and cell sizes (Li et al., 2012a, 2014c). These phenotypes show that overall actin array organization and dynamics cannot universally predict growth patterns. However, they, like the *adf4* observations, do support the hypothesis that longer filament lengths and lifetimes—apparent in *cp*—correlate with longer cells, while shorter filament lengths and lifetimes—*CP-OX*—correlate with shorter cells. The *cp* and *CP-OX* observations of individual actin filament behaviors support the hypothesis that length and lifetime play a predictive role in cell expansion, at least in dark-grown hypocotyls (Henty et al., 2011; Li et al., 2012a, 2014c).

VILLINs (VLN; 5 isoforms in Arabidopsis) are filament bundling and severing proteins that are expressed throughout plant tissues (Khurana et al., 2010; Wu et al., 2015). Rice and

Arabidopsis mutants for several isoforms have been fairly well characterized. Arabidopsis *vln4* and rice *Osvln2* exhibit strong single mutant phenotypes but data indicate that Arabidopsis VLN2 and VLN3 are functionally redundant so they are studied most productively as the double *vln2 vln3* mutant (Zhang et al., 2011b; Bao et al., 2012; van der Honing et al., 2012; Wu et al., 2015). Growth is stunted or abnormal in vegetative tissues of all three *VLN* mutants, and actin filament skewness/bundling is decreased compared with wildtype (Zhang et al., 2011b; Bao et al., 2012; van der Honing et al., 2012; Wu et al., 2015). Wu et al. (2015) extensively characterized individual filament behaviors in rice root epidermal cells, finding that bundling frequency, maximum filament length, and filament lifetime decrease in the absence of OsVLN2, and elongation rates and severing frequencies increase. These data demonstrate that OsVLN2 bundles actin filaments in vivo as well as support the hypothesis that reduction in filament lengths and lifetimes corresponds with reduced cell size.

Cytoplasmic streaming is myosin- and actin-dependent (Williamson, 1972; Foissner and Wasteneys, 2007; Tominaga and Nakano, 2012; Tominaga and Ito, 2015). Myosins are motor proteins that are present in all Eukaryotic cells (Geitmann and Nebenführ, 2015; Nebenführ and Dixit, 2018). Plant myosins fall into two families, myosin VIII and XI. Myosin VIII (4 isoforms in Arabidopsis) are generally associated with the PM and plasmodesmata (Baluska et al., 2001a); myosin XI (13 isoforms) are cytosolic and bind organelles on one side with a "cargo" or "tail" domain and on the other side, a motor domain uses energy provided by ATP hydrolysis to walk along actin filaments (Cai et al., 2014). Considering their role in active transport, it is unsurprising that disruptions to myosin affect growth. Because of functional redundancy in the large family, how myosin effects growth must be studied with either drug treatments that inhibit multiple myosin isoforms at once, or high order mutants.

Studies on a triple knockout mutant (interfering with *myosins XI1, XI2,* and *XIK*; *myosin xi3KO*) found that roots, root hairs, and shoots are smaller, with smaller cells (Peremyslov et al., 2008; Peremyslov et al., 2010; Ueda et al., 2010; Cai et al., 2014). Lateral root patterning as well as cell patterning in the stele is irregular and, interestingly, inflorescence stems were stiffer in the same *myosin xi3KO* (Talts et al., 2016; Abu-Abied et al., 2018), indicating problems with polysaccharide delivery (Zhang et al., 2019). Actin organization in root and hypocotyl epidermal cells is less dense and more bundled, and exhibits higher average filament angles compared with wildtype. However, the mutations have opposing effects on filament parallelness in shoots, where

it is reduced, and in roots, where it increases (Cai et al., 2014). The increased extent of filament organization (in terms of parallelness) in roots, but reduced cell size in both roots and shoots, conflicts with the hypothesis that "more organized" actin corresponds with more growth. Actin in stem inflorescence endodermal cells exhibits average filament angles and parallelness equivalent to wildtype (Talts et al., 2016). There are no data on actin's dynamic properties in inflorescences, but overall array dynamicity decreases in *myosin xi3KO* roots and shoots, probably a function of longer filament lengths and lifetimes (Cai et al., 2014).

It is no surprise that disrupting motors that power cytoplasmic streaming and vesicle delivery negatively affect plant growth. Longer maximum filament lengths and lifetimes in a mutant with smaller cells and tissues appear to contradict the hypothesis that these filament behaviors correlate with elongation. The authors suggest that myosin "acts downstream [of these characteristics] in regulating cell expansion" (Cai et al., 2014), and to that end, there is evidence that myosins XI influence shape of the key player in expansion, the vacuole (Scheuring et al., 2015). However, the stiffer mutant inflorescences measured in Talts et al. (2016) seem confusing, particularly in light of data showing reduced cellulose content in *myosin xi3KO* hypocotyls (Zhang et al., 2019)—though cellulose is not necessarily responsible for the stiffness and polysaccharide content was not reported in the inflorescence study. Interestingly, motor speed (and therefore, cytoplasmic streaming rate) is shown to determine plant size (Tominaga et al., 2013). Chimeric myosins bearing an Arabidopsis cargo-binding domain fused to either a high-speed motor from *Chara* or low-speed motor domain from *Homo sapiens* drastically alter plant and cell size at maturity, with faster myosins producing larger cells and plants (Tominaga et al., 2013). This work implicates cytoplasmic streaming over actin tracks as crucial in growth (Tominaga et al., 2013); potentially, actin organization—in addition to motor speed, contributes to cytoplasmic streaming rate. Together, work on myosin XI shows that the relationship of actin filament dynamics and organization to cell expansion is not straightforward, and drawing universal conclusions based on data from different cell types is not possible.

In addition to ABPs and their activators (such as the Arp2/3 activator SCAR/WAVE) affecting cell expansion, mutations in proteins that regulate actin polymerization cause differences in cell morphology, particularly during the first few stages of growth when cell shape is determined. Rho-like GTPases of plants (ROPs) are signaling proteins that regulate actin polymerization during this early period (Fu, 2002; Fu et al., 2005; Basu et al., 2008). EPC in a constitutively active (CA)

rop2 mutant of Arabidopsis are supersized, circular, and the lobes do not form; F-actin is distributed throughout cells (Fu, 2002). In roots, CA-ROP2 increases lateral root and root hair length, though number of root hairs is reduced (Jones, 2002; Wu et al., 2011). Dominant-negative (DN) *rop2* mutants show smaller EPC and weak lobing, fewer lateral roots, and shorter root hairs than wildtype. The fluorescent signal from F-actin in *DN-ROP2* tissues appears faint and actin patches are absent from the tips of growing root hairs (Fu, 2002; Jones, 2002; Wu et al., 2011). Like *brk1* and the *arp* mutants, *CA-rop2* and *DN-rop2* lack actin-enriched patches at the base of EPC lobes, *CA-rop2* because actin is distributed throughout the cells and *DN-rop2* because these cells appear to contain little actin. Root hairs in *CA-ROP2* exhibit dense actin patches while *DN-ROP2* plants lack these tip-focused patches. The lack of enrichments might be the reason polarized elongation in these regions fails (Fu, 2002; Jones, 2002). Lobe initiation occurs during the first 1–2 days of cell growth in EPC, with some but reduced lobe initiation occurring between days 2–3, and afterwards cells elongate in normal proportions no matter their genotype or treatment (Fu et al., 2002; Zhang et al., 2011a; Armour et al., 2015). It therefore appears that ROP2 influences cell shape only during an initial period (Fu et al., 2002). Fu et al. (2005) and Nagawa et al. (2012) describe a potential mode of action for ROP2: ROP2 signals to RIC4, a ROP effector that stimulates regional F-actin accumulation, promoting growth in that region. Fu et al. (2002) propose that *CA-rop2* EPC appear super-sized because the evenly distributed actin filaments promote abnormal expansion. In root epidermal cells, a similar mechanism is proposed, where ROP6 (as opposed to ROP2 in root hairs) stimulates actin enrichments that lead to cell expansion (Lin et al., 2012). How exactly the upstream RIC4 generates fine arrays of actin filaments remains to be established.

1.5   Statement of Problem: The Relationship between Actin Organization and Growth is Unclear

These previous studies demonstrate that actin plays a major role in cell expansion, and that, in general, mutations that alter actin filament behavior and organization change plant growth. But individual actin filaments behave almost the same in growing and nongrowing cells of the same tissue in wildtype plants (Staiger et al., 2009). The same actin organizations have opposite effects on cell size in roots and shoots (Li et al., 2012a, 2014c). Growth phenotypes and actin arrays in

actin and ABP mutants form part of the basis for the model that "organized" actin arrays contribute to growth. However, the information compiled in **Table 1.2** clearly shows that no single aspect of actin array organization universally correlates with cell size in either direction.

The problem with drawing broad conclusions based on observations of cell size and actin array in actin and ABP mutants is that the observed differences in actin organization or behavior might affect only one aspect of growth. Below, we will discuss the effect of exogenous hormone treatments on actin organization and those studies' further attempts to delineate relationships between actin organization and growth. Like the studies discussed above, these also will show that no direct, universal relationship between actin organization or filament behavior and cell expansion exists, at least based on the actin parameters measured so far. Nor is it clear how actin filaments control growth—are they merely providing tracks for vesicle delivery, or is there something more?

To reach a firm conclusion, we would ideally observe actin in long-term timelapse movies to develop a sense of typical actin dynamics and organization during growth. We would then apply treatments to increase or decrease growth while observing changes in actin dynamics and organization. Such technologies are not readily available. A second-best option would be to evaluate differences in actin dynamics and organization within a single wildtype tissue that exhibits a natural cell elongation gradient, like dark-grown hypocotyls or epidermal cells in the root elongation zone. This is currently feasible. Focusing such work on solely epidermal tissues is reasonable because plants grow from their outside cell layers in; the epidermis expands first. Work in biosynthesis and signaling mutants for brassinosteroids, a hormone involved in growth, shows that cell expansion in roots and shoots is driven by hormone signaling and growth in the epidermis, with deeper tissues responding to epidermal signals (Savaldi-Goldstein and Chory 2008; Hacham et al. 2011). When the receptor for brassinosteroids (*BRI1*), or a biosynthesis gene (*CPD*) is expressed in solely the epidermis of, respectively, a *bri1* (receptor) or *cpd* (biosynthesis) mutant background, each construct rescues mutant growth phenotypes. When each of these constructs is expressed behind a vasculature promoter within the same mutant backgrounds, growth remains entirely or largely deformed (Savaldi-Goldstein and Chory 2008; Hacham et al. 2011). Auxin is another plant hormone involved in growth and much work investigating the relationship between actin and cell expansion uses actin response to auxin to substantiate the model that actin "organization" correlates with expansion.

1.6   Auxin and Plant Growth

1.6.1   General History and Signaling

Auxin, the first plant hormone ever discovered, is present in the freshwater green algae Charophyta, who share a common ancestor with land plants, indicating that the compound evolved before land plants (Lau et al., 2008, 2009; Wang et al., 2014; Mutte et al., 2018; Bowman et al., 2019). Darwin and contemporaries hypothesized the existence of a transported plant hormone when they observed that plants bend towards a light source, but if shoot apexes are covered or removed, the plants no longer bend (Darwin and Darwin, 1880; Sauer et al., 2013). The compound behind the bending phenomenon, indole-3-acetic acid (IAA), is the most abundant natural auxin in plants (Bartel, 1997; Simon and Petrášek, 2011; Sauer et al., 2013; Grones and Friml, 2015), and was first isolated from human urine, then fungi, before finally being isolated from plant tissue in the 1940s (Sauer et al., 2013; Enders and Strader, 2015). Today, auxin is the most widely studied plant hormone and is considered indispensable for nearly all aspects of plant growth and development (Woodward and Bartel, 2005; Teale et al., 2006). However, although auxin is considered to be a growth hormone, at high doses relative to endogenous levels, it inhibits root growth (Went and Thimann, 1937; Thimann, 1937, 1936, 1939), and does so within seconds to minutes of application (Hejnowicz and Erickson, 1968; Fendrych et al., 2018).

The mechanism of cellular auxin perception that leads to transcriptional responses is known: the SKP1–CULLIN1–F-BOX–TRANSPORT INHIBITOR RESPONSE 1 (SCF$^{TIR1/AFB}$) pathway (Dharmasiri et al., 2005a,b; reviewed in Grones and Friml, 2015 and Mutte et al., 2018). The SCF$^{TIR1/AFB}$ complex, including the auxin receptor TIR1, is predominantly localized to the nucleus but with some protein thought to be present in the cytosol (Dindas et al., 2018). In low auxin conditions, members of a family of AUXIN/INDOLE-3-ACETIC-ACID (Aux/IAA) transcriptional repressors are bound to the transcription factors AUXIN RESPONSE FACTORS (ARFs), keeping ARFs inactive. When high concentrations of auxin are present in a cell, the SCF$^{TIR1/AFB}$ receptor complex perceives the auxin signal because auxin binds directly to TIR1 (Dharmasiri et al., 2005a; Kepinski and Leyser, 2005; Tan et al., 2007; Calderon Villalobos et al., 2012). Once bound to SCF$^{TIR1/AFB}$, auxin fills in a space within TIR1 without drastically altering its conformation, and the TIR1–auxin complex is favorable to bind Aux/IAA, recruiting Aux/IAAs from their association with ARFs; auxin acts as "molecular glue" between TIR1 and Aux/IAA

(Tan et al., 2007). The Aux/IAA repressors are ubiquitinated and then destroyed by the proteasome, allowing ARFs to activate (or repress) target genes (Grones and Friml, 2015; Mutte et al., 2018). The Aux/IAA and ARF families contain multiple isoforms (Dharmasiri et al., 2005b; Grones and Friml, 2015); as with the high number of actin and ABP isoforms, this diversity likely contributes to a plant's ability to tightly regulate auxin responses depending on circumstances (Liscum and Reed, 2002; Luo et al., 2018).

In addition to transcriptional reprogramming, which, with a few exceptions (McClure and Guilfoyle, 1987; Hagen and Guilfoyle, 2002; Staswick et al., 2005), generally takes at least 10 minutes (McClure et al., 2007; Labusch et al., 2016), auxin is hypothesized to induce faster, nontranscriptional cellular responses that both do and do not depend on auxin perception by SCF$^{TIR1/AFB}$ (Parry et al., 2009; Titapiwatanakun and Murphy, 2009; Vanneste and Friml, 2013; Schenck et al., 2010; Monshausen et al., 2011; Labusch et al., 2016; Dindas et al., 2018; Fendrych et al., 2018; Paponov et al., 2019). Increases in intracellular H^+ and Ca^{2+} occur within seconds to minutes of auxin treatment (Dindas et al., 2018); influx of these second messengers could very well differentially regulate ABPs (Li et al., 2015b). Since plant growth responds to auxin within seconds, posttranslational regulation in response to auxin is highly likely, even if these nontranscriptional responses are also regulated by TIR1 (Hejnowicz and Erickson, 1968; Dindas et al., 2018; Fendrych et al., 2018). Much less is certain about posttranslational mechanisms of auxin response affecting growth—specifically, the mechanisms by which auxin is perceived ahead of short-term responses; however, they are widely thought to depend on the actin cytoskeleton (Titapiwatanakun and Murphy, 2009; Pan et al., 2015).

1.6.2   Auxin is Necessary for Establishing Cell Polarity

Like actin, auxin is crucial for establishing cell and tissue polarity (Sachs, 1991; Baluska et al., 2003; Sun et al., 2004; Fischer et al., 2006; Boutté et al., 2007; Laskowski et al., 2008; Overvoorde et al., 2010; Pan et al., 2015; Brumos et al., 2018). Auxin can be produced in all plant tissues (Michniewicz et al., 2007; Brumos et al., 2018), but is synthesized primarily in the apexes of shoots and, to a lesser extent, roots, via a tryptophan-dependent pathway—though there is at least one tryptophan-independent pathway to auxin synthesis (Ljung et al., 2001, 2005; Stepanova et al., 2008; Chen et al., 2014a; Zhao, 2014; Wang et al., 2015; Zhu and Geisler, 2015; Brumos et al., 2018). Local auxin synthesis is necessary for proper development of some tissues, like maintaining

the root stem cell niche (Chen et al., 2014a; Brumos et al., 2018), but transported auxin is thought necessary for tissue development and tropisms (Marchant et al., 1999; Marchant et al., 2002; Grieneisen et al., 2007; Laskowski et al., 2008).

Pattern (i.e., tissue) development in plants requires the plant to create regions of high and low auxin concentrations, or auxin gradients (Zhu and Geisler, 2015); plants form these auxin gradients in several ways: biosynthesizing, conjugating or deconjugating, degrading, or directionally transporting auxin among cells (Vanneste and Friml, 2009; Geisler et al., 2014; Grones and Friml, 2015). For long distance bulk transport, auxin travels through the phloem (Michniewicz et al., 2007). Alternatively, auxin can move through a plant via polar auxin transport (PAT), which, like the hormone itself, evolved before land plants (Dibb-Fuller and Morris, 1992; Boot et al., 2012; Zhang and van Duijn, 2014). PAT is known to connect auxin signaling to the actin cytoskeleton (Nick et al., 2009), but the precise molecular mechanisms are not yet fully elucidated (Geisler et al., 2014; Zhu and Geisler, 2015).

Plants use PAT to form auxin gradients to establish polarity (Sachs, 1991; Boutté et al., 2007; Vanneste and Friml, 2009; Xu et al., 2014; Zhu and Geisler, 2015). These gradients themselves then drive a cycle of auxin flow that enforces the patterning (Sachs, 1991). Auxin maxima (localized areas of high auxin concentration) are associated with organ primordia. This movement occurs in one of two ways: chemiosmotic diffusion or active export and reception/import by specialized proteins (Muday and DeLong, 2001; Petrasek and Friml, 2009; Leyser, 2010). In both kinds of PAT, specialized proteins transport auxin out of cells (Michniewicz et al., 2007). Once in the extracellular space, auxin travels through the plant by chemiosmotic diffusion or active reception/import. The chemiosmotic diffusion model posits that in the acidic environment of the apoplast (pH 5.5), the auxin molecule becomes protonated (IAAH, **Figure 1.4**) and therefore nonpolar. In this state, IAAH can diffuse through the PM, but once in the more alkaline environment of the cytoplasm (pH 7.0), IAA is deprotonated to become IAA$^-$ (Michniewicz et al., 2007). No longer a nonpolar molecule, IAA$^-$ relies on active export to leave a cell. Alternatively, auxin must be actively transported into cells (Teale et al., 2006; Michniewicz et al., 2007) or apoplastic auxin binds to a purported auxin receptor, AUXIN BINDING PROTEIN 1 (ABP1). Recent evidence discussed below demonstrates that ABP1 is almost certainly not involved (Dai et al., 2015; Gao et al., 2015).

1.6.3 The Acid–Growth Hypothesis

The general mechanism for plant growth, as described above, is that a cell's vacuole takes up water and exerts pressure on a loosened cell wall; cell wall components traffic along actin filaments to the PM where they are exocytosed and incorporated into the wall. Since the 1970s, a major hypothesis for auxin's role in growth, "the acid–growth hypothesis," posits that auxin is important for cell wall loosening (Rayle et al., 1970). Acids were observed to affect coleoptile elongation even earlier—the mere surroundings of an acidic environment can stimulate growth (Bonner, 1934; Rayle and Cleland, 1992). Within about 20 min of auxin treatment, cells produce additional proton pumps (H^+-ATPases) that work at the PM to pump H^+ into the apoplast, decreasing extracellular pH (Rayle and Cleland, 1992; Kutschera, 1994; Niklas and Kutschera, 2012; Perrot-Rechenman, 2012; Fendrych et al., 2016; Arsuffi and Braybrook, 2018; Majda, 2018). Although other compounds like fusicoccin stimulate growth, fusicoccin, unlike auxin, stimulates only H^+-ATPase activation, but not production or abundance at the PM: only auxin induces H^+-ATPase synthesis (Rayle and Cleland, 1992; Fendrych et al., 2016). Lowered apoplastic pH activates enzymes within the wall, expansins, which change how wall polysaccharides interact with one another (Cosgrove, 2005; Perrot-Rechenman, 2012). Like other components of plant growth, expansins comprise large gene families, ex., 36 isoforms in Arabidopsis (Cosgrove, 2005), once again evidencing that plants use molecular diversity to regulate precise stimulus response (Cosgrove, 1998). By some accounts, the proportion of noncellulosic polysaccharide components of the wall changes within 15 min of IAA treatment (Nishitani and Masuda, 1981; Masuda, 1990). Since the quantity of H^+-ATPases at the PM increases significantly after auxin (Rayle and Cleland, 1992; Fendrych et al., 2016), trafficking and exocytosis of these ATPases from site of production to the PM almost certainly depend on actin. Trafficking of CesA and other wall components is known to rely on actin and myosin (Sampathkumar et al., 2013; Cai et al., 2014; Zhang et al., 2019). This mechanism indirectly connects auxin to actin and growth, but more direct connections also exist.

1.7 Auxin, Actin, and Growth

Very high spatiotemporal resolution imaging experiments demonstrate that auxin stops root growth within 30 s, and does so through posttranscriptional mechanisms (Fendrych et al., 2018). Plant growth requires a dynamic actin cytoskeleton (Baluska et al., 2001b). On a gross scale, long-

term auxin treatments affect actin organization (Rahman et al., 2007; Li et al., 2014a; Scheuring et al., 2015), but the effect of short-term auxin treatments on actin dynamics and organization that might affect growth, particularly in roots, has not been extensively investigated. Since growth is intertwined with both auxin and actin, and specific actin arrays are hypothesized to correlate with growth, it follows that auxin influences growth by modulating actin dynamics, or at least that auxin influence on growth modulates actin dynamics. Because growth changes so fast in response to auxin, it is possible that modulation of the cytoskeleton is posttranslational, like rapid growth cessation itself. Still, examining auxin-induced transcriptional reprogramming or proteomic changes could implicate specific actin isoforms and/or ABPs whose regulation is altered by auxin within minutes of auxin treatments.

Several genes—such as the large family of *SMALL AUXIN UP-RNA* (*SAURs*), an auxin conjugating enzyme (*GH3*), and the *Aux/IAA* transcriptional repressors (Abel et al., 1994; Oeller and Theologis, 1995)—have been shown inducible by auxin within a very short time frame, within 2–5 min! (McClure and Guilfoyle, 1987; Hagen and Guilfoyle, 2002; Staswick et al., 2005). Nevertheless, most research into transcriptomic and proteomic responses to auxin investigate plant response to long-term treatments (Huang et al., 2008; Lee et al., 2009; Xing and Xue, 2012; Chapman et al., 2014; Slade et al., 2017). Several look for differences starting at 10–30 min after auxin treatment (Paponov et al., 2008; Schenck et al., 2010; Labusch et al., 2013; Lewis et al., 2013; Labusch et al., 2016; Kelley et al., 2017; Pu et al., 2019). In most cases, changes to specific cytoskeletal proteins were not reported in these short-term studies; however, changes to genes, gene ontology categories, and proteins broadly related to cell wall, microtubule dynamics, and more generally cytoskeleton reorganization, were reported (Lewis et al., 2013; Mattei et al., 2013; Chapman et al., 2014; Kelley et al., 2017; Pu et al., 2019). The severing protein ADF2, the nucleator FH5, and the bundling protein WLIM1—the few named ABPs whose regulation changes during auxin response—are discussed in more detail in **Chapter 3**. An exception is ACT7, whose expression auxin induces and whose "promoter sequence contains a remarkable number of motifs with sequence similarity to putative phytohormone response elements" (McDowell et al., 1996; McKinney et al., 2001; Kandasamy et al., 2007). For this reason, the ACT7 isoform specifically is thought to be involved in actin response to environmental stimuli.

Figure 1.4 Structure of Auxins Indole-3-Acetic Acid & 1-Naphthylacetic Acid & Their Paths of Entry to and Exit from Cells.

Indole-3-acetic acid$^-$ (IAA$^-$) is a polar molecule and cannot traverse the plasma membrane (PM). IAAH and 1-naphthylacetic acid (NAA) are lipophilic/nonpolar and can diffuse through the PM. The more alkaline environment of the cytosol causes an H$^+$ to dissociate from IAAH, and it becomes the polar form, IAA$^-$. Both forms of auxin, IAA and NAA, can be carried into cells by the auxin influx protein AUXIN RESISTANT 1(AUX1) or family members LIKE AUX1 (LAX, not shown). Once auxin enters a cell, it must be carried out by efflux proteins which are members of either the PIN-FORMED (PIN) or ATP-BINDING CASSETTE/B (ABCB) families. Both PINs and AUX1 are trafficked along actin filaments, implying that auxin treatments might induce actin cytoskeleton reorganization through either or both transport proteins and unidentified actin-binding proteins (black boxes).

The traditional model for short term cellular responses posits that the PM-bound auxin receptor AUXIN BINDING PROTEIN 1 (ABP1), which has been shown to bind both IAA and NAA, transduces the auxin signal into a cell together with its accessory protein TRANSMEMBRANE KINASE (TMK). The auxin signal is amplified through a cell by activation of SPIKE 1 (SPK1), RHO OF PLANTS 6 (ROP6), and ROP INTERACTIVE CRIB MOTIF-CONTAINING 1 (RIC1), which activates the actin-binding ACTIN-RELATED PROTEINS 2 & 3 (Arp2/3) complex, thereby modulating actin cytoskeletal dynamics.

Example is set in the root epidermis. All ABCBs are shown as bidirectional for illustrative purposes only; see text for more information.

Gray arrow indicates change; green arrows indicate flow or movement; purple arrows indicate activation/alteration. Blue background inside the cell indicates the vacuole; illustration shows the cell cortex.
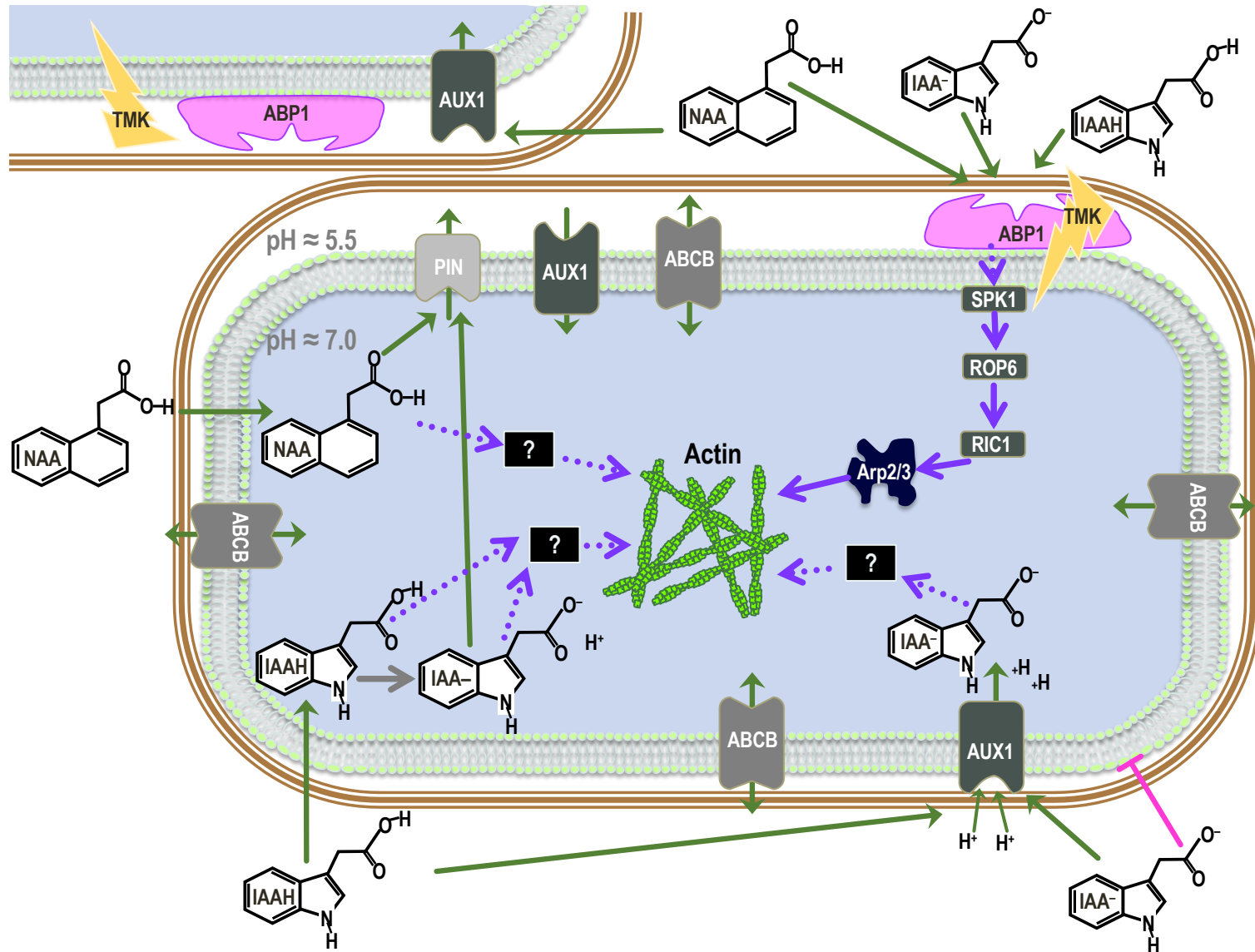
Figure 1.4 Structure of Auxins Indole-3-Acetic Acid & 1-Naphthylacetic Acid & Their Paths of Entry to and Exit from Cells.

Together with actin and growth phenotypes in ABP mutants, experiments that investigate the effect of auxin treatments on actin organization (summarized in **Table 1.3**) contribute to the model that the state of actin organization corresponds with extent of cell expansion. Before GFP-fABD2 was used to visualize actin filaments in plant cells, researchers relied on a fusion of yellow fluorescent protein (YFP) to the mouse ABP, Talin (YFP-mTalin). This construct soon fell out of favor, because it ectopically bundles actin filaments in plant cells and perturbs plant growth (Nick et al., 2009; Dyachok et al., 2014). However, the YFP-mTalin actin reporter was used in experiments that demonstrate that excess actin bundles inhibit rice coleoptile growth and that auxin unbundles filaments in relatively short-term (i.e., 30–60 min) treatments (Nick et al., 2009; Nick, 2010). Compared to a moderate expressing line, plants expressing large amounts of YFP-mTalin displayed copious, thicker, more rigid actin bundles, and exhibited less auxin-induced coleoptile elongation (Nick et al., 2009). PAT moved exogenous auxin more slowly in these highly bundled lines and in treatments with phalloidin, which also induced bundling, indicating that extensive actin bundling inhibits PAT (Nick et al., 2009). High doses of 5–50 µM IAA for 30 min to 1 h stimulated filaments to unbundle, increased filament density, and stimulated coleoptiles to elongate (Holweg et al., 2004; Nick et al., 2009). Importantly, this group corroborated previous evidence that disrupting actin with Lat B or Cyt D inhibits auxin transport in a dose-dependent manner, and that actin bundles form when coleoptiles are depleted of endogenous auxin by decapitation (Butler et al., 1998; Nick et al., 2009). Interestingly, both groups observed that the auxin transport inhibitor 1-N-naphthylphthalamic acid (NPA) could somewhat restore auxin transport after actin was disrupted by Lat B or Cyt D, probably because NPA bundles actin filaments, stabilizing some "tracks" even when most "roads" within a cell are disrupted (Butler et al., 1998; Nick et al., 2009). These studies link extent of actin bundling and filament dynamicity to auxin transport and plant growth (Butler et al. 1998; Nick, Han, and An 2009). How this information fits into the model that increased actin filament organization coincides with growth is interesting: actin bundling is considered a hallmark of "organization" but bundling inhibits growth (Nick et al., 2009). Perhaps it is only excess exogenous bundles (i.e., bundles that are induced by the YFP-mTalin actin reporter), rather than naturally-formed actin bundles, that inhibit growth. To this effect, the group remarks that a certain amount of actin dynamicity is likely necessary for the machinery of PAT to function properly (Waller et al., 2002; Nick et al., 2009; Nick, 2010).

Root growth in the rice *FH* mutant *fh5/bui/rmd* is less sensitive to IAA-induced growth inhibition compared with wildtype, and actin organization in the mutant is nonresponsive to IAA after long-term treatments (Li et al., 2014a). Whereas the high dose of 10 μM IAA typically induces extensive actin bundling in root epidermal cells after 6 h, extent of actin bundling in *fh5/bui/rmd* does not change (Li et al., 2014a). This mutant in particular lends credence to the "organized actin–cell growth" model because filaments in *fh5/bui/rmd* appear transverse, not longitudinal—longitudinality is considered a component of "organization"—and apparently impervious to auxin treatments, and both cells and tissues are shorter than wildtype. PAT is reduced in mutant roots in both directions (rootward and shootward), likely because subcellular localization of auxin export proteins is aberrant (Li et al., 2014a). Plant cell expansion requires a balance of endocytosis and exocytosis (Battey et al., 1999; Frigerio, 2010; Zhang et al., 2019). Both endocytosis and exocytosis are abnormal in *fh5/bui/rmd*: endocytosis of FM-464 dye increases and exocytosis of auxin exporters decreases compared with wildtype (Li et al., 2014a). The authors conclude that *fh5/bui/rmd*'s aberrant actin array prevents PAT by perturbing transporter localization and vesicle trafficking. In *fh5/bui/rmd*, FH5, an ABP that is crucial for normal auxin response at late timepoints, is neither present nor induced in higher quantities by auxin; actin filaments are not modulated, disrupting multiple aspects of growth (trafficking, which disrupts PAT; endocytosis, and exocytosis), which is abnormal compared with wildtype plants (Li et al., 2014a).

This study is a perfect example of how auxin, actin, and growth are intertwined (Li et al., 2014a). However, actin is so involved with the trafficking, endocytosis, and exocytosis of auxin transporters—as well its own functions—that it is impossible to parse which aspects of actin organization and/or behavior are responsible for the typical auxin-induced result of short-term growth cessation. What causes growth cessation: actin bundling or lack of bundles? incorrect filament orientation? the combination? Do the differences in actin organization observed in *fh5/bui/rmd* actively inhibit growth, or do they only fail to contribute to growth? Classical experiments demonstrate that auxin stops plant growth within minutes (Hejnowicz and Erickson, 1968), and a recent high spatiotemporal resolution experiment shows that growth inhibition occurs even faster—within 30 s (Fendrych et al., 2018). The auxin efflux inhibitor NPA also stops root growth quickly—inhibition takes just a few minutes longer than auxin by itself (Fendrych et al., 2018). It is unclear whether growth stops only because of increased auxin levels within cells, or if

growth stops because of altered actin organization. In fact, both widely used auxin transport inhibitors, NPA and tri-iodobenzoic acid (TIBA), alter actin organization by increasing extent of filament bundles and disrupting the actin cytoskeleton (Rahman et al., 2007), so it is not possible to discern whether the increased actin bundling and actin disruption stop growth, or if the increased bundles and filament disruption stop growth by altering auxin transport and then (presumably) deranging other growth cues and/or processes. Studying the effect of auxin on actin organization and dynamics is further complicated by the fact that there is always crosstalk between auxin and other hormones, some of which also stimulate actin reorganization (Lanza et al., 2012).

1.8   Root Gravitropism

Auxin and actin converge in another facet of plant life: gravitropism. Plants sense and respond to gravity, ensuring that roots always grow down. In positive gravitropism, roots use a variation in auxin concentration to coordinate differential growth across a root and point the tissue into growth media where they can obtain nutrition and hydration.

There are three stages to gravitropism: perception, signal transduction, and differential growth. Actin has long been thought to be involved in all three stages, and auxin in signal transduction and differential growth response (Baldwin et al., 2013; Blancaflor, 2013; Sato et al., 2015). Perception is thought to occur primarily in the root columella, a stack of three to four tiers of cells, with four cells in each horizontal tier. These cells are "cytosol-rich"—there appear to be fewer organelles throughout the cytoplasm (Yoder et al., 2001)—and contain special starch-containing plastids, amyloplasts, which are denser than cytoplasm. When a root is reoriented, amyloplasts make their way through a diffuse actin network to resettle on the new bottom within 5 min (Leitz et al., 2009; Blancaflor, 2013). Since endoplasmic reticulum (ER) in columella cells is not distributed throughout the cell, but rather forms a cup-like shape, lining the "walls" as well as the bottom of the cell, a resettling amyloplast will land on the ER, initiating the second phase of gravitropism, signal transduction (Baldwin et al., 2013).

Table 1.3 Actin Response to Auxin in Wildtype Cells.

Tissue/cell type	Auxin	Dose	Duration	Growth phenotype	Actin phenotype
Root EZ epidermis[1d]	IAA	1 μM	2 hours	NE	Apparent increase in actin filaments
Root EZ epidermis[1d]	IAA	30 nM	2 days	**Reduced root & cell elongation**	**Extent of actin filaments increases**
Root EZ epidermis[1d]	2,4-D	1 μM	2 hours	NE	Apparent reduction in actin filaments
Root EZ epidermis[1d]	2,4-D	30 nM	2 days	**Reduced root & cell elongation**	**Extent of actin filaments decreases**
Root EZ epidermis[1d]	NAA	100 nM	2 days	Reduced root & cell elongation	Apparent increase in actin filaments
Root EZ epidermis[1b]	IAA	10 μM	6 hours	**Reduced elongation**	**Increased bundling**
Root EZ epidermis[1e]	NAA	500 nM	6 hours	**NE**	**Increased density**
Root EZ epidermis[1e]	NAA	250 nM	20 hours	**NE**	**Increased skewness**
Coleoptile epidermis[2a]	NAA	10 μM	30 min– 2 hours	NE	Apparent unbundling into "randomly oriented fine strands"
Coleoptile epidermis[2c]	IAA	5 μM	30–60 min	**Increased elongation**	**More, finer filaments**
Coleoptile epidermis[2c]	IAA	10 μM	60 min	**Increased elongation**	**More, finer filaments**
Coleoptile epidermis[2c]	IAA	50 μM	30–60 min	**Increased elongation**	**More, finer filaments**
Coleoptile epidermis[2c]	2,4-D	10 μM	60 min	NE	ND
Coleoptile epidermis[2c]	NAA	10 μM	60 min	NE	**More, finer filaments**
Coleoptile epidermis[2c]	IAA	1 mM	3 hours	**Reduced elongation**	NE

Bold indicates parameters that were quantified (rather than subjectively assessed).

EZ = Elongation zone; ND = No difference; NE = Not evaluated.

[1]*Arabidopsis thaliana*; [2]Rice (*Oryza sativa*).

References: [a]Holweg et al. (2004); [b]Li et al. (2014); [c]Nick et al. (2009).[d]Rahman et al. (2007); [e]Scheuring et al. (2014).

A root will point downwards within hours of gravistimulus (Band et al., 2012). The signal of gravity vector change is transmitted by unknown mechanisms from the columella to the root elongation zone, the growing portion of the root where topside–bottomside differential growth occurs. Auxin efflux carriers relocalize along cell membranes to the direction of the gravity vector, where they direct an auxin gradient—cells accumulate more auxin in the [new] bottom side of the root and less on the [new] top—within 2–10 min of gravistimulus (Friml et al., 2002; Abas et al., 2006; Kleine-Vehn et al., 2010; Baldwin et al., 2013). The greater amount of auxin on the bottom inhibits cell expansion there; less auxin on the top allows these cells to continue to elongate. Formation of this auxin gradient depends on auxin efflux carriers, and plants with mutations in these efflux carriers exhibit gravitropic defects (Friml et al., 2002; Abas et al., 2006; Kleine-Vehn et al., 2010; Baldwin et al., 2013). Loss of signal from the DII-Venus auxin reporter, indicating auxin abundance, is visible at 60 min, and does not occur in a mutant lacking amyloplasts, for the glucose-to-starch–converting enzyme PHOSPHOGLUCOMUTASE 1 (*pgm1*; Band et al., 2012). Quantitative data in Band et al. (2012) show that the total amount of auxin in the root does not change during gravitropic response; only auxin distribution changes.

Efflux carrier trafficking and localization to redistribute auxin require an intact, dynamic actin cytoskeleton (Muday, 2000; Geldner et al., 2001; Friml et al., 2002; Mancuso et al., 2006; Dhonukshe et al., 2007; Kleine-Vehn et al., 2008). When Lat B is applied to 3-day-old Arabidopsis seedlings, plants grow significantly more slowly than control, yet are hypergravitropic, and the transcriptional auxin reporter *DR5-GUS* shows nearly twice as much expression on the bottom side 3–5 h after stimulation, indicating greater auxin flow (Hou et al., 2004). Conversely, actin-stabilizing drugs like phalloidin and JASP strongly inhibit root growth and bending after gravistimulus (Mancuso et al., 2006). Changes in Ca^{2+} and pH are reported in columella cells after gravistimulus (Scott and Allen, 1999), and also occur in "growing root tip" cytosol and extracellular media after plants are turned 90° (Morita, 2010; Monshausen et al., 2011; Toyota and Gilroy, 2013; Vanneste and Friml, 2013). Changes to second messenger concentration can regulate ABP and, therefore, actin organization during, or possibly to cause, differential growth. In the case of gravistimulus, differential growth is the "response" and results in the root pointing downwards once again (Band et al., 2012). Though actin's function with auxin in gravitropic responses is unclear, it is evident that, as in growth, dynamic actin is necessary for PAT and robust differential growth.

1.9   Known Links between Auxin and Actin

1.9.1   The Vacuole

Auxin and actin could influence growth through modulation of vacuole morphology (e.g., vacuole size and volume compared with total cell volume). In transition zone root epidermal cells, relatively high doses of the synthetic membrane-permeable auxin 1-naphthylacetic acid (250 nM NAA) induce vacuole constriction (into smaller, connected—but explicitly *not* fragmented—compartments, imaged with scanning electron microscopy) within 25 min and growth inhibition within 1 hr; in 20 hr treatments, the effect on vacuole morphology is TIR1-dependent (Lofke et al., 2015; Scheuring et al., 2015). Stabilizing or disrupting actin resulted in vacuoles whose morphologies were resistant to NAA-induced constriction (Scheuring et al., 2015). Vacuoles in mutants for *act2 act8*, *act7*, *myosin xi3KO*, and a quadruple *myosin xi4KO* were all more resistant to NAA-induced fractionation, and auxin-induced growth inhibition in these mutants was partially reduced (Scheuring et al., 2015). These studies indicate that auxin stimulates actin to reshape the vacuole which in turn inhibits cell expansion (Lofke et al., 2015; Scheuring et al., 2015). However, since these treatments examining actin were almost all 6–20 hr long (Lofke et al., 2015; Scheuring et al., 2015), it is unclear whether vacuole fractionation is the mechanism by which auxin inhibits growth in the short-term.

1.9.2   PIN-FORMED Proteins (PINs)

So far, we have referred to "auxin export proteins." The predominant auxin efflux carriers involved in PAT are PIN-FORMED proteins (PINs), named for the needlelike phenotype of PIN mutant inflorescences (Galweiler et al., 1998; Křeček et al., 2009). PINs are present in Chlorophytes and all land plants, and direct auxin flow out of cells (Křeček et al., 2009; Bennett et al., 2014; Langdale, 2014; Viaene et al., 2014). The Arabidopsis genome codes for 8 PIN isoforms: two "short" PINs that localize to organelle membranes and 6 "long" PINs that localize to the PM (Křeček et al., 2009). Most studies have focused on long PINs since they were long perceived as the most important regulators of intracellular auxin concentrations (Zhu and Geisler, 2015). These studies assumed that auxin diffuses into cells by chemiosmosis, but once deprotonated in the more alkaline cytosol, the polar IAA$^-$ molecule relies on active transport to exit (Zhu and Geisler, 2015). PINs localize to specific cell faces depending on cell type; because root cells place PIN isoforms on the face to which the PIN isoform usually polarizes, even when the protein is expressed behind another

PIN's promoter in different cell types, proper localization is thought to be encoded for by the protein itself (Wisniewska et al., 2006; Feraru and Friml, 2008).

Root cells in *PIN* mutants are shorter than wildtype but, interestingly, cell lengths are not different from wildtype as cells leave the meristem. It is only once cells enter the transition/elongation zone that *PIN* mutations affect cell size, indicating that the expansion process is aberrant (Křeček et al., 2009). Roots exhibit an endogenous gradient of auxin concentrations along the elongation zone, where auxin concentration is low as cells exit the meristem, then increases gradually but significantly through the elongation zone (Brunoud et al., 2012). Together, these data imply that PIN-directed auxin transport is particularly important for normal growth (Křeček et al., 2009; Brunoud et al., 2012). Indeed, cells in *PIN* knockout mutants would not be able to export auxin, so intracellular auxin levels would increase. In root cells, that leads to growth inhibition. Auxin apparently regulates the length of and/or the duration of a cell's sojourn in the elongation zone (Rahman et al., 2007), so an excess of auxin in *PIN* mutant root cells might trick cells into perceiving that they are at the end of the elongation zone and it is therefore time to stop elongating. Unfortunately, actin organization in PIN mutants has never been examined.

Like many PM proteins in plants, long PIN proteins constitutively cycle between the PM and the endocytic pathway (Geldner et al., 2001; Kleine-Vehn and Friml, 2008). This energy-intensive constitutive cycling likely occurs so that cells can respond rapidly to internal and environmental stimuli (Kleine-Vehn and Friml, 2008). For example, after gravistimulus, PINs in roots relocalize to different faces of a cell in order to direct auxin flow (Friml et al., 2002; Wisniewska et al., 2006; Feraru and Friml, 2008). This constitutive cycling and relocalization of PINs is actin-dependent: when Lat B and Cyt D are used to disrupt actin, PINs mislocalize (Geldner et al., 2001; Kleine-Vehn et al., 2008). Auxin-induced actin polymerization is thought to prevent PIN internalization, which in turn is hypothesized to keep auxin flowing through PM-localized PINs, stimulating cell elongation and sculpting regional expansion and cell shape (Paciorek et al., 2005; Chen et al., 2012; Lin et al., 2012; Nagawa et al., 2012). Stabilizing actin with JASP maintains PINs at the PM but disrupting actin with Lat B leads to PIN internalization (Lin et al., 2012; Nagawa et al., 2012). However, actin response to auxin was never directly visualized in these studies, which also used the fungal toxin Brefeldin A (BFA), under the assumption that the drug specifically inhibits endosome recycling, when in fact BFA targets a wider range of protein transport pathways (Paciorek et al., 2005; Chen et al., 2012; Lin et al., 2012;

Nagawa et al., 2012; Jásik and Schmelzer, 2014; Jásik et al., 2016). A more recent study using the photoconvertible fluorescent reporter Dendra2 shows that auxin stimulates PIN2 synthesis and that most PIN2s observed in BFA bodies were actually newly synthesized (Jásik et al., 2016). Although this group did not investigate the effect of disrupting actin on PIN endocytosis, their results imply that auxin treatments do not prevent PIN endocytosis. Hence, it is unclear why stabilizing actin filaments appears to prevent PIN internalization but disrupting actin filaments increases PIN internalization. Perhaps these observations result from more general changes in trafficking: actin stabilization produces reliable "roads" that can traffic the newly synthesized PINs to the PM more effectively; however, when roads are disrupted, proteins cannot reach their destination. Experiments that visualize actin and PINs are needed to determine whether auxin triggers actin accumulations that prevent PIN endocytosis and alter growth.

1.9.3 ATP-Binding Cassette/B and TWISTED DWARF 1 (ABCBs and TWD1)

The ATP-binding cassette/B (ABCB; also known as MULTIDRUG RESISTANCE, MDR or P-GLYCOPROTEINS, PGP) family of phosphoglycoprotein transporters exists in all Eukaryotes (Zazímalová et al., 2010). ABCB function in auxin transport has been studied less than PINs; however, we will briefly summarize what is known about ABCBs, growth, and actin.

ABCB proteins are thought to function for the most part in "long-distance auxin transport" and development rather than acute environmental responses (Geisler et al., 2005; Peer et al., 2011; Cho et al., 2012). There are 21 ABCB family members in Arabidopsis but only the semi-redundant auxin exporters ABCB1/PGP1 and ABCB19/MDR1/PGP19, and the auxin importer/exporter ABCB4/MDF4/PGP4, are known to participate in auxin signaling (Geisler et al., 2005; Cho et al., 2012). Expression of plant ABCB isoforms in yeast and mammalian cells shows ABCB1 and ABCB19 auxin export and ABCB4 auxin import/export capabilities (Geisler et al., 2005; Terasaka et al., 2005). Mutants *abcb1, abcb4,* and *abcb19* are dwarfed compared with wildtype, but organ formation appears comparable to wildtype plants (Noh et al., 2001; Geisler et al., 2005; Terasaka et al., 2005). Root hairs are longer in *abcb4* and shorter in *ABCB4-OX*: without the major auxin importer/exporter in this cell type, cells fail to maintain intracellular auxin concentrations conducive to growth (Cho et al., 2007).

ABCBs are PM-localized and differentially expressed throughout plant tissues (Noh et al., 2001; Geisler et al., 2005; Blakeslee et al., 2007; Titapiwatanakun and Murphy, 2009). Unlike

PINs, ABCB subcellular localization is largely nonpolar; with the exception of a few tissues (ABCB1 in the root elongation zone endodermis and cortex), ABCBs stably localize around entire cell perimeters (Geisler et al., 2005; Cho et al., 2007; Titapiwatanakun and Murphy, 2009), and do not relocalize to direct auxin flow (Geisler et al., 2005; Cho et al., 2012). ABCB trafficking is slower, or perhaps simply less, than that of PINs: when Cyt D disrupted actin filaments, PINs mislocalized in 2 h while ABCB4 took 3 h to mislocalize. The ABCB4 protein localization appears less sensitive to perturbation by both BFA (disruption to protein trafficking) and Cyt D (inhibition of actin turnover) than PINs (Cho et al., 2012), which reinforces that ABCB localization is more stable than PIN placement. Although ABCBs do not move to direct auxin flow, IAA induces expression of all three auxin transporting ABCBs in high dose, long-term treatments (1–10 µM over 3 h to 5 d; Noh et al., 2001; Geisler et al., 2005; Terasaka et al., 2005).

After exogenous IAA applications, rootward PAT is reduced in *abcb19* and *abcb1 abcb19* but not in *abcb1*; shootward PAT within shoots is not affected in mutants for either isoform or the double mutant (Noh et al., 2001; Geisler et al., 2005). Interestingly, *abcb19* and *abcb1 abcb19* hypocotyls are hypergravitropic because plants respond to gravistimulus faster (Noh et al, 2003). PIN1 is constitutively mislocalized in *abcb19* and *abcb1 abcb19,* so the authors hypothesize that between the loss of ABCB(s) and PIN1 delocalization, auxin flow in the mutants is "more differential" (Noh et al., 2003). Conversely, *abcb4* roots are less gravitropic compared with wildtype, though less agravitropic than other auxin import protein mutants, indicating the importance of auxin import in gravitropism (Terasaka et al., 2005).

Actin organization in *ABCB* mutants has never been examined but actin, notably the ACT7 isoform, is necessary for ABCB localization (Zhu et al., 2016). All three auxin-transporting ABCBs and PIN1 and PIN2 mislocalize from the PM in *act7-4*, as well as in a mutant for TWISTED DWARF 1 (*twd1*), a chaperone that is necessary to traffic ABCBs from the ER to the PM. In fact, TWD1 has been shown to be a crucial integrator between actin, auxin transport, and ABCBs. A study on *twd1* is among the only investigations that, in examining actin's role in auxin transport and/or transport inhibition by NPA, visualizes actin organization and dynamics (Zhu et al., 2016). PAT is reduced in *twd1* and *act7-4* roots (Zhu et al., 2016). The actin array in both hypocotyls and roots of a *twd1* mutant is less bundled and denser than wildtype, and unlike wildtype plants, actin filament organization does not become more bundled after NPA treatment, indicating that NPA modifies actin bundling through TWD1. Individual filament dynamics in *twd1*

hypocotyls show decreased turnover (longer filament length and less filament severing) as well as increased filament debundling frequencies compared with wildtype, which the authors assert likely occurs "in a TWD1-independent manner" (Zhu et al., 2016). These data indicate that in wildtype cells, TWD1 increases filament turnover, and either maintains actin bundles or competes with/inhibits an unidentified actin debundling protein to decrease debundling frequency. Significantly, these results corroborate that a lack of actin debundling (or, conversely, more actin bundles), as induced by NPA, inhibits PAT (Zhu et al., 2016). In conflict with the hypothesis that longer filament lengths and lifetimes correlate with longer cells, filaments in *twd1* exhibit significantly increased—by nearly 50%!—filament lifetimes but shorter cells and shorter hypocotyls (Bailly, et al., 2014; Zhu et al., 2016). It will be interesting to see future studies on actin response to auxin in *twd1* and *act7*.

1.9.4 AUXIN BINDING PROTEIN 1 (ABP1)

AUXIN BINDING PROTEIN 1 (ABP1) was long judged to be the extracellular auxin receptor upstream of actin reorganization. ABP1 is conserved across plants, and the alga *Chlorella sorokiniana* contains a highly conserved ortholog, complete with amino acids important for binding auxin (Khasin et al., 2018). No *Aux/IAA* transcriptional repressors are found in the *C. sorokiniana* genome, indicating that ABP1 is part of an ancient auxin signaling pathway (Khasin et al., 2018). ABP1 is the sole isoform in Arabidopsis (Chen et al., 2001). The ABP1 protein contains no transmembrane domains and most of the protein localizes to the ER (the protein contains an ER retention signal), with only a small amount observed in the apoplast, where ABP1 sits on the extracytoplasmic side of the PM (Jones and Herman, 1993; Sauer and Kleine-Vehn, 2011; Sauer et al., 2013). Traditionally, ABP1 is considered a positive regulator of auxin response and upstream of fast, nontranscriptional responses to auxin, whereas TIR1 regulates auxin-related transcriptional responses (Effendi et al., 2011; Sauer and Kleine-Vehn, 2011; Chen et al., 2014b). A cell-surface auxin receptor is thought necessary for polarized growth: to form polarized auxin gradients, cells must have a mechanism by which they can perceive signal direction. Once auxin is inside a cell, there is no way to determine whence the signal arrived, so any directional perception mechanism must be in place before auxin enters the cell (Sauer and Kleine-Vehn, 2011).

The traditional model considers ABP1 a PM protein that, together with its coreceptor TRANSMEMBRANE KINASE (TMK), binds auxin molecules and transduces the extracellular

auxin signal to ROPs (Lin et al., 2012; Nagawa et al., 2012), activating them in a dose-dependent way (Xu et al., 2014). Once activated, ROPs regulate actin polymerization towards growth-related effects (Sauer and Kleine-Vehn, 2011; Xu et al., 2014; Zhu and Geisler, 2015). ABP1-mediated actin accumulation is connected with inhibition of PIN endocytosis—PIN endocytosis occurs when actin is disrupted, but endocytosis fails to occur when actin is stabilized (Lin et al., 2012; Nagawa et al., 2012). This inhibition of PIN endocytosis is postulated to regulate auxin distribution in roots and epidermal pavement cells by controlling PIN and cell polarity (Lin et al., 2012; Nagawa et al., 2012). Additionally, growth itself was implied to occur through the ABP1 mechanism. Inactivating ABP1 resulted in shorter root lengths since ABP1 presence enables cells to respond to auxin (Tromas et al., 2009). Auxin-induced rapid elongation in hypocotyls was at first shown to require ABP1 but not TIR1 (Sauer and Kleine-Vehn, 2011; Zhu and Geisler, 2015); however now, rapid auxin-induced growth effects—both hypocotyl growth stimulation and root growth inhibition—are demonstrated to depend on TIR1 (Fendrych et al., 2016, 2018).

There is a plethora of data to support a role for ABP1 in auxin signaling. ABP1 directly binds auxins, and auxin can displace anti-ABP1 antibodies from protoplasts (Napier and Venis, 1990; Barbier-Brygoo et al., 1991; Stotz and Hertel, 1994; Tian et al., 1995). Anti-ABP antibodies block typical auxin-induced PM depolarization (Barbier-Brygoo et al., 1991). An *ABP1* T-DNA insertion mutant is embryonic lethal, making the protein difficult to study in vivo (Chen et al., 2001), but plants that are heterozygous for *ABP1* mutant alleles (*abp1/ABP1*) exhibit multiple growth-related defects (Effendi et al., 2011). Compared with wildtype plants, *abp1/ABP1* mutant plants are less phototropic, less gravitropic, produce less auxin-induced transcripts, and have aberrant PAT (Effendi et al., 2011). Interestingly, only shootward transport of radioactive auxin applied to the root apex is abnormal; rootward transport of auxin applied to the base of the *abp1/ABP1* root (i.e., transport towards the root apex) does not differ from wildtype (Effendi et al., 2011). Induced overexpression of *ABP1* generates leaf cells and plants that grow larger than wildtype in response to the same dose of auxin (Jones et al., 1998). A crystal structure for ABP1 in complex with NAA has been solved (Woo et al., 2002), and amino acid residues necessary for auxin binding and inhibition of PIN endocytosis have been identified (Grones et al., 2018). These are just a selection of studies that establish the necessity for ABP1 in auxin signaling; therefore ABP1's importance in auxin signaling should be a closed case.

However, ABP1 has been controversial, and even its discoverer considered its role in auxin signaling to be "a red herring" (Hertel, 1995; Habets and Offringa, 2015). Because a total knockout of *ABP1* is embryonic lethal (Chen et al., 2001), many studies investigating ABP1 use less compelling genetic evidence like point mutants, heterozygotes, inducible knockdowns, or overexpression constructs (Habets and Offringa, 2015). Most ABP1 localizes to the ER, not the PM (Jones and Herman, 1993), but data show that ABP1 can bind auxin only at a fairly acidic pH 5.5 (Tian et al., 1995). At the pH of the ER lumen and the cytosol, close to pH 7.0, ABP1 binds IAA poorly, leading to questions about the purpose of abundant ABP1 where it cannot function in its putative auxin binding role (Tian et al., 1995). In fact, ABP1 binds the synthetic NAA with $1000 \times$ higher affinity than the protein has for the most abundant natural auxin IAA (Napier and Venis, 1990; Stotz and Hertel, 1994; Hertel, 1995).

Furthermore, many, if not most, of the studies that establish ABP1 as necessary for auxin signal perception and transduction across the PM are based wholly or in part on experiments that utilize the membrane permeable auxin NAA (Barbier-Brygoo et al., 1991; Jones et al., 1998; Tromas et al., 2009; Lin et al., 2012; Nagawa et al., 2012; Chen et al., 2014b; Xu et al., 2014). While a legitimate argument can be made for using NAA to study auxin efflux proteins like PINs— a membrane permeable auxin like NAA ensures that auxin perception and entrance to a cell are not an issue and that cells receive a similar dose of auxin—using a PM-permeable auxin to study auxin perception by a PM-localized protein is inappropriate. After all, it is known that once auxin enters a cell, the hormone is perceived by TIR1, which binds NAA (Dharmasiri et al., 2005a; Kepinski and Leyser, 2005). Even assuming TIR1 is in a completely different auxin signaling pathway than ABP1 (Chen et al., 2001), stimulating TIR1 with auxin will confuse results. For example, in the ROP activation study, NAA treatments were used to demonstrate the dose-dependent effect of auxin on ROP activation (Xu et al., 2014). But, it is not clear that ROP activation is not, for example, dependent on TIR1, since it was NAA treatments that stimulated ROP activation and the effect on ROP activation was not examined in a *tir1* mutant (Xu et al., 2014). Many new studies demonstrate that TIR1 does play a role in short-term auxin signaling events that were previously professed to be TIR-independent, such as root growth inhibition and PM depolarization (Fendrych et al., 2016; Dindas et al., 2018; Fendrych et al., 2018; Paponov et al., 2019). And NAA was not employed where it should have been. Some auxin signaling mutants

can be rescued by NAA (Marchant et al., 1999), but no attempt was made to complement embryonic lethality of *abp1* mutants with this auxin variant (Chen et al., 2001).

The most condemning evidence against ABP1's role in short-term auxin signaling comes from a paper in which the authors knock out the protein completely using CRISPR technology so no detectable ABP1 protein is produced (Gao et al., 2015). Plant growth appears equivalent to wildtype, and auxin induces transcription of tested genes equivalent to wildtype (Gao et al., 2015). A second study from the same lab demonstrates that the embryonic lethal *abp1-1* allele causes a disruption in an adjacent gene, *BELAYA SMERT* (*BSM*; Chen et al., 2001; Dai et al., 2015; Habets and Offringa, 2015), which is necessary for plastid transcription and whose mutant (*bsm*) is embryonic lethal (Babiychuk et al., 2011). Since the importance of ABP1 in auxin signaling is in serious doubt, there remains an open question of what protein transmits an incoming auxin signal to the cytoskeleton.

1.9.5   AUXIN RESISTANT 1 (AUX1)

Auxin transport proteins that exclusively import auxin are the final auxin transporter class. A mutant for *AUXIN RESISTANT 1/WAVY ROOTS 5/P83* (*AUX1/WAV5*) was isolated from a screen for auxin-resistant and agravitropic mutants and other alleles followed; these turned out to be the protein AUX1 (Maher and Martindale, 1980; Pickett et al., 1990). The *aux1* mutant (initially called *P83*) exhibits at least an order of magnitude less root growth inhibition by the same doses of IAA and the synthetic auxin 2,4-D compared with wildtype roots. Unlike wildtype roots, which exhibit positive gravitropism where roots grow towards the ground, *aux1* mutant roots grow in all directions, and not into agar (Maher and Martindale, 1980).

At least one *AUX1* homolog appears in all land plants as well as several Chlorophytes (Khasin et al., 2018; Singh et al., 2018). AUX1 is one of 4 members of the AUX/LIKE AUX1 (AUX/LAX1–3) family in Arabidopsis, not to be confused with the transcriptional repressors Aux/IAA (Swarup and Péret, 2012; Peret et al., 2012; Swarup and Bennett, 2014). AUX/LAX are members of the Amino acid/auxin permease (AAAP) family which covers hundreds of proteins throughout Eukaryotes, each with a different level of specificity for amino acids or amino acid-like substrates (Young et al., 1999; Saier, Jr, 2000). AAAPs are membrane proteins with 10–12 transmembrane domains (Young et al., 1999; Saier, Jr, 2000; Swarup et al., 2004). AUX1 likely has 11 transmembrane domains; however, at this point, no crystal structure has been defined

(Singh et al., 2018). The AUX/LAXes are differentially but complementarily expressed in plant tissues with AUX1 expressed in root epidermal cells as well as the lower part of root stele. Expression of all 4 *AUX/LAX* genes is induced by auxin treatments (Paponov et al., 2008; Peret et al., 2012), indicating the importance of auxin importers in auxin response (Band et al., 2014).

Aside from their lack of gravitropism and root growth inhibition by auxin, *aux/lax* plants do not exhibit vast growth defects. *aux1* mutant root cells are larger, plants have fewer lateral roots, and root hairs are shorter (see **Chapter 2**; Pitts et al., 1998; Ugartechea-Chirino et al., 2010; Peret et al., 2012). Interestingly, AUX1 is the only family member necessary for root gravitropism and root growth inhibition by auxin (Peret et al., 2012), likely because it is the sole isoform expressed in the cell type crucial for these responses—root epidermal cells. Promoter swap experiments show that *LAX2* (75.4% sequence identity to *AUX1*) cannot restore proper gravitropic responses to *aux1*, even when expressed behind the *AUX1* promoter, demonstrating that each protein family member is substantially different (Peret et al., 2012; Swarup and Péret, 2012). Lack of root gravitropic response in *aux1* can be rescued by treatment with the membrane permeable auxin NAA (Marchant et al., 1999), which mutant plants appear to take up, though by appearances somewhat less than do wildtype plants (Hayashi et al., 2014). Shootward and rootward PAT in *aux1* roots is also reduced (Swarup et al., 2001; Band et al., 2014).

AUX1 binds to IAA with high affinity (Yang et al., 2006; Carrier et al., 2008). AUX1 heterologously expressed in frog eggs binds IAA with a K_m of ≈ 800 nM (Yang et al., 2006) while ABP1 binds IAA with a K_m of just less than 10 µM (Stotz and Hertel, 1994; Hertel, 1995). The AUX1 protein is responsible for at least 80% of auxin uptake to Arabidopsis root hairs and $\approx 75\%$ of uptake into protoplasts; protoplast uptake was diminished $\approx 80\%$ in the mutant *aux1-22* (Rutschow et al., 2014; Dindas et al., 2018). As a H^+ symporter, AUX1 transports $2\,H^+$ for each auxin molecule it transports (Dindas et al., 2018; Singh et al., 2018); a decrease in cytosolic pH accompanying auxin transport could regulate ABPs and actin. The loss of auxin uptake by *aux1* mutant roots reduces gravitropism and enables growth in the presence of moderate doses of IAA, but NAA inhibits *aux1* growth within seconds, similarly to wildtype (Fendrych et al., 2018). However, like the original study that identified *aux1* (Maher and Martindale, 1980), mutant root growth can be inhibited by high doses of auxin (Fendrych et al., 2018).

Like PIN proteins, in most cell types, AUX1 is generally polarized to discrete cell faces (Swarup et al., 2001; Kleine-Vehn et al., 2006). In the stele, AUX1 localizes to the upper PM,

importing auxin as it flows rootward from the shoot. In the root epidermis, the protein localizes primarily to the upper and lower PM. In columella gravisensing cells, AUX1 is more dynamic and can be seen around entire cell perimeters; in this position, AUX1 can rapidly move auxin upon gravistimulus (Swarup et al., 2001; Kleine-Vehn et al., 2006). Like PINs, AUX1 localization to particular cell faces is actin-dependent (Kleine-Vehn et al., 2006; Du et al., 2011). Lat B causes both PIN1 and AUX1 to mislocalize in root cells (AUX1 is more sensitive to disruption by Lat B); TIBA, which bundles actin filaments, inhibits AUX1 movement in live cell imaging observations (Kleine-Vehn et al., 2006; Rahman et al., 2007). Unlike PIN localization, AUX1 targeting is not as susceptible to BFA, and occurs through a different mechanism than typical BFA-targeted trafficking (Kleine-Vehn et al., 2006).

Clearly, AUX1 is necessary for aspects of auxin signaling, intact actin dynamics are required for AUX1 subcellular localization, and auxin stimulates actin reorganization. A role in short-term auxin signaling to the cytoskeleton was filled by ABP1, and until ABP1's role in auxin reception was recently repudiated (Dai et al., 2015; Gao et al., 2015), AUX1 was not considered to play any substantial role in auxin signaling. Many considered AUX1's contribution to auxin uptake as insignificant: IAAH can diffuse from the acidic apoplast through the PM, so intracellular auxin concentrations and PAT must be controlled solely by export (Zhu and Geisler, 2015). With plenty of IAAH constantly diffusing through the PM, active import would not regulate intracellular auxin levels; only removing excess auxin through active export could control intracellular auxin concentration (Geisler et al 2014; Zhu & Geisler 2015). And perhaps the restored root growth inhibition to *aux1* in the presence of very high auxin *is* a function of the hormone's ability to diffuse (Maher and Martindale, 1980; Fendrych et al., 2018). However, it stands to reason that if active auxin import to cells plays only a minor role in growth, with free diffusion doing most of the work, *aux1* mutant cells would not exhibit strong insensitivity to moderate doses of IAA. Exogenous IAA would readily become IAAH in the apoplast and easily diffuse, so loss of PM-bound AUX1 would be a nonissue. But clearly, *aux1* mutants exhibit insensitivity to IAA while responding to the membrane permeable NAA, indicating that active auxin import does matter (Marchant et al., 1999; Hayashi et al., 2014; Band et al., 2014). Furthermore, the recent work showing that AUX1 is necessary for rapid root growth inhibition by IAA (Fendrych et al., 2018), and responsible for roughly 80% of IAA uptake in root hairs (Dindas et al 2018), especially in

light of the vacancy left by ABP1, implicate AUX1 as a potentially important player, upstream of auxin-induced actin reorganization, that affects plant cell growth.

1.10 Statement of Problem: What Connects Auxin Signaling to the Actin Cytoskeleton Is Unknown

Actin array response to short-term auxin treatments has never been evaluated. The sole work examining actin response to auxin at ≤ 30 min examined cells where actin was ectopically bundled by the actin reporter YFP-mTalin (Nick et al., 2009), but now, actin reporters that do not cause such artifacts exist and are in wide use (Sheahan et al., 2004; Staiger et al., 2009; Dyachok et al., 2014). Auxin stops root growth, which depends on actin, within seconds (Hejnowicz and Erickson, 1968; Fendrych et al., 2018), but whether actin reorganizes to reflect (or cause) that growth cessation is unknown. To decisively uncover relationships between extent of actin organization and degree of cell expansion, testing the hypothesis that "more organized" actin correlates with more expansion, in **Chapter 2**, we characterize actin organization in wildtype root epidermal cells, a cell type that exhibits an inherent expansion gradient. If there is a direct relationship between actin organization and cell expansion, we should find a strong predictive relationship between cell length (but not cell width, which remains essentially constant throughout the visible elongation zone) in conjunction with characteristics of an "organized" actin array, such as bundling, parallelness, and longitudinality. To further test this model (summarized in **Figure 1.3**), we examine actin reorganization in response to short-term auxin treatments at growth-inhibitory doses, with the expectation that a treatment that inhibits growth will rapidly trigger a "less organized" actin array. We measure the individual filament behaviors that cause the auxin-induced actin array reorganization. Together, these data document the first quantitative assessment of actin response to short-term auxin treatments. After the recent findings that demonstrate ABP1's unimportance in short-term auxin signaling (Dai et al., 2015; Gao et al., 2015), what connects auxin signaling to the actin cytoskeleton is unknown. Based on extensive circumstantial evidence, we suspect that the auxin transporter AUX1 has been long overlooked in this role. We use knockout *aux1* mutants to test the hypothesis that AUX1 is in fact necessary for short-term auxin signaling to actin.

1.11 Acknowledgement

1.12 References

Abas, L., Benjamins, R., Malenica, N., Paciorek, T., Wiśniewska, J., Moulinier-Anzola, J.C., Sieberer, T., Friml, J., and Luschnig, C. (2006). Intracellular trafficking and proteolysis of the *Arabidopsis* auxin-efflux facilitator PIN2 are involved in root gravitropism. Nat. Cell Biol. 8: 249–256.

Abel, S., Oeller, P.W., and Theologist, A. (1994). Early auxin-induced genes encode short-lived nuclear proteins. Biochemistry 91: 326–330.

Abu-Abied, M., Belausov, E., Hagay, S., Peremyslov, V., Dolja, V., and Sadot, E. (2018). Myosin XI-K is involved in root organogenesis, polar auxin transport, and cell division. J. Exp. Bot. 69: 2869–2881.

Akkerman, M., Overdijk, E.J.R., Schel, J.H.N., Emons, A.M.C., and Ketelaar, T. (2011). Golgi body motility in the plant cell cortex correlates with actin cytoskeleton organization. Plant Cell Physiol. 52: 1844–1855.

Allwood, E.G., Smertenko, A.P., and Hussey, P.J. (2001). Phosphorylation of plant actin-depolymerising factor by calmodulin-like domain protein kinase. FEBS Lett. 499: 97–100.

Armour, W.J., Barton, D.A., Law, A.M.K., and Overall, R.L. (2015). Differential growth in periclinal and anticlinal walls during lobe formation in Arabidopsis cotyledon pavement cells. Plant Cell 27: 2484–2500.

Arsuffi, G. and Braybrook, S.A. (2018). Acid growth: An ongoing trip. J. Exp. Bot. 69: 137–146.

Babiychuk, E., Vandepoele, K., Wissing, J., Garcia-Diaz, M., De Rycke, R., Akbari, H., Joubes, J., Beeckman, T., Jansch, L., Frentzen, M., Van Montagu, M.C.E., and Kushnir, S. (2011). Plastid gene expression and plant development require a plastidic protein of the mitochondrial transcription termination factor family. Proc. Natl. Acad. Sci. 108: 6674–6679.

Baldwin, K.L., Strohm, A.K., and Masson, P.H. (2013). Gravity sensing and signal transduction in vascular plant primary roots. Am. J. Bot. 100: 126–142.

Bailly, A.,Wang, B., Zwiewka, M., Pollmann, S., Schenck, D., Lüthen, H., Schulz, A., Friml, J., and Geisler, M. (2014). Expression of TWISTED DWARF1 lacking its in-plane membrane anchor leads to increased cell elongation and hypermorphic growth. Plant J. 77: 108–118.

Baluska, F., Barlow, P.W., and Volkmann, D. (2001a). Chapter 26 Actin and myosin VIII in developing root apex cells. Pp. 457–476 in Actin: A Dynamic Framework for Multiple Plant Cell Functions, C.J. Staiger, F. Baluska, D. Volkmann, and P.W. Barlow, eds. Springer: Dordrecht.

Baluska, F., Jasik, J., Edelmann, H.G., Salajová, T., and Volkmann, D. (2001b). Latrunculin B-induced plant dwarfism: Plant cell elongation is F-actin-dependent. Dev. Biol. 231: 113–24.

Baluška, F., Salaj, J., Mathur, J., Braun, M., Jasper, F., Šamaj, J., Chua, N.-H., Barlow, P.W., and Volkmann, D. (2000). Root hair formation: F-actin-dependent tip growth is initiated by local assembly of profilin-supported f-actin meshworks accumulated within expansin-enriched bulges. Dev. Biol. 227: 618–632.

Baluska, F., Vitha, S., Barlow, P.W., and Volkmann, D. (1997). Rearrangements of F-actin arrays in growing cells of intact maize root apex tissues: a major developmental switch occurs in the postmitotic transition region. Eur. J. Cell Biol. 72: 113–121.

Baluska, F., Wojtaszek, P., Volkmann, D., and Barlow, P. (2003). The architecture of polarized cell growth : the unique status of elongating plant cells. BioEssays 25: 569–576.

Band, L.R., Úbeda-Tomás, S., Dyson, R.J., Middleton, A.M., Hodgman, T.C., Owen, M.R., Jensen, O.E., Bennett, M.J., and King, J.R. (2012). Root gravitropism is regulated by a transient lateral auxin gradient controlled by a tipping-point mechanism. Proc. Natl. Acad. Sci. 109: 4668–4673.

Band, L.R., Wells, D.M., Fozard, J.A., Ghetiu, T., French, A.P., Pound, M.P., Wilson, M.H., Yu, L., Li, W., Hijazi, H.I., Oh, J., Pearce, S.P., Perez-Amador, M.A., Yun, J., Kramer, E., Alonso, J.M., Godin, C., Vernoux, T., Hodgman, T.C., Pridmore, T.P., Swarup, R., King, J.R., and Bennett, M.J. (2014). Systems analysis of auxin transport in the *Arabidopsis* root apex. Plant Cell 26: 862–75.

Bao, C., Wang, J., Zhang, R., Zhang, B., Zhang, H., Zhou, Y., and Huang, S. (2012). Arabidopsis *VILLIN2* and *VILLIN3* act redundantly in sclerenchyma development via bundling of actin filaments. Plant J. 71: 962–975.

Barbier-Brygoo, H., Ephritikhine, G., Klambt, D., Maurel, C., Palme, K., Schel, J., and Guern, J. (1991). Perception of the auxin signal at the plasma membrane of tobacco mesophyll protoplasts. 1: 83–93.

Bartel, B. (1997). Auxin Biosynthesis. Annu. Rev. Plant Physiol. Plant Mol. Biol. 48: 51–66.

Baskin, T.I. (2005). Anisotropic expansion of the plant cell wall. Annu. Rev. Cell Dev. Biol. 21: 203–222.

Basu, D., El-Assal, S.E.-D., Le, J., Mallery, E.L., and Szymanski, D.B. (2004). Interchangeable functions of *Arabidopsis* PIROGI and the human WAVE complex subunit SRA1 during leaf epidermal development. Development 131: 4345–4355.

Basu, D., Le, J., Zakharova, T., Mallery, E.L., and Szymanski, D.B. (2008). A SPIKE1 signaling complex controls actin-dependent cell morphogenesis through the heteromeric WAVE and ARP2/3 complexes. Proc. Natl. Acad. Sci. 105: 4044–4049.

Battey, N.H., James, N.C., Greenland, A.J., and Brownlee, C. (1999). Exocytosis and endocytosis. Plant Cell 11: 643–659.

Bennett, T.A., Liu, M.M., Aoyama, T., Bierfreund, N.M, Braun, M., Coudert, Y., Dennis, R.J., O'Connor, D., Wang, X.Y., White, C.D., Decker, E.L., Reski, R., and Harrison, J.C. (2014). Plasma membrane-targeted PIN proteins drive shoot development in a moss. Curr. Biol. 24: 2776–2785.

Bernstein, B.W. and Bamburg, J.R. (2010). ADF/Cofilin: A functional node in cell biology. Trends Cell Biol. 20: 187–195.

Bibeau, J.P., Kingsley, J.L., Furt, F., Tüzel, E., and Vidali, L. (2017). F-actin mediated focusing of vesicles at the cell tip is essential for polarized growth. Plant Physiol. 176: 352–363.

Blakeslee, J.J., Bandyopadhyay, A., Lee, O.R., Mravec, J., Titapiwatanakun, B., Sauer, M., Makam, S.N., Cheng, Y., Bouchard, R., Adamec, J., Geisler, M., Nagashima, A., Sakai, T., Martinoia, E., Friml, J., Peer, W.A., and Murphy, A.S. (2007). Interactions among PIN-FORMED and P-glycoprotein auxin transporters in *Arabidopsis*. Plant Cell 19: 131–47.

Blancaflor, E.B. (2013). Regulation of plant gravity sensing and signaling by the actin cytoskeleton. Am. J. Bot. 100: 143–152.

Blancaflor, E.B., and S. Gilroy. (2000). Plant cell biology in the new millennium: New tools and new insights. Am. J. Bot. 87: 1547–1560.

Blanchoin, L. and Amann, K.J., Higgs, H.N., Marchand, J.-B., Kaiser, D.A., and Pollard, T.D. (2000). Direct observation of dendritic actin filament networks nucleated by Arp2/3 complex and WASP/Scar proteins. Nature 404: 1007–1011.

Blanchoin, L. and Staiger, C.J. (2010). Plant formins: Diverse isoforms and unique molecular mechanism. Biochim. Biophys. Acta Mol. Cell Res. 1803: 201–206.

Bonner, J. (1934). The relation of hydrogen ions to the growth rate of the Avena coleoptile. Protoplasma 21: 406–423.

Boot, K.J.M., Libbenga, K.R., Hille, S.C., Offringa, R., and van Duijn, B. (2012). Polar auxin transport: an early invention. J. Exp. Bot. 63: 4213–4218.

Boutté, Y., Ikeda, Y., and Grebe, M. (2007). Mechanisms of auxin-dependent cell and tissue polarity. Curr. Opin. Plant Biol. 10: 616–623.

Bowman, J.L., Briginshaw, L.N., Fisher, T.J., and Flores-Sandoval, E. (2019). Something ancient and something neofunctionalized—evolution of land plant hormone signaling pathways. Curr. Opin. Plant Biol. 47: 64–72.

Brumos, J., Robles, L.M., Yun, J., Vu, T.C., Jackson, S., Alonso, J.M., and Stepanova, A.N. (2018). Local auxin biosynthesis is a key regulator of plant development. Dev. Cell 47: 306–318.

Brunoud, G., Wells, D.M., Oliva, M., Larrieu, A., Mirabet, V., Burrow, A.H., Beeckman, T., Kepinski, S., Traas, J., Bennett, M.J., and Vernoux, T. (2012). A novel sensor to map auxin response and distribution at high spatio-temporal resolution. Nature 482: 103–6.

Burke, T.A., Christensen, J.R., Barone, E., Suarez, C., Sirotkin, V., and Kovar, D.R. (2014). Homeostatic actin cytoskeleton networks are regulated by assembly factor competition for monomers. Curr. Biol. 24: 579–585.

Butler, J.H., Hu, S., Brady, S.R., Dixon, M.W., and Muday, G.K. (1998). In vitro and in vivo evidence for actin association of the naphthylphthalamic acid-binding protein from zucchini hypocotyls. Plant J. 13: 291–301.

Cabeen, M.T. and Jacobs-Wagner, C. (2010). The bacterial cytoskeleton. Annu. Rev. Genet. 44: 365–92.

Cai, C., Henty-Ridilla, J.L., Szymanski, D.B., and Staiger, C.J. (2014). Arabidopsis myosin XI: a motor rules the tracks. Plant Physiol. 166: 1359–70.

Calderon Villalobos, L.I.A., Lee, S., De Oliveira, C., Ivetac, A., Brandt, W., Armitage, L., Sheard, L.B., Tan, X., Parry, G., Mao, H., Zheng, N., Napier, R., Kepinski, S., and Estelle, M. (2012). A combinatorial TIR1/AFB–Aux/IAA co-receptor system for differential sensing of auxin. Nat. Chem. Biol. 8: 477–485.

Cao, L., Henty-Ridilla, J.L., Blanchoin, L., and Staiger, C.J. (2016). Profilin-dependent nucleation and assembly of actin filaments controls cell elongation in Arabidopsis. Plant Physiol. 170: 220–33.

Cardenas, L., Vidali, L., Domınguez, J., Perez, H., Sanchez, F., Hepler, P.K., and Quinto, C. (1998). Rearrangement of actin microfilaments in plant root hairs responding to *Rhizobium etli* nodulation signals. Plant Physiol. 116: 871–877.

Carlier, A.M., Laurent, V., Santolini, J., Melki, R., Xia, G., Hong, Y., Chua, N., Pantaloni, D., Laurent, V., Santolini, J., and Didry, D. (1997). Actin depolymerizing factor (ADF/Cofilin) enhances the rate of actin depolymerizing filament turnover : Implication in actin-based motility. J. Cell Biol. 136: 1307–1322.

Carrier, D.J., Bakar, N.T.A., Swarup, R., Callaghan, R., Napier, R.M., Bennett, M.J., and Kerr, I.D. (2008). The binding of auxin to the Arabidopsis auxin influx transporter AUX1. Plant Physiol. 148: 529–35.

Chapman, E.J., Greenham, K., Castillejo, C., Sartor, R., Bialy, A., Sun, T., and Estelle, M. (2014). hypocotyl transcriptome reveals auxin regulation of growth-promoting genes through GA-dependent and -independent pathways. PLoS One 7: e36210.

Chen, J., Ullah, H., Young, J.C., Sussman, M.R., and Jones, A.M. (2001). ABP1 is required for organized cell elongation and division in *Arabidopsis* embryogenesis. Genes Dev. 15: 902–911.

Chen, Q., Dai, X., De-Paoli, H., Cheng, Y., Takebayashi, Y., Kasahara, H., Kamiya, Y., and Zhao, Y. (2014a). Auxin overproduction in shoots cannot rescue auxin deficiencies in Arabidopsis roots. Plant Cell Physiol. 55: 1072–1079.

Chen, X., Grandont, L., Li, H., Hauschild, R., Paque, S., Abuzeineh, A., Rakusová, H., Benkova, E., Perrot-Rechenmann, C., and Friml, J. (2014b). Inhibition of cell expansion by rapid ABP1-mediated auxin effect on microtubules. Nature 516: 90–93.

Chen, X., Naramoto, S., Robert, S., Tejos, R., Löfke, C., Lin, D., Yang, Z., and Friml, J. (2012). ABP1 and ROP6 GTPase signaling regulate clathrin-mediated endocytosis in *Arabidopsis* roots. Curr. Biol. 22: 1326–1332.

Cho, M., Lee, S.H., and Cho, H.-T. (2007). P-Glycoprotein4 displays auxin efflux transporter-like action in *Arabidopsis* root hair cells and tobacco cells. Plant Cell 19: 3930–3943.

Cho, M., Lee, Z.-W., and Cho, H.-T. (2012). ATP-binding cassette B4, an auxin-efflux transporter, stably associates with the plasma membrane and shows distinctive intracellular trafficking from that of PIN-FORMED proteins. Plant Physiol. 159: 642–54.

Cooper, J. (1987). Effects of cytochalasin on actin filaments. Cold Spring Harb. Symp. Quant. Biol. 37: 585–593.

Cosgrove, D.J. (1998). Cell wall loosening by expansins. Plant Physiol. 118: 333–339.

Cosgrove, D.J. (2005). Growth of the plant cell wall. Nat. Rev. Mol. Cell Biol. 6: 850–861.

Cosgrove, D.J. (2018). Diffuse growth of plant cell walls. Plant Physiol. 176: 16–27.

Crowell, E.F., Bischoff, V., Desprez, T., Rolland, A., Stierhof, Y.-D., Schumacher, K., Gonneau, M., Höfte, H., and Vernhettes, S. (2009). Pausing of Golgi bodies on microtubules regulates secretion of cellulose synthase complexes in *Arabidopsis*. Plant Cell 21: 1141–1154.

Cvrčková, F. (2012). Formins: Emerging players in the dynamic plant cell cortex. Scientifica 2012: e712605.

Cvrčková, F. (2013). Formins and membranes: anchoring cortical actin to the cell wall and beyond. Front. Plant Sci. 4: 1–7.

Dai, X., Zhang, Y., Zhang, D., Chen, J., Gao, X., Estelle, M., and Zhao, Y. (2015). Embryonic lethality of *Arabidopsis abp1-1* is caused by deletion of the adjacent BSM gene. Nat. Plants 1: e15183.

Darwin, C. and Darwin, F. (1880). The power of movement in plants. John Murray: London, UK.

Dharmasiri, N., Dharmasiri, S., and Estelle, M. (2005a). The F-box protein TIR1 is an auxin receptor. Nature 435: 441–445.

Dharmasiri, N., Dharmasiri, S., Weijers, D., Lechner, E., Yamada, M., Hobbie, L., Ehrismann, J.S., Jürgens, G., and Estelle, M. (2005b). Plant development is regulated by a family of auxin receptor F-Box proteins. Dev. Cell 9: 109–119.

Dhonukshe, P., Aniento, F., Hwang, I., Robinson, D.G., Mravec, J., Stierhof, Y.D., and Friml, J. (2007). Clathrin-mediated constitutive endocytosis of PIN auxin efflux carriers in *Arabidopsis*. Curr. Biol. 17: 520–527.

Dibb-Fuller, J.E. and Morris, D.A. (1992). Studies on the evolution of auxin carriers and phytotropin receptors: Transmembrane auxin transport in unicellular and multicellular Chlorophyta. Planta 186: 219–226.

Dindas, J., Scherzer, S., Roelfsema, M.R.G., Von Meyer, K., Müller, H.M., Al-Rasheid, K.A.S., Palme, K., Dietrich, P., Becker, D., Bennett, M.J., and Hedrich, R. (2018). AUX1-mediated root hair auxin influx governs SCF TIR1/AFB-type Ca^{2+} signaling. Nat. Commun. 9: 1174.

Doolittle, L.K., Rosen, M.K., and Padrick, S.B. (2013). Measurement and analysis of in vitro actin polymerization. Methods Molec. Biol. 1046: 273–293.

Dominguez, R. and Holmes, K.C. (2011). Actin structure and function. Annu. Rev. Biophys. 40:169–186.

Du, C., Xu, Y., Wang, Y., and Chong, K. (2011). Adenosine diphosphate ribosylation factor-GTPase-activating protein stimulates the transport of AUX1 endosome, which relies on actin cytoskeletal organization in rice root development. J. Integr. Plant Biol. 53: 698–709.

Dyachok, J., Sparks, J.A., Liao, F., Wang, Y.S., and Blancaflor, E.B. (2014). Fluorescent protein-based reporters of the actin cytoskeleton in living plant cells: Fluorophore variant, actin binding domain, and promoter considerations. Cytoskeleton 71: 311–327.

Dyachok, J., Zhu, L., Liao, F., He, J., Huq, E., and Blancaflor, E.B. (2011). SCAR mediates light-induced root elongation in *Arabidopsis* through photoreceptors and proteasomes. Plant Cell 23: 3610–3626.

Effendi, Y., Rietz, S., Fischer, U., and Scherer, G.F.E. (2011). The heterozygous *abp1/ABP1* insertional mutant has defects in functions requiring polar auxin transport and in regulation of early auxin-regulated genes. Plant J. 65: 282–294.

Enders, T.A. and Strader, L.C. (2015). Auxin activity: Past, present, and future. Am. J. Bot. 102: 180–196.

Era, A., Tominaga, M., Ebine, K., Awai, C., Saito, C., Ishizaki, K., Yamato, K.T., Kohchi, T., Nakano, A., and Ueda, T. (2009). Application of lifeact reveals F-actin dynamics in *Arabidopsis thaliana* and the liverwort, *Marchantia polymorpha*. Plant Cell Physiol. 50: 1041–1048.

Fayant, P., Girlanda, O., Chebli, Y., Aubin, C.-E., Villemure, I., and Geitmann, A. (2010). Finite element model of polar growth in pollen tubes. Plant Cell 22: 2579–2593.

Fendrych, M., Akhmanova, M., Merrin, J., Glanc, M., Hagihara, S., Takahashi, K., Uchida, N., Torii, K.U., and Friml, J. (2018). Rapid and reversible root growth inhibition by TIR1 auxin signalling. Nat. Plants 4: 453–459.

Fendrych, M., Leung, J., and Friml, J. (2016). Tir1/AFB-Aux/IAA auxin perception mediates rapid cell wall acidification and growth of Arabidopsis hypocotyls. Elife 5: e19048.

Feraru, E., and Friml, J. (2008). PIN Polar Targeting. Plant Physiol. 147: 1553–1559.

Fischer, U., Ikeda, Y., Ljung, K., Serralbo, O., Singh, M., Heidstra, R., Palme, K., Scheres, B., and Grebe, M. (2006). Vectorial information for *Arabidopsis* planar polarity is mediated by combined AUX1, EIN2, and GNOM activity. Curr. Biol. 16: 2143–2149.

Foissner, I. and Wasteneys, G.O. (2007). Wide-ranging effects of eight cytochalasins and latrunculin A and B on intracellular motility and actin filament reorganization in characean internodal cells. Plant Cell Physiol. 48: 585–597.

Frank, M., Egile, C., Dyachok, J., Djakovic, S., Nolasco, M., Li, R., and Smith, L.G. (2004). Activation of Arp2/3 complex-dependent actin polymerization by plant proteins distantly related to Scar/WAVE. Proc. Natl. Acad. Sci. 101: 16379–16384.

Frank, M.J., Cartwright, H.N., and Smith, L.G. (2003). Three Brick genes have distinct functions in a common pathway promoting polarized cell division and cell morphogenesis in the maize leaf epidermis. Development 130: 753–762.

Frank, M.J. and Smith, L.G. (2002). A small, novel protein highly conserved in plants and animals promotes the polarized growth and division of maize leaf epidermal cells. Curr. Biol. 12: 849–853.

Frigerio, L. (2010). Plant Exocytosis, Endocytosis and Membrane Recycling in Turgid Cells. In Encyclopedia of Life Sciences (ELS). John Wiley & Sons, Ltd: Chichester, UK. DOI: 10.1002/9780470015902.a0001676.pub2.

Friml, J., Wiśniewska, J., Benková, E., Mendgen, K., and Palme, K. (2002). Lateral relocation of auxin efflux regulator PIN3 mediates tropism in *Arabidopsis*. Nature 415: 806–809.

Frydman, J. and Hartlt, F.U. (1996). Principles of chaperone-assisted protein folding : differences between in vitro and in vivo mechanisms. Science 272: 1497–1502.

Fu, Y, Li, H., and Yang, Z. (2002). The ROP2 GTPase controls the formation of cortical fine F-actin and the early phase of directional cell expansion during Arabidopsis organogenesis. Plant Cell 14: 777–794.

Fu, Y., Gu, Y., Zheng, Z., Wasteneys, G., and Yang, Z. (2005). *Arabidopsis* interdigitating cell growth requires two antagonistic pathways with opposing action on cell morphogenesis. Cell 120: 687–700.

Galletta, B.J., Chuang, D.Y., and Cooper, J.A. (2008). Distinct roles for Arp2/3 regulators in actin assembly and endocytosis. PLoS Biol. 6: 72–85.

Galweiler, L., Guan, C., Muller, A., Wisman, E., Mendgen, K., Yephremov, A., and Palme, K. (1998). Regulation of polar auxin transport by AtPIN1 in *Arabidopsis* vascular tissue. Science 282: 2226–2230.

Gao, Y., Zhang, Y., Zhang, D., Dai, X., Estelle, M. and, and Zhao, Y. (2015). Auxin binding protein 1 (ABP1) is not required for either auxin signaling or *Arabidopsis* development. Proc. Natl Acad. Sci. USA 112: 2275–2280.

Geisler, M., Blakeslee, J.J., Bouchard, R., Lee, O.R., Vincenzetti, V., Bandyopadhyay, A., Titapiwatanakun, B., Peer, W.A., Bailly, A., Richards, E.L., Ejendal, K.F.K., Smith, A.P., Baroux, C., Grossniklaus, U., Müller, A., Hrycyna, C.A., Dudler, R., Murphy, A.S., and Martinoia, E. (2005). Cellular efflux of auxin catalyzed by the Arabidopsis MDR/PGP transporter AtPGP1. Plant J. 44: 179–194.

Geisler, M., Wang, B., and Zhu, J. (2014). Auxin transport during root gravitropism: Transporters and techniques. Plant Biol. 16: 50–57.

Geitmann, A., Nebenführ, A. (2015). Navigating the plant cell: intracellular transport logistics in the green kingdom. Molec. Biol. Cell 26: 3373–3378.

Geldner, N., Friml, J., Stierhof, Y.D., Jürgens, G., and Palme, K. (2001). Auxin transport inhibitors block PIN1 cycling and vesicle trafficking. Nature 413: 425–428.

Gibbon, B.C., Kovar, D.R., and Staiger, C.J. (1999). Latrunculin B has different effects on pollen germination and tube growth. Plant Cell 11: 2349–2363.

Gilliland, L.U., Kandasamy, M.K., Pawloski, L.C., and Meagher, R.B. (2002). Both vegetative and reproductive actin isovariants complement the stunted root hair phenotype of the Arabidopsis *act2-1* mutation. Plant Physiol. 130: 2199–2209.

Gilliland, L.U., Pawloski, L.C., Kandasamy, M.K., and Meagher, R.B. (2003). *Arabidopsis* actin gene *ACT7* plays an essential role in germination and root growth. Plant J. 33: 319–328.

Grieneisen, V.A., Xu, J., Marée, A.F.M., Hogeweg, P., and Scheres, B. (2007). Auxin transport is sufficient to generate a maximum and gradient guiding root growth. Nature 449: 1008–13.

Grones, P., Chen, X., Simon, S., Kaufmann, W.A., Rycke, R. De, Nodzy, T., and Zažímalová, E. (2018). Auxin-binding pocket of ABP1 is crucial for its gain-of-function cellular and developmental roles. J. Exp. Bot. 66: 5055–5065.

Grones, P. and Friml, J. (2015). Auxin transporters and binding proteins at a glance. J. Cell Sci. 128: 1–7.

Gu, Y., Fu, Y., Dowd, P., Li, S., Vernoud, V., Gilroy, S., and Yang, Z. (2005). A Rho family GTPase controls actin dynamics and tip growth via two counteracting downstream pathways in pollen tubes. J. Cell Biol. 169: 127–138.

Gunning, P.W., Ghoshdastider, U., Whitaker, S., Popp, D., and Robinson, R.C. (2015). The evolution of compositionally and functionally distinct actin filaments. J.Cell Sci. 128: 2009–2019.

Gutierrez, R., Lindeboom, J.J., Paredez, A.R., Emons, A.M.C., and Ehrhardt, D.W. (2009). *Arabidopsis* cortical microtubules position cellulose synthase delivery to the plasma membrane and interact with cellulose synthase trafficking compartments. Nat. Cell Biol. 11: 797–806.

Habets, M.E.J. and Offringa, R. (2015). Auxin binding protein 1 : A red herring after all? Mol. Plant 8: 1131–1134.

Hagen, G. and Guilfoyle, T. (2002). Auxin-responsive gene expression: Genes, promoters and regulatory factors. Plant Mol. Biol. 49: 373–385.

Hansen, W.J., Cowan, N.J., and Welch, W.J. (1999). Prefoldin–nascent chain complexes in the folding of cytoskeletal proteins. J. Cell Biol. 145: 265–277.

Hawes, C.R., and Satiat-Jeunemaitre, B. (1996). Trekking along the cytoskeleton. Plant Physiol. 125: 119–122.

Hayashi, K.K. -i., Nakamura, S., Fukunaga, S., Nishimura, T., Jenness, M.K., Murphy, A.S., Motose, H., Nozaki, H., Furutani, M., and Aoyama, T. (2014). Auxin transport sites are visualized in planta using fluorescent auxin analogs. Proc. Natl. Acad. Sci. 111: 11557–11562.

Hejnowicz, Z. and Erickson, R.O. (1968). Growth inhibition and recovery in roots following temporary treatment with auxin. Physiol. Plant. 21: 302–313.

Henty-Ridilla, J.L., Li, J., Blanchoin, L., and Staiger, C.J. (2013a). Actin dynamics in the cortical array of plant cells. Curr. Opin. Plant Biol. 16: 678–687.

Henty-Ridilla, J.L., Li, J.J., Day, B., and Staiger, C.J. (2014). ACTIN DEPOLYMERIZING FACTOR4 regulates actin dynamics during innate immune signaling in *Arabidopsis*. Plant Cell 26: 340–352.

Henty-Ridilla, J.L., Shimono, M., Li, J., Chang, J.H., Day, B., and Staiger, C.J. (2013b). The plant actin cytoskeleton responds to signals from microbe-associated molecular patterns. PLoS Pathog. 9: e1003290.

Henty, J.L., Bledsoe, S.W., Khurana, P., Meagher, R.B., Day, B., Blanchoin, L., and Staiger, C.J. (2011). *Arabidopsis* actin depolymerizing factor4 modulates the stochastic dynamic behavior of actin filaments in the cortical array of epidermal cells. Plant Cell 23: 3711–3726.

Hertel, R. (1995). Auxin binding protein 1 is a red herring. J. Exp. Bot. 46: 461–462.

Holweg, C., Süßlin, C., and Nick, P. (2004). Capturing in vivo dynamics of the actin cytoskeleton stimulated by auxin or light. Plant Cell Physiol. 45: 855–863.

Hou, G., Kramer, V.L., Wang, Y.S., Chen, R., Perbal, G., Gilroy, S., and Blancaflor, E.B. (2004). The promotion of gravitropism in *Arabidopsis* roots upon actin disruption is coupled with the extended alkalinization of the columella cytoplasm and a persistent lateral auxin gradient. Plant J. 39: 113–125.

Huang, Q.S., Chen, X.J., Li, J.P., Hao, X.Y., Chen, G., Zumuremu, and Shao, L. (2014). The phosphorylation of an actin depolymerizing factor by a calcium-dependent protein kinase regulates cotton fiber elongation. Acta Physiol. Plant. 36: 2627–2636.

Huang, S., Robinson, R.C., Gao, L.Y., Matsumoto, T., Brunet, A., Blanchoin, L., and Staiger, C.J. (2005). Arabidopsis VILLIN1 generates actin filament cables that are resistant to depolymerization. Plant Cell 17: 486–501.

Huang, Y.-C., Chang, Y.-L., Hsu, J.-J., and Chuang, H.-W. (2008). Transcriptome analysis of auxin-regulated genes of *Arabidopsis thaliana*. Gene 420: 118–124.

Hussey, P.J., Ketelaar, T., and Deeks, M.J. (2006). Control of the actin cytoskeleton in plant cell growth. Annu. Rev. Plant Biol. 57: 109–125.

Jásik, J., Bokor, B., Stuchlík, S., Mičieta, K., Turňa, J., and Schmelzer, E. (2016). Effects of auxins on PIN-FORMED2 (PIN2) dynamics are not mediated by inhibiting PIN2 endocytosis. Plant Physiol. 172: 1019–1031.

Jásik, J. and Schmelzer, E. (2014). Internalized and newly synthesized *Arabidopsis* PIN-FORMED2 pass through brefeldin a compartments: a new insight into intracellular dynamics of the protein by using the photoconvertible fluorescence protein Dendra2 as a tag. Mol. Plant 7: 1578–1581.

Jones, A.M. and Herman, E.M. (1993). KDEL-containing auxin-binding protein is secreted to the plasma membrane and cell wall. Plant Physiol. 101: 595–606.

Jones, A.M., Im, K., Savka, M.A., Wu, M., Dewitt, N.G., Shillito, R., and Binns, A.N. (1998). Auxin-dependent cell expansion mediated by overexpressed auxin-binding protein 1. Science 282: 1114–1118.

Jones, M.A. (2002). The Arabidopsis Rop2 GTPase is a positive regulator of both root hair initiation and tip growth. Plant Cell 14: 763–776.

Kandasamy, M.K., Gilliland, L.U., McKinney, E.C., and Meagher, R.B. (2001). One plant actin isovariant, ACT7, is induced by auxin and required for normal callus formation. Plant Cell 13: 1541–1554.

Kandasamy, M.K., Gilliland, L.U., McKinney, E.C., and Meagher, R.B. (2007). Class-specific interaction of profilin and ADF isovariants with actin in the regulation of plant development. Plant Cell 19: 3111–3126.

Kandasamy, M.K., McKinney, E.C., and Meagher, R.B. (2009). A single vegetative actin isovariant overexpressed under the control of multiple regulatory sequences is sufficient for normal *Arabidopsis* development. Plant Cell 21: 701–18.

Kato, T., Morita, M.T., and Tasaka, M. (2010). Defects in Dynamics and Functions of Actin Filament in Arabidopsis Caused by the Dominant-Negative Actin *fiz1*-Induced Fragmentation of Actin Filament. Plant Cell Physiol. 51: 333–338.

Kelley, D.R., Shen, Z., Walley, J.W., Chapman, E.J., Briggs, S.P., and Estelle, M.A. (2017). Quantitative proteomic analysis of auxin signaling during seedling development. bioRxiv October 30. doi: http://dx.doi.org/10.1101/211532.

Kepinski, S., and Leyser, O. (2005). The *Arabidopsis* F-box protein TIR1 is an auxin receptor. Nature 435: 446–451.

Ketelaar, T. (2013). The actin cytoskeleton in root hairs: All is fine at the tip. Curr. Opin. Plant Biol. 16: 749–756.

Ketelaar, T., de Ruijter, N.C.A., and Emons, A.M.C. (2003). Unstable F-actin specifies the area and microtubule direction of cell expansion in Arabidopsis root hairs. Plant Cell 15: 285–292.

Khasin, M., Cahoon, R.R., Nickerson, K.W., and Riekhof, W.R. (2018). Molecular machinery of auxin synthesis, secretion, and perception in the unicellular chlorophyte alga *Chlorella sorokiniana* UTEX 1230. PLoS One 13: 1–13.

Khurana, P., Henty, J.L., Huang, S., Staiger, A.M., Blanchoin, L., and Staiger, C.J. (2010). *Arabidopsis* VILLIN1 and VILLIN3 have overlapping and distinct activities in actin bundle formation and turnover. Plant Cell 22: 2727–2748.

Kijima, S.T., Hirose, K., Kong, S.-G., Wada, M., and Uyeda, T.Q.P. (2016). Distinct biochemical properties of *Arabidopsis thaliana* actin isoforms. Plant Cell Physiol. 57: 46–56.

Kijima, S.T., Staiger, C.J., Katoh, K., Nagasaki, A., Ito, K., and Uyeda, T.Q.P. (2018). *Arabidopsis* vegetative actin isoforms, AtACT2 and AtACT7, generate distinct filament arrays in living plant cells. Sci. Rep. 8: 1–15.

Kleine-Vehn, J., Dhonukshe, P., Swarup, R., Bennett, M., and Friml, J. (2006). Subcellular trafficking of the *Arabidopsis* auxin influx carrier AUX1 uses a novel pathway distinct from PIN1. Plant Cell 18: 3171–81.

Kleine-Vehn, J., Ding, Z., Jones, A.R., Tasaka, M., Morita, M.T., and Friml, J. (2010). Gravity-induced PIN transcytosis for polarization of auxin fluxes in gravity-sensing root cells. Proc. Natl. Acad. Sci. 107: 22344–22349.

Kleine-Vehn, J. and Friml, J. (2008). Polar targeting and endocytic recycling in auxin-dependent plant development. Annu. Rev. Cell Dev. Biol. 24: 447–73.

Kleine-Vehn, J., Leitner, J., Zwiewka, M., Sauer, M., Abas, L., Luschnig, C., and Friml, J. (2008). Differential degradation of PIN2 auxin efflux carrier by retromer-dependent vacuolar targeting. Proc. Natl. Acad. Sci. 105: 17812–17817.

Křeček, P., Skůpa, P., Libus, J., Naramoto, S., Tejos, R., Friml, J., and Zažímalová, E. (2009). The PIN-FORMED (PIN) protein family of auxin transporters. Genome Biol. 10: 249.

Kutschera, U. (1994). Tansley Review No . 66 The current status of the acid-growth hypothesis. New Phytol. 126: 549–569.

Labusch, C., Effendi, Y., Fulda, M., and Scherer, G.F.E. (2016). Transcription of TIR1-controlled genes can be regulated within 10 min by an auxin-induced process. Can TIR1 be the receptor? Front. Plant Sci. 7: 1–13.

Labusch, C., Shishova, M., Effendi, Y., Li, M., and Wang, X. (2013). Patterns and timing in expression of early auxin-induced genes imply involvement of phospholipases A (pPLAs) in the regulation of auxin responses. Molec. Plant 6: 1473–1486.

Langdale, J.A. (2014). Evolution and development: PINpointing the origins of auxin transport mechanisms. Curr. Biol. 24: R1129–R1131.

Lanza, M., Garcia-Ponce, B., Castrillo, G., Catarecha, P., Sauer, M., Rodriguez-Serrano, M., Páez-García, A., Sánchez-Bermejo, E., TC, M., del Puerto, Y.L., Sandalio, L.M., Paz-Ares, J., and Leyva, A. (2012). Role of actin cytoskeleton in brassinosteroid signaling and in its integration with the auxin response in plants. Dev. Cell 22: 1275–1285.

Laskowski, M., Grieneisen, V.A., Hofhuis, H., ten Hove, C.A., Hogeweg, P., Marée, A.F.M., and Scheres, B. (2008). Root system architecture from coupling cell shape to auxin transport. PLoS Biol. 6: e307.

Lau, S., Ju, G., and Smet, I. De (2008). The evolving complexity of the auxin pathway. 20: 1738–1746.

Lau, S., Shao, N., Bock, R., Jürgens, G., and De Smet, I. (2009). Auxin signaling in algal lineages: fact or myth? Trends Plant Sci. 14: 182–188.

Lee, D.J., Park, J.W., Lee, H.W., and Kim, J. (2009). Genome-wide analysis of the auxin-responsive transcriptome downstream of iaa1 and its expression analysis reveal the diversity and complexity of auxin-regulated gene expression. J. Exp. Bot. 60: 3935–3957.

Lee, Y.J., Szumlanski, A., Nielsen, E., and Yang, Z. (2008). Rho-GTPase-dependent filamentous actin dynamics coordinate vesicle targeting and exocytosis during tip growth. J. Cell Biol. 181: 1155–1168.

Leitz, G., Kang, B.-H., Schoenwaelder, M.E.A., and Staehelin, L.A. (2009). Statolith sedimentation kinetics and force transduction to the cortical endoplasmic reticulum in gravity-sensing *Arabidopsis* columella cells. Plant Cell 21: 843–60.

Lewis, D.R., Olex, A.L., Lundy, S.R., Turkett, W.H., Fetrow, J.S., and Muday, G.K. (2013). A kinetic analysis of the auxin transcriptome reveals cell wall remodeling proteins that modulate lateral root development in *Arabidopsis*. Plant Cell 25: 3329–3346.

Leyser, O. (2010). The power of auxin in plants. Plant Physiol. 154: 501–505.

Li, G., Liang, W., Zhang, X., Ren, H., Hu, J., Bennett, M.J., and Zhang, D. (2014a). Rice actin-binding protein RMD is a key link in the auxin-actin regulatory loop that controls cell growth. Proc. Natl. Acad. Sci. 111: 10377–82.

Li, J., Arieti, R., and Staiger, C.J. (2015a). Chapter 5 Actin Filament Dynamics and their Role in Plant Cell Expansion. pp. 127–162 in Plant Cell Wall Patterning and Cell Shape, H. Fukuda, ed. Wiley-Blackwell: Hoboken, NJ. doi:10.1002/9781118647363.ch5.

Li, J., Blanchoin, L., and Staiger, C.J. (2015b). Signaling to actin stochastic dynamics. Annu. Rev. Plant Biol. 66: 415–40.

Li, J., Cao, L., and Staiger, C.J. (2016). Capping protein modulates actin remodeling in response to reactive oxygen species during plant innate immunity. Plant Physiol. 173: 1125–1136.

Li, J., Henty-Ridilla, J.L., Huang, S., Wang, X., Blanchoin, L., and Staiger, C.J. (2012a). Capping protein modulates the dynamic behavior of actin filaments in response to phosphatidic acid in *Arabidopsis*. Plant Cell 24: 3742–3754.

Li, J., Henty-Ridilla, J.L., Staiger, B.H., Day, B., and Staiger, C.J. (2015c). Capping protein integrates multiple MAMP signalling pathways to modulate actin dynamics during plant innate immunity. Nat. Commun. 6: 1–13.

Li, J., Pleskot, R., Henty-ridilla, J.L., Blanchoin, L., Potocký, M., and Staiger, C.J. (2012b). Arabidopsis capping protein senses cellular phosphatidic acid levels and transduces these into changes in actin cytoskeleton dynamics. Plant Signal. Behav. 7: 1727–1730.

Li, J., Staiger, B.H., Henty-Ridilla, J.L., Abu-Abied, M., Sadot, E., Blanchoin, L., and Staiger, C.J. (2014b). The availability of filament ends modulates actin stochastic dynamics in live plant cells. Mol. Biol. Cell 25: 1263–1275.

Li., J., and Staiger, C.J. (2018). Understanding cytoskeletal dynamics during the plant immune response. Annu. Rev. Phytopathol. 56: 23.1–23.21.

Li, L.-J., Ren, F., Gao, X.-Q.; Wei, P.-C., and Wang, X.-C. (2013). The reorganization of actin filaments is required for vacuolar fusion of guard cells during stomatal opening in *Arabidopsis*. Plant Cell Environ. 36: 484–497.

Li, S., Blanchoin, L., Yang, Z., and Lord, E.M. (2003). The putative Arabidopsis Arp2/3 complex controls leaf cell morphogenesis. Plant Physiol. 132: 2034–2044.

Lin, D., Nagawa, S., Chen, J., Cao, L., Chen, X., Xu, T., Li, H., Dhonukshe, P., Yamamuro, C., Friml, J., Scheres, B., Fu, Y., and Yang, Z. (2012). A ROP GTPase-dependent auxin signaling pathway regulates the subcellular distribution of PIN2 in *Arabidopsis* roots. Curr. Biol. 22: 1319–1325.

Liscum, E. and Reed, J.W. (2002). Genetics of Aux/IAA and ARF action in plant growth and development. Plant Mol. Biol. 49: 387–400.

Ljung, K., Bhalerao, R.P., and Sandberg, G. (2001). Sites and homeostatic control of auxin biosynthesis in *Arabidopsis* during vegetative growth. Plant J. 28: 465–474.

Ljung, K., Hull, A.K., Celenza, J., Yamada, M., Estelle, M., Normanly, J., and Sandberg, G. (2005). Sites and regulation of auxin biosynthesis in Arabidopsis roots. Plant Cell 17: 1090–104.

Lofke, C., Dunser, K., Scheming, D., and Kleine-Vehn, J. (2015). Auxin regulates SNARE-dependent vacuolar morphology restricting cell size. Elife 4: e05868.

Lovy-Wheeler, A., Wilsen, K.L., Baskin, T.I., and Hepler, P.K. (2005). Enhanced fixation reveals the apical cortical fringe of actin filaments as a consistent feature of the pollen tube Planta 221: 95–104.

Luo, J., Zhou, J.J., and Zhang, J.Z. (2018). Aux/IAA gene family in plants: Molecular structure, regulation, and function. Int. J. Mol. Sci. 19: 1–17.

Machesky, L.M, Atkinson, S.J., Ampe, C., Vandekerckhove, J., and Pollard, T.D. (1994). Purification of a cortical complex containing two unconventional actins from *Acanthamoeba* by affinity chromatography on profilin-agarose. J. Cell Biol. 127: 107–115.

Maher, E.P. and Martindale, S.J. (1980). Mutants of *Arabidopsis thaliana* with altered responses to auxins and gravity. Biochem. Genet. 18: 1041–1053.

Majda, M. (2018). The role of auxin in cell wall expansion. Int. J. Mol. Sci. 19: 951. doi:10.3390/ijms19040951.

Mancuso, S., Barlow, P.W., Volkmann, D., and Baluska, F. (2006). Actin turnover-mediated gravity response in maize root apices. Plant Signal. Behav. 1: 52–58.

Marchant, A, Bhalerao, R., Casimiro, I., Eklöf, J., Casero, P.J., Bennett, M., and Sandberg, G. (2002). AUX1 promotes lateral root formation by facilitating indole-3-acetic acid distribution between sink and source tissues in the Arabidopsis seedling. Plant Cell 14: 589–597.

Marchant, A., Kargul, J., May, S.T., Muller, P., Delbarre, A., Perrot-Rechenmann, C., and Bennett, M.J. (1999). AUX1 regulates root gravitropism in *Arabidopsis* by facilitating auxin uptake within root apical tissues. EMBO J. 18: 2066–2073.

Masuda, Y. (1990). Auxin-induced cell elongation and cell wall changes. Bot. Mag. Tokyo 103: 345–370.

Mathur, J. (2004). Cell shape development in plants. Trends Plant Sci. 9: 583–590.

Mattei, B., Sabatini, S., and Schininà, M.E. (2013). Proteomics in deciphering the auxin commitment in the *Arabidopsis thaliana* root growth. J. Proteome Res. 12: 4685–4701.

McClure, B.A. and Guilfoyle, T. (1987). Characterization of a class of small auxin-inducible soybean polyadenylated RNAs. Plant Mol. Biol. 9: 611–623.

McClure, B.A., Hagen, G., Brown, C.S., Gee, M.A., and Guilfoyle, T.J. (2007). Transcription, organization, and sequence of an auxin-regulated gene cluster in soybean. Plant Cell 1: 229–239.

McDowell, J.M., An, Y.Q., Huang, S., McKinney, E.C., and Meagher, R.B. (1996). The Arabidopsis *ACT7* actin gene is expressed in rapidly developing tissues and responds to several external stimuli. Plant Physiol. 111: 699–711.

McKinney, E.C., Kandasamy, M.K., and Meagher, R.B. (2001). Small changes in the regulation of one Arabidopsis profilin isovariant, PRF1, alter seedling development. Plant Cell 13: 1179–91.

Melak, M., Plessner, M., and Grosse, R. (2017). Actin visualization at a glance. J. Cell Sci. 0: 1–6. doi:10.1242/jcs.189068.

Michelot, A., Derivery, E., Paterski-Boujemaa, R., Guerin, C., Huang, S., Parcy, F., Staiger, C.J., and Blanchoin, L. (2006). A novel mechanism for the formation of actin-filament bundles by a nonprocessive formin. Curr. Biol. 16: 1924–1930.

Michniewicz, M., Brewer, P.B., and Friml, J. (2007). Polar auxin transport and asymmetric auxin distribution. The Arabidopsis Book e0108. doi:10.1199/tab.0108.

Monshausen, G.B., Miller, N.D., Murphy, A.S., and Gilroy, S. (2011). Dynamics of auxin-dependent Ca^{2+} and pH signaling in root growth revealed by integrating high-resolution imaging with automated computer vision-based analysis. Plant J. 65: 309–318.

Mooren, O.L., Galletta, B.J., and Cooper, J.A. (2012). Roles for actin assembly in endocytosis. Annu. Rev. Biochem 81: 661–86.

Morita, M.T. (2010). Directional gravity sensing in gravitropism. Annu. Rev. Plant Biol. 61: 705–720.

Muday, G.K. (2000). Maintenance of asymmetric cellular localization of an auxin transport protein through interaction with the actin cytoskeleton. J. Plant Growth Regul. 19: 385–396.

Muday, G.K. and DeLong, A. (2001). Polar auxin transport: Controlling where and how much. Trends Plant Sci. 6: 535–542.

Mullins, R.D., Stafford, W.F., and Pollard, T.D. (1997). Structure, subunit topology, and actin-binding activity of the Arp2/3 complex from *Acanthamoeba*. J. Cell Biol. 136: 331–343.

Mullins, R.D., Heuser, J.A., and Pollard, T.D. (1998). The interaction of Arp2 3 complex with actin: Nucleation, high affinity pointed end capping, and formation of branching networks of filaments. Proc. Natl. Acad. Sci. 95: 6181–6186.

Mutte, S.K., Kato, H., Rothfels, C., Melkonian, M., Wong, G.K.-S., and Weijers, D. (2018). Origin and evolution of the nuclear auxin response system. Elife 7: 1–25.

Nagawa, S., Xu, T., Lin, D., Dhonukshe, P., Zhang, X., Friml, J., Scheres, B., Fu, Y., and Yang, Z. (2012). ROP GTPase-dependent actin microfilaments promote PIN1 polarization by localized inhibition of clathrin-dependent endocytosis. PLoS Biol. 10: e1001299.

Napier, R.M. and Venis, M.A. (1990). Monoclonal antibodies detect an auxin-induced conformational change in the maize auxin-binding protein. Planta 182: 313–318.

Nebenführ, A., Gallagher, L.A., Dunahay, T.G., Frohlick, J.A., Mazurkiewicz, A.M., Meehl, J.B., and Staehelin, L.A. (1999). Stop-and-go movements of plant Golgi stacks are mediated by the acto-myosin system. Plant Physiol. 121: 1127–1141.

Nebenführ, A., and Dixit, R. (2018). Kinesins and myosins: molecular motors that coordinate cellular functions in plants. Annu. Rev. Plant Biol. 69: 329–361.

Nick, P. (2010). Probing the actin-auxin oscillator. Plant Signal. Behav. 5: 94–98.

Nick, P., Han, M.-J., and An, G. (2009). Auxin stimulates its own transport by shaping actin filaments. Plant Physiol. 151: 155–167.

Niklas, K.J. and Kutschera, U. (2012). Plant development, auxin, and the subsystem incompleteness theorem. Front. Plant Sci. 3: a37.

Nishimura, T., Yokota, E., Wada, T., Shimmen, T., and Okada, K. (2003). An *Arabidopsis ACT2* dominant-negative mutation, which disturbs F-actin polymerization, reveals its distinctive function in root development. Plant Cell Physiol. 44: 1131–1140.

Nishitani, K. and Masuda, Y. (1981). Auxin-induced changes in the cell wall structure: Changes in the sugar compositions, intrinsic viscosity and molecular weight distributions of matrix polysaccharides of the epicotyl cell wall of Vigna angularis. Physiol. Plant. 52: 482–494.

Noh, B., Bandyopadhyay, A., Peer, W.A., Spalding, E.P., and Murphy, A.S. (2003). Enhanced gravi- and phototropism in plant *mdr* mutants mislocalizing the auxin efflux protein PIN1. Nature 423: 999–1002.

Noh, B., Murphy, A.S., and Spalding, E.P. (2001). *Multidrug Resistance*-like genes of Arabidopsis required for auxin transport and auxin-mediated development. Plant Cell 13: 2441–54.

Oeller, P.W. and Theologis, A. (1995). Induction kinetics of the nuclear proteins encoded by the early indoleacetic acid-inducible genes, *PS-IAA4/5* and *PS-IAA6*, in pea (*Pisum sativum* L.). Plant J. 7: 37–48.

Overvoorde, P., Fukaki, H., and Beeckman, T. (2010). Auxin control of root development. Cold Spring Harb. Perspect. Biol. 2: 1–16.

Paciorek, T., Zazímalová, E., Ruthardt, N., Petrásek, J., Stierhof, Y.-D., Kleine-Vehn, J., Morris, D.A., Emans, N., Jürgens, G., Geldner, N., and Friml, J. (2005). Auxin inhibits endocytosis and promotes its own efflux from cells. Nature 435: 1251–1256.

Pan, X., Chen, J., and Yang, Z. (2015). Auxin regulation of cell polarity in plants. Curr. Opin. Plant Biol. 28: 144–153.

Paponov, I.A., Dindas, J., Król, E., Friz, T., Budnyk, V., Teale, W., Paponov, M., Hedrich, R., and Palme, K. (2019). Auxin-induced plasma membrane depolarization is regulated by auxin transport and not by AUXIN BINDING PROTEIN1. Front. Plant Sci. 9.

Paponov, I.A., Paponov, M., Teale, W., Menges, M., and Chakrabortee, S. (2008). Comprehensive transcriptome analysis of auxin responses in *Arabidopsis*. Mol. Plant 1: 321–337.

Parry, G., Calderon-Villalobos, L.I., Prigge, M., Peret, B., Dharmasiri, S., Itoh, H., Lechner, E., Gray, W.M., Bennett, M., and Estelle, M. (2009). Complex regulation of the TIR1/AFB family of auxin receptors. Proc. Natl. Acad. Sci. 106: 22540–22545.

Peer, W.A., Blakeslee, J.J., Yang, H., and Murphy, A.S. (2011). Seven things we think we know about auxin transport. Mol. Plant 4: 487–504.

Pei, W., Du, F., Zhang, Y., He, T., and Ren, H. (2012). Control of the actin cytoskeleton in root hair development. Plant Sci. 187: 10–18.

Peremyslov, V.V., Prokhnevsky, A.I., Avisar, D., and Dolja, V.V. (2008). Two class XI myosins function in organelle trafficking and root hair development in Arabidopsis. Plant Physiol. 146: 1109–1116.

Peremyslov, V.V., Prokhnevsky, A.I., and Dolja, V.V. (2010). Class XI myosins are required for development, cell expansion, and F-actin organization in *Arabidopsis*. Plant Cell 22: 1883–1897.

Peret, B., Swarup, K., Ferguson, A., Seth, M., Yang, Y., Dhondt, D., James, N., Casimiro, I., Perry, P., Syed, A., Yang, H., Reemmer, J., Venison, E., Howells, C., Perez-Amador, M.A., Yun, J., Alonso, J., Beemster, G.T.S., Laplaze, L., Murphy, A., Bennett, M.J., Nielsen, E., and Swarup, R. (2012). AUX/LAX genes encode a family of auxin influx transporters that perform distinct functions during Arabidopsis development. Plant Cell 24: 2874–2885.

Perrin, B.J. and Ervasti, J.M. (2010). The actin gene family: Function follows isoform. Cytoskeleton 67: 630–634.

Perrot-Rechenman, C. (2012). Cellular responses to auxin: Division versus expansion. Cold Spring Harb Perspect Biol 2: a001446.

Petrasek, J. and Friml, J. (2009). Auxin transport routes in plant development. Development 136: 2675–2688.

Pickett, F.B., Wilson, A.K., and Estelle, M. (1990). The *aux1* mutation of *Arabidopsis* confers both auxin and ethylene resistance. Plant Physiol. 94: 1462–1466.

Pitts, R.J., Cernac, A., and Estelle, M. (1998). Auxin and ethylene promote root hair elongation in *Arabidopsis*. Plant J. 16: 553–560.

Pleskot, R., Li, J., Zarsky, V., Potocky, M., and Staiger, C.J. (2013). Regulation of cytoskeletal dynamics by phospholipase D and phosphatidic acid. Trends Plant Sci. 18: 496–504.

Pu, Y., Walley, J.W., Shen, Z., Lang, M.G., Briggs, S.P., Estelle, M., and Kelley, D.R. (2019). Quantitative early auxin root proteomics identifies GAUT10, a galacturonosyltransferase, as a novel regulator of root meristem maintenance. Mol. Cell. Proteomics. In press. doi.org/10.1074/mcp.RA119.001378.

Rahman, A., Bannigan, A., Sulaman, W., Pechter, P., Blancaflor, E.B., and Baskin, T.I. (2007). Auxin, actin and growth of the *Arabidopsis thaliana* primary root. Plant J. 50: 514–528.

Rayle, D.L. and Cleland, R.E. (1992). The Acid Growth Theory of auxin-induced cell elongation is alive and well. Plant Physiol. 99: 1271–1274.

Rayle, D.L., Evans, M.L., and Hertel, R. (1970). Action of auxin on cell elongation. Proc. Natl. Acad. Sci. 65: 184–191.

Rosero, A., Žárský, V., and Cvrčková, F. (2013). AtFH1 formin mutation affects actin filament and microtubule dynamics in *Arabidopsis thaliana*. J. Exp. Bot. 64: 585–597.

Rotty, J.D. and Bear, J.E. (2014). Competition and collaboration between different actin assembly pathways allows for homeostatic control of the actin cytoskeleton. Bioarchitecture 5: 27–34.

Rotty, J.D., Wu, C., and Bear, J.E. (2013). New insights into the regulation and cellular functions of the ARP2/3 complex. Nat. Rev. Mol. Cell Biol. 14: 7–12.

Rutschow, H.L., Baskin, T.I., and Kramer, E.M. (2014). The carrier AUXIN RESISTANT (AUX1) dominates auxin flux into Arabidopsis protoplasts. New Phytol. 204: 536–544.

Ruzicka, D.R., Kandasamy, M.K., McKinney, E.C., Burgos-Rivera, B., and Meagher, R.B. (2007). The ancient subclasses of Arabidopsis *ACTIN DEPOLYMERIZING FACTOR* genes exhibit novel and differential expression. Plant J. 52: 460–472.

Sachs, T. (1991). Cell polarity and tissue patterning in plants. Dev. Suppl. I: 83–93.

Saier, Jr., M.H. (2000). Families of transmembrane transporters selective for amino acids and their derivatives. Microbiology 146: 1775–1795.

Sampathkumar, A., Gutierrez, R., McFarlane, H.E., Bringmann, M., Lindeboom, J., Emons, A.-M., Samuels, L., Ketelaar, T., Ehrhardt, D.W., and Persson, S. (2013). Patterning and lifetime of plasma membrane-localized cellulose synthase is dependent on actin organization in Arabidopsis interphase cells. Plant Physiol. 162: 675–88.

Satiat-Jeunemaitre, B., Steele, C., and Hawes, C. (1996). Golgi-membrane dynamics are cytoskeleton dependent: a study on Golgi stack movement induced by brefeldin A. Protoplasma 191: 21–33.

Sato, E.M., Hijazi, H., Bennett, M.J., Vissenberg, K., and Swarup, R. (2015). New insights into root gravitropic signalling. J. Exp. Bot. 66: 2155–2165.

Sauer, M. and Kleine-Vehn, J. (2011). AUXIN BINDING PROTEIN1: The Outsider. Plant Cell 23: 2033–2043.

Sauer, M., Robert, S., and Kleine-Vehn, J. (2013). Auxin: Simply complicated. J. Exp. Bot. 64: 2565–2577.

Schenck, D., Christian, M., Jones, A., and Luthen, H. (2010). Rapid auxin-induced cell expansion and gene expression: a four-decade-old question revisited. Plant Physiol. 152: 1183–1185.

Scheuring, D., Löfke, C., Krüger, F., Kittelmann, M., Eisa, A., Hughes, L., Smith, R.S., Hawes, C., Schumacher, K., and Kleine-Vehn, J. (2015). Actin-dependent vacuolar occupancy of the cell determines auxin-induced growth repression. Proc. Natl. Acad. Sci. 113: 452–457.

Scott, A.C. and Allen, N.S. (1999). Changes in cytosolic pH within Arabidopsis root columella cells play a key role in the early signaling pathway for root gravitropism. Plant Physiol. 121: 1291–1298.

Sheahan, M.B., Staiger, C.J., Rose, R.J., and McCurdy, D.W. (2004). A green fluorescent protein fusion to Actin-Binding Domain 2 of Arabidopsis fimbrin highlights new features of a dynamic actin cytoskeleton in live plant cells. Plant Physiol. 136: 3968–3978.

Sheterline, P. and Sparrow, J.C. (1994). Protein profile: Actin. Protein Profile, Vol. 1, P. Sheterline, ed. Academic Press, Ltd.: London, UK.

Simon, S. and Petrášek, J. (2011). Why plants need more than one type of auxin. Plant Sci. 180: 454–460.

Singh, G., Retzer, K., and Vosolsobe, S, and Napier, R. (2018). Advances in understanding the mechanism of action of the auxin permease AUX1. Int. J. Molec. Sci. 19: e3391.

Slade, W.O., Ray, W.K., Hildreth, S.B., Winkel, B.S., and Helm, R.F. (2017). Exogenous auxin elicits changes in the *Arabidopsis thaliana* root proteome in a time-dependent manner. Proteomes 5,16. doi:10.3390/proteomes5030016.

Šlajcherová, K., Fišerová, J., Fischer, L., and Schwarzerová, K. (2012). Multiple actin isotypes in plants: diverse genes for diverse roles ? Front. Plant Sci. 3: a226.

Smertenko, A.P., Jiang, C.J., Simmons, N.J., Weeds, A.G., Davies, D.R., and Hussey, P.J. (1998). Ser6 in the maize actin-depolymerizing factor, ZmADF3, is phosphorylated by a calcium-stimulated protein kinase and is essential for the control of functional activity. Plant J. 14: 187–193.

Smith, L.G. and Oppenheimer, D.G. (2005). Spatial control of cell expansion by the plant cytoskeleton. Annu. Rev. Cell Dev. Biol. 21: 271–295.

Staiger, C.J., Sheahan, M.B., Khurana, P., Wang, X., McCurdy, D.W., and Blanchoin, L. (2009). Actin filament dynamics are dominated by rapid growth and severing activity in the *Arabidopsis* cortical array. J. Cell Biol. 184: 269–280.

Staswick, P.E., Serban, B., Rowe, M., Tiryaki, I., Maldonado, M.T., Maldonado, M.C., and Suzaa, W. (2005). Characterization of an Arabidopsis enzyme family that conjugates amino acids to indole-3-acetic acid. Plant Cell 17: 616–627.

Stepanova, A.N., Robertson-Hoyt, J., Yun, J., Benavente, L.M., Xie, D., Dole, K., Schlereth, A., Jürgens, G., and Alonso, J.M. (2008). *TAA1*-mediated auxin biosynthesis is essential for hormone crosstalk and plant development. Cell 133: 177–191.

Stotz, H.U. and Hertel, R. (1994). Reevaluation of the role of auxin binding site II. J. Plant Growth Regul. 13: 79–85.

Suarez, C. and Kovar, D.R. (2016). Internetwork competition for monomers governs actin cytoskeleton organization. Nat. Rev. Mol. Cell Biol. 17: 799–810.

Suarez, C., Roland, J., Boujemaa-Paterski, R., Kang, H., McCullough, B.R., Reymann, A.C., Guérin, C., Martiel, J.L., De La Cruz, E.M., and Blanchoin, L. (2011). Cofilin tunes the nucleotide state of actin filaments and severs at bare and decorated segment boundaries. Curr. Biol. 21: 862–868.

Sun, H., Basu, S., Brady, S.R., Luciano, R.L., and Muday, G.K. (2004). Interactions between auxin transport and the actin cytoskeleton in developmental polarity of *Fucus distichus* embryos in response to light and gravity. Plant Physiol. 135: 266–78.

Swarup, R., Kargul, J., Marchant, A., Zadik, D., Rahman, A., Mills, R., Yemm, A., May, S., Williams, L., Millner, P., Tsurumi, S., Moore, I., Napier, R., Kerr, I.D., and Bennett, M.J. (2004). Structure-function analysis of the presumptive Arabidopsis auxin permease AUX1. Plant Cell 16: 3069–3083.

Swarup, R. and Bennett, M. (2014). Auxin transport: Providing plants with a new sense of direction. Biochem. Soc. (Lond). April: 12–15.

Swarup, R., Friml, J., Marchant, A., Ljung, K., Sandberg, G., Palme, K., and Bennett, M. (2001). Localization of the auxin permease AUX1 suggests two functionally distinct hormone transport pathways operate in the Arabidopsis root apex. Genes Dev. 15: 2648–2653.

Swarup, R. and Péret, B. (2012). AUX/LAX family of auxin influx carriers—an overview. Front. Plant Sci. 3: a225. doi: 10.3389/fpls.2012.00225.

Szymanski, D.B. and Cosgrove, D.J. (2009). Dynamic coordination of cytoskeletal and cell wall systems during plant cell morphogenesis. Curr. Biol. 19: R800–R811.

Szymanski, D.B., Marks, M.D., and Wick, S.M. (1999). Organized F-actin is essential for normal trichome morphogenesis in Arabidopsis. Plant Cell 11: 2331–2347.

Szymanski, D.B., and C.J. Staiger. (2018). The actin cytoskeleton: functional arrays for cytoplasmic organization and cell shape control. Plant Physiol. 176: 106–118.

Takemoto, D. and Hardham, A.R. (2004). The cytoskeleton as a regulator and target of biotic interactions in plants. Plant Physiol. 136: 3864–3876.

Talts, K., Ilau, B., Ojangu, E., Tanner, K., Peremyslov, V. V, Dolja, V. V, Truve, E., and Paves, H. (2016). *Arabidopsis* myosins XI1, XI2, and XIK are crucial for gravity-induced bending of inflorescence stems. Front. Plant Sci. 7: a1932. doi: 10.3389/fpls.2016.01932.

Tan, X., Calderon-Villalobos, L.I.A., Sharon, M., Zheng, C., Robinson, C. V., Estelle, M., and Zheng, N. (2007). Mechanism of auxin perception by the TIR1 ubiquitin ligase. Nature 446: 2–7.

Teale, W.D., Paponov, I.A., and Palme, K. (2006). Auxin in action: Signalling, transport and the control of plant growth and development. Nat. Rev. Mol. Cell Biol. 7: 847–859.

Terasaka, K., Blakeslee, J.J., Titapiwatanakun, B., Peer, W.A., Bandyopadhyay, A., Makam, S.N., Lee, R., Richards, E.L., Murphy, A.S., Sato, F., and Yazaki, K. (2005). PGP4, an ATP binding cassette p-glycoprotein, catalyzes auxin transport in *Arabidopsis thaliana* roots. Plant Cell 17: 2922–2939.

Thimann, K. V (1936). Auxins and the growth of roots. Am. J. Bot. 23: 561–569.

Thimann, K. V. (1937). On the nature of inhibitions caused by auxin. Am. J. Bot. 24: 407–412.

Thimann, K. V. (1939). Auxins and the inhibition of plant growth. Biol. Rev. 14: 314–337.

Tian, H., Klambt, D., and Jones, A.M. (1995). Auxin-binding protein 1 does not bind auxin within the endoplasmic reticulum despite this being the predominant subcellular location for this hormone receptor. J. Biol. Chem. 270: 26962–26969.

Titapiwatanakun, B. and Murphy, A.S. (2009). Post-transcriptional regulation of auxin transport proteins: Cellular trafficking, protein phosphorylation, protein maturation, ubiquitination, and membrane composition. J. Exp. Bot. 60: 1093–1107.

Tominaga, M. and Ito, K. (2015). The molecular mechanism and physiological role of cytoplasmic streaming. Curr. Opin. Plant Biol. 27: 104–110.

Tominaga, M., Kimura, A., Yokota, E., Haraguchi, T., Shimmen, T., Yamamoto, K., Nakano, A., and Ito, K. (2013). Cytoplasmic streaming velocity as a plant size determinant. Dev. Cell 27: 345–352. doi:10.1016/j.devcel.2013.10.005.

Tominaga, M. and Nakano, A. (2012). Plant-specific myosin XI, a molecular perspective. Front. Plant Sci. 3: a211. doi: 10.3389/fpls.2012.00211.

Toyota, M. and Gilroy, S. (2013). Gravitropism and mechanical signaling in plants. Am. J. Bot. 100: 111–125.

Tromas, A., Braun, N., Muller, P., Khodus, T., Paponov, I.A., Palme, K., Ljung, K., Lee, J., Benfey, P., Murray, J.A.H., Scheres, B., and Perrot-, C. (2009). The AUXIN BINDING PROTEIN 1 is required for differential auxin responses mediating root growth. PLoS ONE 4: e6648.

Ueda, H., Yokota, E., Kutsuna, N., Shimada, T., Tamura, K., Shimmen, T., Hasezawa, S., Dolja, V. V, and Hara-Nishimura, I. (2010). Myosin-dependent endoplasmic reticulum motility and F-actin organization in plant cells. Proc. Natl. Acad. Sci. 107: 6894–6899.

Ugartechea-Chirino, Y., Swarup, R., Swarup, K., Peret, B., Whitworth, M., Bennett, M., and Bougourd, S. (2010). The AUX1 LAX family of auxin influx carriers is required for the establishment of embryonic root cell organization in *Arabidopsis thaliana*. Ann. Appl. Biol. 105: 277–289.

van der Honing, H.S., van Bezouwen, L.S., Emons, A.M.C., and Ketelaar, T. (2011). High expression of Lifeact in *Arabidopsis thaliana* reduces dynamic reorganization of actin filaments but does not affect plant development. Cytoskeleton 68: 578–587.

van der Honing, H.S., Kieft, H., Emons, a. M.C., and Ketelaar, T. (2012). Arabidopsis VILLIN2 and VILLIN3 are required for the generation of thick actin filament bundles and for directional organ growth. Plant Physiol. 158: 1426–1438.

van Gisbergen, P.A.C. and Bezanilla, M. (2013). Plant formins: Membrane anchors for actin polymerization. Trends Cell Biol. 23: 227–233.

Vanneste, S. and Friml, J. (2009). Auxin: A trigger for change in plant development. Cell 136: 1005–1016.

Vanneste, S. and Friml, J. (2013). Calcium: The missing link in auxin action. Plants 2: 650–675.

Viaene, T., Landberg, K., Thelander, M., Medvecka, E., Pederson, E., Feraru, E., Cooper, E.D., Karimi, M., Delwiche, C.F., Ljung, K., Geisler, M., Sundberg, E., and Friml, J. (2014). Directional auxin transport mechanisms in early diverging land plants. Curr. Biol. 24: 2786–2791.

Vidali, L., Augustine, R.C., Kleinman, K.P., and Bezanilla, M. (2007). Profilin is essential for tip growth in the moss *Physcomitrella patens*. Plant Cell 19: 3705–3722.

Vidali, L., Burkart, G.M., Augustine, R.C., Kerdavid, E., Tüzel, E., and Bezanilla, M. (2010). Myosin XI is essential for tip growth in *Physcomitrella patens*. Plant Cell 22: 1868–1882.

Vidali, L., Mckenna, S.T., and Hepler, P.K. (2001). Actin polymerization is essential for pollen tube growth. Molec. Biol. Cell 12: 2534–2545.

Voigt, B., Timmers, A.C.J., Šamaj, J., Müller, J., Baluška, F., and Menzel, D. (2005). GFP-FABD2 fusion construct allows in vivo visualization of the dynamic actin cytoskeleton in all cells of *Arabidopsis* seedlings. Eur. J. Cell Biol. 84: 595–608.

Waller, F., Riemann, M., and Nick, P. (2002). A role for actin-driven secretion in auxin-induced growth. Protoplasma 219: 72–81.

Wang, B., Chu, J., Yu, T., Xu, Q., Sun, X., Yuan, J., Xiong, G., Wang, G., Wang, Y., and Li, J. (2015). Tryptophan-independent auxin biosynthesis contributes to early embryogenesis in *Arabidopsis*. Proc. Natl. Acad. Sci. 112: 4821–4826.

Wang, C., Liu, Y., Li, S.-S., and Han, G.-Z. (2014). Origin of plant auxin biosynthesis in charophyte algae. Trends Plant Sci. 19: 741–743.

Went, F.W. and Thimann, K. V. (1937). Phytohoromones. The Macmillan Company: New York.

Wightman, R. and Turner, S.R. (2010). Trafficking of the plant cellulose synthase complex. Plant Physiol. 153: 427–432.

Williamson, R.E. (1972). A light-microscope study of the action of cytochalasin B on the cells and isolated cytoplasm of the Characeae. J. Cell Sci. 10: 811–819.

Wisniewska, J., Xu, J., Seifertová, D., Brewer, P.B., Ruzicka, K., Blilou, I., Rouquié, D., Benková, E., Scheres, B., and Friml, J. (2006). Polar PIN localization directs auxin flow in plants. Science 312: 883.

Woo, E.J., Marshall, J., Bauly, J., Chen, J.G., Venis, M., Napier, R.M., and Pickersgill, R.W. (2002). Crystal structure of auxin-binding protein 1 in complex with auxin. EMBO J. 21: 2877–2885.

Woodward, A.W. and Bartel, B. (2005). Auxin: Regulation, action, and interaction. Ann. Bot. 95: 707–735.

Wu, H., Hazak, O., Cheung, A.Y., and Yalovsky, S. (2011). RAC/ROP GTPases and Auxin Signaling. Plant Cell 23: 1208–1218.

Wu, S., Xie, Y., Zhang, J., Ren, Y., Zhang, X., Wang, J., Guo, X., Wu, F., Sheng, P., Wang, J., Wu, C., Wang, H., Huang, S., Wan, J. (2015). VLN2 regulates plant architecture by affecting microfilament dynamics and polar auxin transport in rice. Plant Cell 27: 2829–45.

Xing, M. and Xue, H. (2012). A proteomics study of auxin effects in *Arabidopsis thaliana*. Acta Biochim. Biophys. Sin. (Shanghai). 44: 783–796.

Xu, T., Dai, N., Chen, J., Nagawa, S., Cao, M., Li, H., Zhou, Z., Chen, X., De Rycke, R., Rakusová, H., Wang, W., Jones, A.M., Friml, J., Patterson, S.E., Bleecker, A.B., and Yang, Z. (2014). Cell surface ABP1-TMK auxin-sensing complex activates ROP GTPase signaling. Science 343: 1025–1028.

Yanagisawa, M., Desyatova, A.S., Belteton, S.A., Mallery, E.L., Turner, J.A., and Szymanski, D.B. (2015). Patterning mechanisms of cytoskeletal and cell wall systems during leaf trichome morphogenesis. Nat. Plant 1: a15014. DOI: 10.1038/NPLANTS.2015.14.

Yanagisawa, M., Zhang, C., and Szymanski, D.B. (2013). ARP2/3-dependent growth in the plant kingdom: SCARs for life. Front. Plant Sci. 4: 166.

Yang, W., Ren, S., Zhang, X., Gao, M., Ye, S., Qi, Y., Zheng, Y., Wang, J., Zeng, L., Li, Q., Huang, S., and He, Z. (2011). BENT UPPERMOST INTERNODE1 encodes the class II formin FH5 crucial for actin organization and rice development. Plant Cell 23: 661–80.

Yang, Y., Hammes, U.Z., Taylor, C.G., Schachtman, D.P., and Nielsen, E. (2006). High-affinity auxin transport by the AUX1 influx carrier protein. Curr. Biol. 16: 1123–1127.

Yoder, T.L., Zheng, H.Q., Todd, P., and Staehelin, L. a (2001). Amyloplast sedimentation dynamics in maize columella cells support a new model for the gravity-sensing apparatus of roots. Plant Physiol. 125: 1045–1060.

Young, G.B., Jack, D.L., Smith, D.W., Jr, M.H.S., Stu, A., and Stu, A. (1999). The amino acid/auxin-proton symport permease family 1. 1415: 306–322.

Zazímalová, E., Murphy, A.S., Yang, H., Hoyerová, K., and Hosek, P. (2010). Auxin transporters—why so many? Cold Spring Harb. Perspect. Biol. 2: 1–14.

Zhang, S., and van Duijn, B. (2014). Cellular auxin transport in algae. Plants 3: 58–69.

Zhang, W., Cai, C., and Staiger, C.J. (2019). Myosins XI are involved in exocytosis of cellulose synthase complexes. Plant Physiol. 179: 1537–1555.

Zhang, C., Halsey, L.E., and Szymanski, D.B. (2011a). The development and geometry of shape change in *Arabidopsis thaliana* cotyledon pavement cells. BMC Plant Biol. 11: 27. doi:10.1186/1471-2229-11-27.

Zhang, Y., Xiao, Y., Du, F., Cao, L., Dong, H., and Ren, H. (2011b). *Arabidopsis* VILLIN4 is involved in root hair growth through regulating actin organization in a Ca^{2+}-dependent manner. New Phytol. 190: 667–682.

Zhang, Z., Zhang, Y., Tan, H., Wang, Y., Li, G., Liang, W., Yuan, Z., Hu, J., Ren, H., and Zhang, D. (2011c). *RICE MORPHOLOGY DETERMINANT* encodes the type II formin FH5 and regulates rice morphogenesis. Plant Cell 23: 681–700.

Zhao, Y. (2014). Auxin Biosynthesis. Arab. B. 12: e0173.

Zhu, J., Baily, A., Zwiewka, M., Sovero, V., Di Donato, M., Ge, P., Oehri, J., Aryal, B., Hao, P., Linnert, M., Burgardt, N.I., Lücke, C., Weiwad, M., Michel, M., Weiergräber, O.H., Pollmann, S., Azzarello, E., Mancuso, S., Ferro, N., Fukao, Y., Hoffmann, C., Wedlich-Söldner, R., Friml, J., Thomas, C., and Geisler, M. (2016). TWISTED DWARF1 mediates the action of auxin transport inhibitors on actin cytoskeleton dynamics. Plant Cell 28: 930–948.

Zhu, J. and Geisler, M. (2015). Keeping it all together: Auxin–actin crosstalk in plant development. J. Exp. Bot. 66(16): erv308. doi:10.1093/jxb/erv308.

CHAPTER 2.   AUXIN-INDUCED ACTIN CYTOSKELETON REARRANGEMENTS REQUIRE AUX1

2.1   Abstract

The actin cytoskeleton is required for cell expansion and is implicated in cellular responses to the plant growth hormone auxin. However, the molecular and cellular mechanisms that coordinate auxin signaling, cytoskeletal remodeling, and cell expansion are poorly understood. Previous studies have examined actin cytoskeleton responses to long-term auxin treatment, but plants respond to auxin over short timeframes, and growth changes within minutes of exposure to the hormone. To correlate actin arrays with degree of cell expansion, we used quantitative imaging tools to establish a baseline of actin organization, as well as of individual filament behaviors in root epidermal cells under control conditions and after treatment with a known inhibitor of root growth, the auxin indole-3-acetic acid (IAA). We found that cell length was highly predictive of actin array in control roots, and that short-term IAA treatment stimulated denser, more longitudinal, and more parallel arrays by inducing filament unbundling within minutes. By demonstrating that actin filaments were more "organized" after a treatment that stopped elongation, we show there is no direct relationship between actin organization and cell expansion and refute the hypothesis that "more organized" actin universally correlates with more rapidly growing root cells. The plasma membrane-bound auxin transporter AUXIN RESISTANT 1 (AUX1) has previously been shown necessary for archetypal short-term root growth inhibition in the presence of IAA. Although AUX1 was not previously suspected of being upstream of cytoskeletal responses to IAA, we used *aux1* mutants to demonstrate that AUX1 is necessary for the full complement of actin rearrangements in response to auxin, and that cytoplasmic auxin in the form of the membrane permeable auxin 1-naphthylacetic acid (NAA) is sufficient to stimulate a partial actin response. Together, these results are the first to quantitate actin cytoskeleton response to short-term auxin treatments and demonstrate that AUX1 is necessary for short-term actin remodeling.

2.2   Introduction

Despite human dependence on plants for food, fiber, and fuel, we do not fully understand the molecular mechanisms controlling plant growth. Many types of plant cells begin life as roughly isotropic but, during development, the cell establishes polar growth where deposition of cell wall materials is restricted to specific axes of the cell, or expansion is anisotropic, allowing the production of mature cells with a myriad of final shapes and sizes. Turgor pressure drives expansion within the confines of cell wall flexibility: certain areas of the plant cell wall are more flexible than others, and are therefore more susceptible to turgor pressure exerted by the vacuole (Szymanski and Cosgrove, 2009; Guerriero et al., 2014). Vesicles are incorporated into certain areas of the plasma membrane and deposit new cell wall material, increasing the cell's surface area and conducting the cell to grow into specific shapes. Vesicle delivery and exocytosis of vesicle contents of wall materials depend on the actin cytoskeleton (Ketelaar et al., 2003; Hussey et al., 2006; Leucci et al., 2007; Zhang et al., 2019). When actin is disrupted with pharmacological treatments, cells elongate more slowly (Baluška et al., 2001), implicating actin as a crucial player in cell expansion. Although the actin cytoskeleton is required for plant cell expansion (Baluška et al., 2001; Gilliland et al., 2003; Mathur, 2004; Hussey, 2006; Rahman et al., 2007; Kandasamy et al., 2009; Yang et al., 2011; Guerriero et al., 2014), actin's function in this process is not well understood. Actin is accepted to provide tracks for vesicle delivery (Mathur, 2004; Hussey et al., 2006), but connections have also been made between certain actin arrays and plant growth (ex., Nick et al., 2009; Higaki et al., 2010a; Smertenko et al., 2010; Dyachok et al., 2011; Yang et al., 2011, Yanagisawa et al., 2015), resulting in various hypotheses about actin's role and/or the significance of specific actin arrays, each with a degree of supporting evidence, much of it circumstantial (Li et al., 2015a; Szymanski and Staiger, 2017).

Actin arrays form an apparently "organized" orientation, with actin bundles roughly parallel to the longitudinal axis of the cell in rapidly growing root epidermal cells in the light (Dyachok et al., 2011). In the dark, where cell expansion is substantially slower, actin exhibits what appears to be a state of "disorganization": filaments are substantially less aligned relative to the longitudinal axis of root cells (Dyachok et al., 2011). However, data substantiating cause-and-effect are missing from the literature. Whether a longitudinal array is necessary for, coincides with, promotes, or (conversely) is the product of, cell expansion—or whether the "disorganized" array inhibits or coincides with a cessation of expansion—is not understood and is largely unexamined.

In addition to longitudinal actin orientation, various actin arrays have been correlated with cell length or cell expansion. However, there does not seem to be consensus on whether more longitudinal bundles inhibit (Gilliland et al., 2003; Holweg et al., 2004; Rahman et al., 2007) or stimulate (Kandasamy et al., 2009; Yang et al., 2011; Li et al., 2014a) axial cell expansion and tissue growth. Many previous studies linking specific actin organizations with growth or growth inhibition are based on actin or actin-binding protein mutant phenotypes (Gilliland et al., 2003, Kandasamy et al., 2009, Yang et al., 2011; Li et al., 2014a). Others are based on actin responses to drug or hormone treatments (Holweg et al., 2004; Rahman et al., 2007). Therefore, some of the reported actin–cell growth models may be generalized from what might in fact be more discrete responses: cytoskeletal response to a specific external stimulus (drug or hormone) that affects growth via downstream mechanisms; or filament array changes due to an actin-binding protein whose role could be in only one of many aspects of growth.

In fact, what tasks, exactly, actin undertakes during cell expansion and how these tasks drive or participate in expansion are unclear. Bundles potentially inhibit growth by inhibiting transport of growth hormone-related proteins (Nick, 2010). On the other hand, long actin bundles presumably stimulate growth because they provide tracks for vesicle delivery (Szymanski and Cosgrove, 2009; Thomas, 2012). Actin bundles could play a role in regulating osmotic pressure in the vacuole by altering turgor pressure (Higaki et al., 2010a,b; 2011), the main driver of plant cell expansion (Szymanski and Cosgrove, 2009). A recent paper shows that auxin, a known modulator of plant growth that has opposite effects on root or shoot growth (inhibition and stimulation, respectively), constricts vacuolar shape in long-term treatments (6+ h) on root cells, and does so by inducing altered actin arrays (Scheuring et al., 2016). Although this work describes the long-term effects of auxin on actin (Scheuring et al., 2016), what connects short-term auxin treatments with actin rearrangements is not understood. Interactions between auxin signaling pathways and actin are abundant in the literature (reviewed in Zhu and Geisler, 2015), but the mechanics of how the hormone affects the cytoskeleton on a timescale of minutes, and how these interactions stimulate or inhibit growth, are largely unknown.

The molecular players that connect the actin cytoskeleton to auxin perception during short-term responses are unidentified. Auxin reception by AUXIN BINDING PROTEIN 1 (ABP1) was previously suspected to be upstream of cytoskeletal changes in both roots (Chen et al., 2012; Lin et al., 2012) and epidermal pavement cells (Xu et al., 2010; Nagawa et al., 2012; Xu et al., 2014);

however, recent works demonstrate that a CRISPR *abp1-c1* mutant exhibited root growth inhibition in the presence of both the known root growth inhibitor, the auxin indole-3-acetic acid (IAA) and the membrane permeable auxin 1-naphthylacetic acid (NAA), just like wildtype plants, indicating that ABP1 likely does not play a significant role in auxin signaling (Dai et al., 2015; Gao, et al., 2015). AUXIN RESISTANT 1 (AUX1) is a plasma membrane-bound auxin/H^+ symporter in the Amino acid/auxin permease (AAAP) family that is ubiquitous among Eukaryotes. AUX1 appears to be present in all plants as well as some algae, indicating that the protein likely evolved before land plants (reviewed in Swarup and Péret, 2012). Unlike wildtype, *aux1* plants grow in the presence of IAA, but undergo growth inhibition by NAA (Marchant et al., 1999), and AUX1 binds both IAA and NAA with high affinity (Yang et al., 2006; Carrier et al., 2008) and is responsible for 80% of IAA uptake by root hairs (Dindas et al., 2018). AUX1 contributes to short-term, auxin-induced increases in cytosolic H^+ and, together with the intracellular auxin receptor complex SCF$^{TIR1/AFB}$, increases in cytosolic Ca^{2+} (Dindas et al., 2018). The auxin molecule itself is the signal that SCF$^{TIR1/AFB}$ perceives (Dharmasiri et al., 2005a,b; Kepinski and Leyser, 2005), driving both rapid increases in Ca^{2+} (Dindas et al. 2018) and transcriptional reprogramming (Ulmasov et al., 1999).

To correlate actin arrays with degree of cell expansion, we used quantitative tools to establish a baseline of actin architecture and orientation and individual filament behaviors in root epidermal cells under control circumstances. By plotting measurements of each cell's actin array against its length, we found that cell length was highly predictive of actin array. We then used acute treatments with IAA to determine the actin response in presumed non- or very slow-growing cells and documented the first short-term actin responses to these growth-inhibitory doses of IAA. Upon analyzing the actin arrays in two *aux1* alleles (the T-DNA insertion mutant *aux1-100* and the null point mutant *aux1-22*), we found that actin failed to reorganize in response to IAA and actin reorganization was only partially restored by NAA. Our data substantiate that AUX1 and cytosolic auxin play a significant role upstream of actin reorganization in auxin signaling.

2.3   Results

2.3.1   Actin Organization Correlates with Cell Length

Actin organization in living epidermal cells of the root cap and elongation zone, examined with variable angle epifluorescence microscopy (VAEM), displayed a consistent pattern of organization (Baluška et al., 1997; **Figure 2.1A**, **Supplemental Figure 2.6A**[1]). The actin array in thin, rectangular cells closest to the root apex—the root cap—comprised haphazardly arranged bundles. About 200 μm from the apex, in short, square cells emerging from under the root cap, there appeared to be a marked increase in the abundance of actin filaments, with fewer bundles. Array organization appeared to become gradually more bundled, longitudinal, and sparse as cells increased in length, until reaching the end of the root elongation zone (a demarcation indicated by the first visible root hair initiations). Although this pattern has been observed previously (Baluška et al., 1997; Baluška and Mancuso, 2013), we wondered whether there were quantitative differences in actin organization that could be correlated with cell size, and, potentially, with developmental stage. After plant cells are generated in the root meristem, they spend approximately 4 d progressing through the meristematic region (including the root transition zone) before progressing to the zone of rapid elongation, where they spend mere hours (Beemster and Baskin, 1998, 2000; van der Weele et al., 2003). The consistent progression of aging, growing cells allows comparison and quantification of actin arrays in cells in both the slower-growing late meristematic/transition zone and the zone of rapid elongation. Whether actin bundles inhibit (Gilliland et al., 2003; Holweg et al., 2004; Rahman et al., 2007) or promote (Kandasamy et al., 2009; Yang et al., 2011; Li et al., 2014a) cell expansion remains controversial. We hoped to gain insight into the role of actin bundling in expansion of root epidermal cells, since it is the root epidermis that drives cell expansion in all root layers (Savaldi-Goldstein et al., 2007 [shoots]; Hacham et al., 2011).

---

[1]Supplemental Figures start with **Supplemental Figure 2.6**.

Figure 2.1 Actin Organization is Predictive of Epidermal Cell Length in the Root Cap and Elongation Zone.

(A) Mosaic of root cap and elongation zone in an Arabidopsis seedling expressing GFP-fABD2 imaged with variable angle epifluorescence microscopy (VAEM). Arrowhead, root apex; arrow, first root hair initiation. MosaicJ was used to compile 13 original VAEM images. Scale bar, 100 μm.

(B) Representative images of actin organization in two root regions. Scale bar, 10 μm.

(C) to **(G)** Quantification of actin architecture or orientation metrics plotted with respect to corresponding epidermal cell length **(D)**, **(E)**, **(F)**, and **(G)** or cell width **(C)** in the root elongation zone. Filament architecture and orientation were not predictable based on cell width but were highly correlated with cell length. **Supplemental Figure 2.7** shows results for skewness, angle, and parallelness vs. cell width, which also showed no relationship, and **Supplemental Figure 2.6** shows comparisons of Region 2 and Region 3 mean measurements. Mean cell length, Region 2 = 57 ± 28 μm. Mean cell length, Region 3 = 128 ± 34 μm. Region 2 measurements are shown in purple diamonds; Region 3 in blue circles.

N = 60–150 cells per region from 20 roots. NR, no predictive relationship; ***, $p \leq 0.0001$, Bivariate fit/ANOVA for all data points for each parameter. Results are from one experiment.
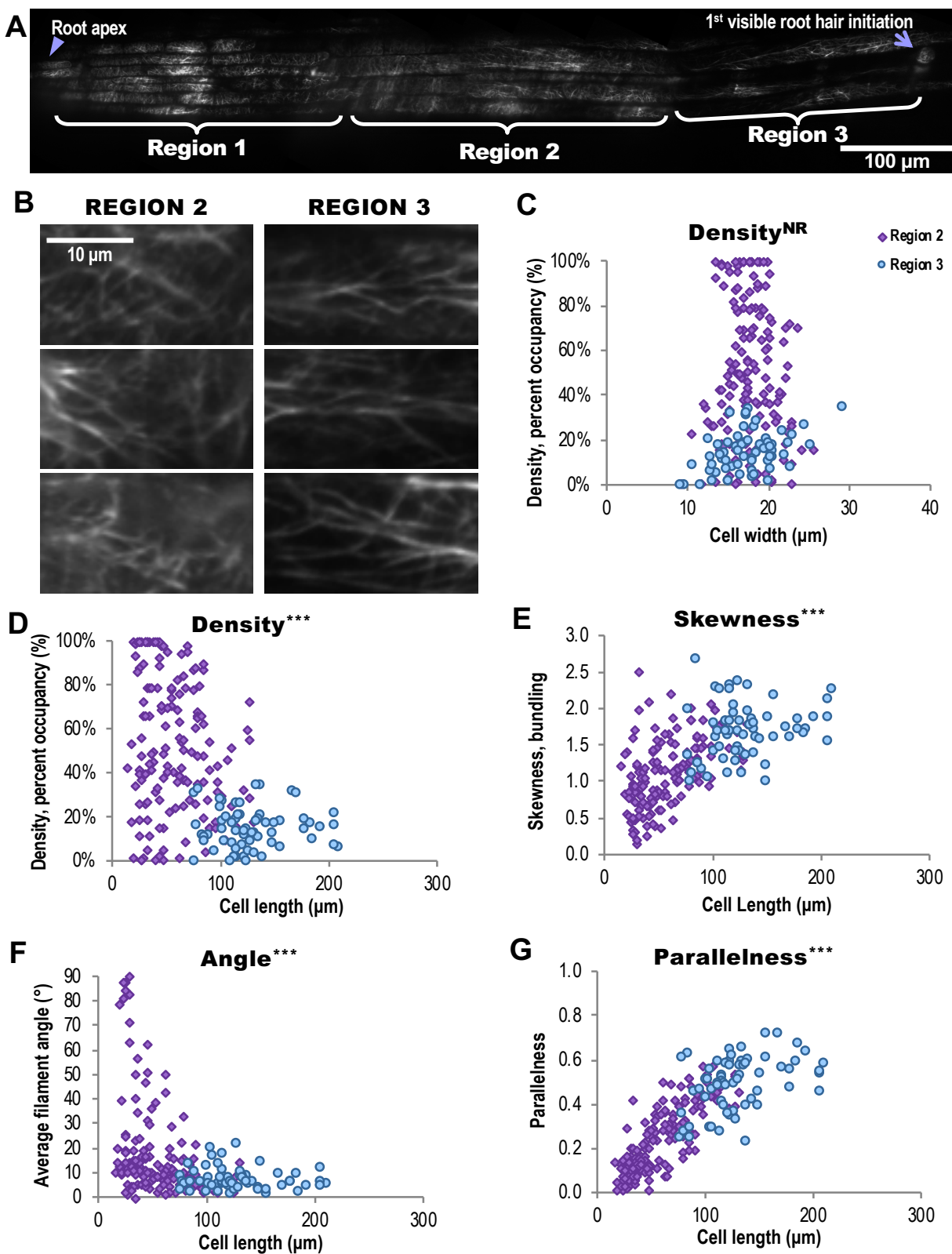
Figure 2.1 Actin Organization is Predictive of Epidermal Cell Length in the Root Cap and Elongation Zone.

To test quantitatively whether actin array organization varies over the course of the root, we took overlapping VAEM images of GFP-fABD2–labeled (green fluorescent protein fused to the second actin-binding domain of Arabidopsis FIMBRIN1) actin filaments from the root apex through the end of the elongation zone. The demarcation between the root cap (here called "Region 1") and what appeared to be the visible transition zone (here called "Region 2") was drastic. Isotropic cells that delineate the late meristematic/early transition zone clearly emerge from under the rectangular cells of the presumed root cap. The distinction between Region 2 and what we call "Region 3" was not nearly so definitive as between Region 1 and Region 2, so we first delineated Region 3 by an observable decrease in actin filament abundance (admittedly, a subjective criterion). Representative images showed conspicuous differences in actin arrays in Region 2 and Region 3 (**Figure 2.1B**; Region 1, i.e., the root cap, in **Supplemental Figure 2.6A**). Aspects of actin organization were quantified as described previously (Higaki et al., 2010b; Ueda et al., 2010; Henty et al., 2011; Li et al., 2012; Cai et al, 2014; Cao et al., 2016). Parameters measured include: percent occupancy or density, the extent of bundling of actin filaments (measured as "skewness" of pixel intensity distribution in an image), parallelness of filaments to each other, and average filament angle relative to a cell's longitudinal axis (Higaki et al., 2010b; Ueda et al., 2010; Henty et al., 2011; Li et al., 2012; Cai et al, 2014; Cao et al., 2016). These quantitative analyses showed (**Supplemental Figure 2.6B–E**) the cortical actin array in root Region 2 was significantly more dense and less bundled than Region 3 (longer cells closer to the first visible root hair initiations). Region 1 was similar in density to Region 2, but more bundled. The filaments and bundles in cells of Region 3 were substantially more longitudinal than those in Region 1 or Region 2. Since cells of the root cap do not follow in the same cell files as Regions 2 and 3 and do not follow the same cell expansion gradient, and since we sought to learn about differences in actin organization over the course of cell expansion, we eliminated Region 1 from further analysis.

Because of the substantial differences in actin organization among epidermal cells within the elongation zone, we hypothesized that if certain actin arrays correlate with expanding cells, cell size should predict actin organization and vice versa. A root cell's shape (length and width) or its actin array should correctly place the cell at a certain point in the expansion gradient of the elongation zone. While cell width could not predict any of the actin measurements—there was no predictive relationship between cell widths and actin filament density, skewness, angle, or

parallelness (**Figure 2.1C**; **Supplemental Figure 2.7**)—cell lengths were highly predictive of each actin metric, using the descriptive statistical analysis bivariate fit (**Figure 2.1D–G**; **Supplemental Figure 2.8**). Short cells exhibited higher actin density (**Figure 2.1D**), lower bundling (**Figure 2.1E**), and what might be perceived as "disorganized" actin, with higher average filament angles (**Figure 2.1F**) and lower parallelness (**Figure 2.1G**) compared with long cells. These highly predictive relationships between cell length and each aspect of actin organization held when we examined actin organization in the Wassilewskija (WS) ecotype expressing GPF-fABD2 and in a T-DNA insertion mutant for the auxin transport protein AUX1 (*aux1-100*, WS background; **Supplemental Figure 2.12**), whose average root epidermal cell lengths are significantly longer than either wildtype. Although we were unable to accurately and consistently measure cell growth rates (based on literature such as Beemster and Baskin, 1998; van der Weele et al., 2003), and so have not determined whether bundles promote or even precede expansion, it is clear that a higher incidence of actin bundling occurred in long cells (**Supplemental Figures 2.8**, **2.12**, and **2.14**).

The parameter that adhered to a fairly linear relationship with cell length is parallelness ($R^2 = 0.68$; **Figure 2.1G**; **Supplemental Figure 2.8D**)—how parallel filaments are to each other. Although these data cannot establish increased filament parallelness as the cause of cell elongation, they demonstrate that filament parallelness is the parameter most directly correlated with cell length. To determine whether any particular combination of the measured parameters (cell length, cell width, filament density, skewness, angle, and parallelness) explains the most variance from the mean for each cell, we performed principal component analysis on each data set, finding that the interactions between cell length, filament parallelness, and to a lesser extent, skewness, explain most of our observations for both wildtype ecotypes (Col-0 and WS) and the *aux1-100* mutant (see **Supplemental Tables 2.3–8**[2]).

Aside from investigating correlations between actin organization and cell size, our intent was to find a more objective way of categorizing cells into "Region 2" or "Region 3" for wildtype plants. By plotting each cell's specific actin metrics against its length or width, we defined maximum cell sizes for each region. The maximum length of a cell included as Region 2 became 85 μm, the mean cell length (57 μm) plus one standard deviation (28 μm); the minimum length of a cell included as Region 3 became 94 μm, the mean cell length (128 μm) minus one standard

---

[2]Supplemental Tables start with **Supplemental Table 2.3**.

deviation (34 µm). These cutoffs were used in assigning "region" in all further experiments on the Col-0;GFP-fABD2 lines (see **Methods**).

2.3.2 Cortical Actin Array Dynamics and Individual Filament Behaviors Differ between Short and Long Cells

Cortical actin arrays constantly remodel depending on the needs of a cell (Staiger et al., 2009; Henty et al., 2011; Henty-Ridilla et al., 2013; Henty-Ridilla et al., 2014; Cao et al., 2016). Arrays in isotropically-growing cotyledon pavement cells are observed to exhibit "more random" and "more dynamic" arrays than the anisotropically-growing cells of the root elongation zone (Smertenko et al., 2010). We hypothesized that the actin network in cells in Region 3 would be less dynamic than in Region 2. We collected 100-s timelapse movies from short and long cells in the same roots and calculated the pairwise correlation coefficient among all possible temporal intervals (Vidali et al., 2010). We found that the actin array dynamicity in Region 2 cells was significantly reduced compared to Region 3 (**Supplemental Figure 2.9**). The array of Region 2 cells was very dense, so we considered that a general comparison of pixel intensities and occupancies among temporal intervals of timelapse movies might not account for the true dynamic behavior of the array.

To determine what specific behaviors contribute to the overall filament array in cells, we quantified individual actin filament behaviors (Li et al., 2015b). We expected increased turnover in short cells and a higher frequency of bundling events in long cells. On average, filaments in short and long cells behaved similarly, except that longer cells exhibited longer, faster-growing filaments (**Figure 2.2**; **Table 2.1**). Upon measuring bundling, unbundling, and annealing frequencies, we were surprised to observe no differences in frequency of bundling or unbundling, but there was a multifold increase in annealing in shorter cells (**Figure 2.2**; **Table 2.1**).

Table 2.1 Individual Actin Filament Behaviors in Regions 2 and 3.

Parameter	Region 2	Region 3
Maximum filament length (µm)	**5.7 ± 0.3**	**8.1 ± 0.4*****
Filament lifetime (s)	23.5 ± 1.5	23.5 ± 1.2[ND]
Elongation rate (µm/s)	**0.96 ± 0.05**	**1.32 ± 0.08*****
Severing frequency (breaks/µm/s)	0.04 ± 0.004	0.04 ± 0.003[ND]
Event frequency/minute per filament		
Bundling[a]	0.111 ± 0.009	0.103 ± 0.009[ND]
Unbundling	0.030 ± 0.004	0.032 ± 0.004[ND]
Annealing	**0.100 ± 0.009**	**0.012 ± 0.003*****

Values are means ± standard error.

[a]Bundling includes both zippering ($\approx$ 90% of observed bundling events) and "other" (remaining $\approx$ 10% of observed bundling events); see **Methods** for more information.

Average number of actin filaments and bundles per 227.7 µm^2 region of interest (ROI): Region 2, 98.7 ± 4.1; Region 3, 64.6 ± 2.4.

Per region, N = at least 50 filaments from more than 25 cells from $\geq$ 15 roots. Bundling, unbundling, and annealing events: per root region, N = ROIs (227.7 µm^2) from a total of 30–37 cells from 30 roots. ND, no statistical differences; ***, $p \leq 0.001$, Student's t-test.

Figure 2.2 Timelapse Imaging of Cortical Actin Filaments in Root Epidermal Cells Shows Differences in the Dynamic Behavior between Short and Long Cells.

(A) and **(C)** The cortical actin cytoskeleton in 6-day-old light-grown root epidermal cells expressing GFP-fABD2 was imaged with timelapse VAEM. Representative images of individual filament dynamics in short cells (up to 85 μm long, Region 2) and long cells (over 94 μm long, Region 3). On average, filaments in short cells **(A; filament highlighted in purple)** elongated over 25% more slowly and grew to be nearly 30% shorter than filaments in long cells **(C; filament highlighted in blue)**. Severing frequencies and filament lifetimes did not vary between regions; see **Table 2.1**. Scale bar, 5 μm.

(B) and **(D)** Regions of interest (ROI; 227.7 $μm^2$) were selected from the same movies as **(A)** and **(C)**. Annealing occurs 10× more frequently in short cells **(B; filaments highlighted in purple)** compared with long cells **(D; filament highlighted in blue)**. Note that four annealing events (white arrowheads) occurred within 6 s in **(B)** compared with only one event in **(D)**. Dots indicate fragments involved in annealing events. Quantification of annealing frequencies as well as bundling and unbundling frequencies are shown in **Table 2.1**. Although actin filament arrays in long cells were substantially more bundled compared with short cells (see **Figure 2.1**), there were no differences in bundling or unbundling frequencies when event frequencies were calculated on a per-minute, per-filament basis. Scale bar, 2 μm.

100-s timelapse movies were collected from short and long cells in the same 30 roots.

Note: Brightness and contrast were enhanced in the montages of **Figure 2.2B** and **Figure 2.2C** to better show the filament and its changes.
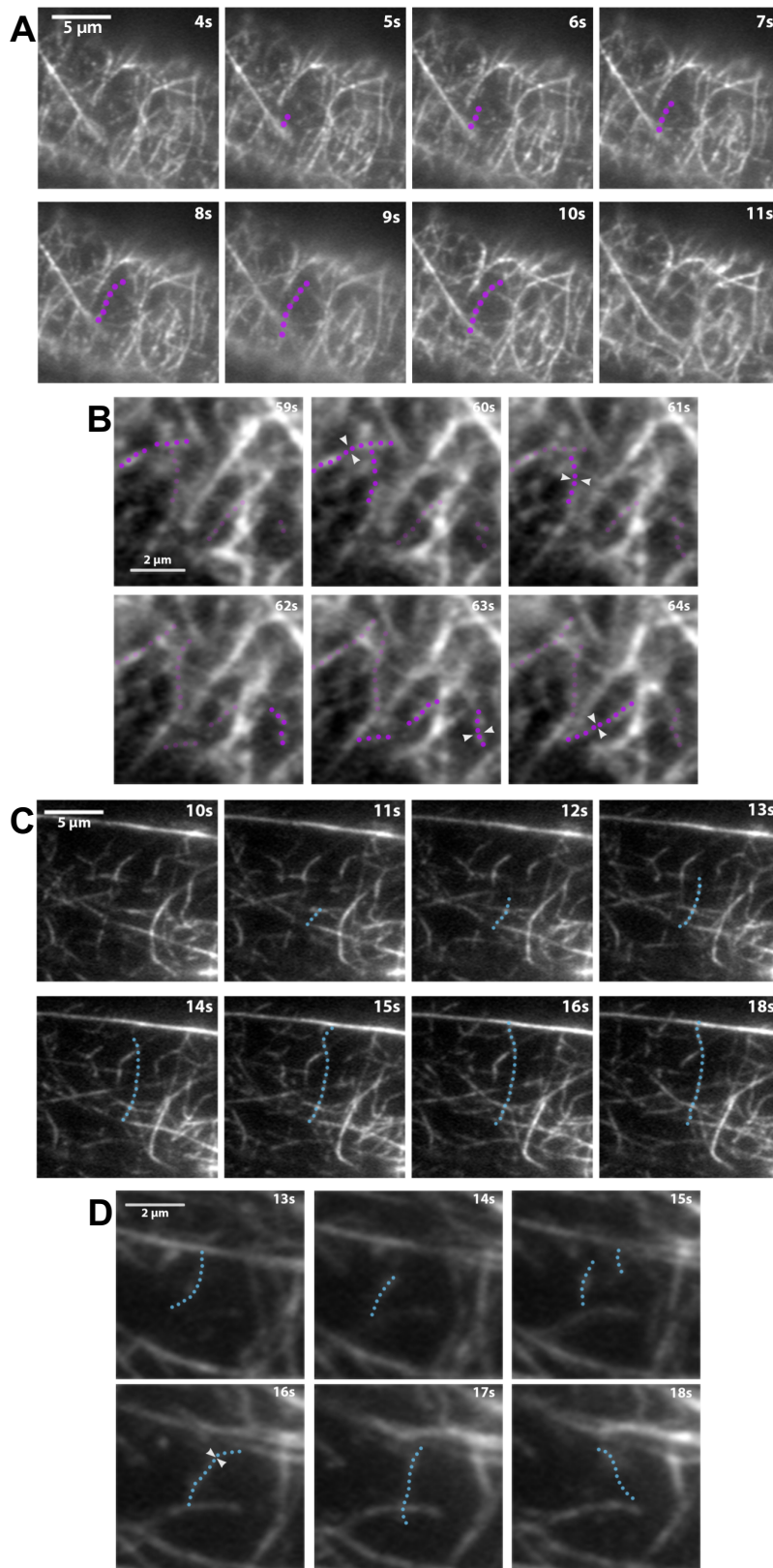
Figure 2.2 Timelapse Imaging of Cortical Actin Filaments in Root Epidermal Cells Shows Differences in the Dynamic Behavior between Short and Long Cells.

2.3.3 Actin Organization Responds to Short-Term IAA Treatments

To decipher which actin parameter(s) coincided with cell expansion, and to find stronger indicators of causality, we treated roots with a known inhibitor of root growth, the naturally occurring auxin, IAA, which has been shown to inhibit root growth within minutes of application (Hejnowicz and Erickson, 1968; Fendrych et al., 2018). Auxin affects actin organization and dynamics and inhibits root growth (reviewed in Zhu and Geisler, 2015; Fendrych et al., 2018), known to depend on an intact cytoskeleton (reviewed in Hussey, 2006 and Li et al., 2015a). Yet, actin response following short-term auxin treatments, i.e., a way to directly link the two, has not been determined. If decreased actin density and increased bundling are indeed hallmarks of growth, and if auxin works by modulating the actin cytoskeleton, then IAA, an agent that inhibits growth, should induce the opposite actin phenotype: after IAA treatment, density should increase and bundling decrease. Further, if a lower average filament angle and higher parallelness are indicative of rapidly growing cells (described in Dyachok at al., 2011, and a natural assumption given that we found increasingly longitudinal actin arrays in longer cells), applying IAA should increase filament angle and decrease parallelness (i.e., there should be a decrease in both longitudinality and apparent "organization").

As expected, 20–30 min IAA treatments induced significant increases in actin filament density and decreases in extent of bundling (**Figure 2.3**), linking actin abundance and a reduction in bundling with plant response to IAA. We were surprised, however, to observe a dose-dependent increase in apparent actin organization after IAA treatments (**Figure 2.3A,D–E**, **Supplemental Figure 2.10**). In another, timeseries experiment, we established that the IAA-induced increase in parallel longitudinality is maintained for at least 60 min after initial treatment (**Supplemental Figure 2.11**; **Supplemental Table 2.9**). Strong changes in filament angle and orientation generally appeared more slowly than the increase in density. Together, these are the first data that quantitatively document actin's short-term response to moderate doses of IAA.

Figure 2.3 Short-Term IAA Treatments Induce Changes in Actin Filament Organization.

(A) Representative VAEM images of GFP-fABD2–labeled actin in epidermal cells from Region 2 (≤ 85 μm long) and Region 3 (≥ 94 μm long), treated for 20–30 min with indicated doses of IAA or mock. Scale bar, 10 μm.

(B) to **(E)** Quantification of actin architecture and orientation in root epidermal cells: IAA triggered an increase in actin filament density **(B)** and decrease in skewness **(C)**. Region 2 measurements are shown in purple; Region 3 in blue. **(D) and (E)** After IAA treatments, actin arrays in both regions were more "organized," with lower average filament angle **(D)** relative to the longitudinal axis of the cell and filaments generally more parallel to each other **(E)**. Changes in actin orientation **(D)** and **(E)** were dose-dependent, see **Supplemental Figure 2.10**.

Cells whose lengths fell between 85 and 94 μm were counted in both regions. N = 8–12 cells per region per root from at least 10 roots per treatment. ND, no statistical differences; *, $p \leq 0.05$; **, $p \leq 0.01$; ***, $p \leq 0.0001$, oneway ANOVA, compared with Dunnett's Method, comparing doses to mock in each Region, in JMP. Results are from one representative experiment of 3 similar experiments with similar results. All IAA experiments were performed and analyzed double blind.
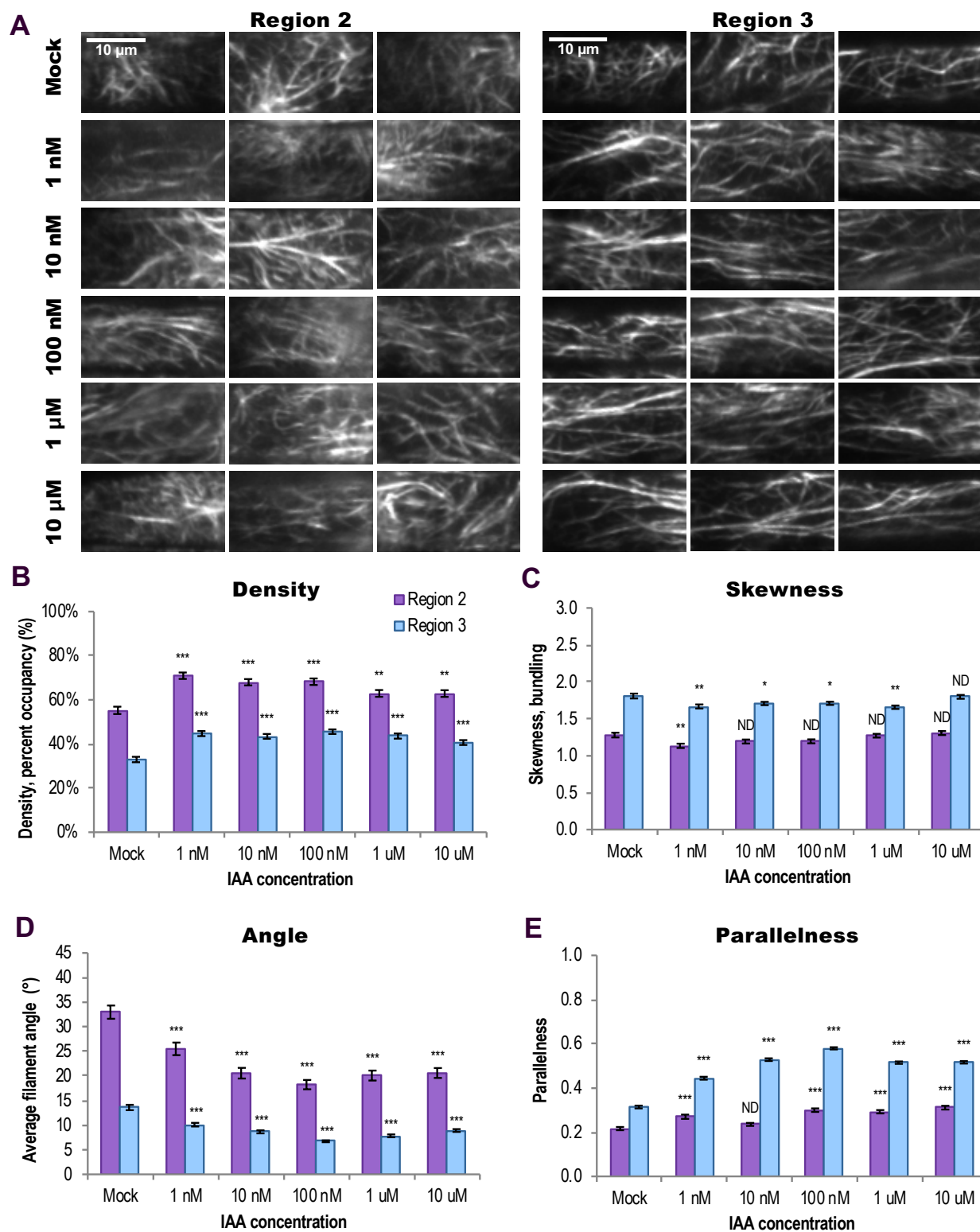
Figure 2.3 Short-Term IAA Treatments Induce Changes in Actin Filament Organization.

2.3.4 Actin Filaments Unbundle in Response to IAA

Links between auxin and actin clearly exist (reviewed in Zhu and Geisler, 2015) but the specific components of these pathways—and actin's role in them—are unresolved, so we evaluated actin's role in IAA perception by measuring whether individual filament behaviors change in the minutes immediately following IAA treatment.

Since substantial increases in actin density and parallel longitudinality occurred within 20–30 min of treatment with IAA, we hypothesized that individual filaments would respond quickly to treatment and might undergo increased severing, faster filament elongation rates, increased unbundling, and/or increased annealing (a result of decreased end-capping; Li et al., 2012). We tested this prediction by quantifying actin dynamics in epidermal cells in Region 2 and Region 3 within 7 min of 10 nM IAA treatment. Surprisingly, we observed no changes in most individual filament behaviors in either shorter or longer cells within this 7-min timeframe (**Table 2.2**). Though the differences in filament elongation rates and maximum filament length we previously observed between regions (**Table 2.1**) were reproduced, 10 nM IAA did not affect any of the measured stochastic dynamics parameters: overall filament length, lifetime, elongation rate, or severing frequency within a region. However, when we measured frequency of bundling, unbundling, and annealing, we observed an IAA-induced doubling of unbundling events in both short and long cells (**Figure 2.4**, **Table 2.2**). In long cells, IAA induced a near 5-fold increase in annealing (**Figure 2.4D**, **Table 2.2**). Actin filaments unbundled and altered annealing frequencies within 7 min of IAA treatment, demonstrating that actin participates in short-term responses to the hormone.

Table 2.2 Actin Filament Dynamics after Treatment with IAA.

Parameter/Treatment	Region 2		Region 3	
	Mock	IAA	Mock	IAA
Maximum filament length (μm)	5.2 ± 0.2	4.6 ± 0.2ND	9.8 ± 0.6	9.7 ± 0.4ND
Filament lifetime (s)	27.4 ± 1.9	24.9 ± 1.2ND	28.8 ± 2.2	33.9 ± 2.1ND
Elongation rate (μm/s)	0.97 ± 0.14	0.88 ± 0.05ND	1.63 ± 0.06	1.62 ± 0.07ND
Severing frequency (breaks/μm/s)	0.05 ± 0.003	0.06 ± 0.003ND	0.03 ± 0.002	0.03 ± 0.002ND
Event frequency/minute per filament				
Bundling[a]	0.216 ± 0.023	0.170 ± 0.015ND	0.239 ± 0.023	0.187 ± 0.015ND
Unbundling	**0.092 ± 0.010**	**0.218 ± 0.017*****	**0.104 ± 0.012**	**0.208 ± 0.025****
Annealing	**0.172 ± 0.009**	**0.133 ± 0.013***	**0.034 ± 0.006**	**0.147 ± 0.020*****

Values are means ± standard error.

[a]Bundling includes both zippering ($\approx$ 90% of observed bundling events) and "other" (remaining $\approx$ 10% of observed bundling events); see **Methods** for more information. These percentages hold for both mock- and IAA-treated plants.

Average number of actin filaments and bundles per 57.8 μm^2 region of interest (ROI): Region 2, 48.6 ± 2.1; Region 2 + IAA, 48.4 ± 1.6; Region 3, 26.9 ± 1.1; Region 3 + IAA, 28 ± 1.3; see **Methods**.

6-day-old roots were treated with 10 nM IAA or mock and epidermal cells were imaged for up to 7 min after treatment.

Per region per treatment, N = at least 50 filaments from $\geq$ 20 cells from $\geq$ 12 roots. ND = no statistical differences, Student's t-test compared with mock for that region.

Bundling, unbundling, and annealing events: per root region per treatment, N = ROIs (57.8 μm^2) from a total of 21–23 cells from 18–22 roots. ND, no statistical differences; *, $p \leq 0.05$; **, $p \leq 0.001$; ***, $p \leq 0.0001$, Student's t-test vs. same region mock-treated.

Figure 2.4 Short-Term Auxin Treatments Cause Actin Filament Unbundling.

Representative images of individual filament bundling, unbundling, and annealing in Region 2 cells **(A)** and **(B)** and Region 3 cells **(C)** and **(D)**; mock **(A)** and **(C)** vs. 10 nM IAA **(B)** and **(D)**. Scale bar, 2 μm.

(A) and **(B)** Timelapse series of VAEM images show that 10 nM IAA **(B)** increased actin filament unbundling in Region 2 within 7 min compared with mock **(A)**. Note that one unbundling event (filament unbundling shown as blue and green dots separating) occurred in **(A)** whereas three occurred in the same timespan in **(B)**. There was also a small but statistically significant decrease in annealing events (white arrowheads) after IAA treatment. Other aspects of individual filament behaviors did not significantly change after treatment; for complete quantification of all measured individual filament dynamics, see **Table 2.2**.

(C) and **(D)** Treatment with 10 nM IAA **(D)** increased actin filament unbundling and filament end annealing in Region 3 within 7 min compared with mock **(C)**. Similarly as in Region 2, IAA stimulated unbundling of actin filaments: two unbundling events are shown in **(D)** compared with only one event in **(C)**. IAA also stimulated an increase in annealing in Region 3, where three annealing events are shown by white arrowheads **(D)**.

Bundling events are shown by either purple and magenta dots coming together (zippering of two independent filaments) or a series of magenta dots increasing in size (fluorescence intensity increase with no visible filament zippering).

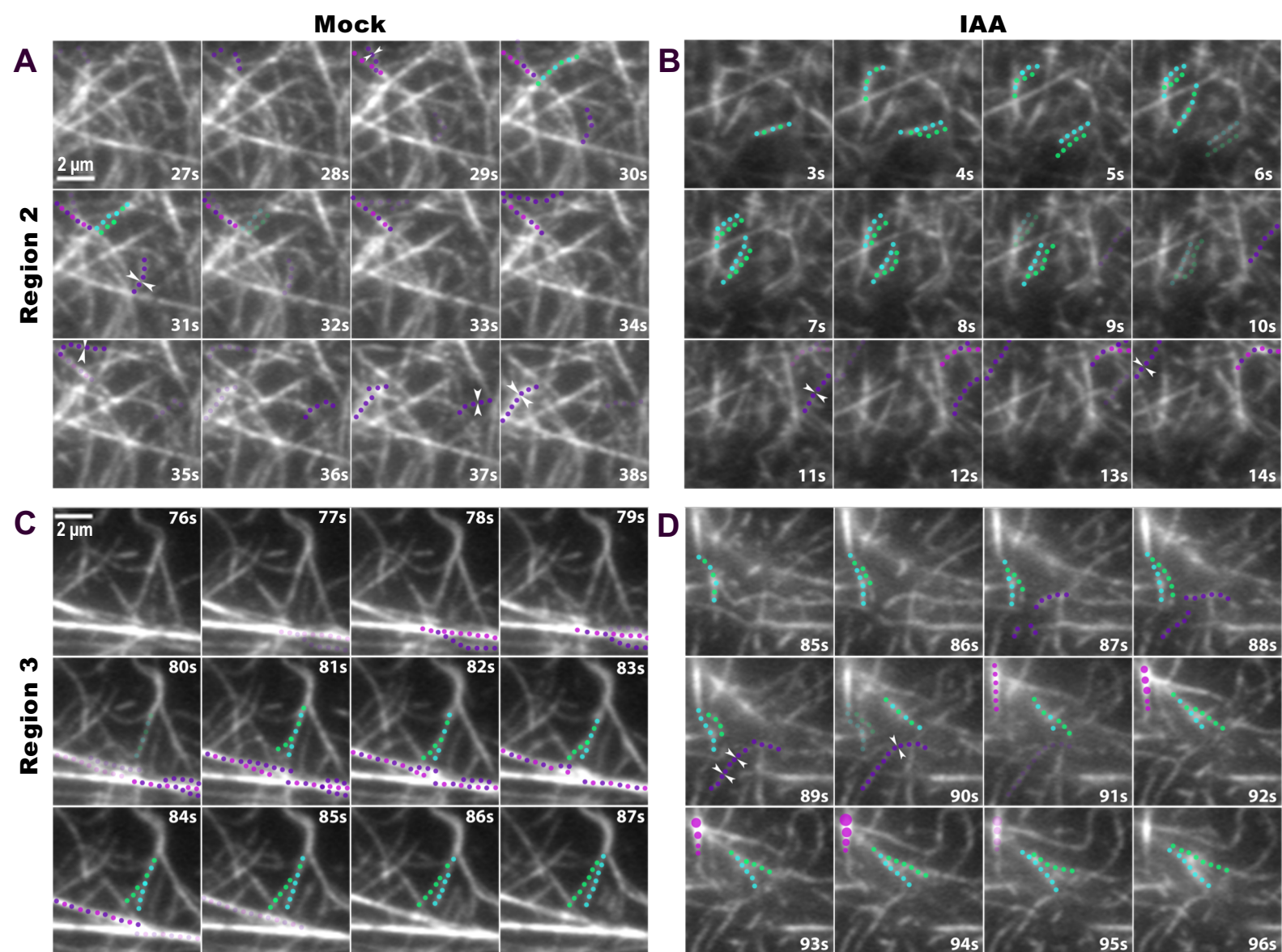100-s timelapse movies were collected from short and long cells in the same 28 6-day-old, light-grown roots.

Figure 2.4 Short-Term Auxin Treatments Cause Actin Filament Unbundling.

2.3.5 The Actin Array in *aux1* Mutants is Insensitive to IAA but Partially Responds to NAA

The auxin importer AUX1 was identified in an ethyl methanesulphonate (EMS) mutant screen for resistance to IAA and 2,4-D (Maher and Martindale, 1980; Pickett et al., 1990), and the protein has been shown to bind IAA with extremely high affinity (Yang et al., 2006; Carrier et al., 2008). AUX1 mutants are agravitropic and exhibit root elongation in the presence of the natural auxin IAA (whereas wildtype roots are growth-inhibited under this condition), but mutant root growth is inhibited to wildtype levels in the presence of the membrane permeable auxin NAA (Maher and Martindale, 1980; Pickett et al., 1990; Bennett et al., 1996; Marchant et al., 1999). Cells in *aux1* mutants take up significantly less IAA (Rashotte et al., 2003; Band et al., 2014; Hayashi et al., 2014; Rutschow et al., 2014, protoplasts; Dindas et al., 2018) and are larger compared with wildtype cells (Ugartechea-Chirino et al., 2010; **Supplemental Figures 2.12** and **2.14**). Intracellular auxin concentrations correlate with cell length, where IAA concentrations are higher in longer root epidermal cells (Brunoud et al., 2012), possibly because IAA concentration regulates the amount of time cells spend in the elongation zone (Rahman et al., 2007). We hypothesized that AUX1 might have a previously uncharacterized role in short-term auxin signaling to the cytoskeleton.

We expressed GFP-fABD2 in the T-DNA insertion mutant for AUX1, *aux1-100* (WS background) and in the point mutant *aux1-22* (Col-0 background; Feldmann, 1991; Roman et al., 1995; Bennett et al., 1996), with the hypothesis that if AUX1 were upstream of cytoskeletal rearrangements in response to IAA, the mutants' actin cytoskeleton would not respond to 20–30 min IAA treatments: neither density nor parallelness would increase, and neither skewness nor average filament angle would decrease. Because root epidermal cells in *aux1* plants were significantly longer than wildtype (**Supplemental Figures 2.12** and **2.14**), analyzing actin response by separating cells into standard "regions" seemed imprecise. For example, a 120 μm-long cell that will grow to a final length of 140 μm in a wildtype plant is at a different point in its development than a 120 μm-long *aux1-100* cell that will reach a final length of 290 μm. Therefore, we quantified changes in actin array on a per-cell basis (see **Methods**).

Both *aux1* mutants had average cell lengths longer than wildtype, as well as overall actin array organization that differed from wildtype under control conditions (**Figure 2.5** and **Supplemental Figures 2.12**, **2.13**, and **2.14**). When each mutant was compared to its respective

wildtype ecotype, both alleles of *aux1* exhibited significantly lower average filament density and increased skewness/bundling. Filaments were overall more longitudinal and parallel to one another. Mutants' longer cells and "more organized" actin filament organization fits the model that higher levels of apparent "organization" are coincident to cell expansion.

Actin organization in wildtype WS plants expressing GFP-fABD2 responded to short-term IAA treatments almost identically as had Col-0. Actin filament density significantly increased, as did parallelness, and average filament angle significantly decreased (**Figure 2.5**). Interestingly, when actin response was quantified on a per-cell basis, WS did not exhibit the small but statistically significant decrease in skewness/bundling (**Figure 2.5E** and **Supplemental Figure 2.12**) that we had previously observed in Col-0 (**Figure 2.3**), perhaps because the ecotype itself is slightly resistant to auxin (Dharmasiri et al., 2005b). The a*ux1-100* mutant's actin array did not significantly reorganize in response to IAA treatment (**Figure 2.5**), indicating that actin cytoskeleton response to IAA required the transporter. To confirm the importance of AUX1 in IAA-triggered actin cytoskeleton rearrangements, we tested a second allele, the null point mutant *aux1-22*. The actin array in *aux1-22* also failed to reorganize in response to IAA treatments (**Supplemental Figure 2.13**).

To understand whether the auxin hormone itself drives cytoskeletal reorganization, or if there is an intermediary between auxin, AUX1, and actin response, we tested the mutant's response to the membrane permeable auxin NAA. If AUX1's role is restricted to transporting IAA into the cell and auxin itself merely needs to enter the cell to stimulate actin reorganization, NAA should be sufficient to induce a wildtype response in *aux1-100* and we should see denser, more parallel, and more longitudinal arrays. But if NAA should fail to induce the established reorganization pattern, we could deduce that the presence of auxin inside the cell is not enough and that the AUX1 protein is required for short-term auxin to actin signaling. **Figure 2.5** shows that WS responds to NAA similarly as to IAA. Interestingly, NAA only partially restores in *aux1-100* a wildtype response to IAA. NAA stimulates increased actin filament density (**Figure 2.5D**) in the mutant, but has no effect on filament angle or parallelness (**Figures 2.5F–G**).

Figure 2.5 Actin Organization in *aux1-100* Fails to Respond to Short-Term IAA Treatments but Partially Responds to the Membrane-Permeable Auxin NAA.

(A) to **(C)** Representative VAEM images of GFP-fABD2–labeled actin in epidermal cells from wildtype and *aux1-100*, treated for 20–30 min with mock **(A)**, 10 nM IAA **(B)**, or 100 nM NAA **(C)**. Scale bar, 5 μm.

(D) to **(G)** Quantification of actin organization in root epidermal cells. IAA failed to trigger an increase in actin filament density in *aux1-100* **(D)** but actin density in *aux1-100* increased in response to NAA. Skewness in both genotypes did not significantly respond to either treatment **(E)**. Wildtype response is shown in blue and *aux1-100* in green; mock, solid; 10 nM IAA, dots; 100 nM NAA, stripes. After IAA and NAA treatments, actin arrays in wildtype plants were more "organized," with lower average filament angle **(F)** relative to the longitudinal axis of the cell and filaments generally more parallel to each other **(G)**. Average actin filament angle and parallelness in *aux1-100* failed to reorganize in response to either IAA (dots) or the membrane-permeable auxin NAA (stripes).

N = 7–32 cells per root; 9–11 roots per genotype per treatment. Different letters indicate statistically significant differences, oneway ANOVA, compared with Tukey-Kramer HSD in JMP. Actin measurements were quantified on a per-cell basis; see **Methods** for description and **Supplemental Figure 2.12** for scatterplots. Results are from one representative experiment of 2 similar experiments with similar results. All auxin experiments were performed and analyzed double blind.
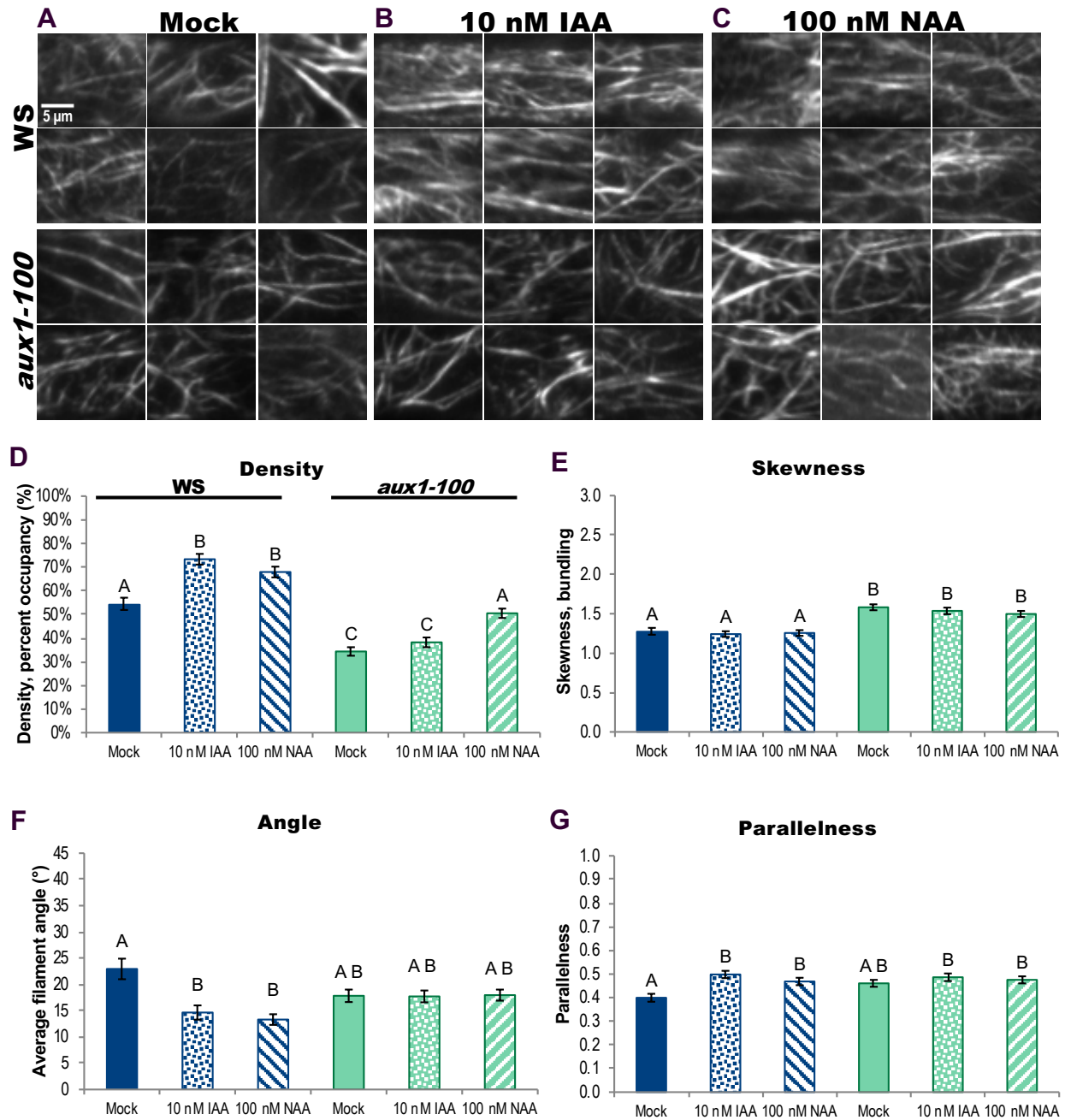
Figure 2.5 Actin Organization in *aux1-100* Fails to Respond to Short-Term IAA Treatments but Partially Responds to the Membrane-Permeable Auxin NAA.

To confirm AUX1's importance in cytoskeletal responses to NAA, we tested the membrane permeable hormone's effects on actin organization in *aux1-22* and its wildtype, Col-0. Recapitulating *aux1-22*'s lack of response to IAA, actin organization in this mutant was largely impervious to NAA, with a sizeable but statistically insignificant reduction in average filament angle. Upon testing the effect of NAA on actin reorganization in Col-0, we found that NAA stimulated an increase in actin filament density in Col-0, but were surprised that, when measured on a per-cell basis, Col-0 exhibited neither a decrease in average filament angle nor an increase in filament parallelness (**Supplemental Figure 2.13**). The Col-0 and WS ecotypes are likely genetically divergent enough to explain why their NAA-prompted actin reorganization is not identical; indeed, previous work identified transcriptional responses for several genes that differ among the two ecotypes under various environmental conditions, including for other proteins involved in hormone signaling (Schultz et al., 2017). Actin organization in both *aux1-100* and *aux1-22* failed to respond to IAA and only partially responded to NAA. These results are the first that place AUX1 upstream of actin in short-term auxin signaling events, as well as demonstrate that the import protein is required for a complete actin response to auxin.

2.4   Discussion

We correlated specific actin architecture and orientation to cell lengths in expanding root epidermal cells and report the first quantitative assessment of actin responses to short-term IAA treatments in roots. Under control conditions, short epidermal cells (Region 2) are characterized by dense actin arrays with high annealing frequencies, whereas long cells (Region 3) exhibit more bundled, more parallel, more longitudinal actin arrays in which filaments elongate faster and grow longer. We found that this same pattern of actin organization occurs in the WS ecotype and *aux1* mutants, indicating that there may be a causal relationship among cell length, skewness/bundling, and filament parallelness. We documented actin responses to growth-inhibitory doses of IAA and were surprised to find that filaments became more dense, parallel, and longitudinally oriented (i.e., lower average filament angle) within 20–30 min, demonstrating that the relationship between higher levels of actin "organization" and increased cell expansion is not as direct as previously hypothesized. Upon analyzing the actin array response to auxin in two *aux1* mutants (the T-DNA insertion mutant *aux1-100* and the null point mutant *aux1-22*), we found that actin failed to reorganize in response to IAA and actin reorganization was only partially restored by NAA.

Although none of our results establishes a cause-and-effect relationship between increased actin bundling and elongating cells, they disprove the hypothesis that actin bundles inherently inhibit cell expansion. Although some specific actin characteristics correlate with longer cells, "more organized" filament arrays do not universally correlate with rapidly growing root cells. We also provide the first evidence that the auxin import protein AUX1 is critical for the actin cytoskeleton's full response to short-term auxin treatments, presumably because it imports the bulk of IAA into cells, and that cytoplasmic auxin is sufficient to trigger some aspects of actin reorganization.

Studies on the long-term (6+ hours) effects of high doses of auxin on actin filaments (Li et al., 2014a; Scheuring et al., 2016) report that actin becomes more bundled after treatment. Several studies (Holweg et al., 2004; Nick et al., 2009) examining the effect of short-term, high dose IAA treatments on mTalin–bundled actin filaments in dark-grown rice coleoptiles demonstrate that relatively high doses of auxin (10 µM NAA, or 50 µM IAA) induced filament unbundling. Auxin transport inhibitors appear to have the opposite effect on actin filaments. Auxin transport inhibitors such as 2,3,5-triiodobenzoic acid (TIBA) induce actin bundling within minutes (Dhonukshe et al., 2008) and inhibit cell elongation (Rahman et al., 2007). Here, we demonstrated that short-term treatment with IAA, closer to endogenous levels (Band et al., 2012), induced an increase in filament density, parallelness, and longitudinality, and decrease in bundles within 20–30 min, as well as an increase in unbundling events in cells throughout the visible root elongation zone within 7 min (**Table 2.2**). These results indicate that, like their role in microbe-associated molecular pattern (MAMP) perception (Cárdenas et al., 1998; Henty-Ridilla et al., 2014; Li et al., 2015b), actin filaments are potentially involved in the initial intracellular perception of IAA. Interestingly, unbundling actin filaments to build a dense array in auxin signaling/response is a different cellular mechanism used to increase filament density vs. the increased density observed in responses to MAMPs in Arabidopsis hypocotyls, where MAMPs inhibit actin depolymerizing factor (ADF)-mediated severing and downregulate capping protein- (CP) mediated barbed end capping to build a denser array (Henty-Ridilla et al., 2014; Li et al., 2014b). This indicates that, despite similar actin readouts of "increased density" after MAMP or 20 min IAA treatment, actin participates in discrete roles in each of these signaling–response pathways, and each stimulus distinctly modulates actin regulation towards separate, precise outcomes.

We found that the auxin import protein AUX1 is required for short-term changes in actin organization in response to auxin. Previously the role of "auxin receptor" was attributed to ABP1

(Chen et al., 2001; Chen et al., 2012; Lin et al., 2012; Nagawa et al., 2012; reviewed in Sauer and Kleine-Vehn, 2011), but immediate cytoskeletal reorganization was never directly linked to the protein because though actin response in roots was implied (Lin et al., 2012), it was never directly visualized. The *aux1* mutants' actin arrays are impervious to IAA, likely because auxin cannot enter cells in sufficient quantities, and are only partially responsive to the membrane-permeable NAA, indicating that while auxin itself elicits some actin rearrangements, AUX1 is necessary for full response. Having an established baseline of auxin's short-term effects on actin filaments in wildtype and *aux1* root epidermal cells will enable further testing of models of actin's role in auxin signaling pathways.

2.4.1 Actin Organization Predicts Cell Length Under Control Conditions but Not Otherwise

Actin's role in cell expansion is established but not understood (reviewed in Li et al., 2015a). It has been generally accepted that cell expansion requires a degree of observable actin "organization" (Smertenko et al., 2010; Dyachok et al., 2011). The hypothesis that an "organized" actin array corresponds with cell growth appeals to an intuitive understanding of growth as a methodical process that requires coordinated elements. However, "organization" can take many forms and exactly what form drives growth is unknown. Indeed, we found in two ecotypes—and in an auxin signaling mutant with significantly longer cells—that filament parallelness, cell length, and skewness affect one another to a similar extent to produce predictable organization across the root elongation zone. By showing that, under control conditions, actin bundling increases as cell length increases, we present definitive evidence that filament bundles do not inhibit cell expansion. Our observation, substantiated by quantitative evidence, that the cytoskeleton changes to a higher level of apparent actin "organization", namely longitudinality and filament parallelness, in response to IAA, a treatment known to inhibit growth within minutes (Hejnowicz and Erickson, 1968; Fendrych et al., 2018), definitively demonstrates that increases in filament "organization" do not, inherently, contribute to cell expansion. Furthermore, the IAA-induced decrease in overall filament bundling (**Figure 2.3c**) and increase in unbundling events (**Table 2.2**) that occurs in Col-0 indicates that an absence of longitudinal bundling does not necessarily coincide with expanding cells. Thus, although our data cannot divulge a cause-and-effect relationship, our correlative study has eliminated two hypotheses for the relationship between actin organization and cell expansion and determined that there is no absolute relationship between actin bundling and cell expansion.

2.4.2 Actin Behaviors Differ in Short and Long Epidermal Cells of the Root Elongation Zone

We evaluated individual filament behaviors in short and long cells to gain insight into what filament behaviors might contribute to cell growth. Although several aspects of individual filament dynamics were previously measured in root epidermal cells in Arabidopsis (Smertenko et al, 2010), we have examined additional filament behaviors, bringing knowledge of Arabidopsis up to that of rice (Wu et al., 2015). Region 2 was significantly denser than Region 3 so we expected a higher rate of filament turnover: increased severing, shorter filaments and filament lifetimes, and faster elongation rates. Filament arrays in Region 3's longer cells were much more bundled than arrays in Region 2 so it was reasonable to expect either a higher bundling frequency in longer cells, a higher incidence of unbundling in shorter cells, or a lower incidence of unbundling in longer cells. In this study, both short and long cells exhibited similar individual filament behaviors (**Table 2.1**), the only major differences being a reduced maximum filament length and elongation rate in shorter cells, and a multifold increase in incidents of annealing in shorter cells. In etiolated hypocotyls, increased filament lengths and lifetimes correlate with longer cells (Henty-Ridilla et al., 2013; Li et al., 2014b). Although shorter root epidermal cells have shorter average filament lengths, lifetime is statistically equivalent to that of filaments in longer cells, demonstrating that the connection between longer lifetime and increased cell length is not evident in roots.

The most marked difference in individual filament behaviors between short cells and long cells was the up to–10-fold increase in annealing frequency observed in shorter cells. Although the correlation coefficient algorithm found Region 2 to be less dynamic than Region 3, pixels occupied by fluorescence do not change as much during annealing events as, for example, when an entirely new filament polymerizes, so it is possible that this method failed to capture the full range of dynamic behaviors in Region 2 cells' actin arrays. The substantial increase in annealing on a per-filament basis indicates there is likely a purpose behind this phenomenon. Annealing in vitro is generally a function of actin concentration, filament length, and/or filament end availability (Adrianantoandro et al., 2001), and in vivo is down-regulated by capping protein (Henty-Ridilla et al., 2014; Li et al., 2014b). Annealing is a way to build filaments quickly and without intensive energy inputs (Smertenko et al., 2010; Li et al., 2014b). Since maximum filament length is reduced in shorter cells that have a higher annealing frequency compared with maximum filament length in longer cells, and since these seem to be transient annealing events that for the most part hold for

only a few frames, the purpose of these events does not appear to be building longer filaments. Perhaps these shorter cells, which are located in the subsection of the elongation zone known as the transition zone, are undergoing more cytoplasmic changes in preparation for rapid elongation.

2.4.3   AUX1 is Necessary for Actin Response to Auxin

It is well-established that signaling between auxin and actin occurs (Kleine-Vehn and Friml, 2008; Nick et al., 2009; Nick, 2010; Lin et al., 2012; Nagawa et al., 2012; Li et al, 2015a; Scheuring et al., 2016; Zhu et al., 2016), but how auxin affects growth, how auxin affects actin, and how auxin affects actin to influence cell expansion are far from being understood. The multiple auxin–actin pathways (reviewed in Overvoode et al., 2010 and Grones and Friml, 2015) assign various roles to actin in auxin response (for example, repositioning auxin transport proteins, or inhibiting endocytosis of auxin transporters), and the pathway thought to link auxin and actin in the very short-term was via the plasma membrane auxin receptor ABP1 (Xu et al., 2010, 2011; Nagawa et al., 2012). Now that ABP1's role in auxin–actin signaling is in doubt (Dai et al., 2015; Gao et al., 2015), the mechanism of auxin–actin signaling and how actin rapidly perceives auxin—through an upstream receptor, second messenger(s) modulating actin-binding proteins, and/or perhaps direct interaction with the hormone itself—remains undetermined.

Before this current work, AUX1 was not suspected of playing a "transceptor" role in signaling upstream of actin organization. AUX1 is an established transporter of auxin (Bennett et al., 1996; Dindas et al., 2018), has homologs in all plants (reviewed in Swarup and Péret, 2012), is necessary for root gravitropism (Maher and Martindale, 1980; Marchant et al., 1999; Swarup et al., 2004), and is responsible for 80% of IAA uptake in root hairs (Dindas et al., 2018) and rapid growth inhibition by IAA (Fendrych et al., 2018). Auxin-induced transcriptional regulation requires that auxin binds to the intracellular auxin receptors $SCF^{TIR1/AFB}$, which complex then binds to AUXIN/INDOLE-3-ACETIC ACID (Aux/IAA) transcriptional repressors (Dharmasiri et al., 2005a,b; Calderón Villalobos et al., 2012). However, the $SCF^{TIR1/AFB}$ pathway is also responsible for short-term intracellular responses to auxin. Within the first 10 min of receiving an auxin signal, there is both an initial influx of H^+ (depolarizing the plasma membrane and reducing cytosolic pH) and, shortly thereafter, increased intracellular Ca^{2+} that propagates through the root (Dindas et al., 2018). Both IAA and NAA are substrates of AUX1 (Yang et al., 2006; Carrier et al., 2008), and

of the SCF$^{TIR1/AFB}$–Aux/IAA complex, though both AUX1 and the protein complex have a higher affinity for IAA (Dharmasiri et al., 2005b; Calderón-Villalobos et al., 2012; Dindas et al., 2018).

Actin in wildtype cells reorganizes to increase filament density in response to both IAA and NAA. Surprisingly, NAA stimulated different effects on actin reorganization in Col-0 and WS: WS responded to NAA as it had to IAA but Col-0 underwent only increased actin filament density, and no changes in parallel longitudinality at 20–30 min. Col-0 might respond to NAA on a timeframe different from WS and different from its response to IAA. Natural and synthetic auxins inhibit root elongation to different extents, depending on ecotype (Delker et al., 2010). Occasionally differential responses to NAA have been detected across ecotypes, for example NAA stimulates a higher number of lateral roots in 9-day-old Col-0 plants compared with WS or Landsberg erecta (Falasca and Altamura, 2003). In addition, IAA and NAA induce in Col-0 different extents of gene expression (Yoshimitsu et al., 2011). It is quite possible that the two ecotypes are more different than is commonly acknowledged, a subject that merits further study.

Actin reorganization in both alleles of *aux1* was resistant to IAA and exhibited only partial responses to NAA, implicating AUX1 as a major player in auxin signaling to actin. After NAA treatments, density increased only in *aux1-100* and angle decreased (although not statistically significantly) only in *aux1-22*. Our results that show attenuated actin reorganization in *aux1-100's* and *aux1-22*'s responses to NAA support the Dindas et al. (2018) model of an intracellular feedback loop that relies on the presence of AUX1. In the *aux1* mutant *wav5-33*, NAA triggers membrane depolarization (at a level similar to wildtype) and H$^+$ influx (though substantially delayed and reduced vs. wildtype), but all *aux1* mutants tested are severely or entirely resistant to IAA in these responses (Dindas et al., 2018). Nor does IAA treatment in *aux1* mutants lead to the typical increased Ca^{2+} and although NAA was not directly tested (Dindas et al., 2018), these results imply that NAA might not induce Ca^{2+} influx in *aux1* mutants. Both H$^+$, which contributes to membrane depolarization, and Ca^{2+} are known regulators of various actin-binding proteins (see below). It is possible that import of IAA through AUX1 is necessary to activate or inhibit other intracellular players which drives, separately, increased actin density, decreased filament angle, and increased parallelness. Alternatively, actin reorganization might be delayed in the mutants. In any case, that previous study (Dindas et al., 2018) and our data showing partial actin response to NAA in *aux1* mutants demonstrate that auxin itself can act as an intracellular signaling molecule

that stimulates some short-term cellular responses, a deviation from the ABP1 model that relied on IAA being perceived at the plasma membrane and its signal amplified within the cell.

2.4.4   Potential Players in the Actin–Auxin Connection

Long-term (6+ h) auxin responses have been shown in rice to rely on the actin-binding protein RMD (Rice Morphology Determinant; FORMIN5, homolog of Arabidopsis FORMIN14), which is downstream of auxin response factors (Zhang et al., 2011; Li et al., 2014a). Less is known about auxin's effect on actin during cellular activities that occur on the order of minutes such as polarized growth or gravitropism (Xu et al., 2014; Zhu et al., 2015). Substantial membrane depolarization, slight acidification of cytosol (in conjunction with significant alkalinization of extracellular pH), and significant but transient increases in cytosolic Ca^{2+} are short-term intracellular responses that were shown to occur independent of transcriptional responses and are AUX1-dependent (Monshausen et al., 2011; Dindas et al., 2018). Actin-binding proteins that are known to be modulated by pH or Ca^{2+}, such as ADF/cofilin or villin, would be good candidates for a target of the hormone and mutants could be evaluated for growth in the presence of IAA or a lack of actin reorganization in response to 20–30 min IAA treatments. The drastic auxin-induced actin reorganization could require more than one actin-binding protein; perhaps ecotype-specific differences in actin-binding protein expression explain Col-0 and WS's dissimilar responses to NAA at 20–30 min.

2.4.5   The Actin–Auxin Connection and Cell Expansion

The mechanisms by which auxin and actin control growth are unknown. Actin could function by providing tracks for trafficking auxin transporters, altering vacuole morphology, and/or operating through another mechanism. Auxin efflux carriers (PIN proteins) and the influx protein AUX1 were previously shown to depend on actin for targeted subcellular localization (Kleine-Vehn et al., 2006; 2008). However, AUX1 is not redistributed in response to NAA (Kleine-Vehn, et al., 2006), to which we observe at least some actin reorganization in Col-0, WS, and both *aux1* mutants. Further, use of a photoconvertible PIN2 shows that it is not maintained at the root epidermal cell plasma membrane after auxin treatments, and that most PIN2 in brefeldin A compartments is newly synthesized rather than recycled (Jasik et al., 2016). These results complicate a role for actin

in trafficking auxin transporters in response to auxin; however, actin reorganization could provide tracks to transport signaling elements into the nucleus.

Turgor pressure exerted by the vacuole (and a loosened cell wall) is a primary driver of cell expansion (Cosgrove, 2005; Kroeger et al., 2011; Braidwood et al., 2013; Guerriero et al., 2014). Six-hour NAA treatments cause actin-dependent vacuole constriction that ultimately leads to reduced cell lengths (Scheuring et al., 2016). If the same mechanism impels growth cessation within minutes, the denser, more longitudinal actin array we detected might effect vacuole constriction.

Auxin-induced actin reorganization could operate primarily in signaling, and be incidental to changes in growth rate rather than driving growth per se. Whereas wildtype (Col-0) roots ceased elongating within 30 s of low-dose IAA treatments, IAA did not significantly affect *aux1-100* root elongation, and 100 nM NAA reduced root growth rate to approximately wildtype levels (Fendrych et al., 2018). At a similar timepoint after 100 nM NAA treatments, we observed that both *aux1-100* and *aux1-22*, exhibited only partial, and divergent, actin reorganization. If there were direct, causative relationships between actin organization and cell expansion or vice versa, NAA should have induced in *aux1* the complete complement of actin rearrangements observed in wildtype cells or at least the same actin response in both mutant alleles.

Actin reorganization is highly energy intensive, costing as much as 1200 ATP-loaded actin monomers per second during filament elongation (Li et al., 2015b), and even if there is no causal relationship between auxin-induced increased actin density and parallel longitudinality, and cell expansion, it seems unlikely that such extensive reorganization would occur for no functional purpose. It is possible that initial actin reorganization after auxin treatment occurs primarily to transduce the auxin signal. Alternatively, cytoplasmic streaming and vesicle delivery could require an exact equilibrium of available tracks and space in which to move, and any actin array that disrupts that balance quickly alters cell expansion. Toward this idea, Tominaga et al. (2013) showed that faster myosins (i.e., faster delivery along actin tracks) grow larger plants with larger cells, and presumably enhanced cell expansion.

Our IAA treatments provide clear evidence that the actin cytoskeleton in cells along the entire root elongation zone responds to the growth cessation signal within minutes by significantly *increasing* filament abundance as well as, in opposition to the current view that organization leads to or is necessary for expansion, apparent actin organization. We show that IAA-induced actin

rearrangements require AUX1, while our NAA results show that auxin itself is able to act as a cytoplasmic signal to modulate actin cytoskeleton organization. We conclude that, however auxin is acting, the relationship between actin organization and cell expansion cannot be explained by a simple model requiring either "organized" or "disorganized" actin, or by a presence or absence of longitudinal bundles.

2.5   Methods

2.5.1   Plant Material and Growth Conditions

Roots for all experiments were from 6-day-old, light-grown seedlings expressing GFP-fABD2: Col-0, WS, *aux1-100,* and *aux1-22*. Seeds were surface sterilized and stratified at 4°C for two days. All plants were grown on 0.5× Murashige and Skoog medium solidified with 0.6% (w/v) agar and no sucrose, as described previously (Sheahan et al., 2004; Dyachok et al., 2011; Henty et al., 2011; Li et al., 2014b; Cai et al., 2014). Seedlings were grown at 21°C, vertically and under long-day conditions (16 h of light, 8 h of darkness).

Seeds for *Arabidopsis thaliana* T-DNA insertion mutant *aux1-100* (CS2360) and EMS point mutant *aux1-22* (CS9585) were obtained from the ABRC stock center and, with WS-0 and Col-0, transformed with GFP-fABD2 (Sheahan et al., 2004) using the floral dip method (Zhang et al., 2006). T1 plants were screened on plates with hygromycin. Plants of *aux1-100* were then genotyped by PCR to confirm homozygosity using DNA primers WT-forward 5'-GCATGCTATGTGGAAACCACAGAAG-3' and WT-reverse 5'-tacCTGACGAGCGGAGGCAGATC-3' and the Feldmann/AZ forward primer for the mutant (Krysan et al., 1996): AZ-forward 5'-gatgcactcgaaatcagccaattttagac-3' with WT-reverse 5'-tacCTGACGAGCGGAGGCAGATC-3'. *aux1-22* mutants were identified by their agravitropic phenotype. T2 plants were used for experiments.

2.5.2   VAEM Imaging, Measuring Cell Lengths, and Quantitative Analysis of Cortical Actin Array Architecture

To measure cell sizes and obtain a corresponding measurement of each actin parameter, we collected overlapping VAEM images (single optical sections) of cortical cytoplasm in root epidermal cells expressing GFP-fABD2. Images were collected from the root apex to the first obviously visible root hair initiations.

VAEM was performed using a TIRF illuminator mounted on an IX-71 microscope equipped with a 60× 1.45–numerical aperture PlanApo TIRF objective (Olympus). Illumination was from a solid-state 50-mW laser (Intelligent Imaging Innovations) attenuated to 3–5% power, depending on the day, but kept the same for a single experiment/replicate. The 488-nm laser emission was captured with an electron multiplying charge-coupled device camera (ORCA-EM C9100-12; Hamamatsu Photonics). The microscope platform was operated and images collected with Slidebook software (version 6; Intelligent Imaging Innovations). A fixed exposure and gain were selected so that individual actin filaments could be seen but higher order filament structures were not intensity-saturated.

Two images were collected per field of view: one to capture actin filaments in focus and one to visualize the cell side and end walls in a higher focal plane, since these are frequently clearly visible in this higher plane without staining. Each image was rotated with an image rotating macro so the longitudinal axes of the cells photographed were parallel to the horizon of the image. All micrographs were cropped and analyzed in FIJI (https://fiji.sc/). For the analysis, we lined up the overlapping images to recreate a full view of the root. In a color (RGB) version of the image stack file, we identified, marked, numbered, and measured cells whose side and end walls were distinguishable, generally choosing cells in the middle of the root to avoid including ones that might present differences in actin architecture due to differences in the cell's angle relative to the objective. On the RGB image stack, to better distinguish cells, we frequently enhanced brightness and contrast; all cropped images used for quantifying actin architecture and orientation were taken from original 8-bit files. Actin images were cropped along the entire length of every specified cell, and numbered to correspond to the specific cell from which they were cropped. Skewness and density were analyzed according to Higaki et al. (2010b) and Henty et al. (2011); angle and parallelness were analyzed according to Ueda et al. (2010) and Cai et al. (2014). The size of crops must be consistent for all images in an experiment and frequently individual crops were smaller than the entire length of a cell; in such cases an actin measurement was obtained for each crop and the final scatter-plotted measurement for each actin parameter for an individual cell was taken as the mean of the measurements from that cell's particular set of crops. In Col-0 root characterization, we analyzed cell size and corresponding actin architecture for more than 180 cells from at least 20 roots total—all the cells with clearly distinguishable end walls. For effects of IAA on Col-0, cells up to 85 μm were counted as belonging to "Region 2", cells more than 94 μm were

categorized as "Region 3", and cells falling between 85–94 µm were counted in both categories. To quantify actin architecture and orientation on a "per-cell" basis for the *WS–aux1-100* and *Col-0–aux1-22* analyses (**Figure 2.5** and **Supplemental Figures 2.12**, **2.13**, and **2.14**), we used the mean value from a single cell's set of crops as the value representing the actin measurement for that cell. For example, to fully account for all the actin in a 160 µm-long cell, 10 crops would be needed. Measurements on a per-cell basis would take the mean of the density values for those 10 crops as a single density value for that cell. In determining *aux1* response to IAA and NAA, we analyzed a minimum of 125 cells (from a total of at least 9 roots) per genotype per treatment. Relationships between actin parameters and cell dimensions were analyzed in Microsoft Excel and JMP.

2.5.3 Auxin Treatments

IAA was obtained from Sigma-Aldrich (I2886) and diluted to a 10 mM stock concentration in ultrapure ethanol (FisherScientific BP2818500). NAA was also from Sigma-Aldrich (N0640) and diluted to a 10 mM stock concentration in ultrapure ethanol. For experiments, each auxin was further diluted to appropriate concentrations into 0.5× MS liquid medium without sucrose; for mock solution, ultrapure ethanol was added to 0.5× MS liquid medium without sucrose to match the highest concentration of IAA or NAA used. To ensure even IAA or NAA treatment of plants during 20–30 min treatments, whole seedlings were cut from agar plates and treated by soaking on their agar block in a 24-well plate. For the very short-term treatments used for 100-s timelapse movies, plants were treated on slides by being mounted in either mock or IAA solution. Imaging began almost immediately and both regions were imaged within 7 min. For 20–30 min treatments, all imaging concluded within 30 min. Because darkness can stimulate degradation of cytoskeletal organizing proteins (Dyachok et al., 2011) and a reorientation of actin filaments in hypocotyls (Breuer et al., 2014), plants were left under grow lights (while soaking in solution during 20-min treatments) and slides were prepared in the light. All IAA and NAA experiments were performed and analyzed double blind.

2.5.4 Individual Actin Filament Dynamics

Individual actin filaments were captured with 100-s timelapse VAEM using a 150× 1.45 NA UApoN TIRF objective (Olympus). To determine differences in actin filament behavior between

shorter and longer cells, we documented cell size by taking snapshots of the entire cells from which the timelapse movies were captured. In general, movies of Region 2 cells were collected from Region 2 cells close to the root cap and movies of Region 3 cells were collected from Region 3 cells close to the end of the elongation zone (i.e., the first cell rootward of the first visible root hair initiation). All timelapse movies and regions of interest were analyzed in FIJI. To best display the representative filaments and their dynamics, brightness and contrast were enhanced in the final montages of **Figure 2.2B** and **Figure 2.2C**. Occasionally, minimal adjustments to brightness and contrast were made during analysis to more definitively follow some filaments or events. Filament severing frequency, maximum filament length, filament lifetime, and elongation rates were measured as described previously (Staiger et al. 2009; Henty et al., 2011; Cai et al., 2014; Henty-Ridilla et al., 2014). To measure bundling, debundling, and annealing frequencies, we cropped ≈ 15 μm $\times$ 15 μm ROIs (exact size 227.7 μm^2). For measuring individual filament responses to IAA, we used ≈ 7 μm $\times$ 7 μm ROIs (exact size 57.8 μm^2). To account for differences in filament density in short and long cells, bundling, unbundling, and annealing frequencies were normalized against filament numbers in each ROI. An incident of bundling was counted as an incident in which filament fluorescence intensity increased, either from an apparent "catch and zip" event (categorized as a "zippering event"; these events comprise approximately 90% of observed incidents of bundling) or, simply, a visible, unambiguous increase with a minimum three-frame persistence (3 s $\geq$ 10% filament lifetime) in fluorescence intensity for which "catch and zip" was not specifically apparent (these were categorized as "other bundling event" and account for the remaining $\approx 10\%$ of bundling incidents). Unbundling events were counted as incidents in which a filament was visible next to a mother filament (usually "unpeeling" over several timelapse frames) and, frequently, fluorescence intensity decreased. In cases without a visible decrease in fluorescence intensity, we included only events where the filament clearly "peeled off" from the mother filament. Incidents of annealing were counted when ends of two F-actin fragments joined together for a minimum of two frames. It was not highly unusual to see this annealing behavior join three pieces of recently severed actin filament; if three distinguishable fragments joined to form an individual filament in the same frame, this was counted as two annealing events, one between each fragment.

When capturing timelapse movies to document individual filament changes in response to IAA within 7 min, we applied ≈ 70 μL of either blinded solution (10 nM IAA or mock) directly to

the microscope slide, then the root and coverslip, and imaged immediately, alternately imaging Region 2 or Region 3 first so the timepoints of each dataset would average out to 0-7 min from applying the treatment to the slide.

2.6   Accession Numbers

Sequence data from this article can be found in the Arabidopsis Information Resource database (https://www.arabidopsis.org/) under the following names and accession numbers: AUX1 (At2G38120).

2.7   Acknowledgements

2.8   Author Contributions

R.S.A and C.J.S conceived the project and designed the experiments. R.S.A performed the experiments and data analysis; and R.S.A and C.J.S. wrote the article.

2.9 Supplemental Tables and Figures[3]

Supplemental Table 2.3 Eigenvectors for Principal Component Analysis of Cell Size vs. Actin Parameters in Col-0.

Item	Prin1	Prin2	Prin3	Prin4	Prin5	Prin6
Cell Length	0.527	0.093	0.048	0.044	0.609	-0.582
Cell Width	-0.032	0.876	-0.392	-0.270	-0.069	-0.014
Density	-0.360	0.096	-0.361	0.813	0.266	-0.000
Skewness	0.440	0.238	0.273	0.495	-0.634	-0.168
Angle	-0.325	0.392	0.797	0.072	0.284	0.137
Parallelness	0.542	0.067	-0.053	0.122	0.266	0.784

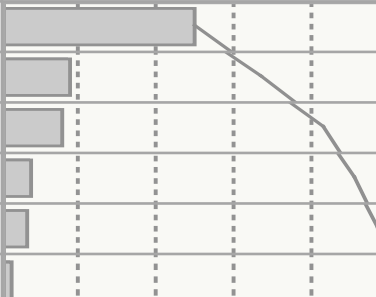Supplemental Table 2.4 Eigenvalues for Principal Component Analysis of Cell Size vs. Actin Parameters in Col-0.

Number	Eigenvalue	Percent		Cum. Percent
1	2.9322	48.871		48.871
2	1.0720	17.867		66.737
3	0.7749	12.914		79.652
4	0.7373	12.288		91.940
5	0.3217	5.362		97.302
6	0.1619	2.698		100.000

---

[3]Supplemental Tables start with **Supplemental Table 2.3**; Supplemental Figures start with **Supplemental Figure 2.6**.

Supplemental Table 2.5 Eigenvectors for Principal Component Analysis of Cell Size vs. Actin Parameters in WS.

Item	Prin1	Prin2	Prin3	Prin4	Prin5	Prin6
WS Cell Length	0.53137	0.13361	0.01256	0.10846	0.34014	0.75643
WS Cell Width	-0.02484	0.91905	0.18593	-0.33084	0.00615	-0.10329
WS Density	-0.33979	0.06901	0.72268	0.57098	-0.06879	0.16357
WS Skewness	0.48014	0.14062	-0.09248	0.30058	-0.80565	-0.04142
WS Angle	-0.32848	0.33435	-0.64176	0.58653	0.15359	0.02918
WS Parallelness	0.51297	0.03429	0.15030	0.34408	0.45483	-0.62276

Supplemental Table 2.6 Eigenvalues for Principal Component Analysis of Cell Size vs. Actin Parameters in WS.
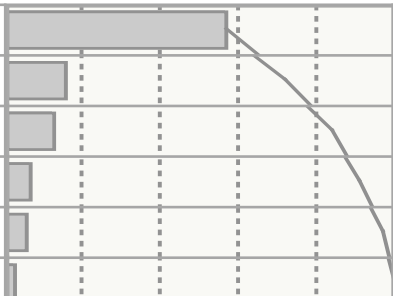
Number	Eigenvalue	Percent		Cum. Percent
1	2.9778	49.630		49.630
2	1.0810	18.016		67.646
3	0.9457	15.762		83.408
4	0.4634	7.724		91.132
5	0.3727	6.212		97.344
6	0.1594	2.656		100.000

Supplemental Table 2.7 Eigenvectors for Principal Component Analysis of Cell Size vs. Actin Parameters in *aux1-100*.

Item	Prin1	Prin2	Prin3	Prin4	Prin5	Prin6
aux1-100 Cell Length	0.47215	-0.16402	0.13255	0.22737	0.62559	-0.53810
aux1-100 Cell Width	0.21551	0.94029	-0.12556	-0.17605	0.14714	-0.03177
aux1-100 Density	-0.39119	0.11131	-0.60851	0.66161	0.10752	-0.12251
aux1-100 Skewness	0.45730	0.10303	0.14257	0.45766	-0.70733	-0.22399
aux1-100 Angle	-0.35628	0.24170	0.74402	0.43920	0.17873	0.19035
aux1-100 Parallelness	0.49148	-0.08679	-0.14993	0.27792	0.20778	0.77976

Supplemental Table 2.8 Eigenvalues for Principal Component Analysis of Cell Size vs. Actin Parameters in *aux1-100*.

Number	Eigenvalue	Percent		Cum. Percent
1	3.4137	56.895		56.895
2	0.9155	15.258		72.153
3	0.7524	12.539		84.692
4	0.4141	6.901		91.593
5	0.3311	5.519		97.112
6	0.1733	2.888		100.000

Supplemental Table 2.9 Actin Organization Measurements after IAA Treatments.

Item	Region 2				Region 3			
Time	Density (%)	Skewness	Angle (°)	Parallelness	Density (%)	Skewness	Angle (°)	Parallelness
$\leq$ 5 min[1]	$67.9 \pm 2.24^{**}$	1.08 ± 0.03^{ND}	22.2 ± 1.75^{ND}	0.24 ± 0.012^{ND}	$38.7 \pm 1.80^{*}$	1.65 ± 0.04^{ND}	$7.3 \pm 0.40^{*}$	0.50 ± 0.011^{ND}
Mock	60.5 ± 2.29	1.13 ± 0.03	24.1 ± 1.77	0.23 ± 0.011	32.2 ± 1.81	1.66 ± 0.04	8.8 ± 0.59	0.51 ± 0.012
10 min	69.9 ± 2.18^{ND}	1.11 ± 0.04^{ND}	$19.8 \pm 1.63^{**}$	$0.26 \pm 0.012^{*}$	$49.5 \pm 1.85^{**}$	$1.45 \pm 0.04^{***}$	8.6 ± 0.55^{ND}	$0.44 \pm 0.010^{*}$
Mock	64.7 ± 2.60	1.20 ± 0.05	28.4 ± 2.24	0.21 ± 0.013	42.1 ± 1.96	1.64 ± 0.04	9.8 ± 0.79	0.47 ± 0.012
20 min	$72.1 \pm 2.00^{***}$	1.04 ± 0.04^{ND}	$20.2 \pm 1.55^{***}$	$0.23 \pm 0.010^{***}$	$43.0 \pm 1.41^{*}$	1.56 ± 0.03^{ND}	$6.2 \pm 0.25^{***}$	$0.52 \pm 0.007^{***}$
Mock	60.4 ± 2.47	1.13 ± 0.04	34.6 ± 2.06	0.14 ± 0.007	37.9 ± 1.67	1.66 ± 0.04	13.4 ± 0.81	0.37 ± 0.009
30 min	$78.9 \pm 1.93^{***}$	$0.98 \pm 0.03^{**}$	$17.1 \pm 1.53^{***}$	0.22 ± 0.010^{ND}	$55.8 \pm 1.76^{***}$	$1.50 \pm 0.04^{***}$	$5.4 \pm 0.41^{***}$	$0.59 \pm 0.009^{***}$
Mock	66.1 ± 2.24	1.13 ± 0.04	32.9 ± 2.35	0.20 ± 0.011	36.1 ± 1.58	1.72 ± 0.04	12.2 ± 0.74	0.44 ± 0.010
60 min	79.6 ± 1.99^{ND}	$0.99 \pm 0.04^{*}$	$21.6 \pm 1.93^{**}$	$0.27 \pm 0.014^{***}$	$56.0 \pm 1.96^{***}$	$1.38 \pm 0.04^{***}$	$6.2 \pm 0.33^{***}$	$0.53 \pm 0.010^{**}$
Mock	76.4 ± 2.12	1.13 ± 0.04	31.3 ± 2.38	0.18 ± 0.008	45.5 ± 1.77	1.63 ± 0.04	10.1 ± 0.62	0.49 ± 0.010

Item	Region 2				Region 3			
Dose IAA	Density (%)	Skewness	Angle (°)	Parallelness	Density (%)	Skewness	Angle (°)	Parallelness
Mock[2]	*55.2 ± 1.67*	*1.28 ± 0.03*	*33.0 ± 1.35*	*0.22 ± 0.007*	*33.0 ± 1.22*	*1.81 ± 0.03*	*13.6 ± 0.54*	*0.31 ± 0.006*
1 nM	70.9 ± 1.45[***]	1.13 ± 0.03[***]	25.5 ± 1.28[***]	0.27 ± 0.010[***]	44.7 ± 1.14[***]	1.67 ± 0.03[***]	10.1 ± 0.37[***]	0.44 ± 0.007[***]
10 nM	68.0 ± 1.42[***]	1.19 ± 0.03[*]	20.6 ± 1.08[***]	0.24 ± 0.007[ND]	43.4 ± 1.08[***]	1.71 ± 0.02[*]	8.6 ± 0.31[***]	0.53 ± 0.006[***]
100 nM	68.2 ± 1.47[***]	1.19 ± 0.03[*]	18.2 ± 0.95[***]	0.30 ± 0.008[***]	45.6 ± 1.03[***]	1.71 ± 0.02[*]	6.7 ± 0.19[***]	0.58 ± 0.005[***]
1 μM	62.9 ± 1.53[***]	1.27 ± 0.03[ND]	20.1 ± 1.01[***]	0.29 ± 0.008[***]	43.6 ± 1.16[***]	1.66 ± 0.02[***]	7.8 ± 0.29[***]	0.51 ± 0.005[***]
10 μM	62.9 ± 1.52[***]	1.31 ± 0.03[ND]	20.6 ± 1.00[***]	0.31 ± 0.008[***]	40.7 ± 1.10[***]	1.80 ± 0.03[ND]	8.9 ± 0.28[***]	0.52 ± 0.006[***]

[1] 10 nM IAA treatments at various times. Density threshold 55.

[2] Dose series imaged at 20–30 min of treatment. Density threshold 45.

Values are ± standard error.

Timeseries, N = Approximately ≥ 10 cells (Region 2) and approx. 4–9 cells (Region 3) per root from 7 roots per treatment per timepoint. ND = no statistically significant difference; *, $p \leq 0.05$; **, $p \leq 0.01$; ***, $p \leq 0.001$, vs. mock on same region at same timepoint, Student's t-test.

Dose series, N = Approximately 8–12 cells per region per root; at least 10 roots per treatment. ND = no statistically significant difference; *, $p \leq 0.05$; **, $p \leq 0.01$; ***, $p \leq 0.001$, vs. mock, Student's t-test.

Supplemental Figure 2.6 Epidermal Cells in Different Root Regions Exhibit Distinct Actin Filament Arrays.

(A) Representative VAEM images of GFP-fABD2–labeled actin in epidermal cells from subjective root regions. Scale bar, 10 μm.

(B) to **(E)** Quantification of individual actin architecture or orientation metrics in three root regions. Results for density **(B)**, skewness **(C)**, angle **(D)**, and parallelness **(E)** showed significantly different actin arrays for most parameters, most notably between Regions 2 and 3. Actin filaments in Region 1 were dense and moderately bundled, with high average filament angle and low parallelness. Region 2 was characterized by a dense filament array, lower bundling, high average filament angle and filaments that were moderately parallel to each other. Region 3 was half as dense as Region 1 or 2, and exhibited a high degree of parallel, longitudinal bundles, with approximately 50% decrease in average filament angle and 40% increase in filament parallelness compared with Region 2.

N = 8–12 cells per region per root for 20 roots. ND, no differences; ***, $p \leq 0.001$, Student's t-test.
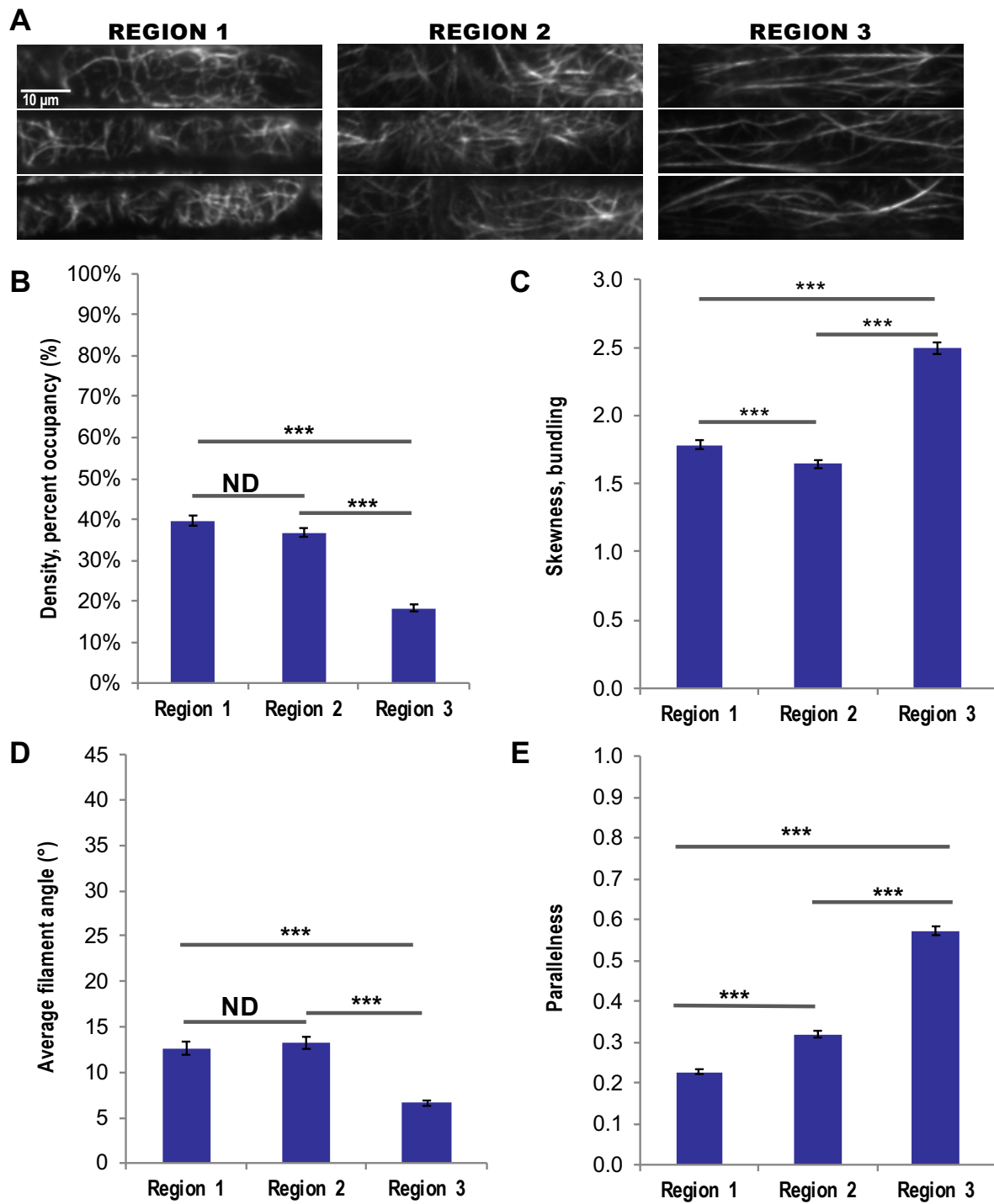
Supplemental Figure 2.6 Epidermal Cells in Different Root Regions Exhibit Distinct Actin Filament Arrays.

Supplemental Figure 2.7 Actin Filament Arrays Are Not Predictive of Cell Width.

(A) to **(C)** Quantification of individual actin architecture or orientation metrics plotted with respect to corresponding cell width in two root regions. Despite the high predictability between actin architecture parameters and cell length (shown in **Figure 2.1**) Filament architecture and orientation were not predictable based on cell width. Results for density **(Figure 2.1)** skewness **(A)**, angle **(B)**, and parallelness **(C)** vs. cell width showed no predictive relationships. Mean cell length, Region 2 = 57 ± 28 μm. Mean cell length, Region 3 = 128 ± 34 μm. Region 2 measurements are shown in purple diamonds; Region 3 in blue circles.

Not shown: mean actin filament density: Region 2 = 52.3 ± 0.02%; Region 3 = 15.4 ± 0.01%. Mean actin filament bundling/skewness: Region 2 = 1.12 ± 0.03; Region 3 = 1.71 ± 0.04. Mean filament angle: Region 2 = 17.5 ± 1.6°; Region 3 = 8.1 ± 0.5°. Mean filament parallelness: Region 2 = 0.24 ± 0.01; Region 3 = 0.50 ± 0.02.

N = 60–150 cells from 20 roots. NR, no predictive relationship, Bivariate fit/ANOVA. Results are from one experiment.

A Skewness^NR

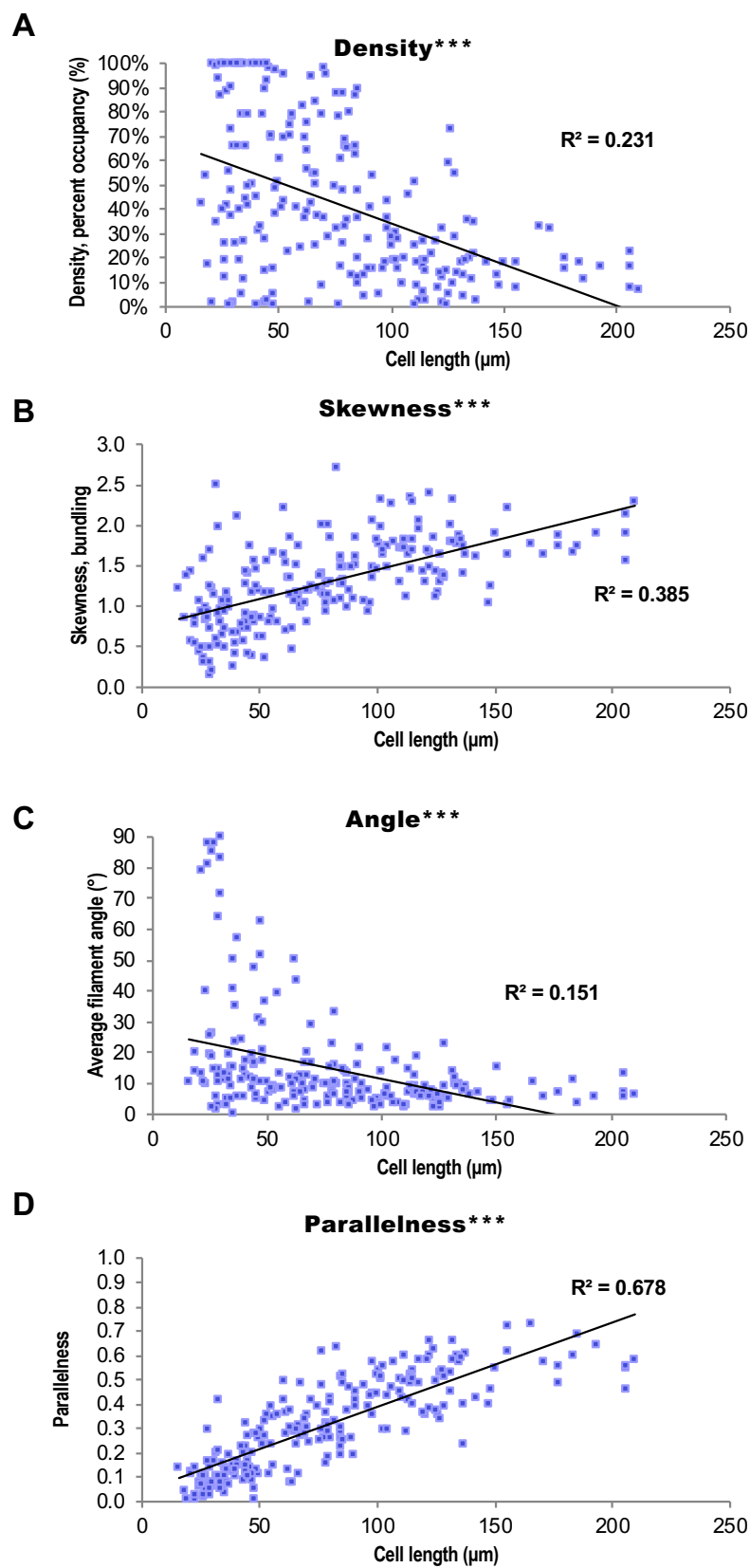**B** Angle^NR

C Parallelness^NR
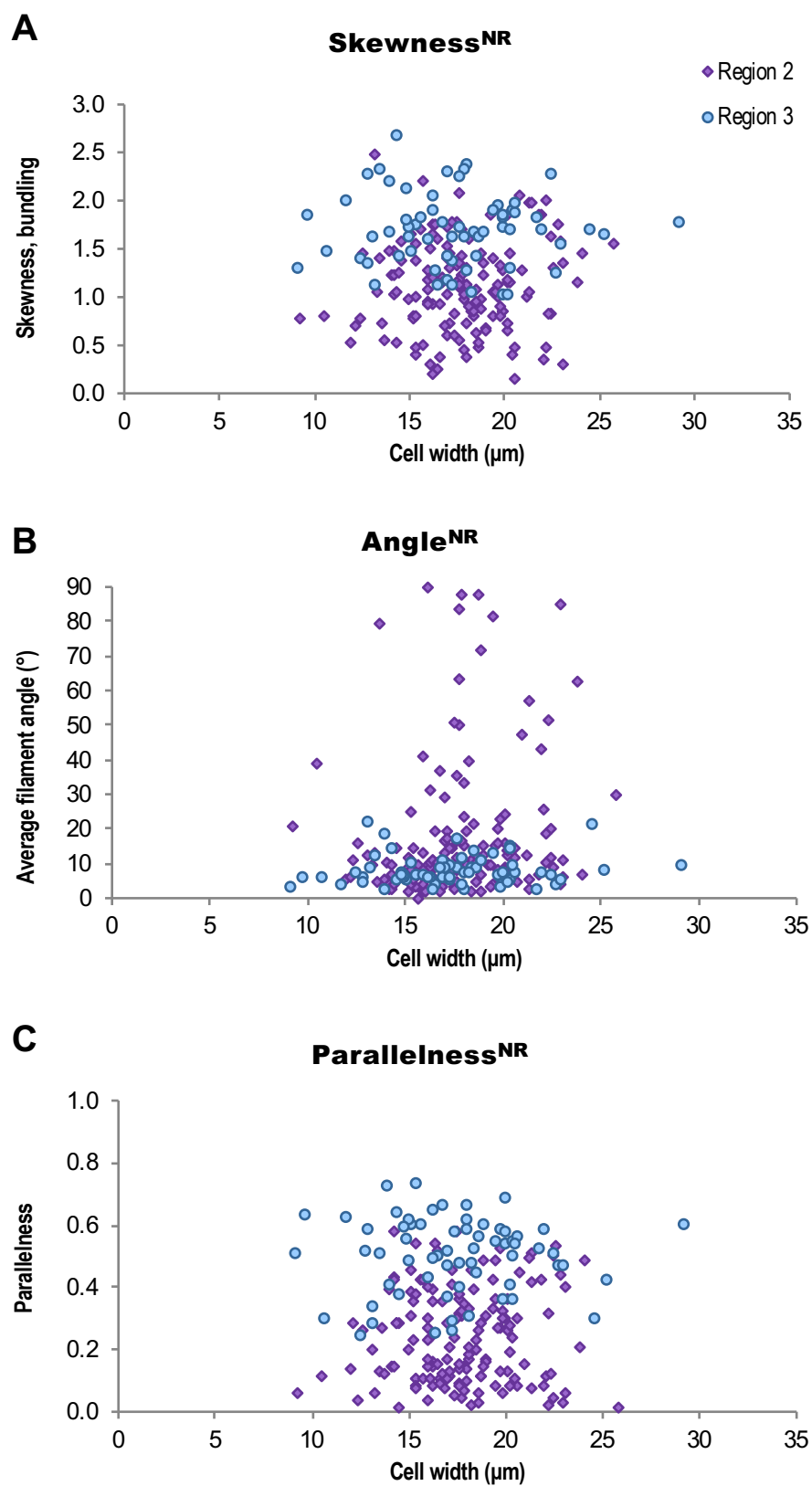
Supplemental Figure 2.7 Actin Filament Arrays Are Not Predictive of Cell Width.

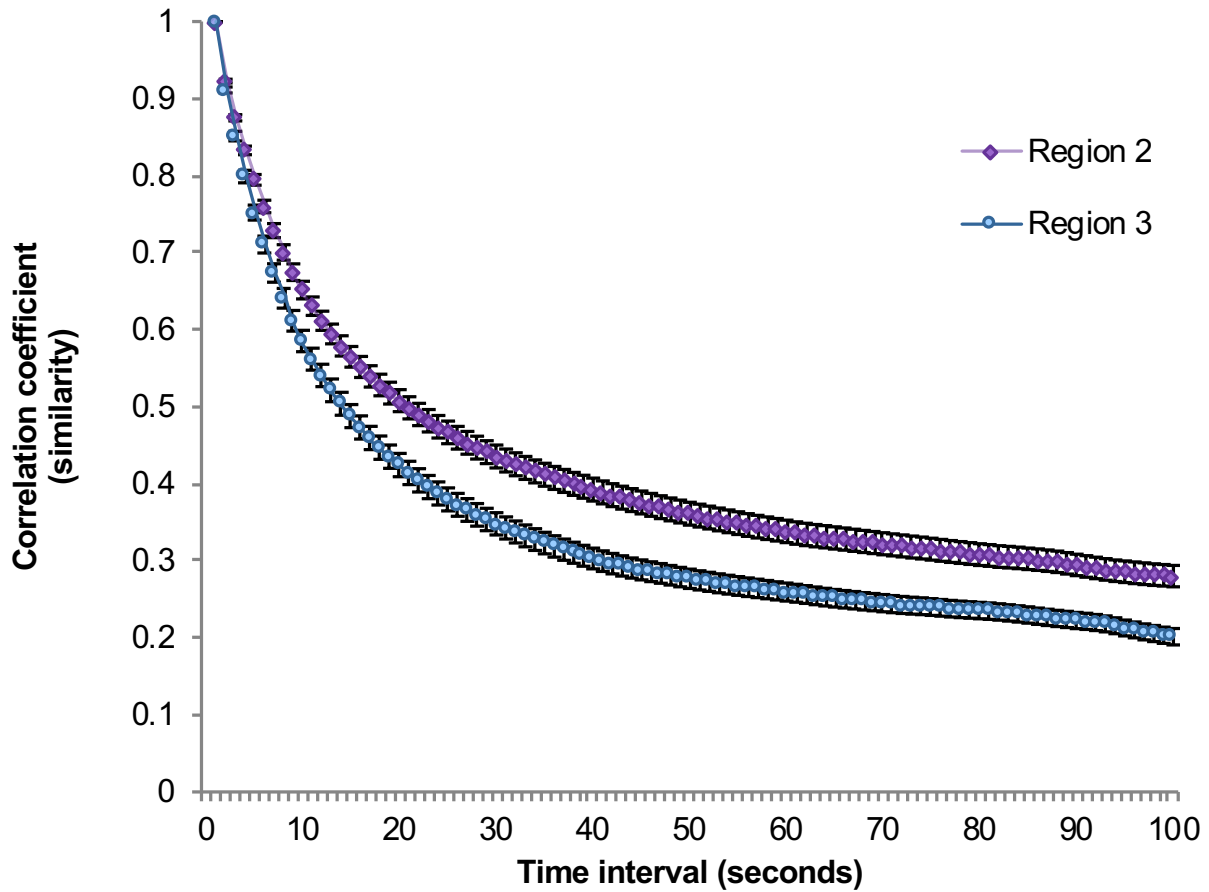Supplemental Figure 2.8 Actin Filament Arrays Are Predictive of Cell Length.

(A) to **(D)** Quantification of individual actin architecture or orientation metrics plotted with respect to corresponding cell length in two root regions, shown with R^2 values (linear fit determined in Excel) for reference only. These graphs are the same as **Figure 2.1** but are not shaded by region. Since it is not possible to know whether cell length or any aspect of actin organization is the independent variable, linear regression analysis is not an appropriate statistical metric on which to base strong conclusions.

$N \geq 200$ cells from a total of 20 roots. ***, $p \leq 0.0001$, Bivariate fit/ANOVA for all data points for each parameter. Results are from one experiment.

A

B

C

D

Supplemental Figure 2.8 Actin Filament Arrays Are Predictive of Cell Length.
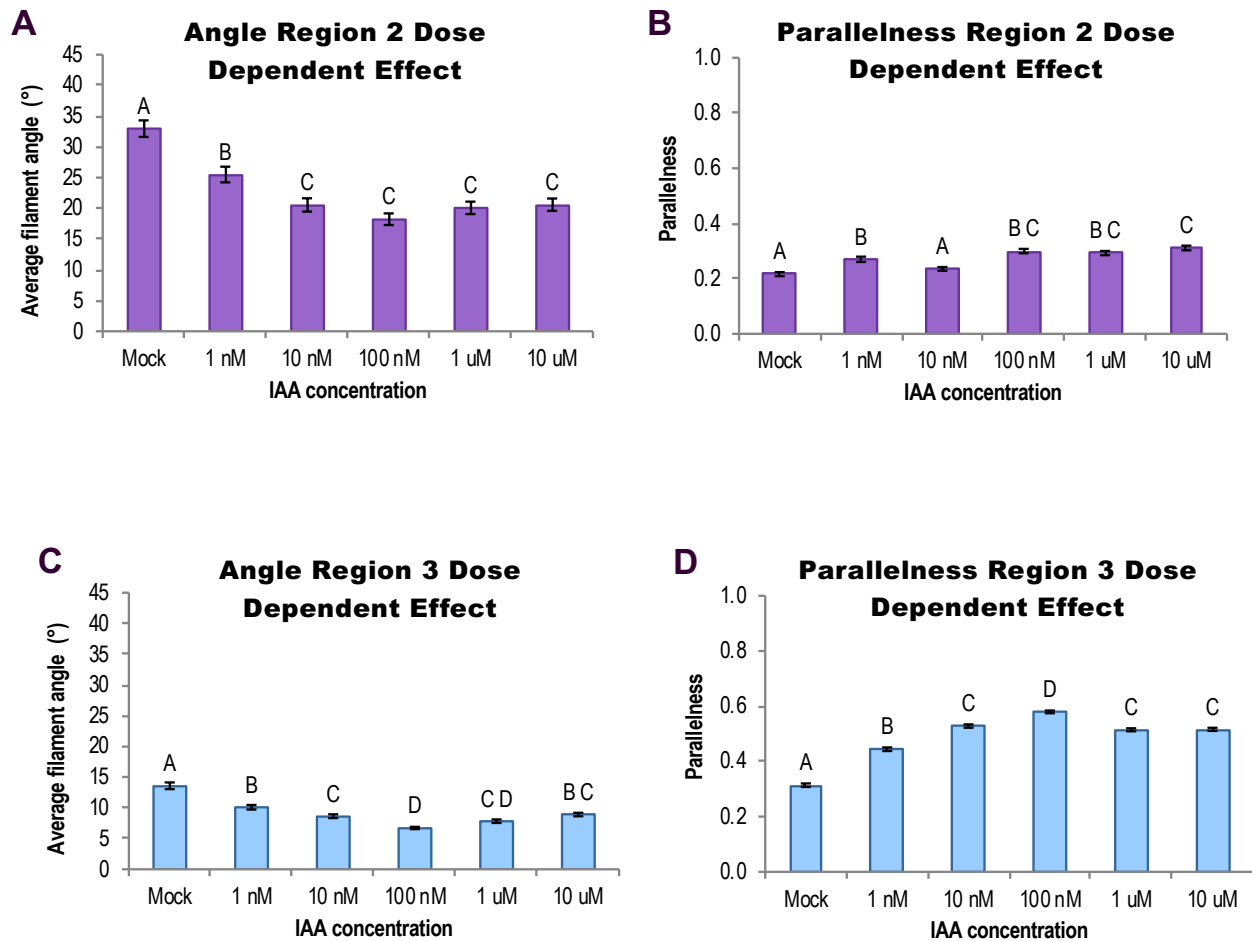
Supplemental Figure 2.9 Actin Arrays in Region 3 Are More Dynamic than in Region 2.

Filament arrays in short cells exhibited less overall dynamicity (i.e., short cells showed a slower decrease in similarity between pixel intensities and location between time intervals) compared with filament arrays of long cells.

100-s timelapse movies were collected from short and long cells in the same 30 roots. N = 80 (Region 3) to 148 (Region 2) cells from the same 30 plants as **Figure 2.2** and **Table 2.1**. ***, F ≤ 0.001, one way ANOVA.

A

Angle Region 2 Dose Dependent Effect

B

Parallelness Region 2 Dose Dependent Effect

C

Angle Region 3 Dose Dependent Effect

D

Parallelness Region 3 Dose Dependent Effect

Supplemental Figure 2.10 Short-Term IAA Treatments Induce Dose-Dependent Changes in Actin Filament Organization.

(A) to **(D)** Quantification of actin orientation in root epidermal cells: IAA triggered a dose-dependent decrease in average filament angle **(A)** and **(C)** and increase in parallelness **(B)** and **(D)**. Region 2 measurements are shown in **(A)** and **(B)**; Region 3 in **(D)** and **(E)**. The dose-dependency was more pronounced in Region 3.

Cells whose lengths fell between 85 and 94 μm were counted in both regions. N = 8–12 cells per region per root from at least 10 roots per treatment. Different letters indicate statistically significant differences, oneway ANOVA, compared with Tukey-Kramer HSD in JMP (see **Methods** for more information). All IAA experiments were performed and analyzed double blind.
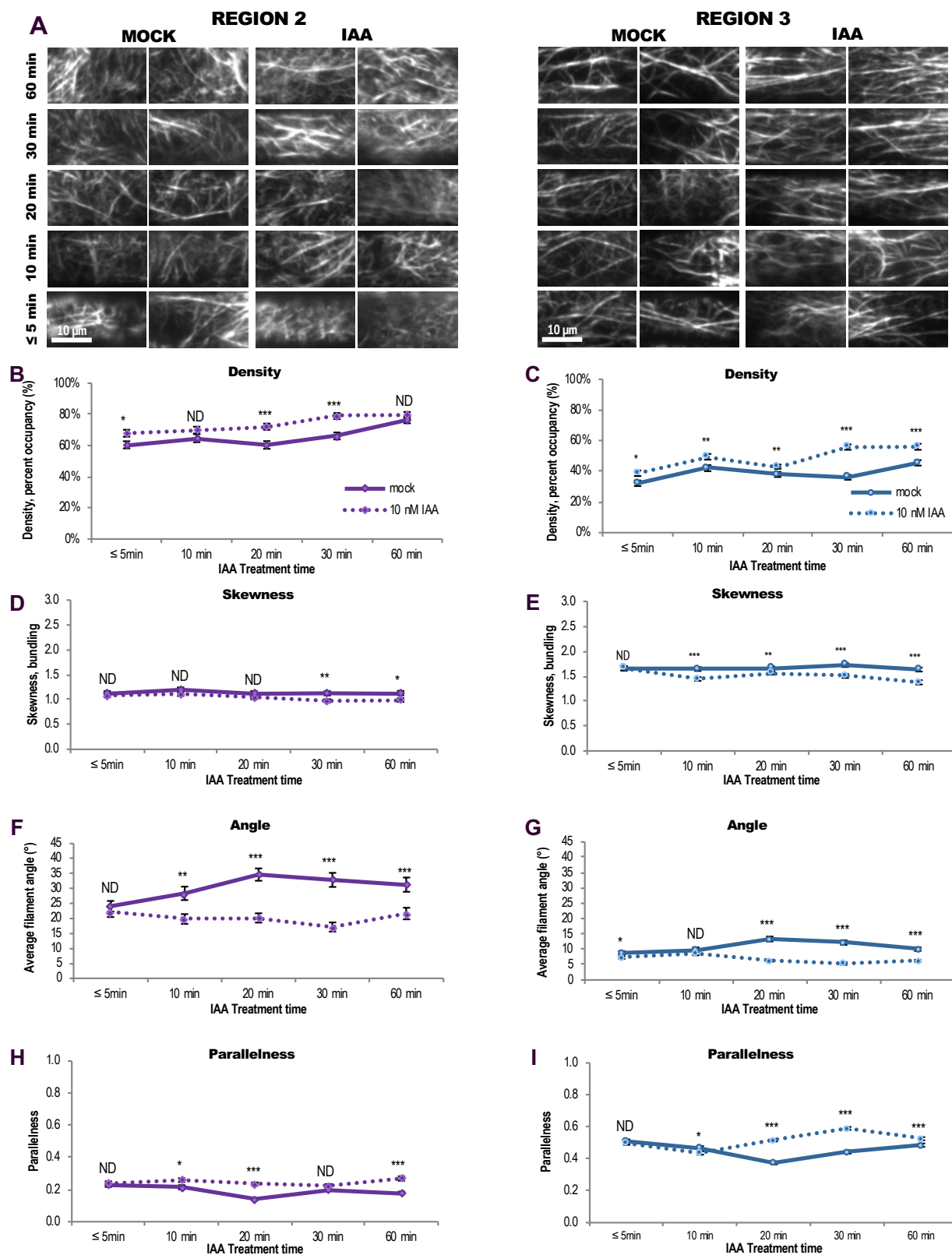
Supplemental Figure 2.11 Short-Term IAA Treatments Induce a Time-Dependent Increase in Actin Filament Density and Longitudinal Orientation.

(A) Representative VAEM images of GFP-fABD2–labeled actin in epidermal cells from Region 2 (left) and Region 3 (right). Scale bar, 10 μm.

(B) to **(E)** Quantification of actin architecture in Regions 2 and 3: 10 nM IAA (dotted lines) triggered a time-dependent increase in actin filament density **(B)** and **(C)** and decrease in skewness **(D)** and **(E)** compared to mock (unbroken lines). Region 2 measurements **(B)**, **(D)**, **(F)**, and **(H)** are shown in purple; Region 3 **(C)**, **(E)**, **(G)**, and **(I)** in blue.

(F) to **(I)** Quantification of actin orientation in Regions 2 and 3: after 10 nM IAA treatments, actin in both regions appeared more "organized", with lower average filament angle **(F)** and **(G)** relative to the longitudinal axis of the cell and filaments generally more parallel to each other **(H)** and **(I)**. These responses were roughly time-dependent, with a peak in parallel longitudinality occurring after 20–30 min of treatment.

N = 7 roots per treatment per timepoint (≥ 10 cells from Region 2 and approx. 4–9 cells from Region 3 from each root). ND, no statistical differences; *, $p \leq 0.05$; **, $p \leq 0.01$; ***, $p \leq 0.001$, Student's t-test of IAA (dotted line) vs. mock (unbroken line) on that region at that timepoint. Results are from one representative experiment of 2 similar experiments with similar results. All IAA experiments were performed and analyzed double blind.

Supplemental Figure 2.11 Short-Term IAA Treatments Induce a Time-Dependent Increase in Actin Filament Density and Longitudinal Orientation.
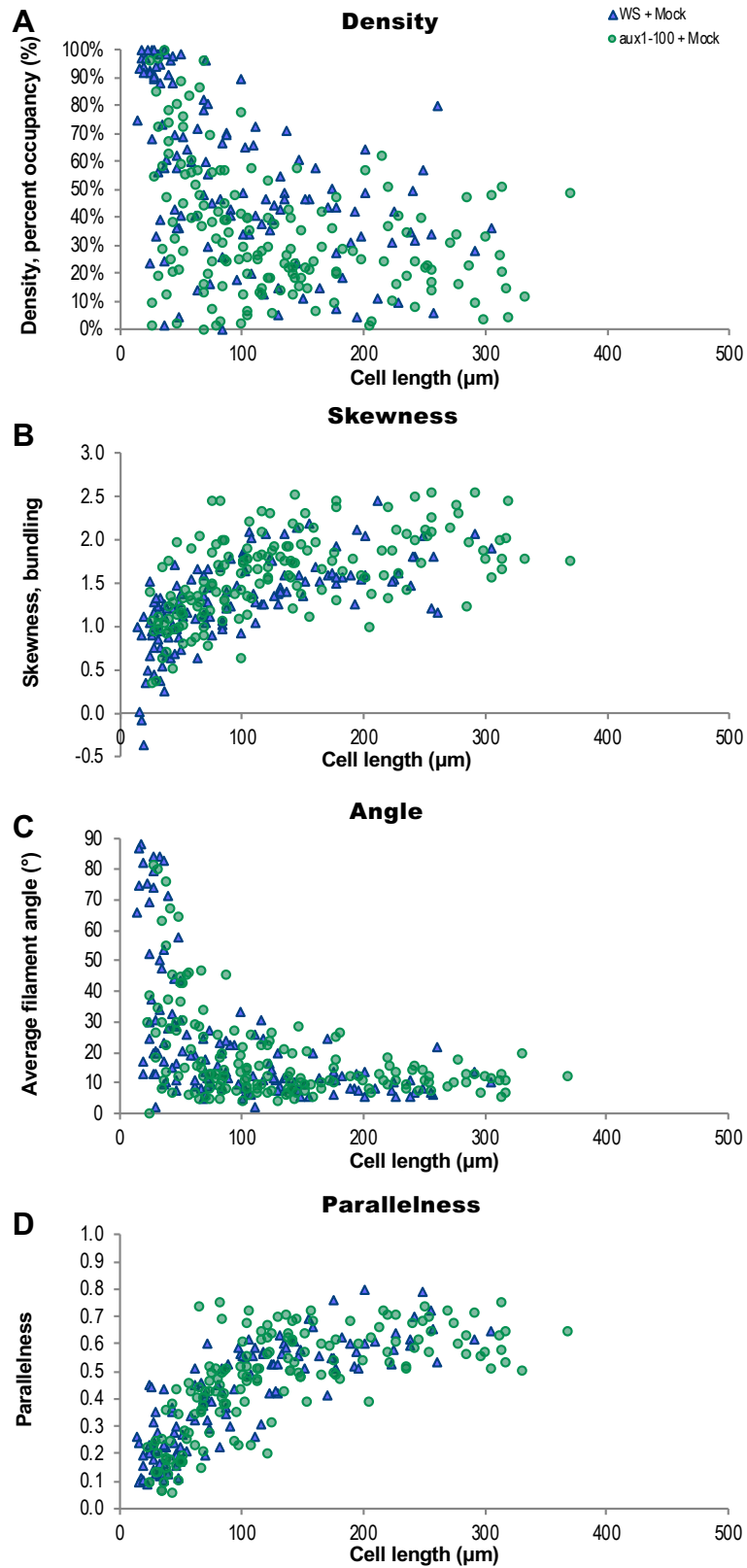
Supplemental Figure 2.12 Actin Filament Organization Plotted with Respect to Corresponding Cell Length in WS and *aux1-100*.

(A) to **(D)** Quantification of individual actin architecture or orientation metrics plotted with respect to corresponding cell length in WS and *aux1-100.*

(E) to **(H)** Quantification of WS individual actin architecture or orientation metrics after treatment with mock, IAA, and NAA, plotted with respect to corresponding cell length.

(I) to **(L)** Quantification of *aux1-100* individual actin architecture or orientation metrics after treatment with mock, IAA, and NAA, plotted with respect to corresponding cell length.

These graphs are scatterplots representing the same dataset as **Figure 2.5**; actin measurements were quantified on a per-cell basis and each data point represents a single cell's actin array plotted against its length.

Supplemental Figure 2.12 Actin Filament Organization Plotted with Respect to Corresponding Cell Length in WS and *aux1-100*.
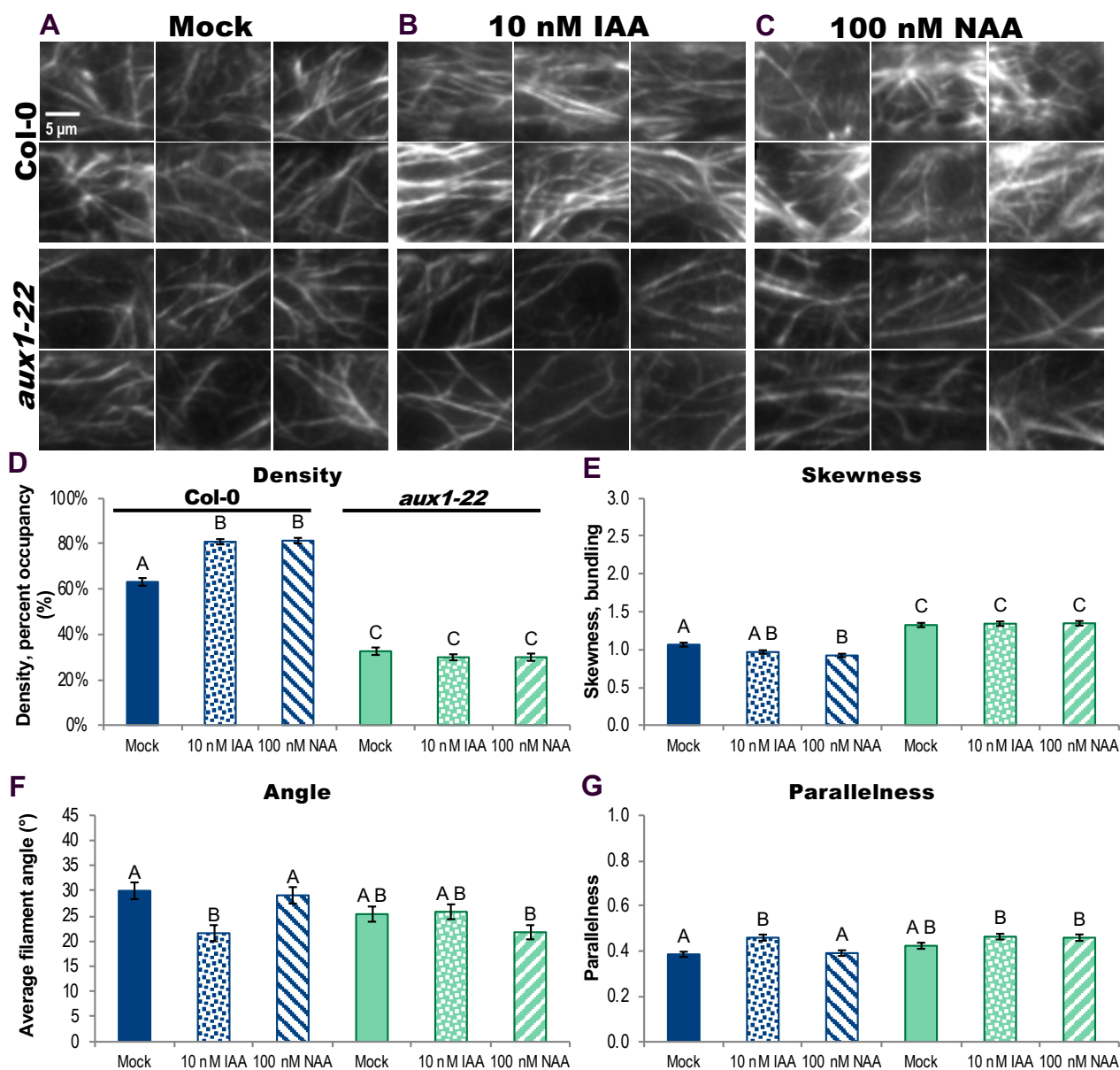
Supplemental Figure 2.12 continued.
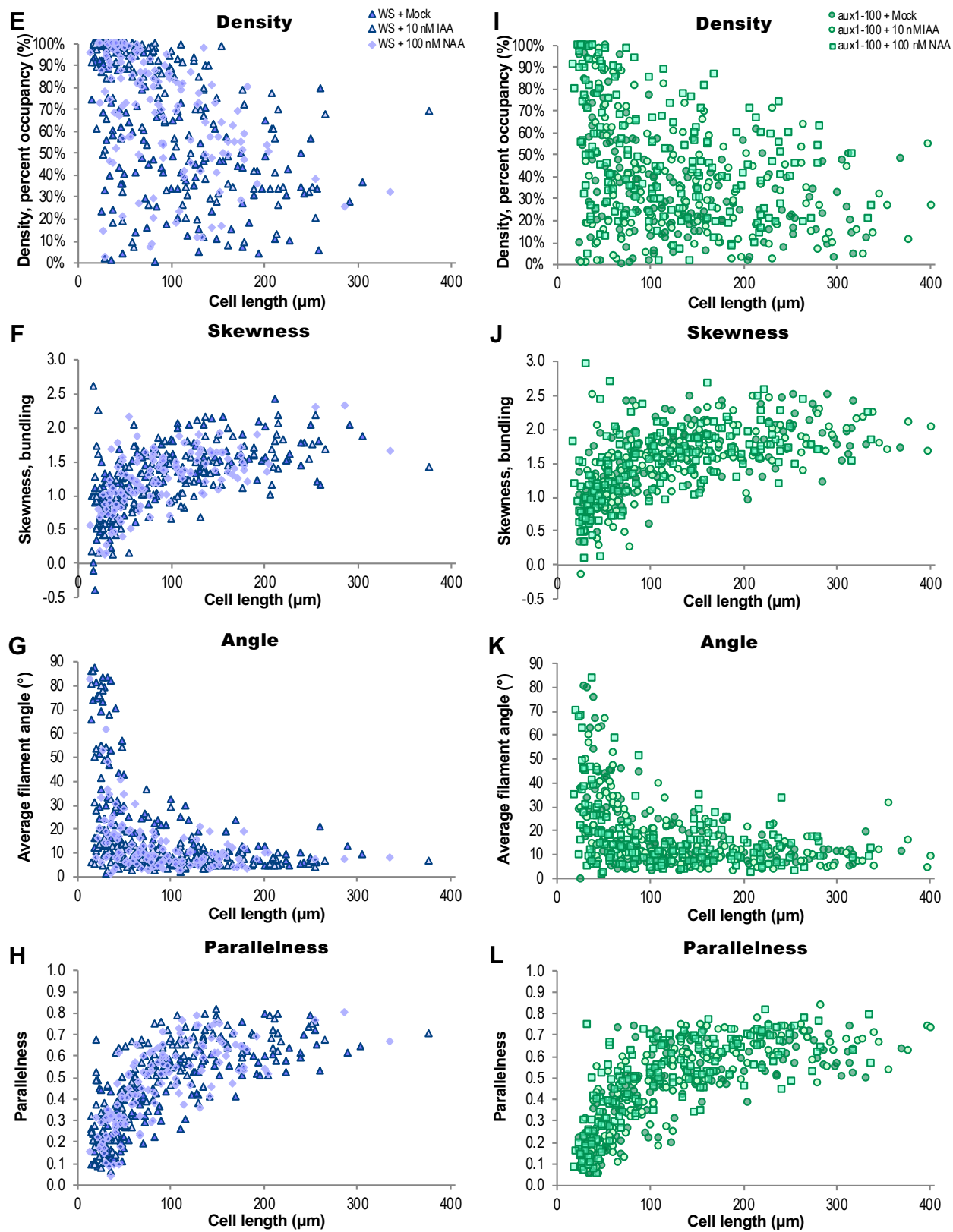
Supplemental Figure 2.13 Actin Organization in *aux1-22* Fails to Respond to Short-Term IAA Treatments but Partially Responds to the Membrane-Permeable Auxin NAA.

(A) to **(C)** Representative VAEM images of GFP-fABD2–labeled actin in epidermal cells from wildtype (Col-0) and *aux1-22*, treated for 20–30 min with mock **(A)**, 10 nM IAA **(B)**, or 100 nM NAA **(C)**. Scale bar, 5 μm.

(D) to **(G)** Quantification of actin organization in root epidermal cells. Both IAA and NAA failed to trigger an increase in actin filament density **(D)** and decrease in skewness **(E)** in *aux1-22* but actin density in wildtype cells increased in response to both IAA and NAA and skewness decreased with both auxin treatments. Wildtype response is shown in blue and *aux1-22* in green; mock, solid; 10 nM IAA, dots; 100 nM NAA, stripes. After IAA treatment, actin arrays in wildtype plants were more "organized," with lower average filament angle **(F)** relative to the longitudinal axis of the cell and filaments generally more parallel to each other **(G)**. NAA triggered the increase in actin density in wildtype plants, but had no effect on angle or parallelness when measured on a per-cell basis. Average actin filament angle and parallelness in *aux1-22* failed to reorganize in response to IAA and only average filament angle decreased (and no increase in parallelness) with the membrane-permeable auxin NAA.

N = 5–38 cells per root; 10 roots per genotype per treatment. Different letters indicate statistically significant differences, oneway ANOVA, compared with Tukey-Kramer HSD in JMP (see **Methods** for more information). Actin measurements were quantified on a per-cell basis; see **Methods** for description. Results are from one experiment. All auxin experiments were performed and analyzed double blind.

Supplemental Figure 2.13 Actin Organization in *aux1-22* Fails to Respond to Short-Term IAA Treatments but Partially Responds to the Membrane-Permeable Auxin NAA.
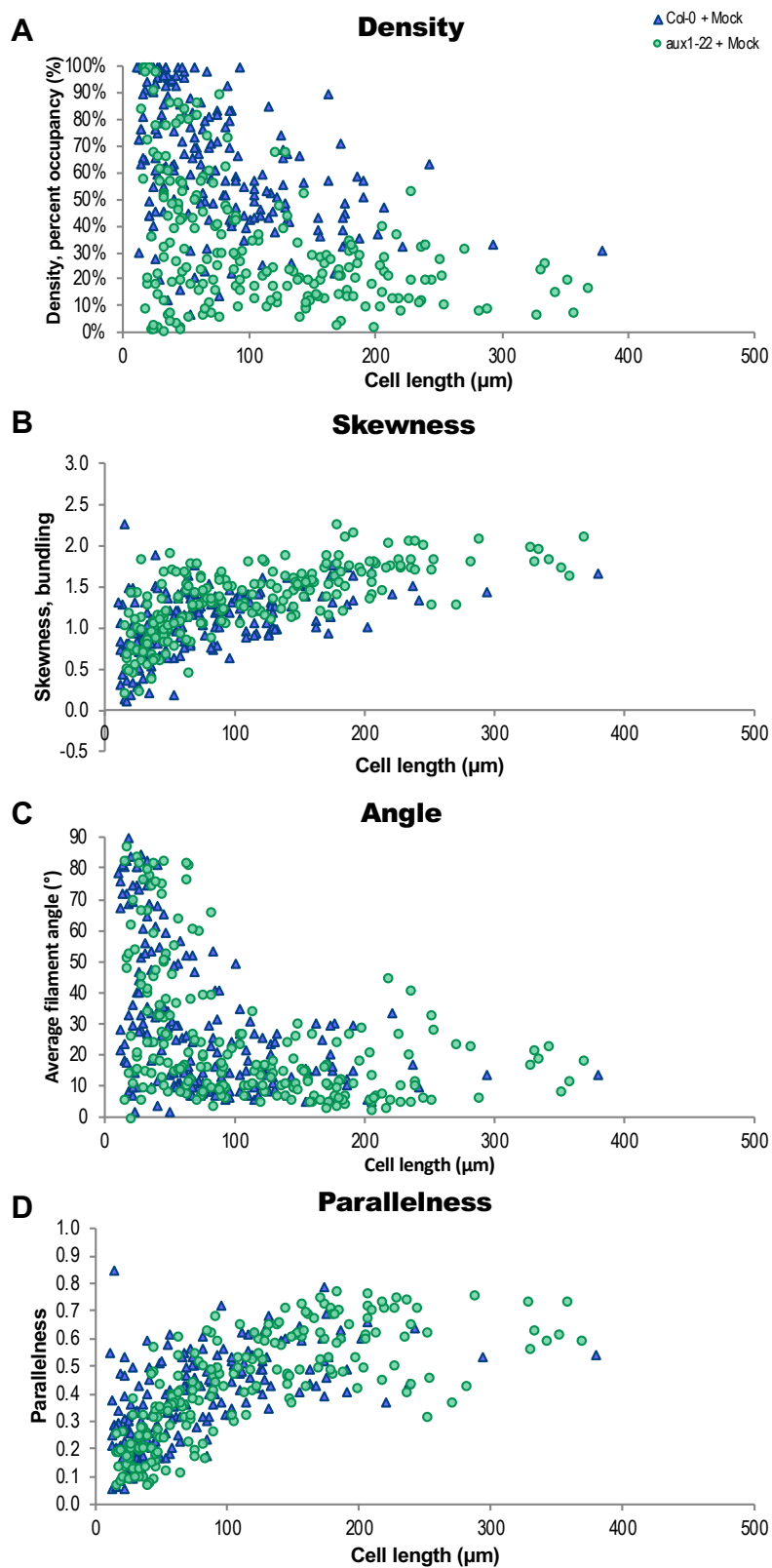
Supplemental Figure 2.14 Actin Filament Organization Plotted with Respect to Corresponding Cell Length in Col-0 and *aux1-22*.

(A) to **(D)** Quantification of individual actin architecture or orientation metrics plotted with respect to corresponding cell length in Col-0 and *aux1-22*.

(E) to **(H)** Quantification of Col-0 individual actin architecture or orientation metrics after treatment with mock, IAA, and NAA, plotted with respect to corresponding cell length.

(I) to **(L)** Quantification of *aux1-22* individual actin architecture or orientation metrics after treatment with mock, IAA, and NAA, plotted with respect to corresponding cell length.

These graphs are scatterplots representing the same dataset as **Supplemental Figure 2.13**; actin measurements were quantified on a per-cell basis and each data point represents a single cell's actin array plotted against its length.

Supplemental Figure 2.14 Actin Filament Organization Plotted with Respect to Corresponding Cell Length in Col-0 and *aux1-22*.

151

Supplemental Figure 2.14 continued.
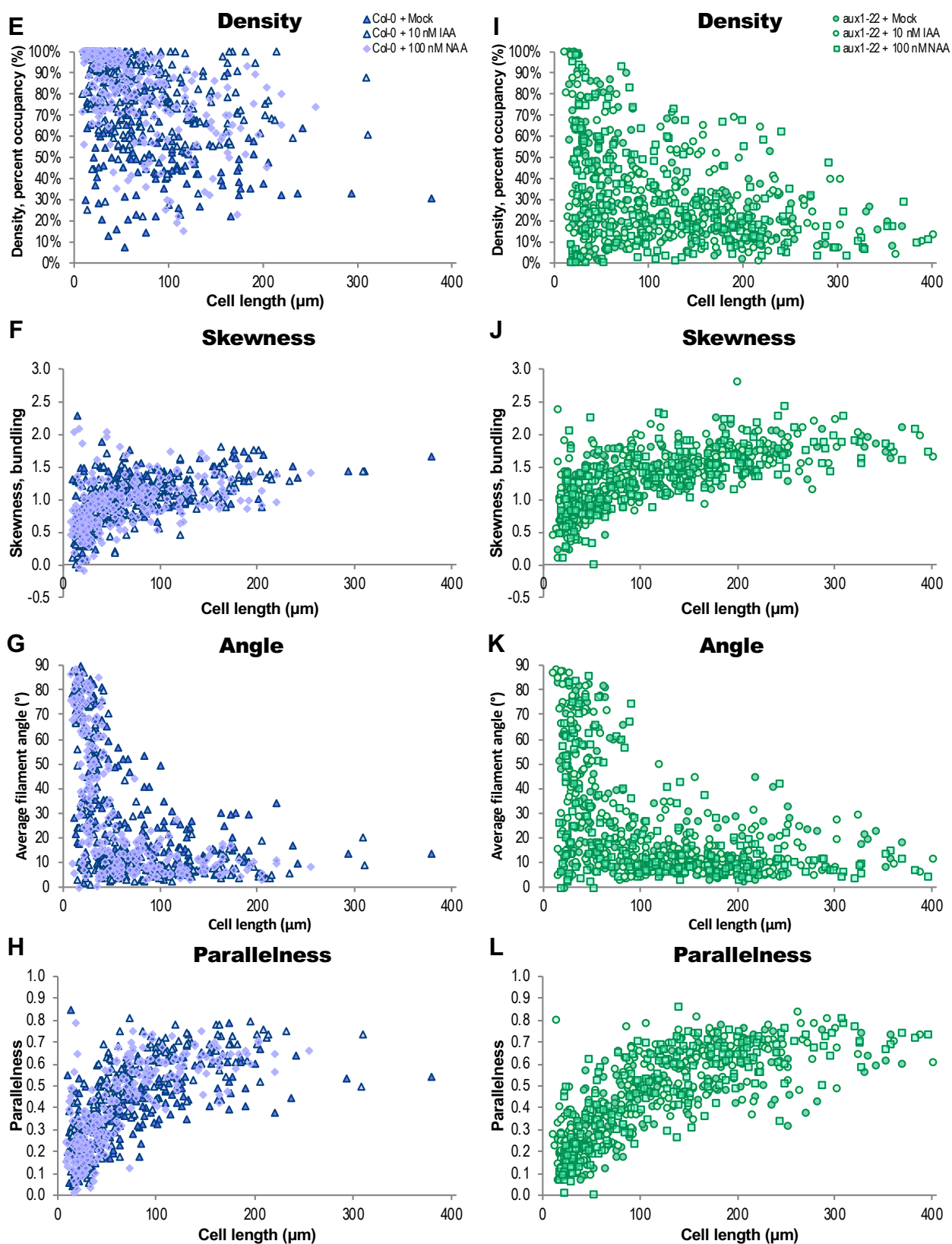
Supplemental Figure 2.15 Hypothetical model of auxin perception by AUX1 upstream of actin cytoskeleton reorganization.

(A) Control conditions: unidentified actin-binding proteins (ABP) -X and -Y are active and maintain actin array; an unidentified intermediary that differs between Col-0 and WS is inactive.

(B) Auxin is transported into a cell by AUX1, activating the unknown intermediary, inactivating both actin-binding proteins, and inducing increased actin filament abundance, decreased filament angle, and increased parallelness.

(C) In the absence of AUX1, the membrane permeable auxin NAA enters a cell, possibly activating the unknown intermediary; ABP-X and ABP-Y are differentially regulated and only either an increase in actin abundance or decrease in filament angle occurs.
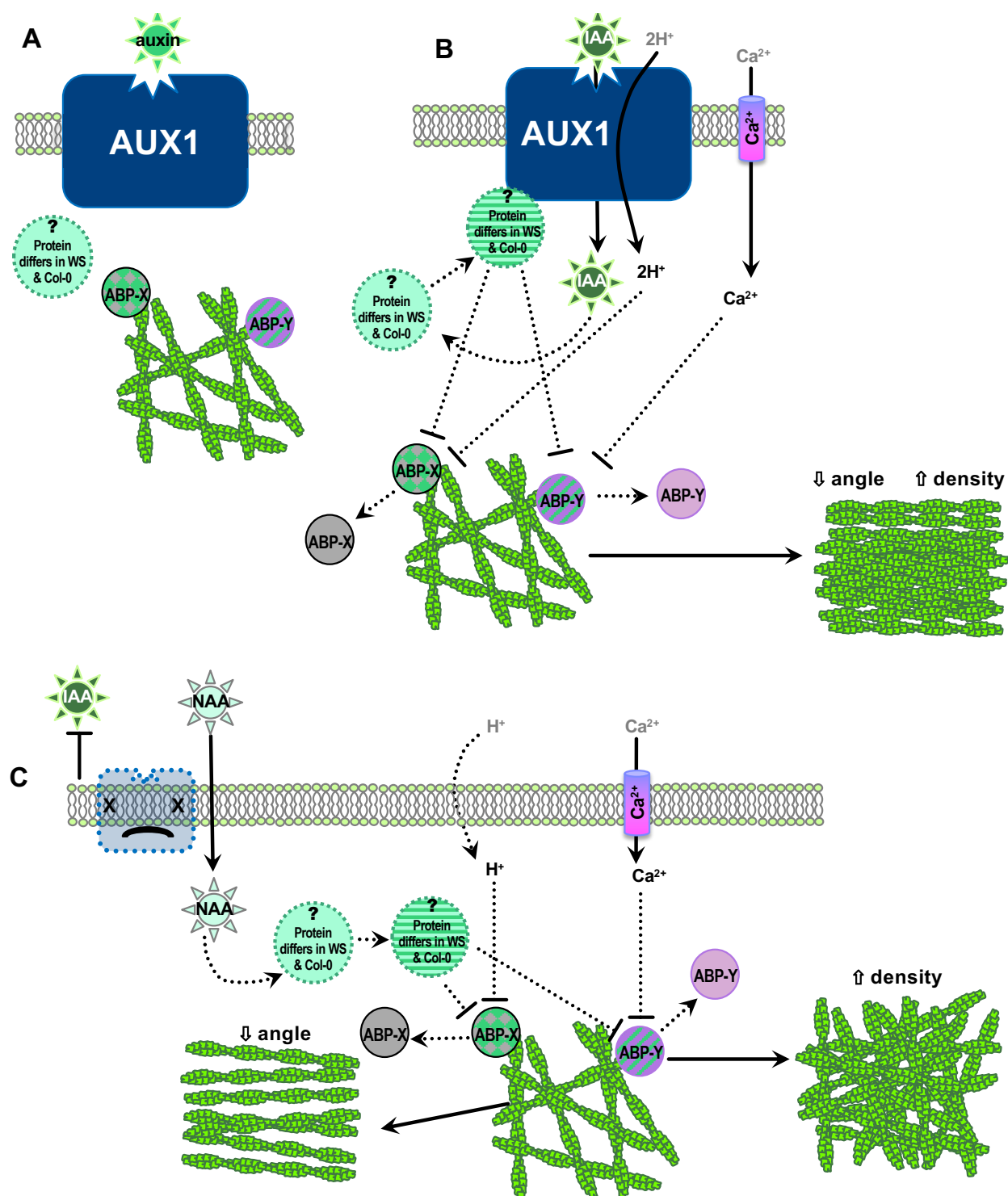
Supplemental Figure 2.15 Hypothetical model of auxin perception by AUX1 upstream of actin cytoskeleton reorganization.

2.10 References

Andrianantoandro, E., Blanchoin, L., Sept, D., McCammon, J.A., and Pollard, T.D. (2001). Kinetic mechanism of end-to-end annealing of actin filaments. J. Mol. Biol. 312: 721–730. doi:10.1006/jmbi.2001.5005.

Baluška, F., Jasik, J., Edelmann, H.G., Salajová, T., and Volkmann, D. (2001). Latrunculin B-induced plant dwarfism: plant cell elongation is F-actin-dependent. Dev. Biol. 231: 113–124. doi:10.1006/dbio.2000.0115.

Baluška, F., and Mancuso, S. (2013). Root apex transition zone as oscillatory zone. Front. Plant Sci. 4: e354. doi:10.3389/fpls.2013.00354.

Baluška, F., Vitha, S., Barlow, P.W., and Volkmann, D. (1997). Rearrangements of F-actin arrays in growing cells of intact maize root apex tissues: a major developmental switch occurs in the postmitotic transition region. Eur. J. Cell Biol. 72: 113–121.

Band, L.R., Wells, D.M., Larrieu, A., Sun, J., Middleton, A.M., French, A.P., Brunoud, G., Sato, E.M., Wilson, M.H., Péret, B., Oliva, M., Swarup, R., Sairanen, I., Parry, G., Ljung, K., Beeckman, T., Garibaldi, J.M., Estelle, M., Owen, M.R., Vissenberg, K., Hodgman, T.C., Pridmore, T.P., King, J.R., Vernoux, T., and Bennett, M.J. (2012). Root gravitropism is regulated by a transient lateral auxin gradient controlled by a tipping-point mechanism. Proc. Natl. Acad. Sci. USA 109: 4668–4673. doi:10.1073/pnas.1201498109.

Band, L.R., Wells, D.M., Fozard, J.A., Ghetiu, T., French, A.P., Pound, M.P., Wilson, M.H., Yu, L., Li, W., Hijazi, H.I., Oh, J., Pearce, S.P., Perez-Amador, M.A., Yun, J., Kramer, E., Alonso, J.M., Godin, C., Vernoux, T., Hodgman, T.C., Pridmore, T.P., Swarup, R., King, J.R., and Bennett, M.J. 2014. Systems analysis of auxin transport in the *Arabidopsis* root apex. *Plant Cell* 26: 862–875. doi: 10.1105/tpc.113.119495.

Beemster, G.T.S., and Baskin, T.I. (1998). Analysis of cell division and elongation underlying the developmental acceleration of root growth in *Arabidopsis thaliana*. Plant Physiol. 116: 1515–1526. doi:10.1104/pp.116.4.1515.

Beemster, G.T.S., and Baskin, T.I. (2000). *STUNTED PLANT 1* mediates effects of cytokinin, but not of auxin, on cell division and expansion in the root of Arabidopsis. Plant Physiol. 124: 1718–1727. doi:10.1104/pp.124.4.1718.

Bennett, M.J., Marchant, A., Green, H.G., May, S.T., Ward, S.P., Millner, P.A., Walker, A.R., Schulz, B., and Feldmann, K.A. (1996). *Arabidopsis AUX1* gene: a permease-like regulator of root gravitropism. Science 273: 948–950. doi:10.1126/science.273.5277.948.

Braidwood, L., Breuer, C., and Sugimoto, K. (2014). My body is a cage: Mechanisms and modulation of plant cell growth. New Phytol. 201: 388–402. doi:10.1111/nph.12473.

Breuer, D., Ivakov, A., Sampathkumar, A., Hollandt, F., Persson, S., and Nikoloski, Z. (2014). Quantitative analyses of the plant cytoskeleton reveal underlying organizational principles. J. Royal Soc. Interface 11: e20140362. doi:10.1098/rsif.2014.0362.

Brunoud, G., Wells, D. M., Oliva, M., Larrieu, A., Mirabet, V., Burrow, A. H., Beeckman, T., Kepinski, S., Traas, J., Bennett, M.J., Vernoux, T. (2012). A novel sensor to map auxin response and distribution at high spatio-temporal resolution. Nature 482: 103–106. doi:10.1038/nature10791.

Cai, C., Henty-Ridilla, J.L., Szymanski, D.B., and Staiger, C.J. (2014). Arabidopsis myosin XI: A motor rules the tracks. Plant Physiol. 166: 1359–1370. doi:10.1104/pp.114.244335.

Calderón Villalobos, L.I.A., Lee, S., De Oliveira, C., Ivetac, A., Brandt, W., Armitage, L., Sheard, L. B., Tan, X., Parry, G., Mao, H., Zheng, N., Napier, R., Kepinski, S., and Estelle, M. (2012). A combinatorial TIR1/AFB-Aux/IAA co-receptor system for differential sensing of auxin. Nat. Chem. Biol 8: 477–485. doi:10.1038/nchembio.926.

Cao, L., Henty-Ridilla, J.L., Blanchoin, L., and Staiger, C.J. (2016). Profilin-dependent nucleation and assembly of actin filaments controls cell elongation in Arabidopsis. Plant Physiol. 170: 220–233. doi:10.1104/pp.15.01321.

Cárdenas, L., Vidali, L., Domínguez, J., Pérez, H., Sánchez, F., Hepler, P.K., and Quinto, C. (1998). Rearrangement of actin microfilaments in plant root hairs responding to rhizobium ETLI nodulation signals. Plant Physiol. 116: 871–877. doi:10.1104/pp.116.3.871.

Carrier, D.J., Bakar, N.T.A., Swarup, R., Callaghan, R., Napier, R.M., Bennett, M.J., and Kerr, I.D. (2008). The binding of auxin to the Arabidopsis auxin influx transporter AUX1. Plant Physiol. 148: 529–535. doi:10.1104/pp.108.122044.

Chen, J.-G, Ullah, H., Young, J. C., Sussman, M.R., and Jones, A.M. (2001). ABP1 is required for organized cell elongation and division in *Arabidopsis* embryogenesis. Genes Dev. 15: 902–911. doi:10.1101/gad.866201.

Chen, X., Naramoto, S., Robert, S., Tejos, R., Löfke, C., Lin, D., Yang, Z., and Friml, J. (2012). ABP1 and ROP6 GTPase signaling regulate clathrin-mediated endocytosis in *Arabidopsis* roots. Curr. Biol. 22: 1326–1332. doi:10.1016/j.cub.2012.05.020.

Cosgrove, D.J. (2005). Growth of the plant cell wall. Nat. Rev. Mol. Cell Biol. 6: 850–861. doi:10.1038/nrm1746.

Dai, X., Zhang, Y., Zhang, D., Chen, J., Gao, X., Estelle, M., and Zhao, Y. (2015). Embryonic lethality of *Arabidopsis abp1-1* is caused by deletion of the adjacent BSM gene. Nat. Plants 1: e15183. doi:10.1038/nplants.2015.183.

Delker, C., Pöschl, Y., Raschke, A., Ullrich, K., Ettingshausen, S., Hauptmann, V., Grosse, I., and Quint, M. (2010). Natural variation of transcriptional auxin response networks in *Arabidopsis thaliana.* Plant Cell 22: 2184-2200. doi:10.1105/tpc.110.073957.

Dharmasiri, N., Dharmasiri, S., and Estelle, M. (2005a). The F-box protein TIR1 is an auxin receptor. Nature 435: 441–445. doi:10.1038/nature03543.

Dharmasiri, N., Dharmasiri, S., Weijers, D., Lechner, E., Yamada, M., Hobbie, L., Ehrismann, J.S., Jürgens, G., and Estelle, M. (2005b). Plant development is regulated by a family of auxin receptor F-box proteins. Dev. Cell 9: 109–119. doi:10.1016/j.devcel.2005.05.014.

Dhonukshe, P., Grigoriev, I., Fischer, R., Tominaga, M., Robinson, D. G., Hašek, J., Paciorek, T., Petrášek, J., Seifertová, D., Tejos, R., Meisel, L.A., Zažímalová, E., Gadella, Jr., T.W.J., Steirhof, Y.-D., Ueda, T., Oiwa, K., Akhmanova, A., Brock, R., Spang, A., and Friml, J. (2008). Auxin transport inhibitors impair vesicle motility and actin cytoskeleton dynamics in diverse eukaryotes. Proc. Natl. Acad. Sci. USA 105: 4489–4494. doi:10.1073/pnas.0711414105.

Dindas, J., Scherzer, S., Roelfsema, M.R.G., Von Meyer, K., Müller, H.M., Al-Rasheid, K.A.S., Palme, K., Dietrich, P., Becker, D., Bennett, M.J., and Hedrich, R. (2018). AUX1-mediated root hair auxin influx governs SCFTIR1/AFB-type Ca^{2+} signaling. Nat. Commun. 9: e1174. doi:10.1038/s41467-018-03582-5.

Dyachok, J., Zhu, L., Liao, F., He, J., Huq, E., and Blancaflor, E.B. (2011). SCAR mediates light-induced root elongation in *Arabidopsis* through photoreceptors and proteasomes. Plant Cell 23: 3610–3626. doi:10.1105/tpc.111.088823.

Falasca, G., and Altamura, M.M. (2003). Histological analysis of adventitious rooting in *Arabidopsis thaliana* (L.) Heynh seedlings. Plant Biosyst. 137: 265–273. dx.doi.org/10.1080/11263500312331351511.

Feldmann, K.A. (1991). T-DNA insertion mutagenesis in *Arabidopsis*: Mutational spectrum. Plant J. 1: 71–82. doi:10.1111/j.1365-313X.1991.00071.x.

Fendrych, M., Akhmanova, M., Merrin, J., Glanc, M., Hagihara, S., Takahashi, K., Uchida, N., Torii, K.U., and Friml, J. (2018). Rapid and reversible root growth inhibition by TIR1 auxin signalling. Nat. Plants 4: 453–459. doi:10.1038/s41477-018-0190-1.

Gao, Y., Zhang, Y., Zhang, D., Dai, X., Estelle, M., and Zhao, Y. (2015). AUXIN BINDING PROTEIN 1 (ABP1) is not required for either auxin signaling or *Arabidopsis* development. Proc. Natl. Acad. Sci. USA 112: 2275–2280. doi:10.1073/pnas.1500365112.

Gilliland, L.U., Pawloski, L.C., Kandasamy, M.K., and Meagher, R.B. (2003). *Arabidopsis* actin gene *ACT7* plays an essential role in germination and root growth. Plant J. 33: 319–328. doi:10.1046/j.1365-313X.2003.01626.x.

Grones, P. and Friml, J. (2015). Auxin transporters and binding proteins at a glance. J. Cell Sci. 128: 1–7. doi:10.1242/jcs.159418.

Guerriero, G., Hausman, J. -F, and Cai, G. (2014). No stress! Relax! Mechanisms governing growth and shape in plant cells. Int. J. Mol. Sci. 15: 5094–5114. doi:10.3390/ijms15035094.

Hacham, Y., Holland, N., Butterfield, C., Ubeda-Tomas, S., Bennett, M.J., Chory, J., and Savaldi-Goldstein, S. (2011). Brassinosteroid perception in the epidermis controls root meristem size. Development 138: 839–848. doi:10.1242/dev.061804.

Hayashi, K.-I, Nakamura, S., Fukunaga, S., Nishimura, T., Jenness, M.K., Murphy, A.S., Motose, H., Nozaki, H., Furutani, M., and Aoyama, T. (2014). Auxin transport sites are visualized in planta using fluorescent auxin analogs. Proc. Natl. Acad. Sci. USA 111: 11557–11562. doi:10.1073/pnas.1408960111.

Hejnowicz, Z., and Erickson, R.O. (1968). Growth inhibition and recovery in roots following temporary treatment with auxin. Physiol. Plantarum 21: 302–313. doi:10.1111/j.1399-3054.1968.tb07254.x.

Henty, J.L., Bledsoe, S.W., Khurana, P., Meagher, R.B., Day, B., Blanchoin, L., and Staiger, C.J. (2011). *Arabidopsis* ACTIN DEPOLYMERIZING FACTOR4 modulates the stochastic dynamic behavior of actin filaments in the cortical array of epidermal cells. Plant Cell 23: 3711–3726. doi:10.1105/tpc.111.090670.

Henty-Ridilla, J.L., Li, J., Blanchoin, L., and Staiger, C.J. (2013). Actin dynamics in the cortical array of plant cells. Curr. Opin. Plant Biol. 16: 678–687. doi:10.1016/j.pbi.2013.10.012.

Henty-Ridilla, J.L., Li, J., Day, B., and Staiger, C.J. (2014). ACTIN DEPOLYMERIZING FACTOR4 Regulates actin dynamics during innate immune signaling in *Arabidopsis*. Plant Cell 26: 340–352. doi:10.1105/tpc.113.122499.

Higaki, T., Kojo, K.H., and Hasezawa, S. (2010a.) Critical role of actin bundling in plant cell morphogenesis. Plant Signal. Behav. 5: 484–488. doi:10.4161/psb.10947.

Higaki, T., Kurusu, T., Hasezawa, S., and Kuchitsu, K. (2011). Dynamic intracellular reorganization of cytoskeletons and the vacuole in defense responses and hypersensitive cell death in plants. J. Plant Res. 124: 315–324. doi:10.1007/s10265-011-0408-z.

Higaki, T., Kutsuna, N., Sano, T., Kondo, N., and Hasezawa, S. (2010b.) Quantification and cluster analysis of actin cytoskeletal structures in plant cells: role of actin bundling in stomatal movement during diurnal cycles in Arabidopsis guard cells. Plant J. 61: 156–165. doi:10.1111/j.1365-313X.2009.04032.x.

Holweg, C., Süßlin, C., and Nick, P. (2004). Capturing in vivo dynamics of the actin cytoskeleton stimulated by auxin or light. Plant Cell. Physiol. 45: 855–863. doi:10.1093/pcp/pch102.

Hussey, P.J., Ketelaar, T., and Deeks, M.J. (2006). Control of the actin cytoskeleton in plant cell growth. Annu. Rev. Plant Biol. 57: 109–125. doi:10.1146/annurev.arplant.57.032905.105206.

Jásik, J., Bokor, B., Stuchlík, S., Mičieta, K., Turňa, J., and Schmelzer, E. (2016). Effects of auxins on PIN-FORMED2 (PIN2) dynamics are not mediated by inhibiting PIN2 endocytosis. Plant Physiol. 172: 1019–1031. doi:10.1104/pp.16.00563.

Kandasamy, M.K., McKinney, E.C., and Meagher, R.B. (2009). A single vegetative actin isovariant overexpressed under the control of multiple regulatory sequences is sufficient for normal *Arabidopsis* development. Plant Cell 21: 701–718. doi:10.1105/tpc.108.061960.

Kepinski, S. and Leyser, O. (2005). The *Arabidopsis* F-box protein TIR1 is an auxin receptor. Nature 435: 446–451. doi:10.1038/nature03542.

Ketelaar, T., De Ruijter, N.C.A., and Emons, A.M.C. (2003). Unstable F-actin specifies the area and microtubule direction of cell expansion in Arabidopsis root hairs. Plant Cell 15: 285–292. doi:10.1105/tpc.007039.

Kleine-Vehn, J., Dhonukshe, P., Sauer, M., Brewer, P.B., Wiśniewska, J., Paciorek, T., Benková, E., and Friml, J. (2008). ARF GEF-dependent transcytosis and polar delivery of PIN auxin carriers in *Arabidopsis*. Curr. Biol. 18: 526–531. doi:10.1016/j.cub.2008.03.021.

Kleine-Vehn, J., Dhonukshe, P., Swarup, R., Bennett, M., and Friml, J. (2006). Subcellular trafficking of the *Arabidopsis* auxin influx carrier AUX1 uses a novel pathway distinct from PIN1. Plant Cell 18: 3171–3181. doi:10.1105/tpc.106.042770.

Kleine-Vehn, J. and Friml, J. (2008). Polar targeting and endocytic recycling in auxin-dependent plant development. Annu. Rev. Cell Dev. Biol. 24: 447–473. doi:10.1146/annurev.cellbio.24.110707.175254.

Kroeger, J.H., Zerzour, R., and Geitmann, A. (2011). Regulator or driving force? The role of turgor pressure in oscillatory plant cell growth. PLoS ONE 6: e18549. doi:10.1371/journal.pone.0018549.

Krysan, PJ, Young, JC, Tax, F, Sussman, MR. 1996. Identification of transferred DNA insertions within *Arabidopsis* genes involved in signal transduction and ion transport. *Proceedings of the National Academy of Sciences of the United States of America* 93: 8145–8150. doi: 10.1073/pnas.93.15.8145.

Leucci, M.R., Di Sansebastiano, G. -P, Gigante, M., Dalessandro, G., and Piro, G. (2007). Secretion marker proteins and cell-wall polysaccharides move through different secretory pathways. Planta 225: 1001–1017. doi:10.1007/s00425-006-0407-9.

Li, G., Liang, W., Zhang, X., Ren, H., Hu, J., Bennett, M.J., and Zhang, D. (2014a). Rice actin-binding protein RMD is a key link in the auxin-actin regulatory loop that controls cell growth. Proc. Natl. Acad. Sci. USA 111: 10377–10382. doi:10.1073/pnas.1401680111.

Li, J., Arieti, R., and Staiger, C.J. (2015a). "Actin filament dynamics and their role in plant cell expansion." pp. 127–162 in *Plant Cell Wall Patterning and Cell Shape*, H. Fukuda, ed. doi:10.1002/9781118647363.ch5.

Li, J., Henty-Ridilla, J.L., Huang, S., Wang, X., Blanchoin, L., and Staiger, C.J. (2012). Capping protein modulates the dynamic behavior of actin filaments in response to phosphatidic acid in *Arabidopsis*. Plant Cell 24: 3742–3754. doi:10.1105/tpc.112.103945.

Li, J., Henty-Ridilla, J.L., Staiger, B.H., Day, B., and Staiger, C.J. (2015b). Capping protein integrates multiple MAMP signalling pathways to modulate actin dynamics during plant innate immunity. Nat. Commun. 6: 7206. doi:10.1038/ncomms8206.

Li, J., Staiger, B.H., Henty-Ridilla, J.L., Abu-Abied, M., Sadot, E., Blanchoin, L., and Staiger, C.J. (2014b). The availability of filament ends modulates actin stochastic dynamics in live plant cells. Mol. Biol. Cell 25: 1263–1275. doi:10.1091/mbc.E13-07-0378.

Lin, D., Nagawa, S., Chen, J., Cao, L., Chen, X., Xu, T., Li, H., Dhonukshe, P., Yamamuro, C., Friml, J., Scheres, B., Fu, Y., Yang, Z. (2012). A ROP GTPase-dependent auxin signaling pathway regulates the subcellular distribution of PIN2 in *Arabidopsis* roots. Curr. Biol. 22: 1319–1325. doi:10.1016/j.cub.2012.05.019.

Maher, E.P., and Martindale, S.J.B. (1980). Mutants of *Arabidopsis thaliana* with altered responses to auxins and gravity. Biochem. Genet. 18: 1041–1053. doi:10.1007/BF00484337.

Marchant, A., Kargul, J., May, S.T., Muller, P., Delbarre, A., Perrot-Rechenmann, C., and Bennett, M.J. (1999). AUX1 regulates root gravitropism in *Arabidopsis* by facilitating auxin uptake within root apical tissues. EMBO J. 18: 2066–2073. doi:10.1093/emboj/18.8.2066.

Mathur, J. (2004). Cell shape development in plants. Trends Plant Sci. 9: 583–590. doi:10.1016/j.tplants.2004.10.006.

Monshausen, G.B., Miller, N.D., Murphy, A.S., and Gilroy, S. (2011). Dynamics of auxin-dependent Ca^{2+} and pH signaling in root growth revealed by integrating high-resolution imaging with automated computer vision-based analysis. Plant J. 65: 309–318. doi:10.1111/j.1365-313X.2010.04423.x.

Nagawa, S., Xu, T., Lin, D., Dhonukshe, P., Zhang, X., Friml, J., Scheres, B., Fu, Y., and Yang, Z. (2012). ROP GTPase-dependent actin microfilaments promote PIN1 polarization by localized inhibition of clathrin-dependent endocytosis. PLoS Biol. 10: e1001299. doi:10.1371/journal.pbio.1001299.

Nick, P. (2010). Probing the actin-auxin oscillator. Plant Signal. Behav. 5: 94–98. doi:10.4161/psb.5.2.10337.

Nick, P., Han, M.-J, and An, G. (2009). Auxin stimulates its own transport by shaping actin filaments. Plant Physiol. 151: 155–167. doi:10.1104/pp.109.140111.

Overvoorde, P., Fukaki, H., and Beeckman, T. (2010). Auxin control of root development. CSH Perspect. Biol. 2: a001537. doi:10.1101/cshperspect.a001537.

Pickett, F.B., Wilson, A.K., and Estelle, M. (1990). The *aux1* mutation of *Arabidopsis* confers both auxin and ethylene resistance. Plant Physiol. 94: 1462–1466. doi:10.1104/pp.94.3.1462.

Rahman, A., Bannigan, A., Sulaman, W., Pechter, P., Blancaflor, E.B., and Baskin, T.I. (2007). Auxin, actin and growth of the *Arabidopsis thaliana* primary root. Plant J. 50: 514–528. doi:10.1111/j.1365-313X.2007.03068.x.

Rashotte, A.M., Poupart, J., Waddell, C.S., and Muday, G.K. (2003). Transport of the two natural auxins, indole-3-butyric acid and indole-3-acetic acid, in Arabidopsis. Plant Physiol. 133: 761–772. doi:10.1104/pp.103.022582.

Roman G, Lubarsky, B., Kieber, J.J., Rothenberg, M., and Ecker, J.R. (1995). Genetic analysis of ethylene signal transduction in *Arabidopsis thaliana*: Five novel mutant loci integrated into a stress response pathway. Genetics 139: 1393–1409.

Rutschow, H.L., Baskin, T.I., and Kramer, E.M. (2014). The carrier AUXIN RESISTANT (AUX1) dominates auxin flux into Arabidopsis protoplasts. New Phytol. 204: 536–544. doi:10.1111/nph.12933.

Sauer, M., and Kleine-Vehn, J. (2011). AUXIN BINDING PROTEIN1: The outsider. Plant Cell 23: 2033–2043. doi:10.1105/tpc.111.087064.

Savaldi-Goldstein, S., Peto, C., and Chory, J. (2007). The epidermis both drives and restricts plant shoot growth. Nature 446: 199–202. doi:10.1038/nature05618.

Scheuring, D., Löfke, C., Krüger, F., Kittelmann, M., Eisa, A., Hughes, L., Smith, R.S., Hawes, C., Schumacher, K., and Kleine-Vehn, J. (2016). Actin-dependent vacuolar occupancy of the cell determines auxin-induced growth repression. Proc. Natl. Acad. Sci. USA 113: 452–457. doi:10.1073/pnas.1517445113.

Schultz, E.R., Zupanska, A.K., Sng, N.J., Paoul, A-L., and Ferl, R.J. (2017). Skewing in Arabidopsis roots involves disparate environmental signaling pathways. BMC Plant Biol. 17: 31. doi:10.1186/s12870-017-0975-9.

Sheahan, M.B., Staiger, C.J., Rose, R.J., and McCurdy, D.W. (2004). A green fluorescent protein fusion to actin-binding domain 2 of Arabidopsis fimbrin highlights new features of a dynamic actin cytoskeleton in live plant cells. Plant Physiol. 136: 3968–3978. doi:10.1104/pp.104.049411.

Smertenko, A.P., Deeks, M.J., and Hussey, P.J. (2010). Strategies of actin reorganisation in plant cells. J. Cell Sci. 123: 3019–3028. doi:10.1242/jcs.071126.

Staiger, C.J., Sheahan, M.B., Khurana, P., Wang, X., McCurdy, D.W., and Blanchoin, L. (2009). Actin filament dynamics are dominated by rapid growth and severing activity in the *Arabidopsis* cortical array. J. Cell Biol. 184: 269–280. doi:10.1083/jcb.200806185.

Swarup, R., Kargul, J., Marchant, A., Zadik, D., Rahman, A., Mills, R., Yemm, A., May, S., Williams, L., Millner, P., Tsurumi, S., Moore, I., Napier, R., Kerr, I.D., Bennett, M.J. (2004). Structure-function analysis of the presumptive Arabidopsis auxin permease AUX1. Plant Cell 16: 3069–3083. doi:10.1105/tpc.104.024737.

Swarup, R., and Péret, B. (2012). AUX/LAX Family of auxin influx carriers-an overview. Front. Plant Sci. 3: e225. doi:10.3389/fpls.2012.00225.

Szymanski, D.B., and Cosgrove, D.J. (2009). Dynamic coordination of cytoskeletal and cell wall systems during plant cell morphogenesis. Curr. Biol. 19: R800–R811. doi:10.1016/j.cub.2009.07.056.

Szymanski, D., and Staiger, C.J. (2017). The actin cytoskeleton: functional arrays for cytoplasmic organization and cell shape control. Plant Physiol. 176: 106–118. doi:https://doi.org/10.1104/pp.17.01519.

Thomas, C. (2012). Bundling Actin filaments from membranes: Some novel players. Front. Plant Sci. 3: e188. doi:10.3389/fpls.2012.00188.

Tominaga, M., Kimura, A., Yokota, E., Haraguchi, T., Shimmen, T., Yamamoto, K., Nakano, A., and Ito, K. (2013). Cytoplasmic streaming velocity as a plant size determinant. Dev. Cell 27: 345–352. doi:10.1016/j.devcel.2013.10.005.

Ueda, H., Yokota, E., Kutsuna, N., Shimada, T., Tamura, K., Shimmen, T., Hasezawa, S., Dolja, V. V., and Hara-Nishimuraa, I. (2010). Myosin-dependent endoplasmic reticulum motility and F-actin organization in plant cells. Proc. Natl. Acad. Sci. USA 107: 6894–6899. doi:10.1073/pnas.0911482107.

Ugartechea-Chirino, Y., Swarup, R., Swarup, K., Péret, B., Whitworth, M., Bennett, M., and Bougourd, S. (2010). The AUX1 LAX family of auxin influx carriers is required for the establishment of embryonic root cell organization in *Arabidopsis thaliana*. Ann. Bot. 105: 277–289. doi:10.1093/aob/mcp287.

Ulmasov, T., Hagen, G., and Guilfoyle, T.J. (1999). Activation and repression of transcription by auxin-response factors. Proc. Natl. Acad. Sci. USA 96: 5844–5849. doi:10.1073/pnas.96.10.5844.

van der Weele, C.M., Jiang, H.S., Palaniappan, K.K., Ivanov, V.B., Palaniappan, K., and Baskin, T.I. (2003). A new algorithm for computational image analysis of deformable motion at high spatial and temporal resolution applied to root growth. roughly uniform elongation in the meristem and also, after an abrupt acceleration, in the elongation zone. Plant Physiol. 132: 1138–1148. doi:10.1104/pp.103.021345.

Vidali, L., Burkart, G.M., Augustine, R.C., Kerdavid, E., Tüzel, E., and Bezanilla, M. (2010). Myosin XI is essential for tip growth in *Physcomitrella patens*. Plant Cell 22: 1868–1882. doi:10.1105/tpc.109.073288.

Wu, S., Xie, Y., Zhang, J., Ren, Y., Zhang, X., Wang, J., Guo, X.,Wu, F., Sheng, P., Wang, J., Wu, C., Wang, H., Huang, S., and Wan, J. (2015). VLN2 regulates plant architecture by affecting microfilament dynamics and polar auxin transport in rice. Plant Cell 27: 2829–2845. doi:10.1105/tpc.15.00581.

Xu, T., Dai, N., Chen, J., Nagawa, S., Cao, M., Li, H., Zhou, Z., Chen, X., De Rycke, R., Rakusová, H., Wang, W., Jones, A.M., Friml, J., Patterson, S.E., Bleecker, A.B., Yang, Z. (2014). Cell surface ABP1-TMK auxin-sensing complex activates ROP GTPase signaling. Science 343: 1025–1028. doi:10.1126/science.1245125.

Xu, T., Nagawa, S., and Yang, Z. (2011). Uniform auxin triggers the Rho GTPase-dependent formation of interdigitation patterns in pavement cells. Small GTPases 2: 227–232. doi:10.4161/sgtp.2.4.16702.

Xu, T., Wen, M., Nagawa, S., Fu, Y., Chen, J. -G, Wu, M. -J, Perrot-Rechenmann, C., Friml, J., Jones, A.M., and Yang, Z. (2010). Cell surface- and Rho GTPase-based auxin signaling controls cellular interdigitation in *Arabidopsis*. Cell 143: 99–110. doi:10.1016/j.cell.2010.09.003.

Yanagisawa, M., Desyatova, A.S., Belteton, S.A., Mallery, E.L., Turner, J.A., and Szymanski, D.B. (2015). Patterning mechanisms of cytoskeletal and cell wall systems during leaf trichome morphogenesis. Nat. Plants 1: e 15014. doi:10.1038/nplants.2015.14.

Yang, W., Ren, S., Zhang, X., Gao, M., Ye, S., Qi, Y., Zheng, Y., Wang, J., Zeng, L., Li, Q., Huang, S., and He, Z. (2011). BENT UPPERMOST INTERNODE1 encodes the class II formin FH5 crucial for actin organization and rice development. Plant Cell 23: 661–680. doi:10.1105/tpc.110.081802.

Yang, Y., Hammes, U.Z., Taylor, C. G., Schachtman, D.P., and Nielsen, E. (2006). High-affinity auxin transport by the AUX1 influx carrier protein. Curr. Biol. 16: 1160. doi:10.1016/j.cub.2006.05.043.

Yoshimitsu, Y., Tanaka, K., Fukuda, W., Asami, T., Yoshida, S., Hayashi, K.-i, Kamiya, Y., Jikumaru, Y., Shigeta, T., Nakamura, Y., Matsuo, T., and Okamoto, S. (2011). Transcription of *DWARF4* plays a crucial role in auxin-regulated root elongation in addition to brassinosteroid homeostasis in *Arabidopsis thaliana*. PLoS ONE 6: e23851. doi:10.1371/journal.pone.0023851.

Zhang, W., Cai, C., and Staiger, C.J. (2019). Myosins XI are involved in exocytosis of cellulose synthase complexes. Plant Physiol. 179: 1537–1555. doi:10.1104/pp.19.00018.

Zhang, X., Henriques, R., Lin, S-S., Niu, Q.W., and Chua, N-H. (2006). Agrobacterium-mediated transformation of *Arabidopsis thaliana* using the floral dip method. Nature Protoc. 1: 641–646. doi:10.1038/nprot.2006.97.

Zhang, Z., Zhang, Y., Tan, H., Wang, Y., Li, G., Liang, W., Yuan, Z., Hu, J., Ren, H., and Zhang, D. (2011). RICE MORPHOLOGY DETERMINANT encodes the type II formin FH5 and regulates rice morphogenesis. Plant Cell 23: 681–700. doi:10.1105/tpc.110.081349.

Zhu, J., Bailly, A., Zwiewka, M., Sovero, V., Di Donato, M., Ge, P., Oehri, J., Aryal, B., Hao, P., Linnert, M., Burgardt, N.I., Lücke, C., Weiwad, M., Michel, M., Weiergräber, O.H., Pollmann, S., Azzarello, E., Mancuso, S., Ferro, N., Fukao, Y., Hoffmann, C., Wedlich-Söldner, R., Friml, J., Thomas, C., and Geisler, M. (2016). TWISTED DWARF1 mediates the action of auxin transport inhibitors on actin cytoskeleton dynamics. Plant Cell 28: 930–948. doi:10.1105/tpc.15.00726.

Zhu, J., and Geisler, M. (2015). Keeping it all together: Auxin-actin crosstalk in plant development. J. Exp. Bot. 66: 4983–4998. doi:10.1093/jxb/erv308.

CHAPTER 3. FUTURE DIRECTIONS

3.1 Actin's Role in Cell Expansion

Actin is necessary for cell expansion because it provides tracks for vesicles to bring growth-related materials to the plasma membrane (PM; Ketelaar et al., 2003; Mathur, 2004; Leucci et al., 2007; Zhang et al., 2019). Cell growth has been attributed to specific actin arrays or dynamic behaviors (Nick et al., 2009; Smertenko et al., 2010; Higaki et al., 2010; Dyachok et al., 2011; Yang et al., 2011; Yanagisawa et al., 2015). The problem with these sorts of models is that the studies upon which they are based look at actin and cell size at a limited number of points in time and make strong conclusions based on mere snapshots. By looking at actin organization over the course of the root cap and elongation zone—a tissue that exhibits an inherent gradient of development—and making limited conclusions that do not attribute cause and effect, we avoid this pitfall, to a degree. We were able to eliminate two hypotheses about actin organization and cell expansion:

1. We dispose of the notion that bundles inherently inhibit cell expansion by demonstrating that a higher incidence of actin bundling occurred in long cells, showing that as cell length increased, so too did extent of actin bundling.

2. By bringing cells to a higher degree of "organization" in terms of lower average filament angle and increased filament parallelness after a treatment that stops growth, we show that "more organized" actin arrays do not necessarily correlate with growth.

These findings are progress, yet they fail to establish cause and effect, and the question remains: Does an actin array shown to correlate with growth precede expansion of a cell, or is the array a byproduct of an expanding cell?

The best way to investigate this question is, in theory, relatively simple: use fluorescent imaging to capture dynamic actin organization in living, expanding cells over time, and within individual cells quantify characteristics of the actin array, overall array dynamics, and individual filament behaviors and correlate these characteristics with rate of cell expansion. This sort of work has been accomplished for microtubules (Chan et al., 2007; Sambade et al., 2012; Vyplelová et al., 2018), but actin filaments, particularly in roots, prove in our experience exceptionally sensitive to disruption by even minimal handling. However, technological advances now provide a possible solution. Lightsheet microscopy affords the proper environmental conditions and requisite

spatiotemporal resolution to undertake this sort of long-term imaging experiment on cell growth and actin dynamics (Ovecka et al., 2015; von Wangenheim et al., 2017; Komis et al., 2018). On some lightsheet platforms, seedlings can be kept upright for long periods of time, so the root can maintain its natural position, and the specimen chamber in the microscope can be equipped with lighting elements to mimic natural photoperiods. As proof of concept, we were able to timelapse image a living Arabidopsis root for a period of 10 h at 15-min intervals using a Bruker/Luxendo MuVi platform during a recent demo at Purdue University. Qualitatitively, we were able to visualize dynamic changes in actin organization in files of epidermal cells from the meristematic region to the differentiation zone with minimal photobleaching or photodamage (**Figures 3.1** and **3.2**). Moreover, axial cell expansion of both root hairs and epidermal cells could be observed throughout the timecourse.

The lightsheet imaging system would allow us not only to establish cause and effect for actin organization and cell expansion, but also to ascertain individual cell growth rates across a range of plant tissues, since growth in the epidermis drives shoot and root growth (Savaldi-Goldstein et al., 2007; Savaldi-Goldstein and Chory, 2008; Hacham et al., 2011; Fridman et al., 2014). Plants exhibit circadian growth but these cycles vary among tissues (Dodd et al., 2005; McClung, 2006; James et al., 2008; de Montaigu et al., 2010; Yazdanbakhsh et al., 2011; Henriques et al., 2018), and although root growth cycles fluctuate with increased growth during dark hours and less growth during the day (Yazdanbakhsh and Fisahn, 2010), individual root cell growth rates have never been directly measured. Uncovering individual cell growth patterns and expansion rates would be useful for putting other cellular phenomena into a context and setting expectations for a range of experiments. For example, if individual cell growth rates were established, we would be able to determine what stimuli alter normal growth, which specific cell types are influenced, and to what degree. With some modeling, knowledge of individual cell expansion rates could allow researchers to formulate a rate for exocytosis of cellulose synthase complexes, or to determine the number of cellulose synthase molecules per unit of cell expansion. Uncovering individual cell growth rhythms could inform best times of day to apply herbicides or other agricultural treatments.

Figure 3.1 Long-Term Imaging Shows Dynamic Actin Filament Behavior and Reorganization in the Arabidopsis Root Cap and Elongation Zone over 10 Hours.

Maximum projection lightsheet images of GFP-fABD2–labeled actin in root epidermal cells from the root cap and the meristematic and elongation zones at indicated timepoints, and representative cropped cells.

(A) to **(F)** Note that the actin array in younger cells appeared denser and less "organized" but by the time cells expanded, actin filaments formed more longitudinal bundles. Root hair elongation is especially visible on the main figures of **(E)** and **(F)**. By the end of 10 h, the entire root cap was no longer visible because it had grown out of the field of view.

T0 = start of imaging; T+2 = 1:45; T+10 = 9:45. Scale bar in whole tissue image at T0, 30 μm. Scale bars in cropped, close up images, 15 μm. Colored arrowheads indicate the upper plasma membrane of selected cells. Lower cropped images, when present, have enhanced brightness to show the actin cytoskeleton, which is less apparent in younger, shorter cells at this magnification.

This root was imaged in media (0.6% agar, sucrose-free ½ MS) on the Bruker/Luxendo MuVi platform; final magnification of 22.2 ×.
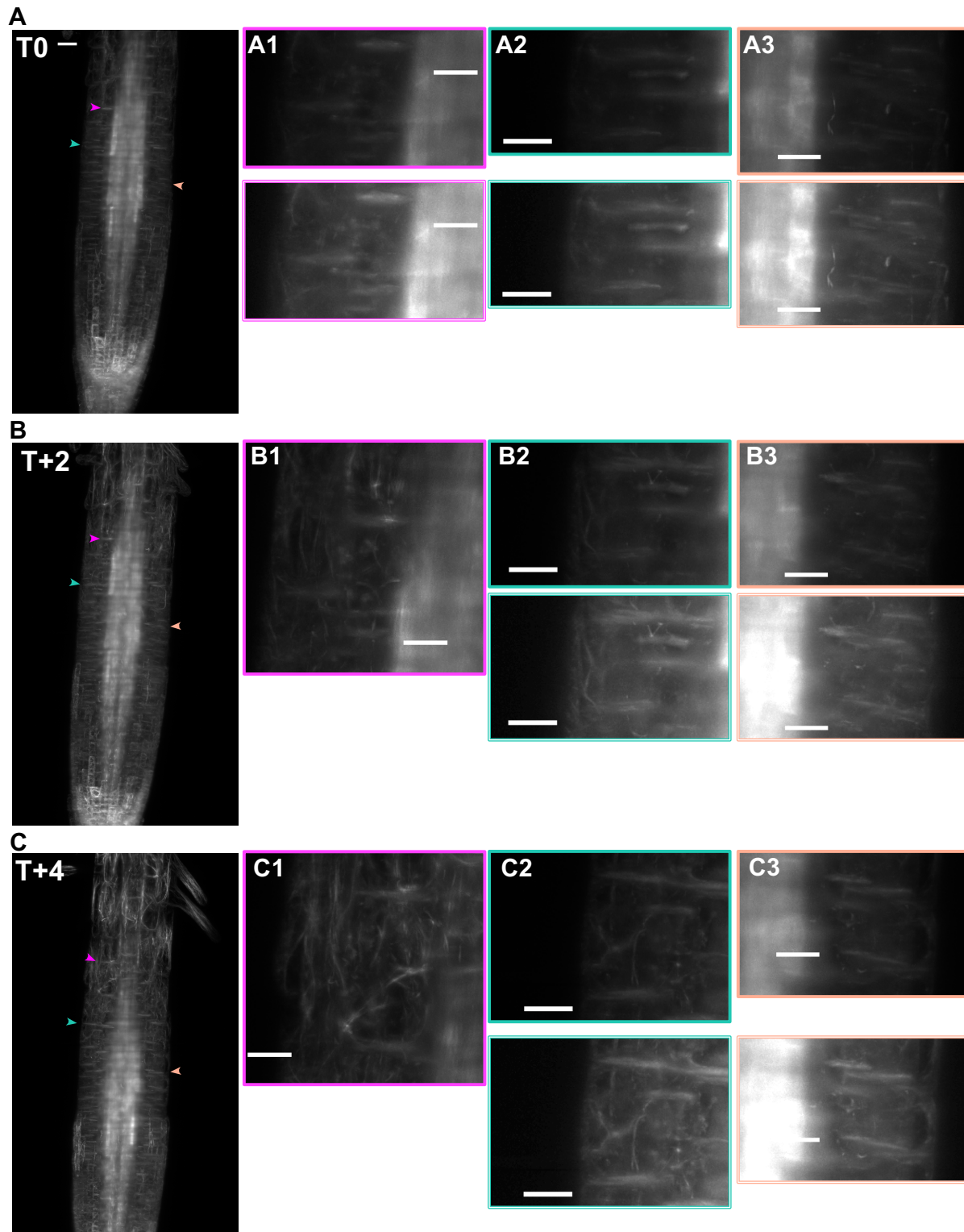
Figure 3.1 Long-Term Imaging Shows Dynamic Actin Filament Behavior and Reorganization in the Arabidopsis Root Cap and Elongation Zone over 10 Hours.
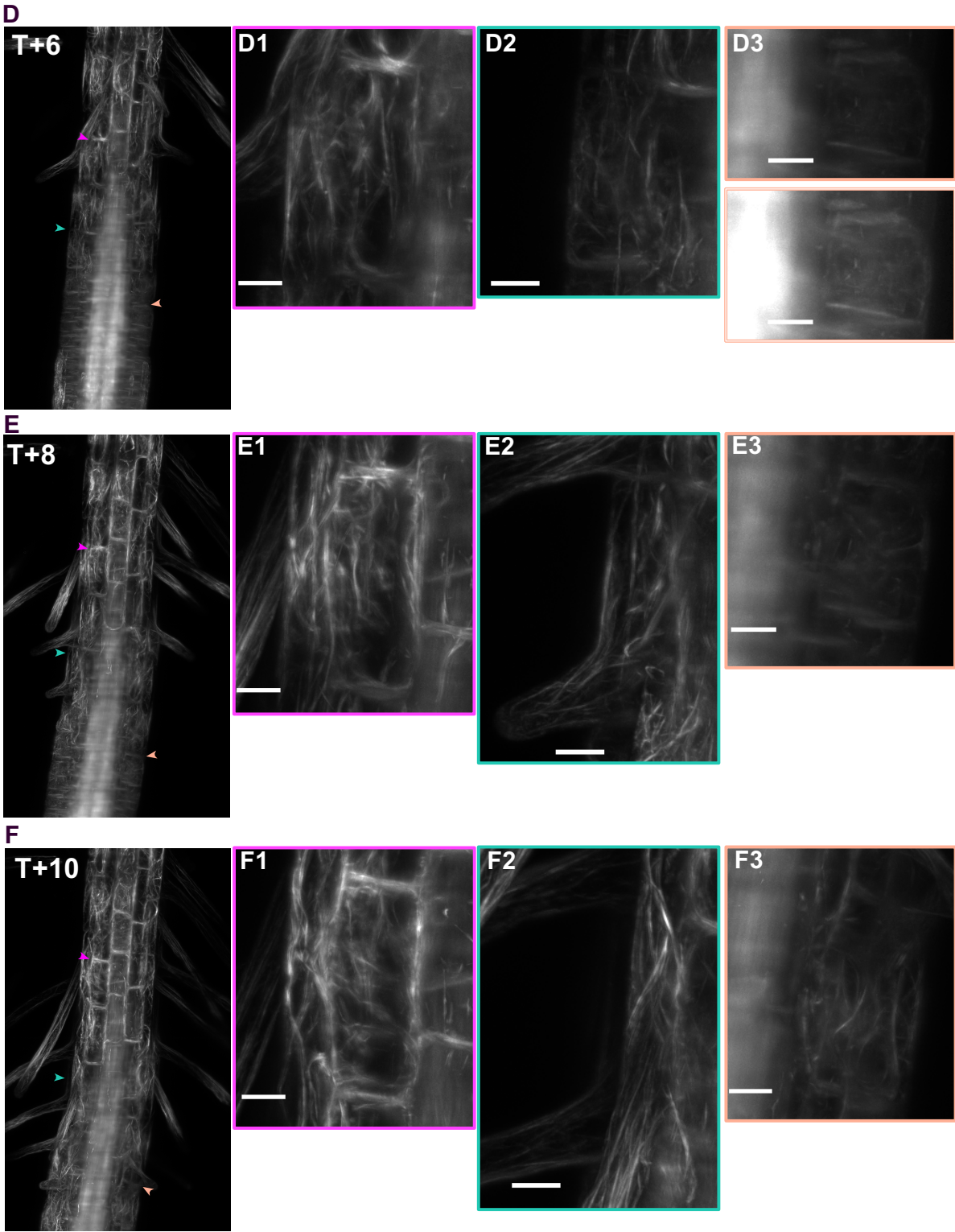
Figure 3.1 continued.

Figure 3.2 Long-Term Imaging Shows Dynamic Actin Filament Behavior in the Arabidopsis Root Differentiation Zone over 10 Hours.

Maximum projection lightsheet images of GFP-fABD2–labeled actin in root epidermal cells from the differentiation zone (just shootward of the images in **Figure 3.1**) at indicated timepoints, and representative cropped cells.

(A) to **(F)** Note that, unlike the elongation zone where the actin array changes dramatically over time in newly differentiated and growing cells, differentiation zone cells have already expanded; though actin filaments are highly dynamic, the overall array does not drastically reorganize, but remains relatively longitudinal over the 10 h. Unlike the root cap/elongation zone images, cells within the differentiation zone do not proliferate and expand out of the field of view .

T0 = start of imaging; T+2 = 1:45; T+10 = 9:45. Scale bar in whole tissue image at T0, 30 μm. Scale bars in cropped, close up images, 15 μm. Colored arrowheads indicate the upper plasma membrane of selected cells.

This root was imaged in media (0.6% agar, sucrose-free ½ MS) on the Bruker/Luxendo MuVi platform; final magnification of 22.2 ×.
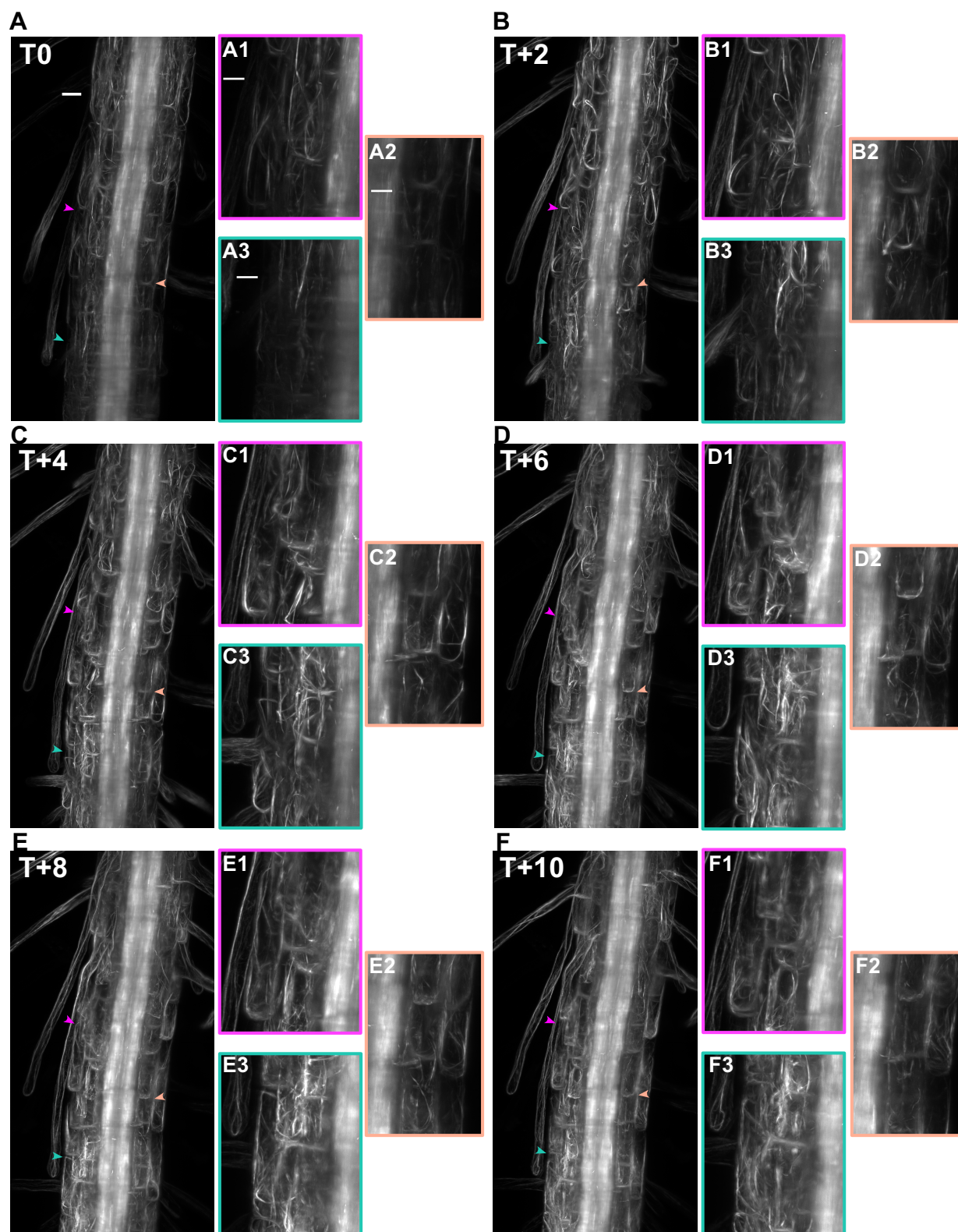
Figure 3.2 Long-Term Imaging Shows Dynamic Actin Filament Behavior in the Arabidopsis Root Differentiation Zone over 10 Hours.

Lightsheet imaging finally provides a method to assess cause and effect between actin organization and cell expansion. It is necessary to first characterize baseline actin organization and reorganization in the root elongation zone over time: track individual cells from first emergence from under the root cap through root hair development (or, for atrichoblasts, until their surrounding cells develop root hairs) and determine broad changes in filament density, skewness/bundling, average filament angle, and filament parallelness that occur in conjunction with growth and changes in expansion rate. It might even be possible to work backwards and trace an individual cell to its production by the meristem. Unlike TIRF/VAEM (total internal reflection fluorescence/variable angle epifluorescence microscopy) which reveals cellular phenomena on the outer periclinal face of the cell, lightsheet imaging facilitates documentation of the inner periclinal face as well, so the actin arrays on both sides of the cell can be compared. Microtubule behavior on each face of the cell has been shown to differ in elongating hypocotyl cells (Chan et al., 2011; Crowell et al., 2011), so it is reasonable to at least investigate the possibility that actin behaves differently on the inner and outer faces of root epidermal cells.

To further divulge relationships between actin organization and cell expansion, this long-term imaging experiment could be augmented to include treatments known to stimulate or inhibit growth. Root cell expansion and actin organization in the presence of a control solution would be documented in the same manner that whole root growth within a chamber was captured in real time in Fendrych et al. (2018). Then, hormone treatments such as auxin and low dose brassinolide could be flooded into the lightsheet chamber to, respectively, inhibit and stimulate root growth. Actin dynamics would be recorded and analyzed in relation to changes in cell expansion rates.

The acid-growth hypothesis has existed in the literature since the 1970s (reviewed in Rayle and Cleland 1992). Briefly, this hypothesis states that auxin stimulates cells to pump H^+ into the apoplastic space, lowering the wall pH, loosening the components of the wall, and allowing the vacuole to exert turgor pressure on the wall, causing cells to expand. Separately from hormones, pH effect on cell expansion rates and actin organization could be evaluated in the same way. Fusicoccin is a fungal toxin that activates PM H^+-ATPases, acidifying the apoplastic space, presumably loosening the cell wall, stimulating growth in both roots (Pillet, 1976) and hypocotyls (Fendrych et al., 2016). Visualizing actin reorganization in response to this pharmacological treatment that stimulates root growth could further test the hypothesis that growth requires "organized" actin arrays.

No matter what relationships between actin organization and cell expansion are uncovered in living cells, the question of "why" actin organization affects cell expansion remains. Why would certain actin arrays lead cells to expand, or prevent cells from expanding, or correlate with states of expansion? A simple explanation might be found by examining cytoplasmic streaming. Cytoplasmic streaming serves to move vesicles within a cell, including delivering materials close to the PM for incorporation into the wall. Cytoplasmic streaming rates, which in Arabidopsis depend on myosin XI, have been shown to determine cell and plant size, where chimeric myosins that combine a fast motor domain from algae fused to wildtype neck and tail domains result in larger cells and plants (Tominaga et al., 2013). Cytoplasmic streaming depends on actin: when actin is disrupted with various drugs (Williamson, 1972; Foissner and Wasteneys, 2007), cytoplasmic streaming ceases because actin tracks are necessary to move vesicles.

It is easy to imagine that targeted delivery of vesicles, requiring that actin tracks are laid toward that specific direction, is particularly important when a cell is coordinating growth in a specific plane, i.e., polarized growth. In the case of the root elongation zone, for example, cells grow in the vertical direction and not laterally. It seems to follow that it is not only the direction of the roads that is important for streaming and growth, but perhaps also their condition that affects vesicle delivery and cytoplasmic streaming. Tracks pointing in haphazard directions will not allow cargoes to reach a polarized destination in the plane of vertical growth. Perhaps an excess of tracks crowded together, or only a few, thick tracks, inhibit targeted vesicle movement. That is to say, perhaps actin organization's role in cell expansion is in the cytoskeleton's ability to support motile vesicles in cytoplasmic streaming. Our own preliminary 3-dimensional lightsheet images show that in both hypocotyl and root epidermal cells, actin appears to form a helical or spiral pattern around the perimeter of mature cells. This spiral actin pattern is in the same directions as described in Foissner and Wasteneys (2000) and Woodhouse and Goldstein (2013), and could underlie cytoplasmic streaming and growth.

Further circumstantial support for the notion that a major role for actin in growth is to provide tracks for cytoplasmic streaming are several pieces of evidence that auxin inhibits cytoplasmic streaming by stimulating actin reorganization. Interestingly, at low doses, auxin increases cytoplasmic streaming rates in *Avena* coleoptiles and at high doses, inhibits it (Thimann and Sweeney, 1937). Our own auxin treatments stimulated substantial increases in filament density. In root hairs, NAA treatments decrease cytoplasmic streaming and cause actin filaments to exhibit

"a random meshwork orientation" (Tominaga et al., 1998). Auxin transport inhibitors tri-iodobenzoic acid (TIBA) and naphthylphthalamic acid (NPA) bundle actin filaments (Rahman et al., 2007), disrupting the "roads", potentially in such a way that vesicles cannot move sufficiently to deliver growth-related materials to the PM. Today it is possible to perform similar experiments—modulating actin organization with various treatments, or finding mutants with aberrant cytoplasmic streaming rates, while evaluating cytoplasmic streaming- and cell growth-rates—while maintaining roots upright in their natural growing position and with the improved spatiotemporal resolution provided by live cell fluorescence imaging. Such experiments could demonstrate that the role of specific actin arrays in cell expansion is to provide an adequate number of proportionately-spaced tracks to allow the vesicle traffic that contributes to growth.

3.2   Auxin–Actin Interactions

It is clear that in any discussion about actin and growth, at least some aspect of cellular responses to auxin eventually arises. Normal plant growth unequivocally requires actin (Baluska et al., 2001; Chen et al., 2007) and normal plant development requires auxin (reviewed in Mockaitis and Estelle 2008). Auxin clearly stimulates actin reorganization (see **Chapter 2**; Rahman et al. 2007; Zhu and Geisler 2015) and auxin transport proteins depend on an intact actin cytoskeleton for proper localization (Geldner et al., 2001; Kleine-Vehn et al., 2006). We have shown that while auxin affects the actin cytoskeleton through the PM-bound auxin influx protein AUXIN RESISTANT 1 (AUX1), an amino acid permease, the hormone itself acts as an intracellular signal to actin when typical entry into the cell is bypassed with the membrane permeable synthetic auxin 1-naphthylacetic acid (NAA). In addition to stimulating actin reorganization, auxin treatments inhibit root elongation (Fendrych et al., 2018), and trigger immediate membrane depolarization and H^+ influx shortly followed by Ca^{2+} influx (Dindas et al., 2018). Ca^{2+} influx is dependent on the $SCF^{TIR1/AFB}$ complex, which can be chemically-inhibited by auxinole (Hayashi et al., 2012; Dindas et al., 2018). To determine whether auxin-induced actin reorganization depends on the intracellular auxin receptor $SCF^{TIR1/AFB}$ complex, one should pretreat roots with auxinole for 20 min, and then administer 20–30 min IAA or NAA. A lack of actin reorganization, or of aspects of actin reorganization, would implicate the $SCF^{TIR1/AFB}$ complex as being upstream of those actin characteristics. Pretreating *aux1* mutants with auxinole and then IAA or NAA could further substantiate AUX1's placement in the $AUX1–SCF^{TIR1/AFB}$–actin auxin response pathway (Dindas

et al., 2018); if AUX1 is upstream of $SCF^{TIR1/AFB}$, we would expect a complete lack of actin reorganization in response to NAA as well as IAA. Auxinole experiments could be completed quickly and substantiated with similar experiments with *tir* mutants and *aux1 tir* double mutants.

In addition to investigating the placement of actin reorganization relative to the intracellular auxin reception machinery in the auxin-response pathway, future work should probe the role of specific actin-binding proteins (ABP) in auxin response. IAA-induced changes in pH and Ca^{2+} are known to modulate ABP activity (Smertenko et al., 1998; Yokota et al., 1999; Allwood et al., 2001; Khurana et al., 2010; Papuga et al., 2010; Bao et al., 2012; van der Honing et al., 2012; Li et al., 2015a; Wu et al., 2015b; Nan et al., 2017), yet it remains unclear whether the actin reorganization we witnessed is mediated by intermediary ABPs or if auxin itself interacts with actin. There are several ways to sort this out.

It is possible that auxin modulates actin organization by binding directly to actin. There is no evidence that this is the case, and other signals that stimulate actin reorganization have either not been evaluated for direct binding or have been shown to act through intermediaries (Goh et al., 1997; Zhu et al., 2016). Still, in vitro binding and TIRF assays using purified actin and IAA could be attempted to ascertain whether there is direct interaction between the hormone and either G-actin or F-actin—would IAA have any effect on filament polymerization, bundling, or unbundling (Bubb et al., 2000; Khurana et al., 2010; Papuga et al., 2010), or would radiolabeled ^{3}H-IAA cosediment with actin filaments (Karger and Mettenleiter, 1996)? In vivo, fluorescent auxins (Hayashi et al., 2014) could be assessed for colocalization with actin filaments.

Though direct auxin–actin binding must be tested before this mode of hormone action on the cytoskeleton may be eliminated from consideration, auxin stimulates influx of known second messengers, as described previously: H^+ (which lowers intracellular pH) and Ca^{2+}. A researcher might use various tests to determine whether one or both of these second messengers is upstream of actin reorganization, and which aspects.

First, the effect of pH itself on actin organization should be tested. In our own preliminary IAA dose series, we found that using ethanol dissolved in MilliQ® water (rather than in liquid ½ MS) for our mock treatment had measurable effects on both average filament angle and filament parallelness (unfortunately, the microscope settings used to collect data in this experiment were ill-suited to seeing effects on density and skewness). The pH of MilliQ® water is more alkaline,

and close to 1.2 points higher[4] compared to ½ MS which has a pH of approximately 5.8. Compared to a mock treatment using ½ MS as the carrier, average filament angle was significantly higher and filament parallelness significantly lower when plants were treated with a water-ethanol control, and these differences in effects of each mock treatment held for both Regions 2 and 3. Furthermore, when we later used NaOH as a solvent for IAA and NAA, drastically increasing the pH of our solutions, we found that all aspects of actin reorganization were less responsive to auxin. It is not guaranteed that the variations we observed are due strictly to differences in pH, but it seems highly likely considering that pH was, in the IAA/NAA experiment, the only condition that changed vs. other experiments.

Extracellular pH significantly affects the extent of IAA-induced membrane depolarization, where alkaline extracellular pH reduces or nullifies the effects of IAA (Dindas et al., 2018). To investigate effect of pH on actin organization, differences in actin organization could be measured in roots treated with a range of buffered solutions with and without auxin. If auxin's effects on actin are driven largely by immediate acidification of cytosol, treatments with low pH solutions could recapitulate some or all of the IAA-induced reorganization we observed. Alternatively, if actin reorganization responds primarily to auxin itself or other intracellular signals, differences in only pH should not affect actin organization.

Interestingly, most auxin-induced H^+ influx (and accompanying apoplastic alkalinization) depends on AUX1 because the influx protein cotransports two H^+ for each IAA that is transported into a cell (Monshausen et al., 2011; Dindas et al., 2018). Furthermore, H^+ transport and membrane depolarization in response to IAA was reduced in CYCLIC NUCLEOTIDE-GATED CHANNEL 14 (*cngc14-2*) mutants, indicating feedback between CNGC14 and AUX1 (Dindas et al., 2018). Actin organization in the *cncg14-2* mutant could be used to test the hypothesis that actin reorganization in response to auxin is a two-part response. If actin array density, average filament angle, and filament parallelness are separately regulated by H^+ and Ca^{2+}, actin in *cncg14-2* should not reorganize in response to auxin since the mutant does not exhibit increases in either intracellular second messenger (Dindas et al., 2018). But a treatment that reduces intracellular pH, certainly in conjunction with auxin, should restore to the mutant some actin reorganization, informing whether any aspect is regulated by pH. To understand whether any aspects of actin

---

[4]   (https://www.emdmillipore.com/US/en/water-purification/learning-centers/applications/inorganic-analysis/ph-measurement/water-impact/MK6b.qB.3g4AAAFUNWISsxU6,nav)

reorganization are regulated by calcium, the nonfunctional mutant channel could perhaps be bypassed with auxin plus drugs that transport Ca^{2+} into cells (ionophores) such as calcimycin or ionomycin (De Vriese et al., 2018).

Besides for H^+, Ca^{2+} is the other second messenger that increases within minutes of auxin treatments (Monshausen et al., 2011; Dindas et al., 2018), and fluctuations in intracellular Ca^{2+} could cause actin to reorganize. Ca^{2+} manipulates actin by modulating ABP activity and more indirectly by modulating calcium-dependent protein kinases that modulate ABP activity (Smertenko et al., 1998; Yokota et al., 1999; Qian and Xiang, 2019). Blocking Ca^{2+} channels with pharmacological treatments and then treating plants with auxin would show which, if any, aspects of actin reorganization are driven by Ca^{2+} fluctuations. For example, if only filament-filament annealing increases after IAA treatments on plants pretreated with the Ca^{2+} channel blocker lanthanum, we would determine that Ca^{2+} modulates unbundling while other factors, likely pH, modulate annealing. Since Ca^{2+} influx in response to auxin is lacking in *aux1* mutants (Dindas et al., 2018), presumably because of a broken feedback loop, ionophores could be applied with and without NAA to learn whether Ca^{2+} is sufficient to instigate auxin-induced actin reorganization, whether Ca^{2+} restores reorganization only in the presence of NAA, and whether all aspects of reorganization are fully restored. By using the *aux1* mutant to eliminate actin response to H^+ (membrane depolarization and H^+ influx are severely reduced or eliminated in *aux1*; Dindas et al. 2018) and using ionophores to (potentially) restore only the actin responses stimulated by Ca^{2+}, and then using ionophores with NAA to restore actin responses organized by Ca^{2+} and auxin, this experiment would divulge which aspects of actin reorganization are coordinated by which signal.

3.2.1 Auxin-Induced Actin Modulation via Actin-Binding Proteins

More likely than direct auxin–actin binding is that auxin modulates actin behavior and organization via regulating activity of one or more ABPs. As described above, short-term cellular response to auxin involves substantial increases in cytosolic Ca^{2+} and slight acidification of cytosol (in conjunction with significant alkalinization of extracellular pH), both shown to be independent of transcriptional responses (Monshausen et al., 2011; Dindas et al., 2018; Fendrych et al., 2018). Since actin is likely necessary on the signaling side of auxin response, any ABPs that are known to be modulated by pH or Ca^{2+} would be reasonable candidates for targeting by the hormone. Unless auxin does bind directly to actin, any ABP mutants whose actin organization is

nonresponsive to IAA would almost certainly be nonresponsive to the membrane permeable NAA in at least some aspects. Actin reorganization is downstream of IAA entry to cells (which we have shown requires AUX1) and likely mediated by ABPs. In the absence of a required ABP, presence of the stimulating signal will be inadequate to initiate actin reorganization. However, differences in response to IAA and NAA might provide insight into what causes ecotypes Col-0 and WS's differential responses to IAA and NAA.

Candidate ABP targets for auxin signaling are members of the VILLIN (VLN) family, which has five isoforms in Arabidopsis (Huang et al., 2005). Though specific protein isoform activity varies, VLNs are in general good candidates for ABPs that might be downregulated in response to auxin. VLNs can cap, sever, and, most relevantly, bundle actin filaments, and with the exception of VILLIN 1 (VLN1; Huang et al. 2005), VLNs are known to respond to fluctuations in Ca^{2+}. VLN3 (VILLIN 3) of Arabidopsis is a bundling and severing protein expressed throughout the plant, including in root epidermal cells of the elongation zone. VLN3's bundling activity in vitro is unaffected by changes to Ca^{2+} concentration, but its severing activity responds to increased Ca^{2+} concentrations (Khurana et al., 2010). Interestingly, when both VLN1 and VLN3 are present in vitro, increasing Ca^{2+} concentrations enable VLN3 to sever filament bundles (Khurana et al., 2010). While our own experiments never counted bundle severing frequencies after IAA, minutes-long movies (rather than the seconds-long movies we collected) would be reasonable to collect and allow measurement of this phenomenon in vivo. We predict that if VLN3 plays a role in IAA response, bundle severing frequencies would increase after IAA and be absent in a *vln3* (or higher order, see below) mutant.

While *vln3* and *vln2* individual isoform mutants do not exhibit strong growth phenotypes, double mutant *vln2 vln3* plants are dwarfed and have wavy roots due to imbalanced cell expansion on each side of the plant, where some cells grow longer than others (van der Honing et al., 2012), a phenotype which is commonly due to aberrant auxin signaling (Swarup et al., 2004; Lanza et al., 2012; Li et al., 2014a; Wu et al., 2015a, 2015b). Furthermore, *vln2 vln3* exhibits an actin phenotype with apparently increased density and, quantified, reduced skewness/bundling, reminiscent of auxin-treated root epidermis cells, although the actin organization parameters angle and parallelness were not measured (Bao et al., 2012; van der Honing et al., 2012). In cosedimentation assays in vitro, increasing Ca^{2+} concentrations with VLN2 reduced the amount of actin filaments

in the pellet, indicating that Ca^{2+} might destabilize VLN-originated actin filaments and bundles in vivo (Bao et al., 2012), potentially in response to IAA-induced Ca^{2+} influx.

Rice VLN2 is closely related to Arabidopsis VLN2 and VLN3 (Khurana et al., 2010; Wu et al., 2015b). Mutant *osvln2* plants grow with wavy roots, root epidermal cells exhibit reduced actin filament skewness/bundling (phenocopying our IAA treatments), roots are hypergravitropic and less sensitive to auxin transport inhibitors, and plants demonstrate substantially reduced rootward and shootward polar auxin transport, although *osvln2* actin response to IAA was never examined (Wu et al., 2015b). Ca^{2+} regulates OsVLN2: cosedimentation experiments show that purified protein bundles actin filaments in a Ca^{2+}-dependent manner, with increased Ca^{2+} reducing the amount of actin in the pellet (Wu et al., 2015b). Our own short-term auxin treatments (see **Chapter 2**) resulted in a doubling of filament unbundling events and no change in bundling. Unbundling in *osvln2* was no different from wildtype, though unbundling in the mutant is likely at a steady state vs. responding to a novel stimulus, and filament dynamic behaviors, with their potential differences, were not studied in the context of individual root regions within the elongation zone. Based on VLN2 and VLN3's responses to Ca^{2+} in Arabidopsis and rice, and the *osvln2* and *vln2 vln3* double mutant's overall actin arrays that appear (Khurana et al., 2010; Bao et al., 2012; van der Honing et al., 2012; Wu et al., 2015b) to phenocopy that of our IAA-treated plants, we feel that VLN2 and/or VLN3 are good candidate ABPs for potential targets of cytosolic changes induced by IAA, with IAA (or its secondary effects on Ca^{2+}) inhibiting VLN activity. We predict that IAA-induced Ca^{2+} influx downregulates VLN2 and/or VLN3 activity, so *vln2 vln3* mutants' actin arrays will not reorganize in response to IAA or NAA, though calcium ionophores should restore some actin reorganization in *aux1* if VLN2 and/or VLN3 are downstream of AUX1.

VLN4 is in a different VLN subfamily from VLN2 and VLN3, and is also expressed in roots (Arabidopsis eFP Browser, Winter et al. 2007; Khurana et al. 2010). Similar to VLN3, VLN4 bundles actin filaments in vitro, but produces significantly shorter bundles with increasing concentrations of Ca^{2+} (Zhang et al., 2011a). The absence of VLN4 leads to short root hairs, reduced cytoplasmic streaming, and the actin array in these T-DNA insertion mutants is like that of *vln2 vln3*: significantly less skewed, indicating less bundling (Zhang et al., 2011a). This ABP could be another candidate for involvement in auxin response where we expect *vln4* mutant actin organization to be impervious to IAA.

Our data show that IAA induces a doubling in filament unbundling, and also alters annealing behavior: we observed a small but statistically significant decrease in incidents of annealing in Region 2; incidents of annealing in Region 3 increased multifold to more closely resemble annealing frequencies in Region 2. CAPPING PROTEIN (CP) is a prime suspect for provoking these changes. CP, a heterodimer comprised of the subunits CPA and CPB, binds to an actin filament's barbed end, preventing further elongation. CP can be regulated by reactive oxygen species and, more pertinent to hormone signaling, by phosphatidic acid (PA; Li et al., 2012a; Li et al., 2012b; Pleskot et al. 2013; Li et al. 2014b). Though there are several metabolic routes to producing PA, the PA that participates in microbe-associated molecular pattern (MAMP) and auxin signaling is produced by members of the PHOSPHOLIPASE D (PLD) family, whose PA-producing activity can be inhibited with the alcohol 1-butanol (Li and Xue, 2007; Mancuso et al., 2007; Li et al., 2015b; Wang et al., 2019).

Mutant root cells in *cp* are shorter than wildtype, and actin organization in *cp* mutants phenocopies auxin treatments: cells exhibit higher filament density and multifold increases in annealing, though average filament angle and parallelness were not measured (Li et al., 2012a, 2014b). CP's effect on filament density appears to be PA-regulated: while PA significantly increases filament density and annealing incidents in wildtype hypocotyl epidermal cells, actin density and annealing in the *cpb-1* mutant is insensitive to such treatments. 1-butanol inhibits PA production, thereby inhibiting CP downregulation, which reduces density in wildtype but not *cpb-1* (Li et al., 2012a, 2014b).

PA downregulates CP in MAMP signaling to actin to increase actin density (Li et al., 2015b), and there are limited studies showing that PA plays a role in regulating auxin responses, (though effects on actin have not been investigated). PLDζ2 expression is increased by IAA, and PLDζ2 activity is necessary for auxin flow through the root transition zone (which almost certainly corresponds to the rootward side of our own Region 2), where auxin flow was reduced by about 40% in a *pldζ2* mutant (Li and Xue, 2007; Mancuso et al., 2007). The *pldζ2* mutant is less sensitive to auxin overall, and 1-butanol treatments on wildtype phenocopy the effect of the mutation (Li and Xue, 2007). PA itself binds to PINOID (PID) kinase, which activates PIN2. When PIN2 and PID are ectopically expressed in *Xenopus* oocytes, applying PA increases the rate of auxin efflux over untreated cells expressing PIN2 and PID, and the rate of auxin efflux increases because PA

activates PID in a dose-dependent manner (Wang et al., 2019). How auxin modulates PLD activity to increase levels of PA remains unclear.

Though there is a link between PA and auxin signaling, and PA modulates actin organization, PA has not yet been shown to operate in short-term auxin signaling to actin. The *cp* mutants and overexpression lines (CP-OX) could be used to test the model that auxin-induced PLD activity stimulates PA production to downregulate CP and increase filament–filament annealing. Auxin should not affect annealing rates in *cp* (because the protein's activity is already effectively "downregulated"), so auxin-induced actin reorganization will be reduced or absent in *cp* compared with wildtype, and it is possible that mutant root growth will be less responsive to inhibition by auxin. Auxin signaling in CP-OX should also be aberrant, with these plants exhibiting diminished auxin-induced actin reorganization that would be salvageable by high doses of exogenous PA. Exogenous PA would downregulate CP, so this treatment in conjunction with NAA might partially or entirely salvage actin reorganization in *aux1*, whereas 1-butanol applied to wildtype plants (with either auxin) would inhibit annealing and, if CP is in the AUX1–actin pathway, at least some aspects of array organization would phenocopy *aux1*. We expect that exogenous PA would have no effect on auxin-induced actin reorganization in *aux1 cp* double mutants but that PA treatment in conjunction with NAA would restore the phenomenon in *aux1 CP-OX*. These experiments would reveal whether CP regulates auxin-induced actin reorganization.

We find VLN and CP the most likely candidates of auxin-based regulation of actin, where the second messenger Ca^{2+} potentially downregulates VLN activity to induce unbundling and auxin-stimulated PA production downregulates CP to perturb annealing frequency. What is known about other ABP regulation by H^+ and Ca^{2+} seems incompatible with the established intracellular responses to auxin. However, much investigation into ABP function is in vitro, and almost every plant ABP family includes multiple isoforms; family members frequently exhibit differential regulation (Khurana et al., 2010; Papuga et al., 2010; Nan et al., 2017). A proteomic study on Arabidopsis seedling and root responses to auxin at 30 min shows that both ACTIN DEPOLYMERIZING FACTOR 2 (ADF2) and LIM-DOMAIN CONTAINING PROTEIN 1 (WLIM1) are upregulated (Kelley et al., 2017). There are 11 ADF/COFILINs in Arabidopsis (which fall into four subclasses and exhibit differential expression throughout the plant) and 6 LIMs (including three widely expressed WLIMs and three PLIMs that are enriched in pollen; Kandasamy et al. 2007; Ruzicka et al. 2007; Thomas et al. 2007; Thomas et al. 2009; Papuga et al.

2010; Henty et al. 2011; Nan et al. 2017). Because quantities of the proteins ADF2 and WLIM1 appear to be increased in response to auxin, the role of each protein in auxin signaling warrants some investigation.

ADFs bind to ADP-actin with much higher affinity than to ATP- or ADP-Pi-actin. Typical ADFs (those in Subclasses I, II, and IV) bind the ADP region of an actin filament and alter the filament's natural twist to destabilize it and induce a break, producing initiation sites for new filaments, and increasing actin turnover (Carlier et al., 1997; de la Cruz, 2009; Suarez et al., 2011; Henty et al., 2011; Nan et al., 2017). Lily ADF1 can bind actin at low pH, but severing and depolymerizing activities occur at higher pH (Allwood et al., 2002; Li et al., 2015a; Nan et al., 2017). Atypical ADFs, ADF5 and ADF9, belong to Subclass III and bundle filaments, with bundling activity in vitro more pronounced at acidic pH (Tholl et al., 2011; Nan et al., 2017), though actin phenotype in vivo might reflect different function. In any case, because auxin immediately decreases cytosolic pH and we observed unbundling after auxin treatments, Subclass III ADFs are unlikely to be involved in auxin response—and our unpublished results (**Figure 3.3**) show that actin organization in an *adf9* mutant responds normally to auxin. However, typical ADF activity is regulated by both pH and Ca^{2+} (Smertenko et al., 1998; Sengupta et al., 2018; Nan et al., 2017). In vitro work demonstrates that maize ADF3 (a Subclass I ADF) is regulated by Ca^{2+}, where a calcium-dependent protein kinase (CDPK) reversibly phosphorylates ZmADF3 to prevent it from associating with actin (Smertenko et al., 1998), effectively down regulating ZmADF3 activity. Extensive experiments in living plants have characterized Arabidopsis ADF4 function, showing ADF4 severs filaments (severing is substantially reduced in *adf4*, reducing overall turnover and lowering filament density) and the protein is inhibited during MAMP response, so filaments are more stable and build a denser array (Henty et al., 2011; Henty-Ridilla et al., 2014).

ADF2 is in the same subclass as ADF4 and was identified as a protein that is upregulated 30 min after auxin treatment (Kelley et al., 2017), indicating a potential role in auxin signaling. Little information on ADF2 is available. However, one study shows that nematode infection of roots causes ADF2 expression to be upregulated, leading vascular cells to expand into "giant cells" that contain the nematodes, and neighboring cells to form a gall. When RNAi is induced to reduce ADF2 expression, actin appears denser and progression of nematode infection is blocked. The researchers suggest that knocking down ADF2 increases actin stability, altering plant growth to

reduce "giant cell" ultimate size and make a less hospitable habitat, thus preventing nematodes from finishing their reproductive cycle (Clement et al., 2009). It is difficult to see a clear connection to auxin signaling, but there is evidence that nematode-induced galls alter auxin flow towards the gall site (Kyndt et al., 2016), providing more circumstantial evidence that auxin signaling (a byproduct of nematode infection) requires ADF2. Because the nematode data imply that active ADF2 leads to more bundled filaments and that inducing ADF2-RNAi to knock down the protein increases apparent filament density (Clement et al., 2009), it seems likely that ADF2 would function at timepoints in late auxin response where actin becomes more bundled (Rahman et al., 2007; Li et al., 2014a), rather than in short-term signaling where ADF2 activity would likely be downregulated by auxin transport-lowered intracellular pH, immediately deactivating ADF2 and stabilizing actin filaments to build a denser array (Clement et al. 2009). Though, in vitro data about general ADF regulation do not necessarily guarantee ADF2 activity in vivo. In any case, it would be simple enough to measure whether there are differences between auxin-induced actin reorganization in an *adf2* mutant vs. wildtype. Long-term auxin responses by the *adf2* mutant could be investigated with a simple root growth inhibition assay in which less growth inhibition by *adf2* would indicate the protein's involvement in auxin signaling. If ADF2 is downregulated by second messengers in short-term auxin responses, we would expect less actin reorganization after auxin treatments in *adf2* compared with wildtype.

Figure 3.3 Actin Organization in *adf9-1* Responds to Short-Term IAA Treatments Similarly as Wildtype.

(A) Representative VAEM images of GFP-fABD2–labeled actin in epidermal cells from wildtype and *adf9-1*, treated for 20–30 min with mock or 10 nM IAA, as indicated. Scale bar, 5 μm.

(B) to **(I)** Quantification of actin architecture and orientation in root epidermal cells: IAA triggers an increase in actin filament density **(B)** and **(C)** and decrease in skewness **(D)** and **(E)** in both regions of both genotypes (*adf9-1 -/-* mutant, shown in sea green; wildtype sibling ADF9++, shown in mauve). **(F)** to **(I)**, After IAA treatments, actin arrays in both regions of both genotypes were more "organized," with lower average filament angle **(F)** and **(G)** relative to the longitudinal axis of the cell and filaments generally more parallel to each other **(H)** and **(I)**.

Cells were subjectively categorized into regions (see **Chapter 2 Figure 2.1**). N ≈ 8–12 cells per region per root from 10 roots per treatment. Different letters indicate statistically significant differences, oneway ANOVA, compared with Tukey-Kramer HSD in JMP. Results are from one experiment, which was performed and analyzed double blind.
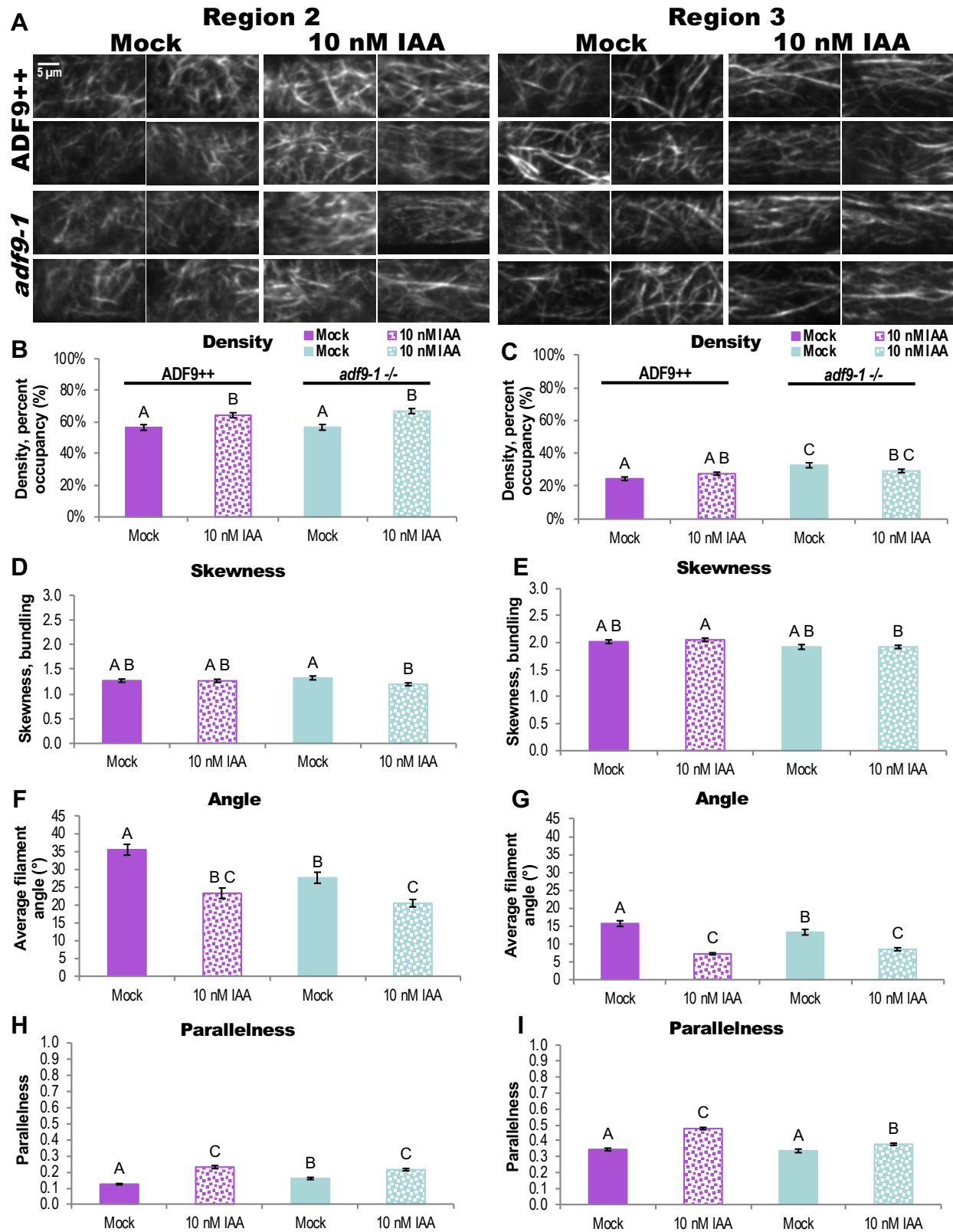
Figure 3.3 Actin Organization in *adf9-1* Responds to Short-Term IAA Treatments Similarly as Wildtype.

In addition to ADF2, the recent proteomic study at 30 min after IAA found increased WLIM1 (Kelley et al., 2017). LIMs bind with high affinity, stabilize, and bundle actin filaments. High pH, and for PLIM2c, high Ca^{2+}, promotes PLIM dissociation from actin filaments to lessen these effects, while WLIM function is insensitive to both pH and Ca^{2+} (Papuga et al., 2010). Expressing fluorescence-labeled LIMs, as well as the Arabidopsis eFP browser, shows that all LIM isoforms—including PLIMs, which in theory are predominantly expressed in pollen—are present in various tissues, including the root epidermis and expression is variably induced (PLIM2c) or downregulated (WLIM1, WLIM2a, PLIM2b) by 2-h auxin treatment (Winter et al., 2007; Papuga et al., 2010; Bargmann et al., 2013). Interestingly the Kelley et al. (2017) proteomic study found increased WILM1 after auxin. The proteomic study authors explicitly report finding frequent inconsistencies between auxin-induced transcriptomic and proteomic data, which they attribute to regulation of translation as well as protein degradation (Kelley et al., 2017). Given the proteomic and in vitro data available for LIMs, WLIM1 and PLIM2c are the most likely candidates of this ABP family to act as intermediaries between auxin signaling and actin reorganization. Cells in both *wlim1* and *plim2c* mutants would be shorter, and mutant actin arrays would be less bundled overall and would fail to unbundle in response to auxin.

Other ABPs shown to play a role in aspects of auxin signaling are members of the myosin XI family (motor proteins that walk along actin filaments and bundles) and rice FORMIN 5 (nucleate, elongate, bundle, and cap filaments). What is known about both myosin and formin in auxin response, however, shows that the two proteins appear to act in longer-term aspects signaling that require transcriptional regulation (Yang et al., 2011; Zhang et al., 2011b; Li et al., 2014a; Scheuring et al., 2016; Abu-Abied et al., 2018; Ojangu et al., 2018), rather than immediate cytoplasmic changes. Work in rice demonstrates that BUI/RMD/FORMIN5 (BENT UPPERMOST INTERNODE/RICE MORPHOLOGY DETERMINANT, a Class II formin homologous to Arabidopsis FORMIN14), drives an increase in actin filament bundles after long-term (6+ h) auxin treatment (Li et al., 2014a). RMD is downstream of ARFs (auxin response factors); the *rmd* mutant is dwarfed compared with wildtype and its actin array fails to respond to long-term (6+ h) IAA treatments with increased bundling, which disrupts polar auxin transport (Zhang et al., 2011b; Li et al., 2014a). The RMD promoter region contains auxin response elements motifs, sequences demonstrated to bind auxin response factors (ARFs), transcription factors that induce RMD transcription in the presence of auxin. Mutants for two ARFs, OsARF23 and

OsARF24 were shown to be upstream of RMD expression, and *osarf23* exhibited similar root and actin phenotypes as the *rmd* mutant, both recoverable with RMD overexpression (Li et al., 2014a). To find other ABPs active in auxin signaling, one might search ABP promoter regions—or the whole Arabidopsis genome—for such auxin response element motifs. This search could yield candidate ABPs upregulated in the presence of auxin, though ABPs regulated through transcriptional responses might be more relevant to long-term auxin responses than to short-term changes in growth.

As for myosins XI, cytoplasmic streaming drives growth and depends on this protein's functionality (Tominaga and Ito, 2015), whose mobility is inhibited by Ca^{2+} (Yokota et al., 1999). Since auxin induces a rapid influx of Ca^{2+}, there is a reasonable mechanism by which auxin could halt myosin XI activity to control cytoskeletal rearrangements within minutes. It appears that actin phenotypes from a *myosin xi triple knockout* (*xi3KO*) mutant do not totally fit a model of myosin XI actin in auxin response (Cai et al., 2014). If myosin XI were downregulated by auxin-induced Ca^{2+} influx, we might expect to see systemic auxin-resistant phenotypes in the mutant: longer root epidermal cells and longer roots, lower filament density and average filament angle, and higher parallelness. However, *xi3KO* exhibits shorter roots and root cells and only some actin phenotypes expected for auxin resistance—lower density and higher parallelness (Cai et al., 2014), indicating that inactivation of myosin XI is likely not solely responsible for auxin-induced actin reorganization. To test a model of auxin-induced actin reorganization that depends on myosin XI, with auxin downregulating myosin XIs to halt cytoplasmic streaming (and therefore, growth), we recommend using the drugs 2,3-butanedione monoxime (BDM) or pentabromopseudilin (PBP), which interfere with ATP-hydrolysis in the myosin motor domain, to inhibit myosin XI activity in wildtype plants in advance of auxin treatments (Zhang et al., 2019). We would expect that actin organization in the *xi3KO* mutant is nonresponsive to auxins, and, assuming Ca^{2+} downregulates myosin XI activity, the actin response to auxin would appear identical in *cngc14-2*, *cngc14-2* treated with BDM/PBP, and *cngc14-2 xi3KO*. If myosin XIs are in the AUX1–actin response pathway, inhibiting myosin XI in *aux1* with BDM or PBP would be expected to phenocopy aspects of actin organization in auxin-treated wildtype. Experiments that investigate the role of Ca^{2+} regulation of myosin (ex., exogenously opening or inhibiting calcium channels to regulate specifically myosin at will) would be difficult to decipher because of auxin's endogenous effect on Ca^{2+} levels, and are not recommended.

At present, there are no data on ABP involvement in short-term auxin response. We suggest using reverse genetics approaches to focus on the ABP discussed above—VLN, CP, and possibly ADF and myosin XI; alternatively, a query for ABPs with ARF sequences in their promoter (Li et al., 2014a), or a large-scale ABP mutant screen for plants lacking auxin-induced root growth inhibition could be conducted. Once candidate ABP are shown to have a role in rapid auxin responses, mutants for these ABP should be crossed with *aux1* to produce double mutants to ensure that the ABP in question is downstream of AUX1 (if both are in the same pathway, actin reorganization in response to IAA should be similar to *aux1* and should only partially occur in response to NAA). With thoughtful effort, the auxin pathway that depends on AUX1 may be resolved.

3.3   References

Abu-Abied, M., Belausov, E., Hagay, S., Peremyslov, V., Dolja, V., and Sadot, E. (2018). Myosin XI-K is involved in root organogenesis, polar auxin transport, and cell division. J. Exp. Bot. 69: 2869–2881.

Allwood, E.G., Anthony, R.G., Smertenko, A.P., Reichelt, S., Drobak, B.K., Doonan, J.H., Weeds, A.G., and Hussey, P.J. (2002). Regulation of the pollen-specific actin-depolymerizing factor LlADF1. Plant Cell 14: 2915–2927.

Allwood, E.G., Smertenko, A.P., and Hussey, P.J. (2001). Phosphorylation of plant actin-depolymerising factor by calmodulin-like domain protein kinase. FEBS Lett. 499: 97–100.

Baluska, F., Jasik, J., Edelmann, H.G., Salajová, T., and Volkmann, D. (2001). Latrunculin B-induced plant dwarfism: Plant cell elongation is F-actin-dependent. Dev. Biol. 231: 113–24.

Bao, C., Wang, J., Zhang, R., Zhang, B., Zhang, H., Zhou, Y., and Huang, S. (2012). Arabidopsis *VILLIN2* and *VILLIN3* act redundantly in sclerenchyma development via bundling of actin filaments. Plant J. 71: 962–975.

Bargmann, B.O.R., Vanneste, S., Krouk, G., Nawy, T., Efroni, I., Shani, E., Choe, G., Friml, J., Bergmann, D.C., Estelle, M., and Birnbaum, K.D. (2013). A map of cell type-specific auxin responses. Mol. Syst. Biol. 9:688.

Bubb, M.R., Spector, I., Beyer, B.B., and Fosen, K.M. (2000). Effects of jasplakinolide on the kinetics of actin polymerization: An explanation for certain in vivo observations. J. Biol. Chem. 275: 5163–5170.

Cai, C., Henty-Ridilla, J.L., Szymanski, D.B., and Staiger, C.J. (2014). Arabidopsis myosin XI: a motor rules the tracks. Plant Physiol. 166: 1359–70.

Carlier, A.M., Laurent, V., Santolini, J., Melki, R., Xia, G., Hong, Y., Chua, N., Pantaloni, D., Laurent, V., Santolini, J., and Didry, D. (1997). Actin depolymerizing factor (ADF/Cofilin) enhances the rate of actin depolymerizing filament turnover : Implication in actin-based motility. J. Cell Biol. 136: 1307–1322.

Chan, J., Calder, G., Fox, S., and Lloyd, C. (2007). Cortical microtubule arrays undergo rotary movements in *Arabidopsis* hypocotyl epidermal cells. Nat. Cell Biol. 9: 171–5.

Chan, J., Eder, M., Crowell, E.F., Hampson, J., Calder, G., and Lloyd, C. (2011). Microtubules and CESA tracks at the inner epidermal wall align independently of those on the outer wall of light-grown *Arabidopsis* hypocotyls. J. Cell Sci. 124: 1088–1094.

Chen, T., Teng, N., Wu, X., Wang, Y., Tang, W., Šamaj, J., Baluška, F., and Lin, J. (2007). Disruption of actin filaments by latrunculin B affects cell wall construction in *Picea meyeri* pollen tube by disturbing vesicle trafficking. Plant Cell Physiol. 48: 19–30.

Clement, M., Ketelaar, T., Rodiuc, N., Banora, M.Y., Smertenko, A., Engler, G., Abad, P., Hussey, P.J., and de Almeida Engler, J. (2009). Actin-depolymerizing factor 2-mediated actin dynamics are essential for root-knot nematode infection of *Arabidopsis*. Plant Cell Online 21: 2963–2979.

Crowell, E.F., Timpano, H., Desprez, T., Franssen-Verheijen, T., Emons, A.-M., Hofte, H., and Vernhettes, S. (2011). Differential regulation of cellulose orientation at the inner and outer face of epidermal cells in the *Arabidopsis* hypocotyl. Plant Cell 23: 2592–2605.

de la Cruz, E.M. (2009). How cofilin severs an actin filament. Biophys. Rev. 1: 51–59.

de Montaigu, A., Tóth, R., and Coupland, G. (2010). Plant development goes like clockwork. Trends Genet. 26: 296–306.

De Vriese, K., Costa, A., Beeckman, T., and Vanneste, S. (2018). Pharmacological strategies for manipulating plant Ca^{2+} signalling. Int. J. Mol. Sci. 19: e1506.

Dindas, J., Scherzer, S., Roelfsema, M.R.G., Von Meyer, K., Müller, H.M., Al-Rasheid, K.A.S., Palme, K., Dietrich, P., Becker, D., Bennett, M.J., and Hedrich, R. (2018). AUX1-mediated root hair auxin influx governs SCF TIR1/AFB -type Ca^{2+} signaling. Nat. Commun. 9: e1174.

Dodd, A.N., Toth, R., Kevei, E., Webb, A.A.R., Salathia, N., Hibberd, J.M., Nagy, F., Millar, A.J., and Hall, A. (2005). Plant circadian clocks increase photosynthesis, growth, survival, and competitive advantage. Science 309: 630–633.

Dyachok, J., Zhu, L., Liao, F., He, J., Huq, E., and Blancaflor, E.B. (2011). SCAR mediates light-induced root elongation in *Arabidopsis* through photoreceptors and proteasomes. Plant Cell 23: 3610–3626.

Fendrych, M., Akhmanova, M., Merrin, J., Glanc, M., Takahashi, K., Uchida, N., and Torii, K.U. (2018). Rapid and reversible root growth inhibition by TIR1 auxin signalling. Nat. Plant 4: 453–459.

Fendrych, M., Leung, J., and Friml, J. (2016). TIR1/AFB-Aux/IAA auxin perception mediates rapid cell wall acidification and growth of Arabidopsis hypocotyls. Elife 5: e19048.

Foissner, I. and Wasteneys, G.O. (2000). Microtubule disassembly enhances reversible cytochalasin-dependent disruption of actin bundles in characean internodes. Protoplasma 214: 33–44.

Foissner, I. and Wasteneys, G.O. (2007). Wide-ranging effects of eight cytochalasins and latrunculin A and B on intracellular motility and actin filament reorganization in characean internodal cells. Plant Cell Physiol. 48: 585–597.

Fridman, Y., Elkouby, L., Holland, N., Vragović, K., Elbaum, R., and Savaldi-Goldstein, S. (2014). Root growth is modulated by differential hormonal sensitivity in neighboring cells. Genes Dev. 28: 912–920.

Geldner, N., Friml, J., Stierhof, Y.D., Jürgens, G., and Palme, K. (2001). Auxin transport inhibitors block PIN1 cycling and vesicle trafficking. Nature 413: 425–428.

Goh, E.L.K., Pircher, T.J., Wood, T.J.J., Norstedt, G., Graichen, R., and Lobie, P.E. (1997). Growth hormone-induced reorganization of the actin cytoskeleton is not required for STAT5 (signal transducer and activator of transcription-5)-mediated transcription. Endocrinology 138: 3207–3215.

Hacham, Y., Holland, N., Butterfield, C., Ubeda-Tomas, S., Bennett, M.J., Chory, J., and Savaldi-Goldstein, S. (2011). Brassinosteroid perception in the epidermis controls root meristem size. Development 138: 839–848.

Hayashi, K.-i., Neve, J., Hirose, M., Kuboki, A., Shimada, Y., Kepinski, S., and Nozaki, H. (2012). Rational design of an auxin antagonist of the SCF^{TIR1} auxin receptor complex. ACS Chem. Biol. 7: 590–598.

Hayashi, K.K. -i., Nakamura, S., Fukunaga, S., Nishimura, T., Jenness, M.K., Murphy, A.S., Motose, H., Nozaki, H., Furutani, M., and Aoyama, T. (2014). Auxin transport sites are visualized in planta using fluorescent auxin analogs. Proc. Natl. Acad. Sci. 111: 11557–11562.

Henriques, R., Papdi, C., Ahmad, Z., and Bögre, L. (2018). Circadian regulation of plant growth. Annu. Plant Rev. 1: 1–29.

Henty-Ridilla, J.L., Li, J.J., Day, B., and Staiger, C.J. (2014). ACTIN DEPOLYMERIZING FACTOR4 regulates actin dynamics during innate immune signaling in *Arabidopsis*. Plant Cell 26: 340–352.

Henty, J.L., Bledsoe, S.W., Khurana, P., Meagher, R.B., Day, B., Blanchoin, L., and Staiger, C.J. (2011). *Arabidopsis* actin depolymerizing factor4 modulates the stochastic dynamic behavior of actin filaments in the cortical array of epidermal cells. Plant Cell 23: 3711–3726.

Higaki, T., Kojo, K.H., and Hasezawa, S. (2010). Critical role of actin bundling in plant cell morphogenesis. Plant Signal. Behav. 5: 484–8.

Huang, S., Robinson, R.C., Gao, L.Y., Matsumoto, T., Brunet, A., Blanchoin, L., and Staiger, C.J. (2005). Arabidopsis VILLIN1 generates actin filament cables that are resistant to depolymerization. Plant Cell 17: 486–501.

James, A.B., Monreal, J.A., Nimmo, G.A., Kelly, C.L., Herzyk, P., Jenkins, G.I., and Nimmo, H.G. (2008). Clock in roots is a slave version of clock in shoots. Science 322: 1832–1836.

Kandasamy, M.K., Burgos-Rivera, B., McKinney, E.C., Ruzicka, D.R., and Meagher, R.B. (2007). Class-specific interaction of profilin and ADF isovariants with actin in the regulation of plant development. Plant Cell 19: 3111–26.

Karger, A., and Mettenleiter, T.C. (1996). Identification of cell surface molecules that interact with pseudorabies virus. J. Virol. 70: 2138–2145.

Kelley, D.R., Shen, Z., Walley, J.W., Chapman, E.J., Briggs, S.P., and Estelle, M.A. (2017). Quantitative proteomic analysis of auxin signaling during seedling development. bioRxiv October 30. http://dx.doi.org/10.1101/211532.

Ketelaar, T., de Ruijter, N.C. a, and Emons, A.M.C. (2003). Unstable F-actin specifies the area and microtubule direction of cell expansion in Arabidopsis root hairs. Plant Cell 15: 285–292.

Khurana, P., Henty, J.L., Huang, S., Staiger, A.M., Blanchoin, L., and Staiger, C.J. (2010). *Arabidopsis* VILLIN1 and VILLIN3 have overlapping and distinct activities in actin bundle formation and turnover. Plant Cell 22: 2727–2748.

Kleine-Vehn, J., Dhonukshe, P., Swarup, R., Bennett, M., and Friml, J. (2006). Subcellular trafficking of the *Arabidopsis* auxin influx carrier AUX1 uses a novel pathway distinct from PIN1. Plant Cell 18: 3171–81.

Komis, G., Novák, D., Ove, M., Olga, Š., and Jozef, Š. (2018). Advances in imaging plant cell dynamics. Plant Physiol. 176: 80–93.

Kyndt, T., Goverse, A., Haegeman, A., Warmerdam, S., Wanjau, C., Jahani, M., Engler, G., De Almeida Engler, J., and Gheysen, G. (2016). Redirection of auxin flow in *Arabidopsis thaliana* roots after infection by root-knot nematodes. J. Exp. Bot. 67: 4559–4570.

Lanza, M., Garcia-Ponce, B., Castrillo, G., Catarecha, P., Sauer, M., Rodriguez-Serrano, M., Páez-García, A., Sánchez-Bermejo, E., TC, M., del Puerto, Y.L, Sandalio, L.M., Paz-Ares, J., and Leyva, A. (2012). Role of actin cytoskeleton in brassinosteroid signaling and in its integration with the auxin response in plants. Dev. Cell 22: 1275–1285.

Leucci, M.R., Di Sansebastiano, G. Pietro, Gigante, M., Dalessandro, G., and Piro, G. (2007). Secretion marker proteins and cell-wall polysaccharides move through different secretory pathways. Planta 225: 1001–1017.

Li, G., Liang, W., Zhang, X., Ren, H., Hu, J., Bennett, M.J., and Zhang, D. (2014a). Rice actin-binding protein RMD is a key link in the auxin-actin regulatory loop that controls cell growth. Proc. Natl. Acad. Sci. 111: 10377–82.

Li, G. and Xue, H.-W. (2007). *Arabidopsis PLDζ2* regulates vesicle trafficking and is required for auxin response. Plant Cell 19: 281–295.

Li, J., Blanchoin, L., and Staiger, C.J. (2015a). Signaling to actin stochastic dynamics. Annu. Rev. Plant Biol. 66: 415–40.

Li, J., Henty-Ridilla, J.L., Huang, S., Wang, X., Blanchoin, L., and Staiger, C.J. (2012a). Capping protein modulates the dynamic behavior of actin filaments in response to phosphatidic acid in *Arabidopsis*. Plant Cell 24: 3742–3754.

Li, J., Henty-Ridilla, J.L., Staiger, B.H., Day, B., and Staiger, C.J. (2015b). Capping protein integrates multiple MAMP signalling pathways to modulate actin dynamics during plant innate immunity. Nat. Commun. 6: 1–13.

Li, J., Pleskot, R., Henty-Ridilla, J.L., Blanchoin, L., Potocký, M., and Staiger, C.J. (2012b). Arabidopsis capping protein senses cellular phosphatidic acid levels and transduces these into changes in actin cytoskeleton dynamics. Plant Signal. Behav. 7: 1727–1730.

Li, J., Staiger, B.H., Henty-Ridilla, J.L., Abu-Abied, M., Sadot, E., Blanchoin, L., and Staiger, C.J. (2014b). The availability of filament ends modulates actin stochastic dynamics in live plant cells. Mol. Biol. Cell 25: 1263–1275.

Mancuso, S., Marras, A.M., Mugnai, S., Schlicht, M., Žársky, V., Song, L., and Baluška, F. (2007). PhospholipaseDζ2 drives vesicular secretion of auxin for its polar cell-cell transport in the transition zone of the root apex. Plant Signal. Behav. 2: 240–244.

Mathur, J. (2004). Cell shape development in plants. Trends Plant Sci. 9: 583–590.

McClung, C.R. (2006). Plant circadian rhythms. Plant Cell 18: 792–803.

Mockaitis, K. and Estelle, M. (2008). Auxin receptors and plant development: a new signaling paradigm. Annu. Rev. Cell Dev. Biol. 24: 55–80.

Monshausen, G.B., Miller, N.D., Murphy, A.S., and Gilroy, S. (2011). Dynamics of auxin-dependent Ca^{2+} and pH signaling in root growth revealed by integrating high-resolution imaging with automated computer vision-based analysis. Plant J. 65: 309–318.

Nan, Q., Qian, D., Niu, Y., He, Y., Tong, S., Niu, Z., Ma, J., Yang, Y., An, L., Wan, D., and Xiang, Y. (2017). Plant actin-depolymerizing factors possess opposing biochemical properties arising from key amino acid changes throughout evolution. Plant Cell 29: 395–408.

Nick, P., Han, M.-J., and An, G. (2009). Auxin stimulates its own transport by shaping actin filaments. Plant Physiol. 151: 155–167.

Ojangu, E.-L., Ilau, B., Tanner, K., Talts, K., Ihoma, E., Dolja, V. V., Paves, H., and Truve, E. (2018). Class XI myosins contribute to auxin response and senescence-induced cell death in *Arabidopsis*. Front. Plant Sci. 9: 1–21.

Ovecka, M., Vaškebová, L., Komis, G., Luptoviak, I., Smertenko, A., and Šamaj, J. (2015). Preparation of plants for developmental and cellular imaging by light-sheet microscopy. Nat. Protoc. 10: 1234–1247.

Papuga, J., Hoffmann, C., Dieterle, M., Moes, D., Moreau, F., Tholl, S., Steinmetz, A., and Thomas, C. (2010). *Arabidopsis* LIM proteins: a family of actin bundlers with distinct expression patterns and modes of regulation. Plant Cell 22: 3034–52.

Pillet, P.E. (1976). Fusicoccin and auxin effects on root growth. Plant Sci. Lett. 7: 81–84.

Pleskot, R., Li, J., Zarsky, V., Potocky, M., and Staiger, C.J. (2013). Regulation of cytoskeletal dynamics by phospholipase D and phosphatidic acid. Trends Plant Sci. 18: 496–504.

Qian, D. and Xiang, Y. (2019). Actin cytoskeleton as actor in upstream and downstream of calcium signaling in plant cells. Int. J. Mol. Sci. 20: 1403.

Rahman, A., Bannigan, A., Sulaman, W., Pechter, P., Blancaflor, E.B., and Baskin, T.I. (2007). Auxin, actin and growth of the *Arabidopsis thaliana* primary root. Plant J. 50: 514–528.

Rayle, D.L. and Cleland, R.E. (1992). The Acid Growth Theory of auxin-induced cell elongation is alive and well. Plant Physiol. 99: 1271–1274.

Ruzicka, D.R., Kandasamy, M.K., McKinney, E.C., Burgos-Rivera, B., and Meagher, R.B. (2007). The ancient subclasses of Arabidopsis *ACTIN DEPOLYMERIZING FACTOR* genes exhibit novel and differential expression. Plant J. 52: 460–472.

Sambade, A., Pratap, A., Buschmann, H., Morris, R.J., and Lloyd, C. (2012). The influence of light on microtubule dynamics and alignment in the *Arabidopsis* hypocotyl. Plant Cell 24: 192–201.

Savaldi-Goldstein, S. and Chory, J. (2008). Growth coordination and the shoot epidermis. Curr. Opin. Plant Biol. 11: 42–48.

Savaldi-Goldstein, S., Peto, C., and Chory, J. (2007). The epidermis both drives and restricts plant shoot growth. Nature 446: 199–202.

Scheuring, D., Löfke, C., Krüger, F., Kittelmann, M., Eisa, A., Hughes, L., Smith, R.S., Hawes, C., Schumacher, K., and Kleine-Vehn, J. (2016). Actin-dependent vacuolar occupancy of the cell determines auxin-induced growth repression. Proc. Natl. Acad. Sci. 113: 452–7.

Sengupta, S., Rajasekaran, K., and Baisakh, N. (2018). Natural and targeted isovariants of the rice actin depolymerizing factor 2 can alter its functional and regulatory binding properties. Biochem. Biophys. Res. Commun. 503: 1516–1523.

Smertenko, A.P., Deeks, M.J., and Hussey, P.J. (2010). Strategies of actin reorganisation in plant cells. J. Cell Sci. 123: 3019–3028.

Smertenko, A.P., Jiang, C.J., Simmons, N.J., Weeds, A.G., Davies, D.R., and Hussey, P.J. (1998). Ser6 in the maize actin-depolymerizing factor, ZmADF3, is phosphorylated by a calcium-stimulated protein kinase and is essential for the control of functional activity. Plant J. 14: 187–193.

Suarez, C., Roland, J., Boujemaa-Paterski, R., Kang, H., McCullough, B.R., Reymann, A.C., Guérin, C., Martiel, J.L., De La Cruz, E.M., and Blanchoin, L. (2011). Cofilin tunes the nucleotide state of actin filaments and severs at bare and decorated segment boundaries. Curr. Biol. 21: 862–868.

Swarup, R., Kargul, J., Marchant, A., Zadik, D., Rahman, A., Mills, R., Yemm, A., May, S., Williams, L., Millner, P., Tsurumi, S., Moore, I., Napier, R., Kerr, I.D., and Bennett, M.J. (2004). Structure-function analysis of the presumptive Arabidopsis auxin permease AUX1. Plant Cell 16: 3069–3083.

Thimann, K.V., and Sweeney, B.M. (1937). The effect of auxins upon protoplasmic streaming. J. Gen. Physiol. Nov 20;21: 123–135.

Tholl, S., Moreau, F., Hoffmann, C., Arumugam, K., Dieterle, M., Moes, D., Neumann, K., Steinmetz, A., and Thomas, C. (2011). *Arabidopsis* actin-depolymerizing factors (ADFs) 1 and 9 display antagonist activities. FEBS Lett. 585: 1821–1827.

Thomas, C., Moreau, F., Dieterle, M., Hoffmann, C., Gatti, S., Hofmann, C., Van Troys, M., Ampe, C., and Steinmetz, A. (2007). The LIM domains of WLIM1 define a new class of actin bundling modules. J. Biol. Chem. 282: 33599–33608.

Thomas, C., Tholl, S., Moes, D., Dieterle, M., Papuga, J., Moreau, F., and Steinmetz, A. (2009). Actin bundling in plants. Cell Motil. Cytoskeleton 66: 940–957.

Tominaga, M. and Ito, K. (2015). The molecular mechanism and physiological role of cytoplasmic streaming. Curr. Opin. Plant Biol. 27: 104–110.

Tominaga, M., Kimura, A., Yokota, E., Haraguchi, T., Shimmen, T., Yamamoto, K., Nakano, A., and Ito, K. (2013). Cytoplasmic streaming velocity as a plant size determinant. Dev. Cell 27: 345–352.

Tominaga, M., Sonobe, S., and Shimmen, T. (1998). Mechanism of inhibition of cytoplasmic streaming by auxin in root hair cells of *Hydrocharis*. Plant Cell Physiol. 39: 1342–1349.

van der Honing, H.S., Kieft, H., Emons, A.M.C., and Ketelaar, T. (2012). Arabidopsis VILLIN2 and VILLIN3 are required for the generation of thick actin filament bundles and for directional organ growth. Plant Physiol. 158: 1426–1438.

von Wangenheim, D., Hauschild, R., and Friml, J. (2017). Light sheet fluorescence microscopy of plant roots growing on the surface of a gel. J. Vis. Exp. 119: e55044.

Vyplelová, P., Ovečka, M., Komis, G., and Šamaj, J. (2018). Chapter 7: Advanced microscopy methods for bioimaging of mitotic microtubules in plants. pp. 129–158 in Methods in Cell Biology, vol. 145. doi.org/10.1016/bs.mcb.2018.03.019.

Wang, P., Shen, L., Guo, J., Jing, W., Qu, Y., Li, W., Bi, R., Xuan, W., Zhang, Q., and Zhang, W. (2019). Phosphatidic acid directly regulates PINOID-dependent phosphorylation and activation of the PIN-FORMED2 auxin efflux transporter in response to salt stress. Plant Cell 31: 250–271.

Williamson, R.E. (1972). A light-microscope study of the action of cytochalasin B on the cells and isolated cytoplasm of the Characeae. J. Cell Sci. 10: 811–819.

Winter, D., Vinegar, B., Nahal, H., Ammar, R., Wilson, G. V, and Provart, N.J. (2007). An "Electronic Fluorescent Pictograph" Browser for Exploring and Analyzing Large-Scale Biological Data Sets. PLoS ONE 8: e718.

Woodhouse, F.G. and Goldstein, R.E. (2013). Cytoplasmic streaming in plant cells emerges naturally by micro filament self-organization. Proc. Natl. Acad. Sci. 110: 14132–14137.

Wu, L., Luo, P., Di, D-W., Wang, L., Wang, M., Lu, C-K., Wei, S-D., Zhang, L., Zhang, T-Z., Amakorová, P., Strnad, M., Novák, O., and Guo, G-Q. (2015a). Forward genetic screen for auxin-deficient mutants by cytokinin. Sci. Rep. 5: e11923.

Wu, S., Xie, Y., Zhang, J., Ren, Y., Zhang, X., Wang, J., Guo, X., Wu, F., Sheng, P., Wang, J., Wu, C., Wang, H., Huang, S., Wan, J. (2015b). VLN2 Regulates plant architecture by affecting microfilament dynamics and polar auxin transport in rice. Plant Cell 27: 2829–45.

Yanagisawa, M., Desyatova, A.S., Belteton, S.A., Mallery, E.L., Turner, J.A., and Szymanski, D.B. (2015). Patterning mechanisms of cytoskeletal and cell wall systems during leaf trichome morphogenesis. Nat. Plants 1: 15014.

Yang, W., Ren, S., Zhang, X., Gao, M., Ye, S., Qi, Y., Zheng, Y., Wang, J., Zeng, L., Li, Q., Huang, S., and He, Z. (2011). BENT UPPERMOST INTERNODE1 encodes the class II formin FH5 crucial for actin organization and rice development. Plant Cell 23: 661–80.

Yazdanbakhsh, N. and Fisahn, J. (2010). Analysis of *Arabidopsis thaliana* root growth kinetics with high temporal and spatial resolution. Ann. Bot. 105: 783–791.

Yazdanbakhsh, N., Sulpice, R., Graf, A., Stitt, M., and Fisahn, J. (2011). Circadian control of root elongation and C partitioning in *Arabidopsis thaliana*. Plant Cell Environ. 34: 877–894.

Yokota, E., Muto, S., and Shimmen, T. (1999). Inhibitory regulation of higher-plant myosin by Ca^{2+} ions. Plant Physiol. 119: 231–240.

Zhang, W., Cai, C., and Staiger, C.J. (2019). Myosins XI are involved in exocytosis of cellulose synthase complexes. Plant Physiol. 179: 1537–1555.

Zhang, Y., Xiao, Y., Du, F., Cao, L., Dong, H., and Ren, H. (2011a). *Arabidopsis* VILLIN4 is involved in root hair growth through regulating actin organization in a Ca^{2+}-dependent manner. New Phytol. 190: 667–682.

Zhang, Z., Zhang, Y., Tan, H., Wang, Y., Li, G., Liang, W., Yuan, Z., Hu, J., Ren, H., and Zhang, D. (2011b). RICE MORPHOLOGY DETERMINANT encodes the type II formin FH5 and regulates rice morphogenesis. Plant Cell 23: 681–700.

Zhu, J., Baily, A., Zwiewka, M., Sovero, V., Di Donato, M., Ge, P., Oehri, J., Aryal, B., Hao, P., Linnert, M., Burgardt, N.I., Lücke, C., Weiwad, M., Michel, M., Weiergräber, O.H., Pollmann, S., Azzarello, E., Mancuso, S., Ferro, N., Fukao, Y., Hoffmann, C., Wedlich-Söldner, R., Friml, J., Thomas, C., and Geisler, M. (2016). TWISTED DWARF1 mediates the action of auxin transport inhibitors on actin cytoskeleton dynamics. Plant Cell 28: 930–948.

Zhu, J. and Geisler, M. (2015). Keeping it all together: Auxin–actin crosstalk in plant development. J. Exp. Bot. 66: 4983–4998. doi:10.1093/jxb/erv308.

VITA

Ruthie S. Arieti
Purdue University
Hansen Life Sciences Research Building
201 South University Street, West Lafayette, IN 47907
ORCID: 0000-0001-8706-635X

a. Professional Preparation

George Mason University, VA	Biology, *cum laude*	B.A., 2005
Purdue University	Ph.D., Biological Sciences/PULSe	Exp. Aug 2019

b. Appointments

2012–present   Graduate Research Assistant, Purdue University Life Sciences Interdisciplinary Program (PULSe)
Purdue University, West Lafayette, IN

2008–2012   Research Associate
Board on Agriculture and Natural Resources
The National Academy of Sciences, Washington, DC

2006–2008   Senior Program Assistant
Board on Agriculture and Natural Resources
The National Academy of Sciences, Washington, DC

2006   Program Assistant
Board on Agriculture and Natural Resources
The National Academy of Sciences, Washington, DC

c. Publication and Presentations

(i) *Publications*

Arieti, R. S., and Staiger, C. J. (submitted). Auxin-Induced Actin Cytoskeleton Rearrangements Require AUX1. Available online at https://www.biorxiv.org/content/10.1101/630798v1.

Li, J., **Arieti, R.**, and Staiger, C. J. (2015). Chapter 5 Actin Filament Dynamics and their Role in Plant Cell Expansion. Pp. 127–162 in *Plant Cell Wall Patterning and Cell Shape First Edition*, H. Fukuda, ed. John Wiley & Sons, Inc., Boston. Available online at: https://onlinelibrary.wiley.com/doi/10.1002/9781118647363.ch5.

(ii) *Selected Posters and Presentations*

Poster: Auxin-Induced Actin Cytoskeleton Rearrangements Require AUX1. **Arieti, R. S.** and Staiger C. J. Chicago Cytoskeleton, Northwestern University, Chicago, March 15, 2019.

Poster: Root epidermal cell length predicts actin organization in the elongation zone. **Arieti, R. S.** and Staiger, C. J. Midwest Plant Cell Dynamics, University of Wisconsin, Madison, May 29–June 1, 2018.

Presentation: Auxin stimulates the actin cytoskeleton through AUX1. **Arieti, R. S.** and Staiger, C. J. Midwest Plant Cell Dynamics, University of Wisconsin, Madison, May 30, 2018.

Poster: Root epidermal cell length predicts actin organization in the elongation zone. **Arieti, R. S.** and Staiger C. J. Chicago Cytoskeleton, Northwestern University, Chicago, March 16, 2018.

Poster: Investigating the relationship between actin organization and root epidermal cell expansion. **Arieti, R. S.** and Staiger, C. J. Fourth Midwest Membrane Trafficking and Signaling Symposium, Purdue University, October 27, 2017.

Presentation: Auxin stimulates actin cytoskeleton dynamics. **Arieti, R. S.** and Staiger, C. J. Fourth Midwest Membrane Trafficking and Signaling Symposium, Purdue University, October 27, 2017.

d. Synergistic Activities

Teaching Assistant, Department of Biological Sciences, Purdue University

BIOL 110 Fundamentals of Biology I	Fall 2015, Fall 2016, Fall 2017
BIOL 111 Fundamentals of Biology II	Spring 2018

*In introductory level biology courses for science majors, **Fundamentals of Biology I** and **Fundamentals of Biology II** (BIOL 110 and 111), I worked with hundreds of students over four semesters to reinforce lecture material through guided problem-solving in labs and recitations.*

BIOL 286 Introduction to Ecology & Evolution	Spring 2015, Spring 2016, Spring 2017

*In **Introduction to Ecology and Evolution** (BIOL 286), for three semesters, I held weekly office hours; graded short-answer questions on homework, weekly quizzes, and tests; and delivered several guest lectures on aspects of evolution within a cell biology framework.*

PULSe Graduate Student Organization, Purdue University

Activities Coordinator	May 2015–April 2016
Co-Activities Coordinator	May 2013–April 2014

Transformed the fundamental framework of socials, increasing turnout, involvement, and PULSe esprit de corps by diversifying activity times and locations.

e. Collaborators & Other Affiliations

(i) *Collaborator*

A. Bhat and G. Monshausen (PI), Huck Institute of the Life Sciences, Penn State University, University Park, PA

(ii) *Graduate Advisor*

Chris J. Staiger, Department Head and Distinguished Professor, Department of Botany and Plant Pathology, Purdue University, West Lafayette, IN